Le magmatisme des Vosges : conséquence des subductions paléozoïques (datation, pétrologie, géochimie, ASM)

Anne-Sophie Tabaud

UNIVERSITÉ DE STRASBOURG

ÉCOLE DOCTORALE Sciences de la Terre, de l'Univers et de l'Environnement (ED 413)

Institut de Physique du Globe de Strasbourg (UMR 7516)

THÈSE présentée par :

Anne-Sophie TABAUD

soutenue le : **14 Juin 2012**

pour obtenir le grade de : **Docteur de l'université de Strasbourg**

Discipline/ Spécialité : Sciences de la Terre - Géologie/Géochimie

Le magmatisme des Vosges : conséquence des subductions paléozoïques

(datation, pétrologie, géochimie, ASM)

THÈSE dirigée par :

M. WHITECHURCH Hubert	Prof., Université de Strasbourg
M. ROSSI Philippe	Bureau de Recherches Géologiques et Minières

RAPPORTEURS :

M. BARBEY Pierre	Prof., Centre de Recherches Pétrographiques et Géochimiques
M. JANOUŠEK Vojtěch	Czech Geological Survey
M. MANATSCHAL Gianreto	Prof., Université de Strasbourg

EXAMINATEUR :

M. SCHULMANN Karel	Prof., Université de Strasbourg

UNIVERSITÉ DE STRASBOURG

Géosciences pour une Terre durable

THÈSE présentée par :

Anne-Sophie TABAUD

soutenue le : **14 Juin 2012**

pour obtenir le grade de : **Docteur de l'Université de Strasbourg**

Discipline/ Spécialité : Sciences de la Terre - Géologie/Géochimie

Le magmatisme des Vosges : conséquence des subductions paléozoïques

(datation, pétrologie, géochimie, ASM)

THÈSE dirigée par :

M. WHITECHURCH Hubert	Prof., Université de Strasbourg
M. ROSSI Philippe	Bureau de Recherches Géologiques et Minières

RAPPORTEURS :

M. BARBEY Pierre	Prof., Centre de Recherches Pétrographiques et Géochimiques
M. JANOUŠEK Vojtěch	Czech Geological Survey
M. MANATSCHAL Gianreto	Prof., Université de Strasbourg

EXAMINATEUR :

M. SCHULMANN Karel	Prof., Université de Strasbourg

Remerciements

C’est le moment de remercier toutes les personnes qui ont contribué à ce travail de thèse et de leur faire part de toute ma gratitude.

Je remercie vivement mes deux directeurs de thèse, Hubert Whitechurch et Philippe Rossi, pour m’avoir fait confiance et m’avoir confiée ce beau projet. La qualité de l’encadrement a fortement contribué à la réussite de ce travail, et je suis très sincèrement reconnaissante envers Hubert et Philippe pour toute la disponibilité dont ils ont fait preuve au cours de ces années.

Je remercie également les membres du jury : Gianreto Manatschal, Pierre Barbey, Vojtěch Janoušek et Karel Schulmann, d’avoir accepté de juger ce travail et de leur apport dans l’amélioration de ce manuscrit. Mes remerciements vont aussi à toute l’équipe de la Dynamique de la Lithosphère et des Bassins Sédimentaires (DyLBaS) pour m’avoir accueillie et pour leur aide.

Je remercie le BRGM et la région Alsace pour la bourse de thèse ainsi que pour le support financier sans lequel ce travail n’aurait pas été aussi complet.

Ce travail a été mené en collaboration avec Etienne Skrzypek, Karel Schulmann, Jean-Bernard Edel et Zuzana Kratinová qui m’ont apportée leurs nombreuses connaissances sur le Massif Vosgien ainsi que sur l’orogène Varisque en général. Je remercie sincèrement Etienne et Zuzana pour leur participation très active aux campagnes de forage pour l’ASM, épaulés par Ludovic Jeanniot, Vlada Kusbach et Francis Chopin.

Enfin, au cours de ce travail de nombreuses personnes ont été mises à contributions pour l’obtention des échantillons et des analyses : Amélie Aubert, Gilles Morvan, Geoffroy Mohn et Tsvetomila Mateeva (Université de Strasbourg) ; Catherine Guerrot, Guillaume Wille, Alain Cocherie, Dominique Guinamant et Jérémie Melleton (BRGM, Orléans) ; Philippe Robion et Fabien Humbert (Université Cergy-Pontoise) et Jean-Louis Paquette (Laboratoire Magmas et Volcans, Clermont-Ferrand), je tiens à les remercier vivement pour m’avoir facilitée mon travail de recherche et aidée à faire progresser la connaissance des Vosges.

Et encore merci à tous pour l’aide et le soutien.

Sommaire

Introduction

Le large éventail de composition des roches magmatiques (plutonites et volcanites), constituants majeurs de la croûte continentale, reflète la diversité de la nature de leur source et/ou des modalités (conditions T, P, P fluides) de la fusion du protolite et des possibles interactions-hybridations avec des magmas mantelliques. Ces roches se sont mises en place quels que soient les types de régime tectonique (compression, extension, transtension) et dans des contextes géodynamiques aussi variés que rifting, subduction ou collision.

L'origine des roches magmatiques que l'on observe dans la croûte continentale peut être recherchée dans la fusion d'une source crustale ou mantellique ou bien encore mixte. Ces composants crustaux et mantelliques présentent chacun des signatures géochimiques distinctes qui permettent généralement de tracer leur présence (et éventuellement de quantifier leurs proportions respectives) au sein des magmas.

L'étude de la composition chimique des roches magmatiques, d'abord à partir de celle des éléments majeurs (Cross, Iddings, Pearson, Washington, Peacock, Harker etc …) a rapidement permis, dès le début du XX siècle, de distinguer au sein des roches magmatiques des familles calco-alcaline, alumineuse, alcaline … en considérant en particulier l'aluminium 'feldspathisable' ou non 'feldspathisable'. Déjà, à cette époque, un essai de relation avait été établi entre la composition des roches magmatiques et leur position géographique (cf. famille calco-alcaline ou 'atlantique'). En considérant le comportement du fer opposé à celui du magnésium, Kuno (1968), à partir de l'étude du volcanisme du Japon, a affiné le concept de série magmatique (différenciation) et défini la série tholéiitique.

Dans les années 1970-80, la géochimie des éléments en traces, puis des isotopes est venue compléter et affiner les outils de discrimination entre les différentes séries magmatiques (Floyd & Winchester, 1975 ; Petro et al., 1979 ; Pitcher, 1983 ; Pearce et al., 1984 ; Maniar et Piccoli, 1989 ; Barbarin, 1990 ; Foerster et al., 1997) et permis d'associer, de façon souvent très étroite, la composition chimique des roches volcaniques et celle de leur site de genèse dans le cadre de la tectonique des plaques. La géochimie est ainsi devenue un outil très puissant pour les géodynamiciens, et, en prenant en compte l'actualisme, pour les paléogéodynamiciens. Les discriminations établies à partir des roches volcaniques, dont la composition se rapproche (globalement) de celles de liquides et auxquelles le concept de cristallisation fractionnée peut s'appliquer (Allègre, Treuil etc …) ont été ensuite étendues aux roches plutoniques (Pearce et al., 1984 ; Maniar & Piccoli, 1989 ; Barbarin, 1990 ; Foerster et al., 1997) cependant l'application 'aveugle' ou comme 'boîtes noires' des diagrammes discriminants, spécialement dans le cas des plutonites, a conduit à des résultats souvent décevants voire incohérents. En effet, les modalités de cristallisation des roches plutoniques au sein de la croûte continentale ne permettent pas d'assimiler directement les magmas à leur origine a des liquides ; en effet, dans la

mesure où, si l'on prend en compte leur temps de migration depuis leur site de genèse à celui de leur mise en place, des phénomènes d'assimilation et/ou mélange et/ou cumulation peuvent intervenir dans cette durée.

Ainsi si le croisement systématique des données géologiques et structurales avec l'information géochimique, minéralogique, ou géochronologique reste une approche indispensable dans l'étude des roches magmatiques, il prend encore plus de pertinence dans le cas des roches plutoniques.

D'après Condie (1998), 75 à 80 % de la croûte continentale juvénile a été extraite du manteau durant l'Archéen et le Paléoprotérozoïque, en revanche la contribution varisque consiste principalement en un recyclage d'éléments crustaux plus anciens (Downes & Duthou, 1988 ; Pin & Duthou, 1990). Dans la chaîne varisque, caractérisée par l'abondance des intrusions acides résultant de la fusion de la croûte inférieure (Downes & Duthou, 1988 ; Pin & Duthou, 1990 ; Shaw et al., 1993 ; Williamson et al, 1996 ; Downes et al., 1997), les granitoïdes peuvent fournir une image transposée de la composition de cette croûte inférieure granulitique.

Au sein des massifs varisques, les Vosges s'avèrent constituer un site d'étude particulièrement adéquat pour étudier l'évolution et le développement de la croûte continentale lors de l'orogène varisque. En effet ce massif est caractérisé par la présence de nombreuses extrusions et intrusions magmatiques d'affinités variées, affleurant dans un cadre bien circonscrit et facilement accessible, permettant d'y conduire une analyse détaillée de leur composition et de l'éventuelle filiation entre les différents termes pétrographiques. En outre on y rencontre des formations métamorphiques avec des granulites de moyenne pression formées à la base de la croûte et un métamorphisme barrovien au niveau de la croûte moyenne dont l'étude a fait, pour partie, l'objet du travail de thèse d'E. Skrzypek (2011).

Les Vosges ont été divisées en deux domaines séparés par un accident majeur : la faille de Lalaye-Lubine (Kossmatt, 1927). Dans les Vosges centrales et méridionales, qui appartiennent au domaine Moldanubien, affleure le magmatisme le plus ancien de ce massif, tandis que dans les Vosges septentrionales, appartenant au domaine Saxo-Thuringien, se trouve un magmatisme plus jeune. Chacune de ces deux zones apporte donc des éléments permettant d'affiner la connaissance de l'environnement géodynamique de ce massif varisque et de mieux contraindre sa paléoposition par rapport aux autres massifs de la chaîne.

Lors du lever des premières cartes géologiques, les relations existant entre les roches métamorphiques et magmatiques ont été mises en évidence (Rosenbusch, von Eller…) et une première chronologie relative esquissée. Dès cette époque, certaines roches : les 'durbachites' et les

granitoïdes associés sont très vite apparus singulières par rapport à celles connues aussi bien dans leur environnement que dans d'autres orogènes.

La connaissance géologique s'est ensuite concurremment poursuivie par des études pétrographiques (Hameurt, Fluck, Gagny) ; structurales (Rey) ; pétrostructurales (école de Gagny : Blanchard, Cottard, Blumenfeld etc … ; école de Strasbourg, Edel, Schulmann, Skrzypek…) et enfin géochimiques (Altherr et al., 2000). Ces derniers auteurs ont procédé à une utilisation systématique des éléments en traces (Terres Rares et éléments incompatibles) et des isotopes du Sr et Nd sur les granitoïdes des Vosges septentrionales. Ils ont pu montrer que les diorites de la bande du Champ du Feu des Vosges septentrionales seraient issues de la fusion d'une lithosphère mantellique « enrichie » et que les granodiorites et granites résulteraient de la fusion, à différents taux, d'une croûte profonde (sans grenat, laissant un résidu d'amphibole) à composition variable de métabasaltes, méta-andésites, tonalites ou métagrauwackes. Enfin, les granites circonscrits (Andlau, Natzwiller, Senones), toujours de type I, proviendraient de la fusion d'une croûte plus profonde dans laquelle le grenat est présent (Altherr et al, 2000). Ces auteurs concluent que ces granitoïdes se seraient formés, soit au-dessus de la zone de subduction vers le Sud de l'océan Rhéno-hercynien sous le Saxo-Thuringien et le Moldanubien, soit au début de la collision continentale entre le domaine Rhéno-Hercynien au Nord et le domaine Saxo-Thuringien au Sud.

Des datations U-Pb sur zircon ont été effectuées dans les Vosges centrales et méridionales (Schaltegger et al., 1996 ; 1999 ; Schulmann et al, 2002 ; Kratinová et al., 2007) en accompagnement d'analyses structurales par la méthode « ASM » (Anisotropie de la Susceptibilité Magnétique, Kratinová et al., 2007). Aucune donnée géochimique (majeurs et traces) ni isotopique n'était jusqu'à présent disponible pour cette zone.

Le présent travail a pour objectif premier d'utiliser l'étude du magmatisme des Vosges pour comprendre ses conditions de genèse et de mise en place et de combiner ces résultats avec ceux de la littérature afin de mieux contraindre la dynamique varisque dans ce secteur de l'orogène et de la comparer à celle des autres secteurs de la chaîne. Pour parvenir à ces fins il a été nécessaire d'entreprendre une caractérisation géochimique systématique des différentes séries volcaniques et plutoniques des Vosges et de définir avec précision la chronologie de mise en place des différentes associations magmatiques en combinant les informations relatives, issues des données de terrain, avec des données géochronologiques robustes (U-Pb sur zircon, U-Th-Pb sur monazite) déjà publiées ou bien acquises dans le cadre de notre recherche. En outre, des analyses structurales (mesures sur le terrain et ASM) ont été effectuées conjointement afin de bien contraindre l'environnement tectonique de la mise en place des magmas. Tous les éléments acquis aussi bien sur le terrain, en ASM, en pétrographie-minéralogie, ou bien en géochimie vont être mis en relation pour établir un modèle

géodynamique de genèse et de mise en place de ces venues magmatiques.

Enfin, le magmatisme des Vosges sera comparé à celui des autres massifs de l'orogène varisque (Massif de Bohème, Massif Cristallins Externes des Alpes, Massif Corso-Sarde, Forêt Noire).

Ce mémoire est présenté sous la forme de 6 chapitres : 4 chapitres de résultats sous la forme de publications soumises dans des revues internationales dont 3 sur les Vosges moyennes et méridionales et 1 sur les Vosges septentrionales. L'agencement des chapitres suit la chronologie des évènements magmatiques affectant le massif vosgien.

Le premier chapitre est consacré aux généralités de la chaine varisque en Europe et à la présentation des terrains constituants le massif vosgien.

Le Chapitre 2, est constitué d'une publication publiée dans *International Journal of Earth Sciences* et concerne le magmatisme le plus ancien (gabbros et lherzolite) des Vosges moyennes et méridionales exposés dans la « ligne des Klippes » (Schneider, 1990).

Le Chapitre 3, est constitué d'une publication soumise à *Journal of Petrology* et traite d'un point de vue pétrologique, géochimique, isotopique et géochronologique de deux principaux évènements magmatiques (Granites des Crêtes et des Ballons et Granite fondamental) affectant les Vosges moyennes et méridionales. Ces données sont comparées avec les données existantes sur les autres massifs de la chaine varisque (Massif de Bohème, Forêt Noire, Alpes, Massif Corso-Sarde).

Le Chapitre 4, est constitué d'une publication qui sera soumise à *Tectonics* et concerne les données d'Anisotropie de la Susceptibilité Magnétique (ASM) sur les deux principaux évènements des Vosges moyennes et méridionales et permet de connaître les contraintes affectant la croûte continentale lors de la mise en place de ces phases magmatiques.

Le Chapitre 5, est constitué d'une publication qui sera soumise dans *International Journal of Earth Sciences ou* dans le Bulletin de la *Société Géologique de France (spécial publication* après le meeting Variscan 2012 à Sassari, Sardaigne*)*, traite des analyses pétrographiques, géochimiques, isotopiques et géochronologiques des différentes phases magmatiques (volcanisme du Massif de Schirmeck-Rabodeau, Massif du Champ du Feu, volcanisme du Nideck) affectant les Vosges septentrionales. Les données acquises sont complétées par les données déjà existantes pour cette partie des Vosges.

Enfin, le Chapitre 6 présente les conclusions de ce travail en proposant un modèle d'évolution de l'ensemble du Massif Vosgien de 360 Ma à 290 Ma.

Ce travail, supporté par le BRGM et la région Alsace, s'inscrit dans le cadre de l'opération de synthèse géodynamique des Vosges menée au sein du programme RGF (Référentiel Géologique de la France), qui vise à une actualisation de la connaissance thématique et régionale du territoire national. Une partie des données recueillies dans le cadre de ce travail permettra d'assurer la mise en relation des formations magmatiques de la carte de synthèse à 1/250 000 du massif vosgien. Ce travail complète les précédents travaux de E. Skrzypek (Thèse soutenue en 2011) sur la synthèse tectonique.

Chapitre 1 : l'orogène Varisque

L'extension de la chaine Varisque à travers le monde est immense. Elle s'étend d'Ouest en Est du Texas au Massif de Bohème en passant par les Appalaches et le Maroc.

1. L'Orogène Varisque en Europe

En Europe, la chaine Varisque s'étend sur près de 3000 km du Massif de Bohème jusqu'à la péninsule ibérique (Matte, 1986 ; 1991). Elle est formée de roches d'âge Protérozoique à Carbonifère moyen et constitue le socle anté-permien de toute l'Europe occidentale et centrale. Ces terrains affleurent au sein de différents massifs, tel que le Massif Ibérique, les Pyrénées, le Sud de l'Angleterre, le Massif Armoricain, le Massif Central, les Vosges-Forêt Noire, les Ardennes, la Corse, la Sardaigne, le Massif des Maures, dans les Massifs Cristallins externes des Alpes et le Massif de Bohème. Les structures tectoniques et les évènements métamorphiques et magmatiques observés sont les témoins de la collision entre trois continents (Fig.1) : La Laurussia au nord, la Baltica au centre et le Gondwana au Sud ainsi que des microcontinents comme le groupe Armorica et l'Avalonia (Autran et Cogné, 1980; Bard et al., 1980, Paris et Robardet, 1990, Van der Voo, 1993; Tait et al., 1997; Cocks, 2000; Franke, 2000; Robardet, 2003; Von Raumer et al., 2003). La collision finale intervient entre 380 et 350 Ma. Elle fait suite à la disparition de plusieurs domaines océaniques (Fig.2) qui permettent de diviser la chaine Varisque en Europe en trois domaines lithotectoniques majeurs, du Nord au Sud : le domaine Rhénohercynien, le domaine Saxothuringien et le domaine Moldanubien.

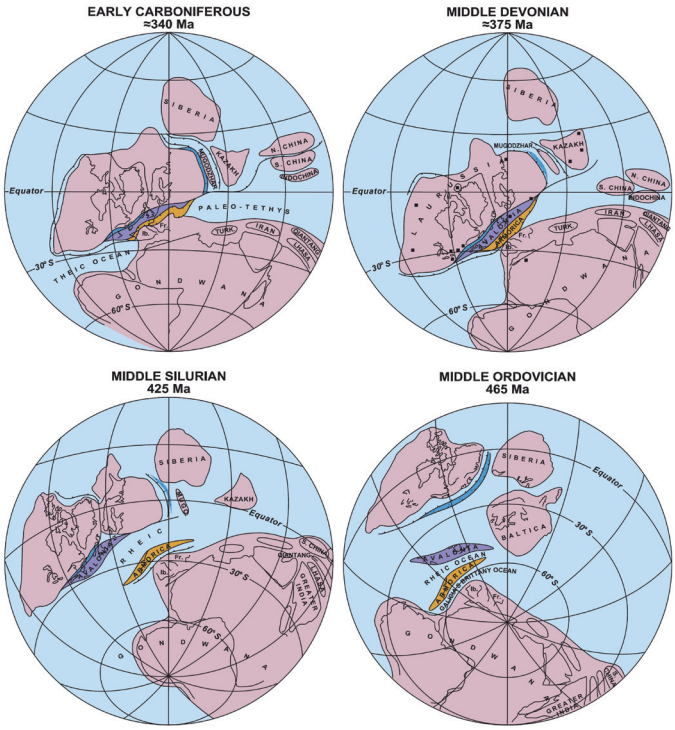

Figure 1 : Reconstitution paléozoïque depuis l'Ordovicien moyen (465 Ma) jusqu'à la fin du Carbonifère (340 Ma) d'après Matte (2001).

Le domaine Rhénohercynien (Fig.3) affleure au sein de plusieurs massifs comme le Massif Schisteux-Rhénan, les Ardennes, le Massif de Harz et en Cornouaille (sud-ouest de l'Angleterre) et représente le socle cadomien-avalonien. Ce socle est surmonté par des sédiments de dépôts de marge passive datés du début jusqu'au milieu du Dévonien suivi par le dépôt de flyschs datés fin Dévonien - début Carbonifère (Franke, 1995). La présence de basaltes de type-MORB dans le Massif Rhénan suggère la présence d'un océan Rhénohercynien au Sud qui s'ouvre au début du Dévonien et se ferme au Carbonifère (Fig.2). Son existence est aussi prouvée par la présence de séries ophiolitiques et sédiments d'âge Dévonien inférieur à Carbonifère en Cornouaille (Floyd, 1984 ; Holder et Leveridge, 1986 ; Leveridge et Hartley, 2006) et Moravie (Hladil et al, 1999 ; Hartley et Otava, 2001 ; Kalvoda et al., 2008). La fermeture de l'océan Rhénohercynien est enregistrée dans les grauwackes turbiditiques dérivant de la marge active située au SE dans le « Mid-German Crystalline High » (Franke, 2000) et forme des plis à vergence Nord au Nord du domaine Avalonia (Oncken et al., 1999 ; Shail et Leveridge, 2009).

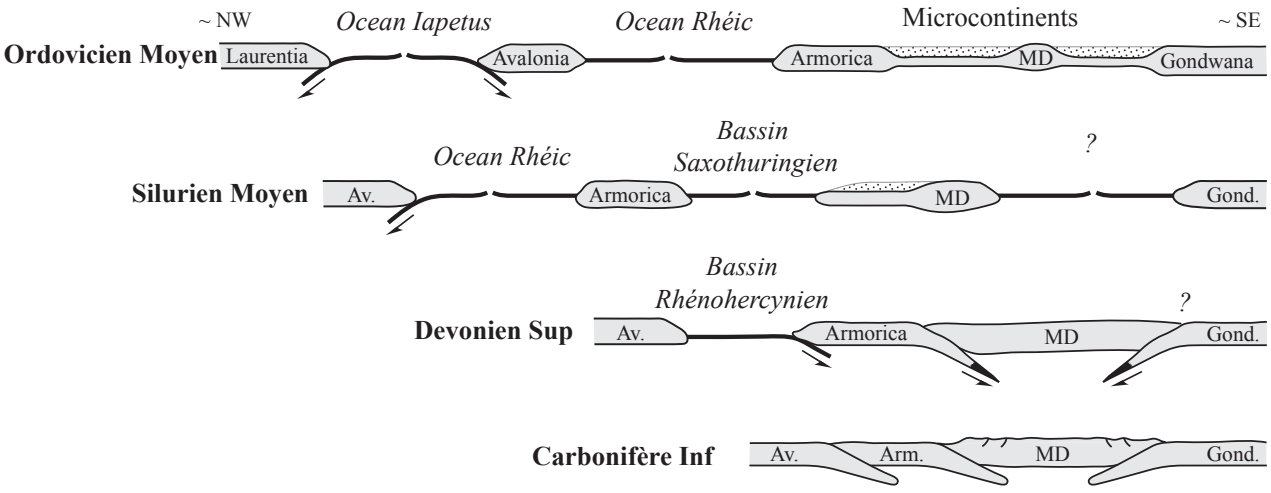

Figure 2 : Modèle d'évolution de la chaine varisque pendant le Paléozoïque d'après Tait et al. (2000) ; Winchester et al. (2002) ; Cocks & Torsvik (2002).

Ce domaine est séparé du domaine Saxothuringien au Sud par la zone « Mid-German Crystalline High » (Fig.3) formée d'un socle d'âge Paléozoïque inférieur, d'un magmatisme d'arc Carbonifère et de sédiments d'affinité rhénohercynienne. Cette unité est interprétée comme résultant d'un système d'accrétion frontal et basal des différentes unités (Oncken, 1997).

La zone Saxothuringienne (Fig.3) est constituée d'un socle d'âge Cadomien (Protérozoïque à Cambrien inférieur). Ce socle est surmonté par des séries sédimentaires d'âge Paléozoïque (Franke, 1984 ; 1989). Cette zone est reconnue surtout dans la partie Centrale et Est de l'Europe. Les roches magmatiques ainsi que les ophiolites affleurant au Nord du Massif de Bohême montrent la présence d'un épisode de rifting au Cadomien et l'ouverture de l'océan Saxothuringien (Fig.2) durant le Cambro-Ordovicien (Bowes & Aftalion, 1991 ; Kemnitz et al., 2002). Du Dévonien au Carbonifère, la subduction océanique devient continentale au sud-est du domaine Saxothuringien et entraine une déformation intense du socle avec son exhumation dans de larges anticlinaux ainsi que le plissement de la couverture sédimentaire (Franke, 1984 ; Schäfer et al., 2000).

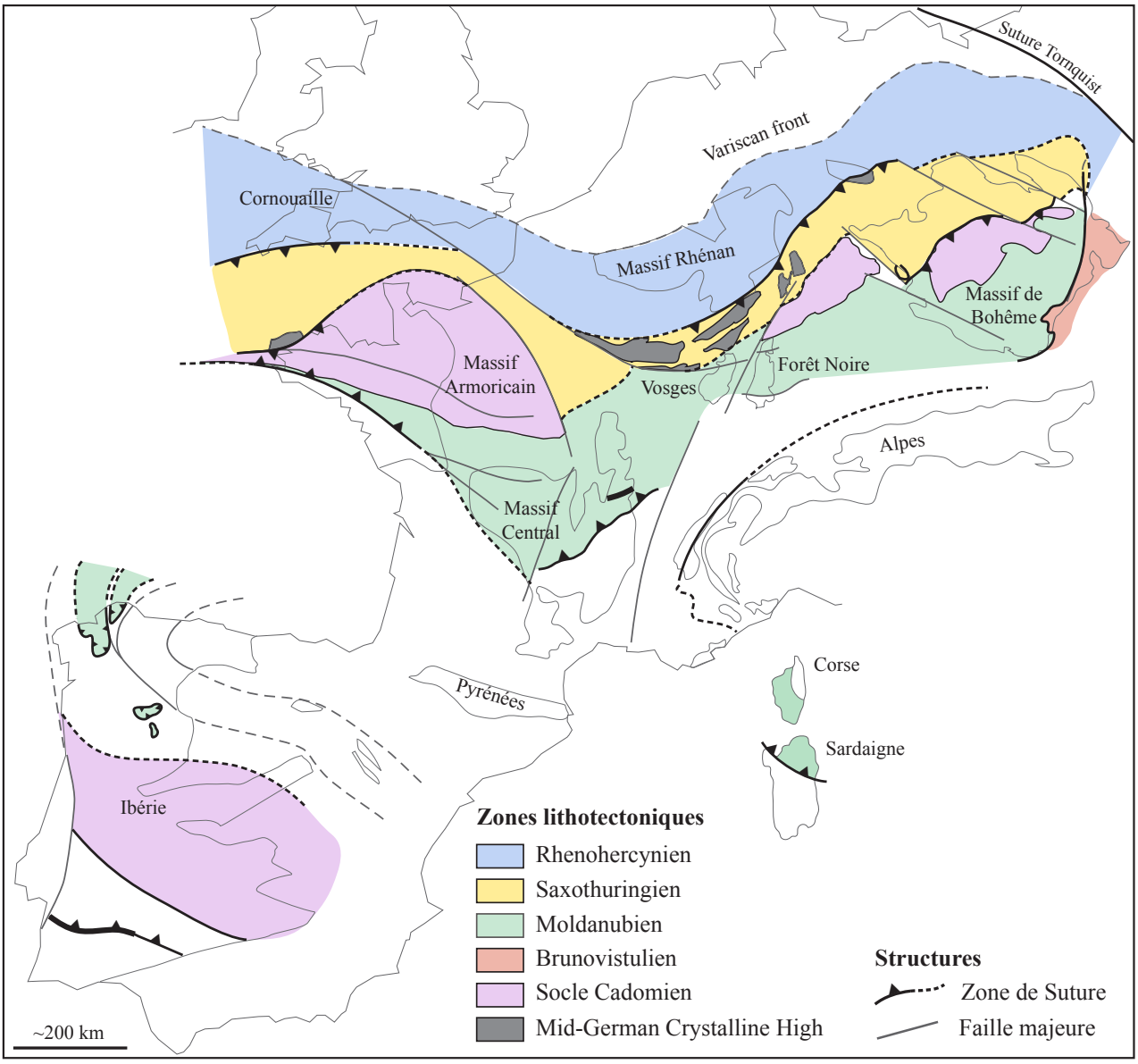

Figure 3 : Carte des unités lithotectoniques de la chaine varisque en Europe modifié d'après Edel & Schulmann (2009); Ballèvre et al. (2009) ; Pitra et al. (2010).

Ce domaine présente au Sud des chevauchements majeurs de la zone Moldanubienne sur la zone Saxothuringienne de direction NW à W.

La zone Moldanubienne (Fig.3) est considérée comme étant la racine métamorphique de l'orogène Varisque (Schulmann et al., 2009). Cette zone peut être suivie d'Est en Ouest en Europe. Elle est bordée par des blocs discontinus d'âge Cadomien qui correspondent, au Nord, à des reliques des microcontinents et, au Sud, au Gondwana (Linnemann et al., 2004). Le Nord de ce domaine chevauche la zone saxothuringienne par des décrochements majeurs de direction NW à W alors que la marge Sud de ce domaine montre plutôt des structures de vergence Sud où les unités de haut métamorphisme surmontent les unités de plus bas métamorphisme d'âge Paléozoïque inférieur à Neoprotérozoïque (Schulmann et al., 2005). Ces structures de vergence Sud sont observées dans le Massif Armoricain, le Massif Central, les Vosges, la Forêt Noire et le Massif de Bohême (Burg & Matte, 1978; Maass et al., 1990; Schulmann et al., 2008; Ballèvre et al., 2009). Ceci montre l'existence d'un domaine océanique entre la zone Moldanubienne et la marge Nord du Gondwana (Fig.2 ; Finger & Steyrer, 1990; Finger et al., 1997; Loeschke et al, 1998; Lardeaux et al., 2001; von Raumer et al., 2003; Guillot & Ménot, 2009; Rossi & Oggiano, 2009).

Figure 4 : Carte des synthétique du Massif des Vosges d'après Fluck et al., 1991. Figure ci-contre

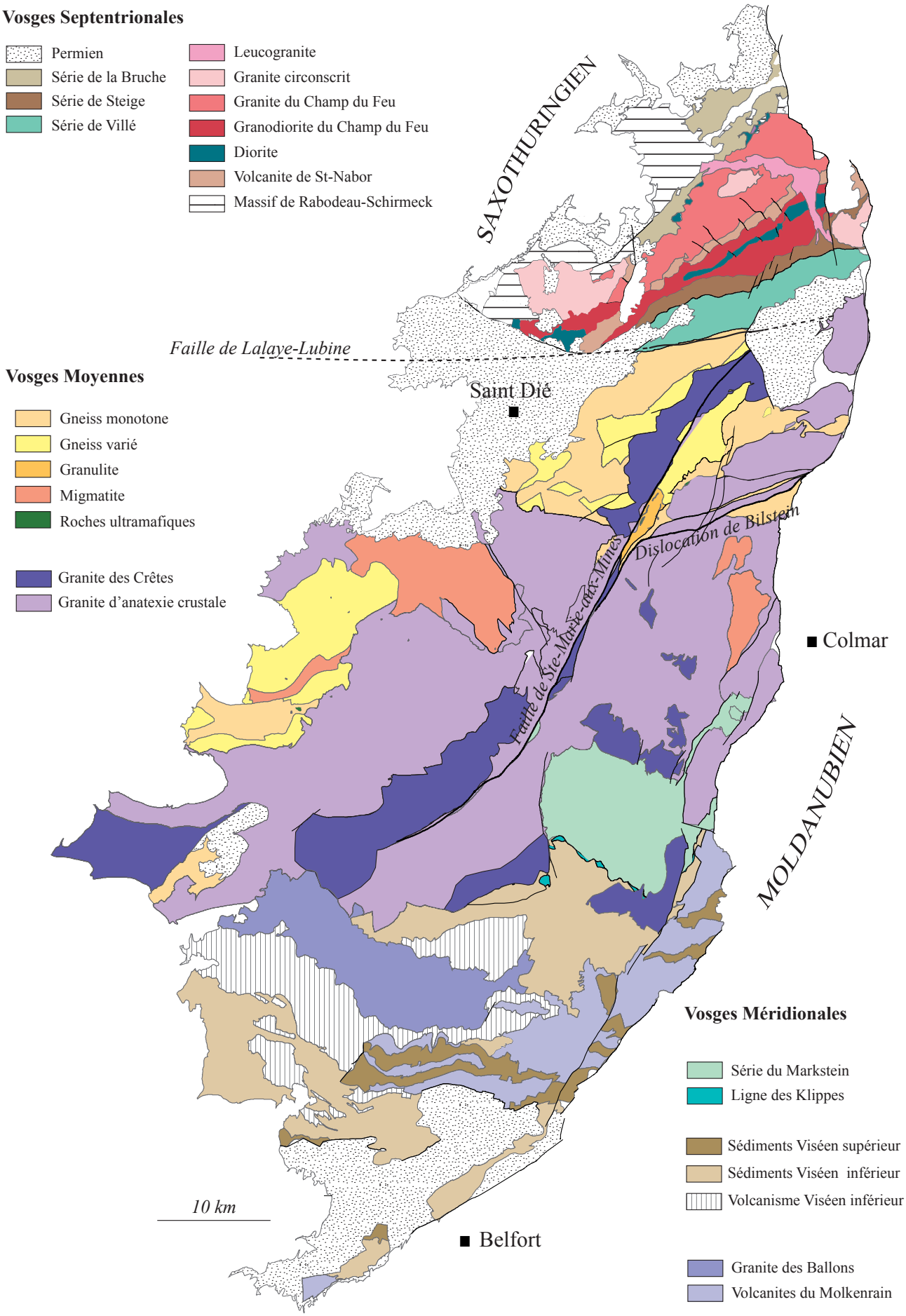
Vosges Septentrionales
Permien
Série de la Bruche
Série de Steige
Série de Villé
Leucogranite
Granite circonscrit
Granite du Champ du Feu
Granodiorite du Champ du Feu
Diorite
Volcanite de St-Nabor
Massif de Rabodeau-Schirmeck
SAXOTHURINGIEN
Faille de Lalaye-Lubine
Vosges Moyennes
Gneiss monotone
Gneiss varié
Granulite
Migmatite
Roches ultramafiques
Granite des Crêtes
Granite d'anatexie crustale
Saint Dié
Dislocation de Bilstein
Faille de Ste-Marie-aux-Mines
Colmar
MOLDANUBIEN
Vosges Méridionales
Série du Markstein
Ligne des Klippes
Sédiments Viséen supérieur
Sédiments Viséen inférieur
Volcanisme Viséen inférieur
Granite des Ballons
Volcanites du Molkenrain
10 km
Belfort

2. Description et Evolution de la chaine Varisque dans les Vosges

Le Massif des Vosges (~3650 km²) est divisé en deux parties par la discontinuité de Lalaye-Lubine (Fig.4). La partie Nord des Vosges fait partie du domaine Saxothuringien et les Vosges moyennes et méridionales font partie du domaine Moldanubien (Kossmat, 1927).

2.1. Les séries sédimentaires et métamorphiques des Vosges septentrionales

Les séries sédimentaires et métamorphiques des Vosges septentrionales (Fig.5) forment trois unités distinctes, du Nord au Sud : Série de la Bruche, Série de Steige et Série de Villé. La série de la Bruche (Fig.5) commence par des coulées de laves basaltiques, de roches acides et de sédiments grossiers d'âge probablement Dévonien (Juteau, 1971). Cette séquence est surmontée par des conglomérats et grès du Dévonien moyen (Benecke et Bucking, 1898) suivis d'une alternance de grauwackes et pélites associées à un volcanisme bimodal Givétien (Firtion, 1945 ; 1957). Ce volcanisme est constitué de basalte submarin, de spilite-kératophyre et de brèche pyroclastique (Ikenne et Baroz, 1985 ; Rizki et Baroz, 1988). L'âge Givétien est reconnu aussi dans des lentilles de carbonates de dépôts récifaux influencés par des continents proches. Le Dévonien moyen est donc associé à une érosion du socle Cambrien, à une sédimentation conglomératique et à un développement de calcaires récifaux dans un bassin siliciclastique peu profond localisé à l'Est. Cette série sédimentaire passe graduellement vers un épais dépôt de pélites au Frasnien et Famenien (Dévonien supérieur) associées à des radiolarites et des débris de plantes (Figge, 1968 ; Blanalt et Lilié, 1973 ; Braun et al, 1992 ; Aghai Soltani et al., 1996). Les dépôts du Dévonien supérieur présentent des clastes de grauwackes et pélites du Viséen inférieur (Corsin et Dubois, 1932 ; Dubois, 1946 ; Corsin et al., 1960). L'activité tectonique culmine durant le Viséen moyen (lacune de sédimentation, contact métamorphique et activité magmatique au Sud ; Bonhomme et Prévot, 1968).

Les séries de Steige et de Villé (Fig.5) montrent des structures orientées NE-SW. La série de Villé présente les plus vieux dépôts des Vosges et est formée par des pélites Cambriennes et Ordoviciennes suivies par des dépôts de pélites quartziques avec des intercalations de quartzites et de tuffs acides. La série est métamorphisée dans le faciès des schistes verts (Doubinger et von Eller, 1963a ; Ross, 1964 ; Reitz et Wickert, 1989). La série de Villé est surmontée par la série de Steige de plus faible métamorphisme qui est composée de pélites d'âge Ordovicien à Silurien (Doubinger et von Eller, 1963b ; Ross, 1964). Tobschall (1974) suggère que ces séries se sont déposées dans un bassin marin peu profond de type environnement de plateforme.

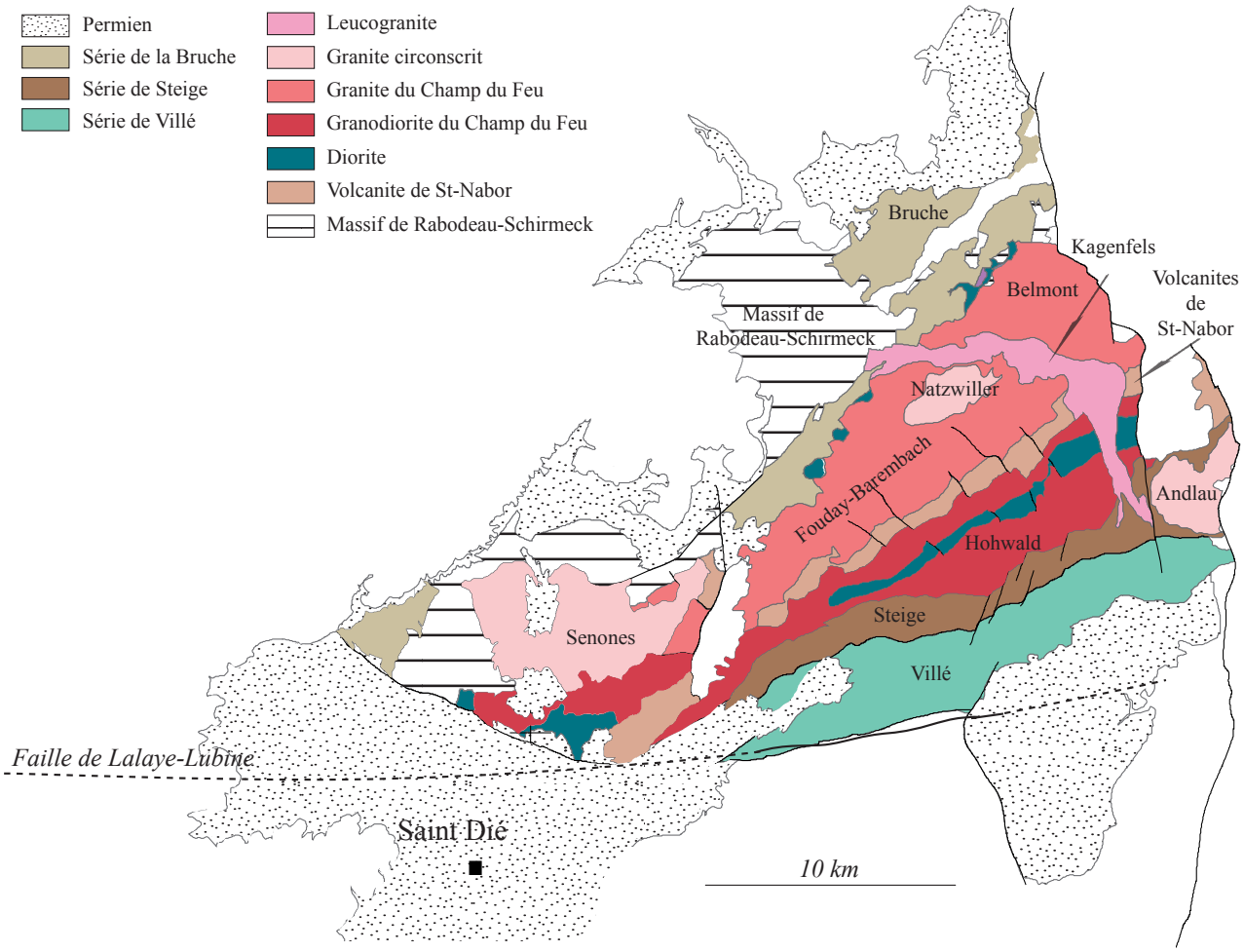

Figure 5 : Carte géologique simplifiée des Vosges Septentrionales

2.2. Les séries métamorphiques et (volcano-)sédimentaires des Vosges moyennes et méridionales

Les Vosges moyennes (Fig.6) sont composées de séquences de haut degré métamorphique (granulite, amphibolite, gneiss, migmatite) qui ont fait partie d'une étude menée par Skrzypek (2011). Ces séquences sont recoupées par plusieurs plutons de compositions granitiques.

Ces séries métamorphiques peuvent être divisées en deux unités : les granulites felsiques d'origine ignée et les séries gneissiques (monotones et variées) de protolithe sédimentaire (Fig.6). Skrzypek (2011) par datation U-Pb sur zircons montre que l'âge du protolithe igné des granulites est d'environ 500Ma. L'étude de la provenance des zircons montre que cet évènement magmatique est suivi par le dépôt du protolithe des séries gneissiques pendant l'Ordovicien (début Ordovicien pour la série des gneiss monotones et fin Ordovicien pour la série des gneiss variés). Le dépôt se fait directement sur le socle granitique Cambrien.

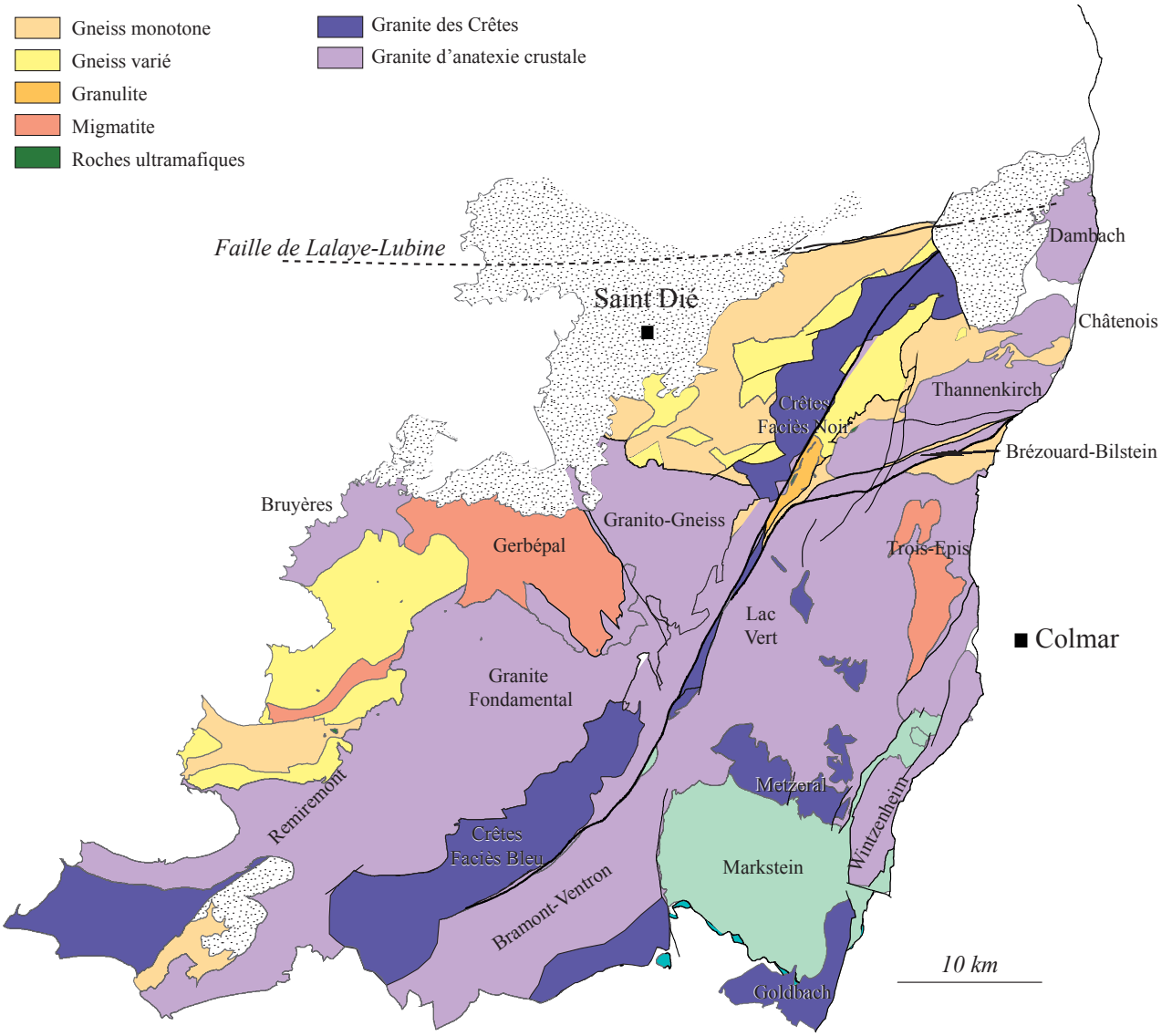

Figure 6 : Carte géologique simplifiée des Vosges Moyennes

Les Vosges méridionales (Fig.7) sont composées surtout de bassins (volcano-)sédimentaires divisés en unité allochtone et autochtone (Jung, 1928). La limite entre ces deux séries est proche de la ligne des Klippes (Fig.7) décrites par Schneider et al. (1990) et qui est constituée de matériel ophiolitique. L'unité allochtone est représentée par la série du Markstein (Fig.7) et la ligne des klippes qui forme la base de l'unité (Jung, 1928 ; Schneider et al., 1990). Les klippes sont surmontées par des pélites siliceuses Fameniennes (Maass et Stoppel, 1982) suivies par une alternance de pélites et grauwackes du Viséen inférieur formant la série du Markstein avec quelques conglomérats et carbonates (Corsin et Mattauer, 1957 ; Corsin et Ruhland, 1959). La sédimentation se termine au Viséen supérieur (Krecher, 2005). L'unité allochtone montre la présence d'un bassin profond d'âge Dévonien supérieur rempli par des flyschs turbiditiques au Viséen inférieur qui indique un système progradant de fans marins (Krecher et al., 2007).

L'unité autochtone composée des séries de Thann et Oderen (Fig.7) est formée de trois lithologies principales, de la base vers le sommet : calcaire Frasnien et de pélite Famenienne qui préserve une faune de plateforme du Dévonien supérieur et sont associés à des grauwackes turbiditiques (Maass & Stoppel, 1982). Cette série sédimentaire est associée à un volcanisme bimodal composé de rhyolites et basaltes (Schaltegger et al., 1996), interprété comme étant soit des tholéiites d'arc (Lefèvre et al. 1994) soit des tholéiites continentales (Bébien & Gagny, 1978). Cette série est surmontée, en discordance, par des shales et grauwackes turbiditiques marines mises en place au cours du Viséen (Corsin et al., 1956, Corsin et Mattauer, 1957 ; Mattauer et Théobald, 1957 ; Mattauer, 1959 ; Coulon et al., 1975 ; Doubinger & Rauscher, 1966 ; Hahn et al, 1981 ; Vogt, 1981 ; Maass, 1988). Ces sédiments sont recoupés par des laves volcaniques syn-sédimentaires (andésites à rhyolites). La présence d'olistostromes (Schneider et al., 1990), de structures de glissement intercalées par des conglomérats et brèches montrent que cette série s'est mise en place dans un environnement de dépôt de pente sous-marine (Krecher, 1997). Le sommet de la série est composée de séquences terrigènes datées du Namurien au Westpalien (Carbonifère supérieur, Doubinger & Rauscher, 1966 ; Traiser et al., 1998). La base de cette succession est formée par une séquence de grauwackes et pélites (Schneider, 1990), intercalée par des roches pyroclastiques d'origine ignimbritique (rhyolite dacitique à rhyolite). Ces dépôts sont suivis par des dépôts sédimentaires continus de type terrestre (canaux fluviatiles, barres de sable fluviales et sédiments de plaine d'inondation, Maass & Schneider, 1995) et des dépôts lacustres.

Les roches volcaniques dans la série inférieure sont de type mafique et présentent des anomalies positives en Cr et Ni. Les roches volcaniques des deux autres lithologies sont de type intermédiaire à felsique et montrent un enrichissement en éléments incompatibles comme le Th, Ba et Zr ainsi qu'une anomalie négative en Nb ce qui révèle la dominance d'une source d'arc (Eisele et al., 2000).

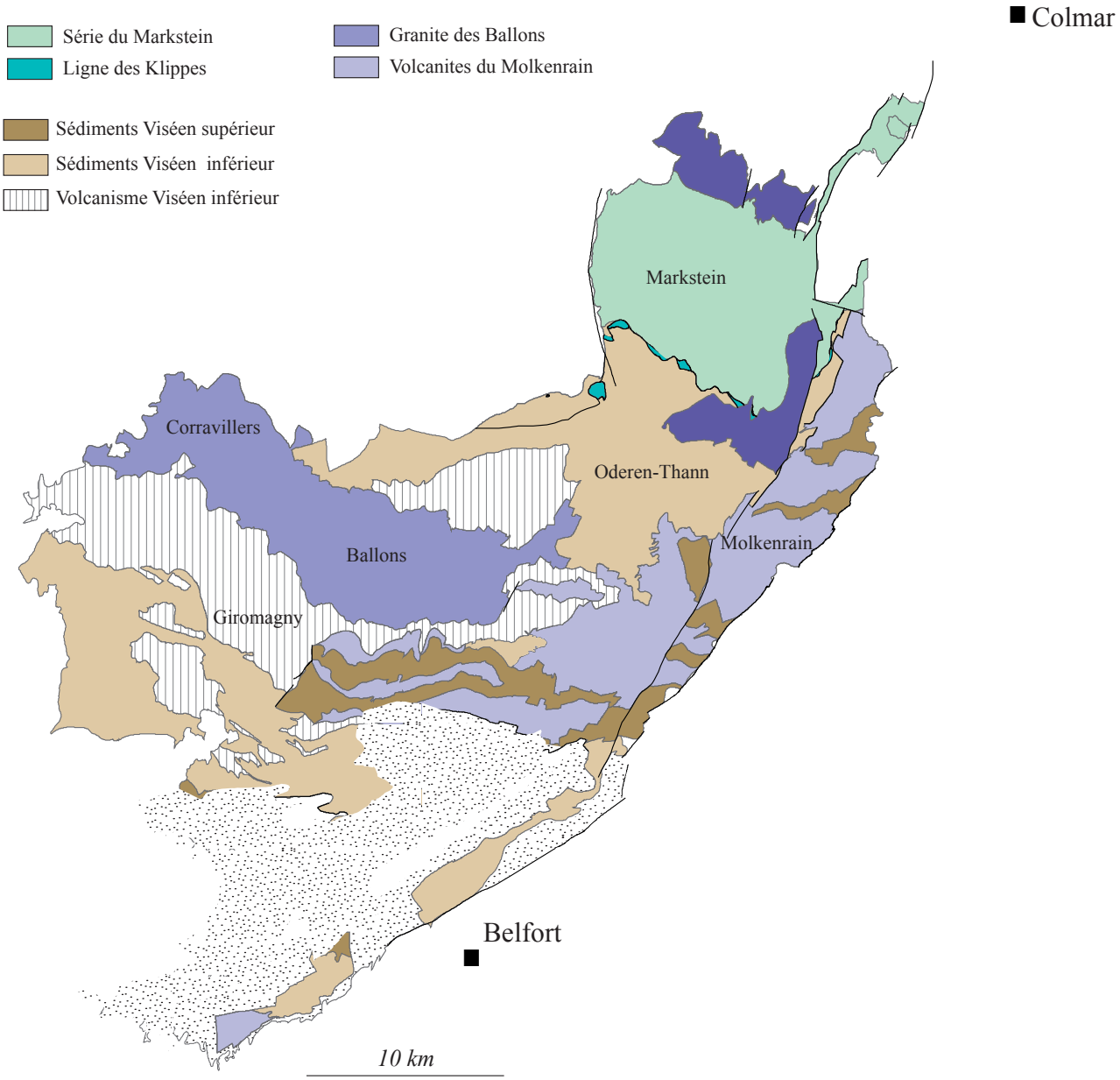

Figure 7 : Carte géologique simplifiée des Vosges Méridionales

3. Le magmatisme des Vosges

Les roches magmatiques (granites et volcanites) ont une grande importance dans les Vosges car elles recouvrent une grande surface à l'affleurement, surtout dans la partie moldanubienne des Vosges.

3.1. Les Vosges septentrionales

Le premier évènement magmatique des Vosges septentrionales est daté au Dévonien-Dinantien et se retrouve dans deux massifs principaux : le massif de Schirmeck et le massif de Rabodeau (Fig.5). Le massif de Rabodeau présente des roches hypovolcaniques (dolérite, microdiorite, rhyolite) mises en place surtout en masses et peu en filons. Ces roches sont recoupées par des plutons granitiques et dioritiques et montrent un métamorphisme de contact de type cornéenne. Le massif de Schirmeck montre le plus vaste ensemble volcanique des Vosges septentrionales. Il est formé d'une série volcanique très diversifiée et constituée de laves basiques à acides et de roches pyroclastiques dont l'évolution régulière et continue des éléments majeurs et traces montre leur cogénétisme (Elsass et al., 2008). Les roches du massif de Schirmeck évoluent suivant l'ordre de cristallisation des roches tholéiitiques avec la cristallisation précoce du plagioclase et un enrichissement en Ti équivalent à celui des arcs insulaires évolués (Rizki, 1992). Quant au massif du Rabodeau, il présente deux lignée magmatiques : une lignée tholéiitique d'arc et une lignée calco-alcaline (Ikenne & Baroz, 1985).

Cet évènement est suivi par la mise en place en bandes orientées ENE-WSW du magmatisme du Champ du Feu (Fig.5). La géochimie (éléments majeurs, traces et quelques isotopes) du Champ du Feu donne trois ensembles magmatiques (Elsass et al., 2008 ; Fluck et al., 1991) : un ensemble calco-alcalin à calco-alcalin potassique montré par les volcanites de Saint Nabor (Fig.5) datées par la méthode U-Pb sur zircon à 334 ± 5 Ma (Cocherie, 2007), les granodiorites du Hohwald (Fig.5) datées à 329 ± 2 Ma (datation sur zircon, Cocherie, 2007) et les granites Belmont-Fouday-Barembach (Fig.5) datés par la méthode U-Pb sur zircon à 319 ± 3 Ma (Cocherie, 2007). Le second ensemble est calco-alcalin magnésio-potassique ou shoshonitique. Il est représenté par le monzogranite de Senones, le granite de Natzwiller et le granite d'Andlau (Fig.5) et est daté à environ 314 Ma (Cocherie, communication personnelle). Les magmas à l'origine de ces granites seraient initialement shoshonitiques (Altherr et al, 2000). Le troisième ensemble est péralumineux et est représenté par les leucogranites à deux micas de Kreuzweg, Kagenfelds et Grendelbruch (Fig.5).

L'ensemble des roches magmatiques des Vosges septentrionales montre un caractère typique de zone de convergence des plaques (Rizki, 1992).

3.2. Vosges moyennes et méridionales

Le premier évènement magmatique des Vosges moldanubienne met en place les granites des Crêtes dans les Vosges moyennes (Fig.6) et le granite des Ballons dans les Vosges méridionales (Fig.7) lors d'une phase de plissement régional (Petrini & Burg, 1998).

Le granite des Crêtes, daté à 340 ± 1 Ma (U-Pb sur zircon ; Schaltegger et al., 1996), affleure en différents pointements de tailles variables. Il présente deux faciès, un faciès bleu et un faciès noir, (Gagny, 1968) et est composé de biotite et d'actinote et phénocristaux de feldspaths potassiques. Ce granite est associé à un cortège filonien de microsyénite (durbachite, Sauer, 1893) à pyroxène, actinote et phénocristaux de feldspaths, (von Eller, 1961 ; Gagny, 1968). L'étude des éléments majeurs montre que ces différentes intrusions granitiques font partie des séries shoshonitiques et qu'elles proviennent d'un mélange de magma acide et basique. Le magma basique a une origine mantellique à tendance alcaline de type gabbro ou syéno-gabbro et le magma acide provient de l'anatexie en profondeur de roches profondes. Une différenciation par gravité dans la chambre magmatique va donner naissance aux durbachites et au faciès noir du granite des Crêtes (Gagny, 1968).

Le granite des Ballons et ses plutonites basiques en bordure sont datés à 340 ± 4 Ma et 342 ± 1 Ma respectivement (U-Pb sur zircon ; Schaltegger et al., 1996). Cet ensemble s'est mis en place en deux périodes successives d'intrusions. La première met en place les plutonites basiques et la seconde le pluton monzogranitique. L'analyse des éléments majeurs suggère que les plutonites font partie soit d'une lignée shoshonitique (Pagel, 1981), soit d'une lignée tholéiitique (Bébien & Gagny, 1978 ; Schneider, 1990). L'étude des éléments majeurs du monzogranite des Ballons suggère que ce granite peut avoir la même source mantellique que le granite des Crêtes, leur différence provient dans l'hybridation précoce en profondeur du granite des Crêtes et dans la différenciation magmatique tardive en surface du granite des Ballons (Gagny, 1968 ; Fluck et al., 1991)

Cet évènement magmatique est suivi par la mise en place conjointe du granite fondamental (Hameurt, 1967), des granites dits alumineux (Châtenois, Thannenkirch, Vic, Barbey-Seroux et Tholy) et des granites à biotites et deux micas (Bramont, Ventron, Thiéfosse, Lac Vert, Bilstein, Brézouard, Remiremont…) dans les Vosges moyennes (Fig.6). La partie Est de cet ensemble est daté entre 330 Ma et 325 Ma (Schaltegger et al, 1999 ; Kratinová et al., 2007). Certains de ces granites montrent des affinités pétrologiques avec le granite des Crêtes (Hameurt, 1967). Ces granites sont décrits comme étant des granites d'anatexie crustale ou granites de type-S riche en potassium (Hameurt, 1967 ; Kratinová et al., 2007). Ils se mettent en place dans un niveau crustal élevé lors d'une phase de bombement (Hameurt, 1967).

REFERENCES CITED

Aghai Soltani, L., Bender, P., Braun, A. & Schmidt-Effing, R. (1996). Oberdevonische Radiolarien aus Kieselgesteinen des Breuschtales (Vallé de la Bruche, Nord-Vogesen, Frankreich). *Jahresbericht und Mitteilungen des oberrheinischen geologischen Vereins*, **78**, 183-208.

Altherr, R., Holl, A., Hegner, E., Langer, C. & Kreuzer, H. (2000). High-potassium, calc-alkaline I-type plutonism in the European Variscides: northern Vosges (France) and northern Schwarzwald (Germany). *Lithos*, **50**, 51-73.

Autran, A. et Cogné, J. (1980). La zone interne de l'orogenèse varisque dans l'Ouest de la France et sa place dans le développement de la chaîne hercynienne. In : *Géologie de l'Europe. 26° C.G.I. Paris. Mémoire BRGM, Orléans,* **108**, 90 –111.

Ballèvre, M., Bosse, V., Ducassou, C. & Pitra, P., 2009. Palaeozoic history of the Armorican Massif: Models for the tectonic evolution of the suture zones. *Comptes Rendus Géoscience*, **341**, 174-201.

Bard J.P., Burg J.P., Matte P. & Ribeiro A. (1980). La chaîne hercynienne d'Europe occidentale en termes de tectonique des plaques. In : *Géologie de l'Europe. 26e C.G.I. Paris. Mémoire BRGM*, *Orléans*, **108**, 233 – 246.

Bébien, J. & Gagny, C. (1978). Le plutonisme viséen des Vosges méridionales : un nouvel exemple de combinaison magmatique entre roches tholéiitiques et calco-alcalines. *Comptes Rendus de l'Académie des Sciences*, **286**, 1045-1047.

Benecke, E. W. & Bücking, H. (1898). Calceola sandalina im oberen Breuschtal. *Mittheilungen der geologischen Landesanstalt von Elsass - Lothringen*, **4**, 105-111.

Blanalt, J. G. & Lillié, F. (1973). Données nouvelles sur la stratigraphie des terrains sédimentaires dévono-dinantiens de la vallée de la Bruche (Vosges septentrionales). *Sciences Géologiques*, **26**, 69-74.

Bonhomme, M. & Prévôt, L. (1968). Application de la méthode Rubidium-Strontium à l'étude de l'âge radiométrique de quelques dépôts dévono-dinantiens du massif de la Bruche (Vosges du Nord). *Bulletin du Service de la Carte Géologique d'Alsace-Lorraine*, **21**, 219-248.

Bowes, D. R. & Aftalion, M. (1991). U-Pb isotopic evidence for early Ordovician and Late Proterozoic units in the Mariánské Lázně Complex, Central European Hercynides. *Neues Jahrbuch für Mineralogie Abhandlungen*, **7**, 315-326.

Braun, A., Maass, R. & Schmidt-Effing, R. (1992). Oberdevonische Radiolarien aus dem Breuschtal (Nord-Vogesen, Elsaß) und ihr regionaler und stratigraphischer Zusammenhang. *Neues Jahrbuch für Geologie und Paläontologie. Abhandlungen*, **185**, 161-178.

Burg, J.-P. & Matte, P. (1978). A cross-section through the French Massif Central and the scope of its Variscan geodynamic evolution. *Zeitschrift der Deutschen Geologischen Gesellschaft*, **109**, 429-460.

Cocherie A. (2007). Datations U-Pb (laser-ICPMS-MC) sur zircons des Vosges (projet carte 50 000). *Note N° MMA/ISO-2007/262*, 15 p.

Cocks, L. R. M. & Torsvik, T. H. (2002). Earth geography from 500 to 400 million years ago: a faunal and palaeomagnetic review. *Journal of the Geological Society, London*, **159**, 631-644.

Cocks, L. R. M. (2000). The Early Palaeozoic geography of Europe. *Journal of the Geological Society of London*, **157**, 1-10.

Corsin, P., Danze-Corsin, Millot, G. & Ruhland, M. (1960). Sur l'âge viséen inférieur des schistes de Schwarzbach (vallée de la Bruche) dans les Vosges du Nord. *Bulletin du Service de la Carte Géologique d'Alsace-Lorraine*, **13**, 163-164.

Corsin, P. & Ruhland, M. (1959). Les gisements à plantes du Viséen dans les Vosges méridionales. *Comptes Rendus de l'Académie des Sciences*, **248**, 2145-2149.

Corsin, P. & Mattauer, M. (1957). Quelques nouveaux gisements fossilifères du Massif des Ballons (Vosges méridionales). *Comptes rendus sommaires de la Société Géologique de France*, **5**, 92-94.

Corsin, P., Gagny, C. & Mattauer, M. (1956). Découverte d'une florure d'âge viséen dans les schistes et grauwackes des environs de Fellering (Haut-Rhin). *Comptes Rendus de l'Académie des Sciences*, **242**, 1908-1909.

Corsin, P. & Dubois, G. (1932). Description de la flore dinantienne de Champenay. *Bulletin du Service de la Carte Géologique d'Alsace-Lorraine*, **2**, 1-33.

Coulon, M., Fourquin, C., Paicheler, J. C. & Point, R. (1975). Contribution à la connaissance du tectorogène varisque dans les Vosges méridionales. II-Le Culm de la région comprise entre Giromagny et Bourbach-le-Bas. *Bulletin de la Société Géologique de France,* **28,** 109-139.

Doubinger, J. & Rauscher, R. (1966). Spores du Viséen marin de Bourbach-le-Haut dans les Vosges du Sud. *Pollen et Spores*, **8**, 361-405.

Doubinger, J. & von Eller, J. P. (1963a). Découverte de Chitinozoaires d'âge silurien dans les schistes de Steige (vallée de l'Andlau, Vosges). *Comptes Rendus de l'Académie des Sciences*, **256**, 469-471.

Doubinger, J. & von Eller, J. P. (1963b). Présence de Spongiaires dans les schistes précambriens métamorphiques des Vosges. *Bulletin du Service de la Carte Géologique d'Alsace-Lorraine*, **16**, 111-123.

Dubois, G. (1946). Répartition des gisements certainement et vraisemblablement dinantiens dans la région de la Bruche (Vosges moyennes). *Comptes rendus sommaires de la Société Géologique de France*, **12**, 222-223.

Edel, J. B. & Schulman, K. (2009). Geophysical constraints and model of the ''Saxothuringian and Rhenohercynian subductions–magmatic arc system'' in NE France and SW Germany. *Bulletin de la Société Géologique de France* **180,** 545–558.

Eisele, J., Gertisser, R. & Montenari, M. (2000). Geochemistry and provenance of Devono-Carboniferous volcanosedimentary sequences from the southern Vosges basin and the geodynamic implications for the western Moldanubian Zone. In: Franke, W., Haak, V. Oncken,O. & Tanner, D. (eds.) *Orogenic Processes: Quantification and Modelling in the Variscan Belt, Geological Society of London, special publication*, **179**, 35-61.

Elsass, P., von Eller, J. P. & Stussi, J. M. (2008). Géologie du massif du Champ du Feu et de ses abords. Eléments de notice pour la feuille géologique 307 Sélestat. *Rapport BRGM/RP-56088-FR*, 184 p.

Figge, K. (1968). Ober-Devon im Breuschtal der Vogesen. *Neues Jahrbuch für Geologie und Paläontologie. Monatshefte*, **4**, 195-199.

Finger, F., Roberts, M. P., Haunschmid, B., Schermaier, A. & Steyrer, H. P. (1997). Variscan granitoids of central Europe: their typology, potential sources and tectonothermal relations. *Mineralogy and Petrology*, **61**, 67-96.

Finger, F. & Steyrer, H. P. (1990). I-type granitoids as indicators of a late Paleozoic convergent ocean-continent margin along the southern flank of the central European Variscan orogen. *Geology*, **18**, 1207-1210.

Firtion, F. (1957). Les éléments paléontologiques dévoniens du Val de Bruche. *Annales Universitatis Saraviensis, Scientia*, **5-6**, 97-184.

Firtion, F. (1945). Apports à la connaissance paléontologique du Dévono-Dinantien de la région de Schirmeck. *Comptes rendus sommaires de la Société Géologique de France*, **4**, 39-41.

Floyd, P. A. (1984). Geochemical characteristics and comparison of the basic rocks of the Lizard Complex and the basaltic lavas within the Hercynian troughs of SW England. *Journal of the Geological Society of London*, **141**, 61-70.

Fluck, P., Piqué, A., Schneider, J. L. & Whitechurch, H. (1991). Le socle vosgien. *Sciences Géologiques Bulletin*, **44**, 207-235.

Franke, W. (2000). The mid-European segment of the Variscides: tectonostratigraphic units, terrane boundaries and kinematic evolution. In: Franke, W., Haak, V., Oncken, O. & Tanner, D. (eds.) *Orogenic Processes: Quantification and Modelling in the Variscan Belt, Geological Society Special Publication, London,* **179**, 35-63.

Franke, W. (1995). Rhenohercynian Foldbelt: Autochton and Nonmetamorphic Nappe Units - Stratigraphy. In: Dallmeyer, D., Franke, W. & Weber, K. (eds) *Pre-Permian Geology of Central and Western Europe*, 33-49.

Franke, W. (1989). Tectonostratigraphic units in the Variscan belt of central Europe. *Geological Society of America, Special Paper*, **230**, 67 –90.

Franke, W. (1984). Variszischer Deckenbau im Raume der Münchberger Gneismasse, abgeleitet aus der Fazies, Deformation und Metamorphose im umgebenden Paläozoikum. *Geotektonische Forschungen*, **68**, 1-253.

Gagny, C. (1968). Pétrogenèse du granite des Crêtes, Vosges méridionales, France. Thèse de doctorat, Université de Nantes, p.515.

Guillot, S. & Ménot, R. P. (2009). Paleozoic evolution of the External Crystalline Massifs of the Western Alps. *Comptes Rendus Géoscience*, **341**, 253-265.

Hahn, G., Hahn, R. & Maass, R. (1981). Trilobiten aus dem Unterkarbon der S-Vogesen. O*berrheinische geologische Abhandlungen*, **30**, 1-26.

Hameurt, J. (1967). Les terraines cristallins et cristallophylliens du versant occidental des Vosges moyennes. *Mémoires du Service de la Carte géologique d'Alsace-Lorraine*, **26**, 402 p.

Hartley, A. J. & Otava, J. (2001). Sediment provenance and dispersal in a deep marine foreland basin: the Lower Carboniferous Culm Basin, Czech Republic. *Journal of the Geological Society of London*, **158**, 137-150.

Hladil, J., Melichar, R., Otava, J., Galle, A., Krs, M., Man, O., Pruner, P., Cejchan, P. & Orel, P. (1999). The Devonian in the Easternmost Variscides, Moravia: a Holistic Analysis Directed Towards Comprehension of the Original Context. *Abhandlungen der geologischen Bundesanstalt*, **54**, 27-47.

Holder, M. T. & Leveridge, B. E. (1986). A model for the tectonic evolution of South Cornwall. *Journal of the Geological Society of London*, **143**, 125-134.

Ikenne, M. & Baroz, F. (1985). Mise en évidence des caractères orogénique, tholéïtique et calco-alcalin du volcanisme dévono-dinantien dans le massif du Rabodeau (Vosges septentrionales) : apport à la reconstitution géotectonique des Vosges. *Comptes Rendus de l'Académie des Sciences*, **301**, 529-532.

Jung, J. (1928). Contribution à la géologie des Vosges hercyniennes d'Alsace. *Mémoires du Service de la Carte géologique d'Alsace-Lorraine*, **2**, 463 p.

Juteau, T. (1971). Nouvelles données cartographiques, pétrographiques et chimiques sur le massif dévono-dinantien du Rabodeau (Vosges septentrionales). Pétrogénèse d'une série spilite-kératophyre « hercynotype » complexe. *Sciences de la Terre*, **16**(1), 45-106.

Kalvoda, J., Bábek, O., Fatka, O., Leichmann, J., Melichar, R., Nehiba, S. & Spacek, P. (2008). Brunovistulian terrane (Bohemian Massif, Central Europe) from late Proterozoic to late Paleozoic: a review. *International Journal of Earth Sciences*, **97**, 497-518.

Kemnitz, H., Romer, R. L. & Oncken, O. (2002). Gondwana breakup and the northern margin of the Saxothuringian belt (Variscides of Central Europe). *Geologische Rundschau*, **91**, 246-259.

Kossmat, F. (1927). Gliederung der varistischen Gebirgsbaues. *Abhandlungen des Sächsischen Geologischen Landesamts*, **1**, 1-39.

Kratinová, Z., Schulmann, K., Edel, J. B., Ježek, J. & Schaltegger, U. (2007). Model of successive granite sheet emplacement in transtensional setting: Integrated microstructural and anisotropy of magnetic susceptibility study. *Tectonics*, **26**, TC6003.

Krecher, M., Behrmann, J. H. & Müller-Sigmund, H. (2007). Sedimentology and tectonic setting of Devonian-Carboniferous turbidites and debris flow deposits in the Variscan Vosges Mountains (Markstein Group, NE-France). *Zeitschrift der Deutschen Gesellschaft für Geowissenschaften*, **158**, 1063-1087.

Krecher, M. (2005). Die Turbiditsandstein-Komplexe der devono-karbonischen Markstein Gruppe im Oberelsass (NE-Frankreich) und ihre Beziehungen zu den moldanubischen Gesteinseinheiten von Schwarzwald und Vogesen. Dissertation, Albert-Ludwigs-Universität, Freiburg im Breisgau, 386 p.

Krecher, M. (1997). Visean slope sedimentation in the Southern Vosges (NE-France). *Terra Nova, Abstract supplement*, **1**, 9-264.

Lardeaux, J. M., Ledru, P., Daniel, I. & Duchene, S. (2001). The Variscan French Massif Central - a new addition to the ultrahigh pressure metamorphic 'club': exhumation processes and geodynamic consequences. *Tectonophysics*, **332**, 143-167.

Lefèvre, C., Lakhrissi, M. & Schneider, J. L. (1994). Les affinités magmatiques du volcanisme dinantien des Vosges méridionales (France) ; approche géochimique et interprétation. *Comptes Rendus de l'Académie des Sciences*, **319**, 79-86.

Leveridge, B. E. & Hartley, A. J. (2006). The Variscan Orogeny: the development and deformation of Devonian/Carboniferous basins in SW England and South Wales. In: Brenchley, P. J. & Rawson, P. F. (eds) *The Geology of England and Wales, Geological Society, London*, 225-255.

Linnemann, U., McNaughton, N. J., Romer, R. L., Gehmlich, M., Drost, K. & Tonk, C. (2004). West African provenance for Saxo-Thuringia (Bohemian Massif): did Armorica ever leave pre-Pangean Gondwana?—U–Pb-SHRIMP zircon evidence and the Nd isotopic record. *International Journal of Earth Sciences*, **93**, 683-705.

Loeschke, J., Güldenpfennig, M., Hann, H. P. & Sawatzki, G. (1998). Die Zone von Badenweiler-Lenzkirch (Schwarzwald): Eine variskische Suturzone. *Zeitschrift der deutschen geologischen Gesellschaft*, **149**, 197-212.

Maass, R. & Schneider, J. L. (1995). Die südlichen Vogesen. *Jahresberichte und Mitteilungen des Oberrheinischen Geologishen Vereins Neue Folge*, **77**, 139-153.

Maass, R., Prosch, T. & Schuler, D. (1990). The zone of Badenweiler-Lenzkirch – a Carboniferous accretionary wedge? *Neues Jahrbuch für Geologie und Paläontologie. Monatshefte*, **12**, 717-734.

Maass, R. (1988). Die Südvogesen in variszischer Zeit. *Neues Jahrbuch für Geologie und Paläontologie. Monatshefte*, **10**, 611-638.

Maass, R. & Stoppel, D. (1982). Nachweis von Oberdevon bei Markstein (Bl. Munster, Südvogesen). *Zeitschrift der Deutschen Geologischen Gesellschaft*, **133**, 403-408.

Mattauer, M. (1959). Découverte d'une faune viséenne près de Rimbach (Vosges méridionales). *Comptes Rendus de l'Académie des Sciences*, **248**, 433.

Mattauer, M. & Théobald, N. (1957). Présence de Lepidostrobus browni (Unger) Schimper dans le Dinantien de la Haute-Vallée de la Thur. *Bulletin du Service de la Carte Géologique d'Alsace-Lorraine*, **10**, 133-142.

Matte, P. (2001). The Variscan collage and orogeny (480-290 Ma) and the tectonic definition of the Armorica microplate: a review. *Terra Nova*, **13**, 122-128.

Matte P. (1991), Accretionary history and crustal evolution of the Variscan belt in Western Europe. *Tectonophysics*, **196**, 309-337.

Matte, P. (1986). Tectonics and plate tectonics model for the Variscan Belt of Europe. *Tectonophysics*, **126**, 329-374.

Oncken, O., von Winterfeld, C. & Dittmar, U. (1999). Accretion of a rifted passive margin: The Late Paleozoic Rhenohercynian fold and thrust belt (Middle European Variscides). *Tectonics*, **18**, 75-91.

Oncken, O. (1997). Transformation of a magmatic arc and an orogenic root during oblique collision and its consequences for the evolution of the European Variscide (Mid-German Crystalline Rise). *Geologische Rundschau*, **86**, 2-20.

Pagel, M. (1981). Facteurs de distribution et de concentration de l'uranium et du thorium dans quelques granites de la chaîne hercynienne d'Europe. Thèse Sciences C.R.P.G. et C.R.E.G.U., I.N.P.L., Nancy, 566p.

Paris, F. & Robardet, M. (1990). Early Paleozoic paleogeography of the Variscan regions. *Tectonophysics*, **177**, 193-213.

Petrini, K. & Burg, J. P. (1998). Relationships between deformation, plutonism and regional metamorphism in the Markstein area (southern Vosges). *Géologie de la France*, **2**, 13-23.

Pitra, P., Ballèvre, M. & Ruffet, G. (2010). Inverted metamorphic field gradient towards a Variscan suture zone (Champtoceaux Complex, Armorican Massif, France). *Journal of Metamorphic Geology*, **28**, 183-208.

Reitz, E. & Wickert, F. (1989). Late Cambrian to early Ordovician acritarchs from the Villé unit, northern Vosges Mountains (France). *Neues Jahrbuch für Geologie und Paläontologie. Monatshefte*, **6**, 375-384.

Rizki, A. (1992). Le volcanisme dévono-dinantien du Versant Alsacien des Vosges du Nord (Massif de Schirmeck-Bande Médiane du Champs du Feu). Pétrogenèse et apport à la compréhension de l'évolution géodynamique de la Chaine Varisque. Thèse de doctorat, Nancy, p.156.

Rizki, A. & Baroz, F. (1988). Le volcanisme tholéïtique du massif de Schirmeck (Vosges septentrionales, France), témoin d'une zone de convergence de plaques au Paléozoïque supérieur. *Comptes Rendus de l'Academie des Sciences*, **307**, 511-516.

Robardet, M. (2003). The Armorica «microplate»: fact or fiction ? Critical review of the concept and contradictory paleobiogeographical data. *Palaeogeography, Palaeoclimatology, Palaeoecology*, **195**, 125-148.

Ross, P. H. (1964). Fossilfunde in den Steiger und Weiler Schiefern (Vogesen). *Nachrichten der Akademie der Wissenschaften zu Göttingen, Mathematisch-Physikalische Klasse*, **3**, 37-43.

Rossi, P. & Oggiano, G. (2009). A restored section of the ''southern Variscan realm'' across the Corsica–Sardinia microcontinent. *Comptes Rendus Géoscience*, **341**, 224-238.

Sauer, A. (1893). Der Granitit von Durbach im nordlichen Schwarzwald un seine Grenzfacies von Glimmersyenit (Durbachit). *Mitteilungsblatt der Badischen Geologischen Landesanstalt* **2**, 233-276.

Schäfer, F., Oncken, O., Kemnitz, H. & Romer, R. (2000). Upper-plate deformation during collisional orogeny: a case study from the German Variscides (Saxo-Thuringian Zone). In: Franke, W., Haak, V. Oncken,O. & Tanner, D. (eds.) *Orogenic Processes: Quantification and Modelling in the Variscan Belt, Geological Society of London, Special publication* , **179**, 281-302.

Schaltegger, U., Fanning, C. M., Günther, D., Maurin, J. C., Schulmann, K. & Gebauer, D. (1999). Growth, annealing and recrystallization of zircon and preservation of monazite in high-grade metamorphism: conventional and in situ U-Pb isotope, cathodoluminiscence and microchemical evidence. *Contributions to Mineralogy and Petrology*, **134**, 186–201.

Schaltegger, U., Schneider, J.-L., Maurin, J.-C. & Corfu, F. (1996). Precise U-Pb chronometry of 345–340 Ma old magmatism related to syn-convergence extension in the Southern Vosges (Central Variscan Belt). *Earth and Planetary Sciences Letters,* **144**, 403–419.

Schneider, J. L. (1990). Enregistrement de la dynamique varisque dans les bassins volcano-sédimentaires dévono-dinantiens : exemple des Vosges du Sud (zone moldanubienne). Thèse de doctorat, Université de Strasbourg, 222 p.

Schneider, J. L., Hassenforder, B. & Paicheler, J.-C. (1990). Une ou plusieurs « Ligne des Klippes » dans les Vosges du Sud (France)? Nouvelles données sur la nature des « klippes » et leur signification dans la dynamique varisque. *Comptes Rendus de l'Académie des Sciences*, **311**, 1221-1226.

Schulmann, K., Konopásek, J., Janoušek, V., Lexa, O., Lardeaux, J.-M., Edel, J.-B., Štípská, P. & Ulrich, S. (2009). An Andean type Palaeozoic convergence in the Bohemian Massif. *Comptes Rendus Geoscience*, **341**, 266-286.

Schulmann, K., Lexa, O., Štípská, P., Racek, M., Tajčmanová, L., Konopásek, J., Edel, J. B., Peschler, A. & Lehmann, J. (2008). Vertical extrusion and horizontal channel flow of orogenic lower crust: key exhumation mechanisms in large hot orogens? *Journal of Metamorphic Geology*, **26**, 273–297.

Schulmann, K., Kröner, A., Hegner, E., Wendt, I., Konopásek, J., Lexa, O. & Štípská, P. (2005). Chronological constraints on the pre-orogenic history, burial and exhumation of deep-seated rocks along the eastern margin of the Variscan orogen, Bohemian Massif, Czech Republic. *American Journal of Science*, **305**, 407-448.

Shail, R. K. & Leveridge, B. E. (2009). The Rhenohercynian passive margin of SW England: Development, inversion and extensional reactivation. *Comptes Rendus Géoscience*, **341**, 140-155.

Skrzypek, E. (2011). Contribution structurale, pétrologique et géochronologique à la tectonique intracontinentale de la chaîne hercynienne d'Europe (Sudètes, Vosges). Thèse de doctorat, Université de Strasbourg, p.381.

Tait, J., Schätz, M., Bachtadse, V. & Soffel, H. (2000). Paleomagnetism and Palaeozoic palaeogeography of Gondwana and European terranes. In: Franke, W., Haak, V., Oncken, O. & Tanner, D. (eds.) *Orogenic Processes: Quantification and Modelling in the Variscan Belt*, *Geological Society Special Publication, London***, 179**, 21-34.

Tait, J., Bachtadse, V., Franke, W. & Soffel, H. C. (1997). Geodynamic evolution of the European Variscan fold belt: paleomagnetic and geological constraints. *Geologische Rundschau*, **86**, 585-598.

Tobschall, H. J. (1974). Geochemische Untersuchungen zum stofflichen Bestand und Sedimentationsmilieu paläozoischer mariner Tone: Die Gehalte der Hauptelemente und der Spurenelemente Ni, Cu, Zn, Rb, Sr, Y, Zr, Nb und Ba in den Steiger Schiefern (Vogesen). *Habilitationsschrift, Mainz*, 142 p.

Traiser, C., Montenari, M. & Speck, T. (1998). The Upper Unit of the Southern Vosges Basin (Central Variscan Belt): a genetic model and a stratigraphic discussion. *Terra Nostra*, **98**, 189-190.

Van der Voo, R. (1993). Paleomagnetism of the Atlantic, Tethys and Iapetus oceans. *Cambridge University press, Cambridge*, 411p.

Vogt, C. (1981). Benthonische Klein-Foraminiferen aus dem Unter-Karbon der Südvogesen. *Neues Jahrbuch für Geologie und Paläontologie. Monatshefte*, **6**, 363-384.

von Eller, J. P. (1961). Les gneiss de Sainte-Marie-aux-Mines et les séries voisines des Vosges moyennes. *Mémoires du Service de la Carte géologique d'Alsace-Lorraine*, **19**, 160 p.

von Raumer, J. F., Stampfli, G. M. & Bussy, F. (2003). Gondwana-derived microcontinents-the constituents of the Variscan and Alpine collisional orogens. *Tectonophysics*, **365**, 7-22.

Winchester, J. A., Pharaoh, T. C. & Verniers, J. (2002). Palaeozoic amalgamation of Central Europe: an introduction and synthesis of new results from recent geological and geophysical investigations. In: Winchester, J. A., Pharaoh, T. C. & Verniers, J. (eds.) *Palaeozoic Amalgamation of Central Europe*, *Geological Society Special Publication, London*, **201**, 1-18.

Chapitre 2 : la «ligne des Klippes»

Ce chapitre présente l'étude lithologique, structurale, géochimique et géochronologique des fragments d'ophiolite et de gneiss de la « ligne des Klippes » située dans les Vosges moyennes et méridionales. Ces différentes klippes préservent des harzburgites serpentinisées, des ophicalcite, des gabbros, des gneiss et des conglomérats.

L'ensemble des ces études nous a permis de proposer la formation d'un bassin profond au cours de la fin du Dévonien qui se ferme durant le Viséen. En corrélant ces données avec les observations faites par d'autres auteurs dans les autres massifs varisques (Brévennes, Forêt Noire), nous avons proposé que ces klippes préservent des reliques de roches formées dans un contexte de bassin d'arrière-arc mature qui s'est développé loin de la zone de subduction vers le nord de l'océan Paléotéthys situé au sud du domaine Moldanubien.

Ce chapitre résulte d'un travail en collaboration avec Etienne Skrzypek. Il a consisté en des travaux de terrain (microcartographie des différentes klippes), de données structurales, de nouvelles datations en U-Pb sur zircons (Alain Cocherie, BRGM) et en Sm-Nd sur minéraux et roches totales (Catherine Guerrot, BRGM) et de l'étude pétrologique et géochimique des gabbros.

Cette partie a été publiée dans *International Journal of Earth Sciences* où je suis second auteur (participation à 40%).

Int J Earth Sci (Geol Rundsch)
DOI 10.1007/s00531-011-0709-4

ORIGINAL PAPER

The significance of Late Devonian ophiolites in the Variscan orogen: a record from the Vosges Klippen Belt

E. Skrzypek · A.-S. Tabaud · J.-B. Edel · K. Schulmann · A. Cocherie · C. Guerrot · P. Rossi

Received: 30 March 2011 / Accepted: 16 July 2011

Abstract The present work examines the lithological, structural, geochemical and geochronological records from the Klippen Belt located in the southern Vosges Mountains (NE France). The Klippen Belt is represented by discontinuous exposures of serpentinized harzburgite, ophicalcite, gabbro, gneiss and polymictic conglomerate overlain by deep marine pelitic sediments. Structural data and Bouguer anomalies reveal that the Klippen Belt coincides with a significant discontinuity now occupied by a granitic ridge. Gabbro geochemistry indicates a MOR-type affinity similar to recent slow-spreading ridges, but positive Ba, Sr, Th or U anomalies do not exclude the influence of fluids expelled from a subduction zone. A Sm–Nd isochron age of 372 ± 18 Ma is thought to reflect gabbro emplacement from a highly depleted mantle source ($\varepsilon_{Nd} = +11.3$), and U–Pb zircon ages from a gneiss sample indicate that the basement found in the Klippen has a Neoproterozoic origin. Combined data indicate the formation of a deep basin during Late Devonian rifting. The Klippen lithologies could testify for the presence of an ocean–continent transition environment subsequently inverted during the Early Carboniferous. Basin inversion during the Middle Visean was probably controlled by rift-related structures, and resulted in folding of the sedimentary successions as well as exhumation along thrust zones of deep parts of the basin represented by the Klippen Belt. Based on correlations with the neighbouring Variscan massifs, it is proposed that the southern Vosges sequences represent a back-arc basin related to the North-directed subduction of the southern Palaeotethys Ocean. This geodynamic reconstruction is tentatively correlated with similar ophiolitic remnants in the northern part of the French Massif Central (Brévenne) and with the evolution of the southern Black Forest. The Late Devonian ophiolites are interpreted as relicts of small back-arc marginal basins developed during general closure of the Palaeozoic subduction systems.

Keywords Variscan orogeny · Devonian ophiolites · Palaeozoic oceans · Klippen Belt · Vosges Mountains

E. Skrzypek (✉) · A.-S. Tabaud · J.-B. Edel · K. Schulmann
Ecole et Observatoire des Sciences de la Terre—UMR 7516, Université de Strasbourg, 1, rue Blessig, 67084 Strasbourg, France
e-mail: etienne.skrzypek@eost.u-strasbg.fr

A. Cocherie · C. Guerrot · P. Rossi
BRGM, BP 36009, Orléans cedex 02, France

Introduction

Two major episodes of oceanic crust generation are clearly documented in the Variscan Belt of Europe (Behr et al. 1984; Matte 1986; Ziegler 1986; Pin 1990). The first Cambro-Ordovician event is associated with the formation of the large Rheic oceanic realm and rifting of continental blocks away from the northern Gondwana margin (Crowley et al. 2000; Tait et al. 2000; Matte 2001; von Raumer and Stampfli 2008). The second event corresponds to a well-documented Early Devonian oceanic stage (Holder and Leveridge 1986; Franke 2000), while some Late Devonian ophiolites may reflect back-arc spreading (Pin and Paquette 1997).

The episodes of Palaeozoic rifting led to the formation of basins with contrasted sedimentary and deformational records. The basins which opened during the Cambro-Ordovician preserve Ordovician to Devonian autochtonous sediments that are indicative of long-lived oceanic

Published online: 09 September 2011

domains. They are also characterised by Devonian to Visean flysch deposits (e.g. Saxothuringian stratigraphy; Falk et al. 1995). Subsequent inversion of these relatively old sequences was associated with the growth of a thick oceanic wedge and resulted in large thrust imbrications of sedimentary units, ophiolites and back-thrusted high-pressure rocks (Franke 1984). By contrast, Devonian basin sequences are related to short-lived oceanic domains. They comprise Early to Middle Devonian undisturbed marine sediments followed by a Middle Devonian to Carboniferous input of flysch sediments (e.g. Rhenohercynian stratigraphy; Franke 1995; Leveridge and Hartley 2006). Inversion of the Devonian basins produced a fold and thrust belt geometry (Oncken et al. 1999) with imbrications of non-metamorphosed to weakly metamorphosed sediments and obduction of ophiolites (Shail and Leveridge 2009) with some high-pressure remnants (Massone and Schreyer 1983; Ganssloser et al. 1996). In a similar way, Late Devonian successions are related to very short-lived back-arc domains because they exhibit Late Devonian sediments shortly followed by Early Carboniferous flyschoid sedimentation (Hartley and Otava 2001). Inversion of these probably small basins is characterised by an exhumation of the deepest parts of the basin in between younger sediments (e.g. the Horní Benešov-Šternberk Belt in Moravia, Dvořák 1995).

Thus, the life span of an oceanic basin seems to be a key parameter controlling its future inversion. It is all the more important for Late Devonian remnants because this period corresponds to a general closure of the Variscan subduction systems and a widespread exhumation of HP rocks (e.g. Matte 1998; Stampfli and Borel 2002; Ballèvre et al. 2009). It is therefore critical to assess the timing and tectonic evolution of the Late Devonian oceanic domains in order to better understand their origin and significance during Variscan orogeny.

The opportunity to address such problems is given by the ophiolitic remnants exposed in the southern Vosges Klippen Belt ('Ligne des Klippes', Jung 1928). There, the closure of a Devonian oceanic basin was documented by Krecher and Behrmann (2007), but information on the preceding opening stage is lacking. This contribution therefore proposes a re-evaluation of ophiolitic rocks from the Klippen Belt. Detailed mapping of the Klippen Belt together with structural and geophysical data from the adjacent units are used to decipher the tectonic history of the southern Vosges. In addition, geochemical analyses on gabbroic rocks and geochronological data from oceanic and basement lithologies mixed in the Klippen Belt are combined to constrain the origin, geodynamic setting and timing of the basin. A tectonic evolution is proposed and implications for the dynamics of the Variscan Belt are discussed.

Geological background

Devonian ophiolites in the Variscan belt of Europe

Two groups of Devonian ophiolitic remnants can be distinguished in the Variscan Belt of Europe (Fig. 1). The first group is comprised of oceanic rocks of the Lizard Complex which document Early to Middle Devonian extension in SW England (Floyd and Styles 1993; Clark et al. 1998; Cook et al. 2002), and the Giessen and Harz MOR-type metabasalts overlain by Middle Devonian sediments in NW Germany (Franke 1995; Floyd 1995). These ophiolites are interpreted as relicts of the Early Devonian Rhenohercynian oceanic basin which was subsequently inverted in the Middle to Late Devonian (Franke 2000). The second group is represented by the Brévenne Séries in the French Massif Central which preserve Late Devonian subduction-related magmatic rocks (Pin and Paquette 1997; Leloix et al. 1999) and by Devonian deep marine sediments and arc to back-arc magmatic rocks of the Vrbno and Drahany Facies in Moravia (Patočka and Valenta 1996; Hladil et al. 1999; Janoušek et al. 2006). The Beja-Acebuches Ophiolite Complex indicating opening of a basin at 400–370 Ma in SW Iberia (Ribeiro et al. 2010) could also be associated with the group of Late Devonian ophiolites, though this interpretation is still debated (Azor et al. 2008; Pin et al. 2008). This group of ophiolites is generally related to the existence of small back-arc domains during Devonian times.

Southern Vosges Mountains

In the southern Vosges, ophiolitic rocks (sensu Coleman 1977) are found in the so-called Klippen Belt, which represents a discontinuous exposure of exotic rocks between two sedimentary basins (Fig. 2). Based on structural observations, Jung (1928) originally distinguished between a northern allochtonous unit (Markstein unit) and a southern group of autochtonous units (Oderen and Thann units). The allochtonous sedimentary unit is composed of interbedded pelite and greywacke (Fig. 3) and represents an Early Carboniferous (Corsin and Mattauer 1957; Corsin and Ruhland 1959) siliciclastic turbidite basin preserving distinct facies of sandy submarine fans (Gagny 1962; Krecher et al. 2007). To the South, the autochtonous units chiefly correspond to Lower to Upper Visean volcano-sedimentary rocks. The base of the Oderen unit (Fig. 3) is characterised by a relatively thin succession of Frasnian (?) carbonates conformably overlain by Fammenian sediments (Asselberghs 1926) and Early Carboniferous pelite and greywacke, whereas the thick Lower to Middle Visean deposits involve interbedded pelite and greywacke turbidites accompanied by mostly submarine basaltic ('spilitic') volcanism (Vogt 1981; Schneider 1990; Hammel 1996;

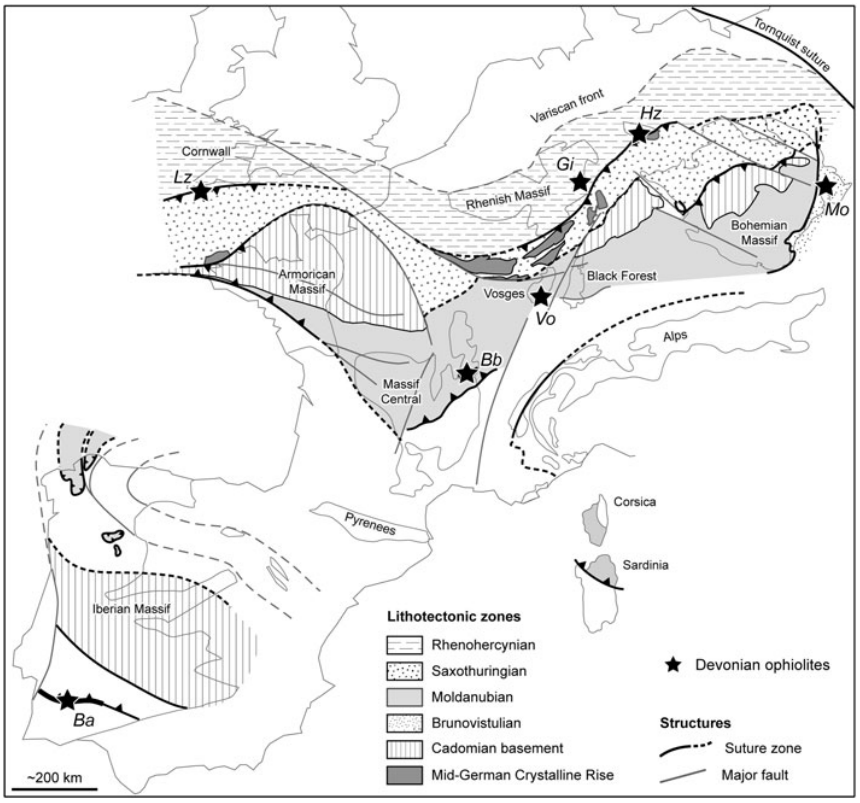

Fig. 1 Devonian ophiolites in the Variscan Belt of Europe. *Ba* Beja-Acebuches Ophiolite Complex, *Lz* Lizard Complex, *Bb* Brévenne-Beaujolais, *Vo* Vosges Klippen Belt, *Gi* Giessen and *Hz* Harz Nappes, *Mo* Vrbno-Drahany Facies and Horní Benešov-Šternberk Belt in Moravia. Variscan framework is modified after Edel and Schulman (2009), Ballèvre et al. (2009) and Pitra et al. (2010)

Montenari et al. 2002). The Upper Visean continental deposits of the Thann unit (Fig. 3) are represented by coarse-grained greywacke and conglomerate alternating with volcanic rocks that range from trachyte and andesite to rhyodacite and rhyolite (Coulon et al. 1978). The sedimentary basins are surrounded by amphibole–biotite-bearing granite ('Crêtes' granite) and voluminous anatectic granite (Fig. 2) emplaced at ca. 340 Ma and ca. 326 Ma, respectively (Schaltegger et al. 1996, 1999).

The deformation in the sedimentary units mostly involves folding of the primary bedding. In the allochtonous unit, Ruhland (1958) recognised N–S trending folds at the border of the massif, and dominant NW–SE trending folds in the centre. The NW–SE folding event is believed to be broadly coeval with granitic intrusions at ca. 340 Ma (Petrini and Burg 1998). On the contrary, Krecher and Behrmann (2007) interpreted the structural record in the southern Vosges basins as a result of southward thrusting followed by dextral transpression.

The Vosges Klippen Belt

Enigmatic occurrences of serpentinite and gabbro within sediments of the southern Vosges have long been recognised (Delesse 1847; Delbos and Kœchlin-Schlumberger 1866). The first detailed description of the associated gneiss, conglomerates and pelites was proposed by Linck (1892). Later, von Seidlitz (1914) suggested a tectonic origin for these rocks, and Jung (1928) interpreted them as thrust-derived slices of deep parts of the allochtonous sedimentary basin. The latter author introduced the term Klippen Belt by analogy with the Pieniny Klippen Belt found in the Western Carpathians. The tectonic origin was contested by Fluck (1987) who proposed that the contrasted lithologies represent olistoliths lying in a greywacke matrix. However, Wickert and Eisbacher (1988) observed shear criteria in the surrounding sediments which indicate a dextral strike-slip and thrusting. Based on a review of all Klippen, Schneider et al. (1990) more recently distinguished between a tectonically derived Klippen Belt to the West (LK1), and an alignment of resedimented conglomeratic lenses to the East (LK2) (Fig. 2).

The mineralogy of basic and ultrabasic rocks of the Klippen Belt was detailed by Weigand (1875) and Linck (1892). They observed that the serpentinite was originally harzburgitic in composition and may be linked with the presence of gabbroic rocks. Based on recalculated highly positive ε_{Nd} values (+7.1 to +8.8), Pin and Carme (1988) proposed that the gabbroic rocks were probably derived from the partial melting of a strongly depleted mantle source. Because the chemistry of both serpentinite and

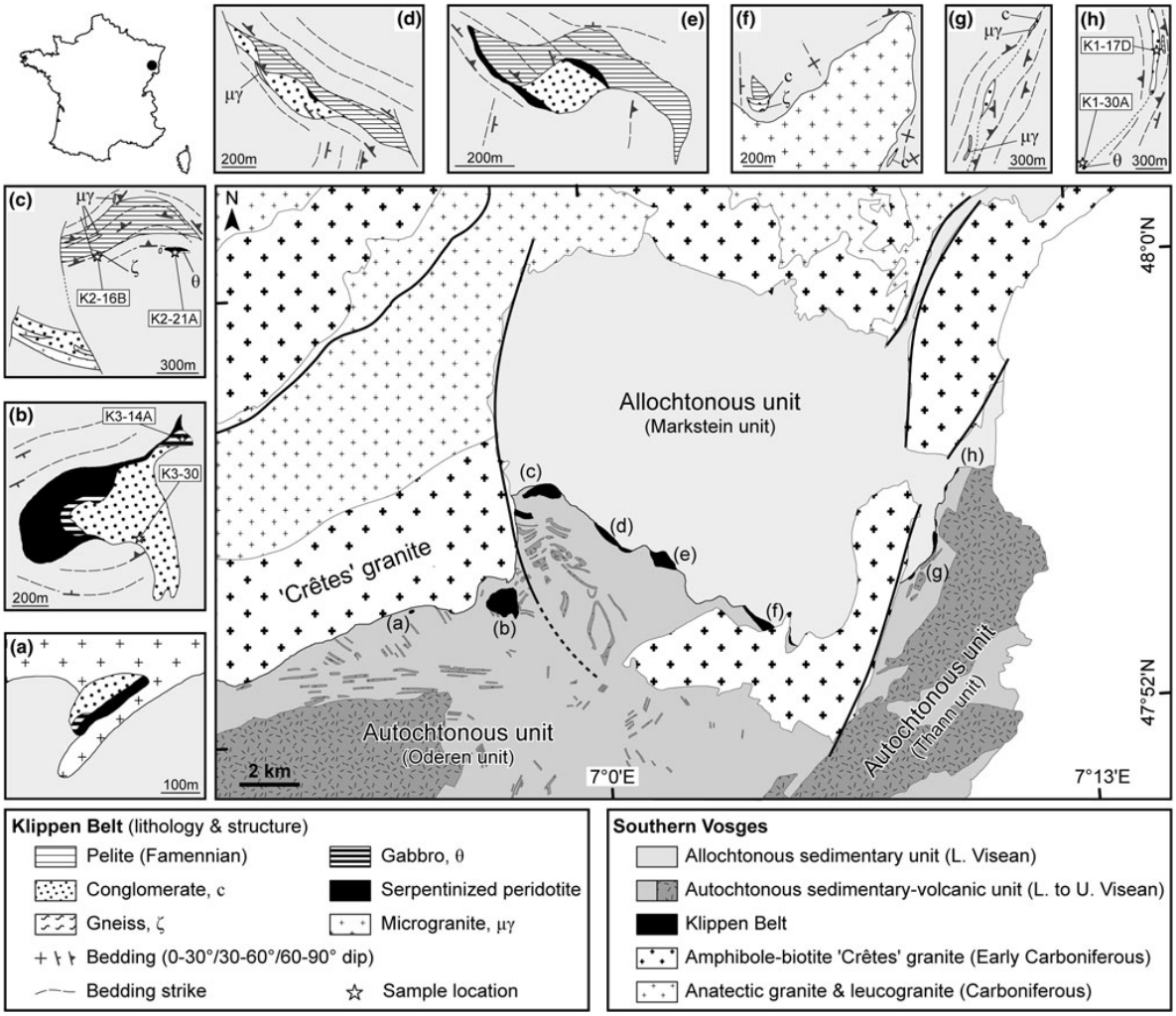

Fig. 2 Lithological map of the southern Vosges and detailed maps of the different Klippen. Klippen names: **a** Drumont, **b** Thalhorn, **c** Kruth-Sauwas, **d** Treh, **e** Markstein, **f** Arutsch-Rennenbachfels, **g** Lautenbach, **h** Murbach-Rimbach

gabbro indicates a tholeiitic affinity, Kam (1983) suggested that these rocks may represent a fragment of an ophiolitic complex.

The age of the ophiolitic rocks has remained poorly investigated. Pin and Carme (1988) tried to constrain the age of the gabbroic material, but the Sm–Nd mineral isochron yielded a ca. 300 Ma age interpreted as late isotopic re-homogenisation. The only time constraints concerning the Klippen Belt were therefore derived from the palaeontological records in pelites. Doubinger and Ruhland (1963) first used chitinozoans to propose an Early to Middle Devonian age, but conodonts found by Maass and Stoppel (1982) indicate that sedimentation more likely occurred during the Famennian. In addition, conventional U–Pb dating of detrital zircon from the pelites points to the existence of a magmatic or metamorphic event at ca. 386 Ma (Schaltegger et al. 1996), i.e. close to the Givetian–Frasnian boundary.

Lithology

The Klippen are dominantly composed of siliceous pelite and coarse-grained to conglomeratic greywacke with local occurrences of peridotite, gabbro and gneiss (Fig. 3). Detailed mapping (Fig. 2a–h, Table 1) reveals that a consistent succession is preserved, and involves ultrabasic to basic rocks and basement lithologies overlain by conglomeratic greywacke and fine-grained sediments. This superposition is only observed in the western Klippen (Fig. 2a–f), i.e. in the LK1 after Schneider et al. (1990).

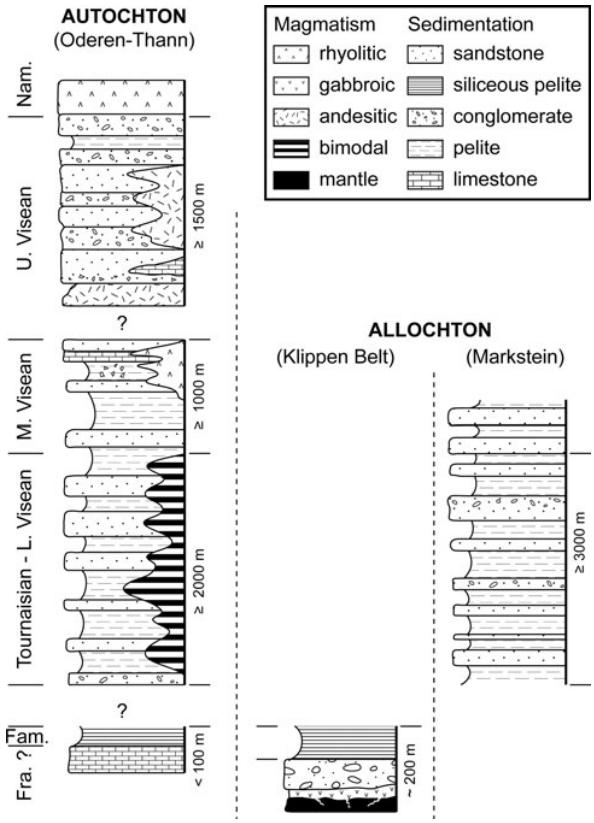

Fig. 3 Lithostratigraphic columns of the southern Vosges allochtonous and autochtonous units

Ultrabasic rocks are represented by massive outcrops of serpentinized peridotite. Some rocks have also been identified for the first time as ophicalcite (Fig. 4a). Serpentinized peridotite shows a typical ochre alteration and preserves abundant macroscopic serpentine and calcite veins. The intense serpentinization leaves only few relicts of brownish spinel and orthopyroxene which suggest that the rock was originally of harzburgitic composition. Ophicalcite is observed either as the product of in situ fracturing of peridotite, or as pebbles within the conglomeratic greywacke (respectively OC1 and OC2 after Lemoine et al. 1987). It corresponds to clasts of serpentinized spinel-peridotite cemented by fine-grained calcite veins where detrital spinel is abundant.

Basic rocks occur as massive gabbro and dolerite, or as gabbroic and doleritic pebbles in the conglomerate. These rocks display a continuous evolution from a rare fine-grained doleritic texture to a widespread cumulative texture (Fig. 4b). Gabbro is composed of sericitized plagioclase, ortho and clinopyroxene variably replaced by greenish amphibole, minor quartz and opaque minerals.

Basement rocks are found as isolated blocks or as pebbles in the conglomeratic greywacke. They are represented by weakly deformed gneiss, mylonitic orthogneiss, garnet amphibolite or amphibole gneiss. The weakly deformed gneiss (Fig. 4c) displays features indicative of cataclastic deformation and shows coarse-grained quartz–K-feldspar–plagioclase lenses surrounded by muscovite, few biotite, and small garnet (0.25–0.5 mm in diameter). The mylonitic orthogneiss (so-called 'leptynite') exhibits a fine-grained, almost granulitic texture (Fig. 4d) with large (1–7 mm in length) K-feldspar porphyroclasts and a small amount of biotite. Amphibolite is composed of green to brown hornblende, plagioclase, some garnet porphyroblasts (0.75–7 mm in diameter), and minor biotite and titanite.

The conglomerate covers large zones of the different Klippen (Fig. 2). The matrix is a coarse-grained greywacke with quartz and plagioclase clasts surrounded by anastomosing bands of fine-grained quartz, chlorite, biotite and clay minerals. Occasionally, detrital pyroxene, amphibole or spinel are observed. The conglomerate is composed of cm-scale pebbles to m-scale blocks of all the above-described lithologies. Gneiss pebbles are commonly rounded, whereas gabbro or dolerite pebbles have a toothed shape, and ultrabasic rocks form only small angular clasts (Fig. 4e). The conglomeratic greywacke is locally strongly deformed showing significant grain size reduction, and in places it is difficult to distinguish between deformed massive blocks of gneiss or gabbro and the deformed greywacke and pebbles.

Fine-grained siliceous sediments generally overlie the conglomeratic greywacke and the exotic blocks. Whereas the upper yellowish siltstone may belong to the base of the overlying allochtonous unit, the lower red and green pelites (the so-called 'Treh shales') are a common feature of the Klippen Belt. They are finely laminated siltstones that display a clear sedimentary bedding defined by alternating quartz-rich and clay-rich layers.

Microgranite does not strictly belong to the lithological succession, but is an important feature of the Klippen Belt. Several m-thick intrusive bodies of pinkish microgranite (Fig. 4f) are almost always found in the different Klippen, and are commonly localised at their periphery (Fig. 2). In thin section, the microgranite exhibits abundant biotite phenocrysts (1–2.5 mm in size) which are partly chloritized, large (0.5–2 mm in length) actinolitic amphibole needles, and rare anhedral quartz lying in a microcrystalline matrix.

Structural setting

The primary bedding (S0) is the dominant structure that can extensively be mapped in sediments around the Klippen Belt (Fig. 5a). It is also rarely observed in the fine-grained pelite in some Klippen (Fig. 2). The sedimentary bedding is commonly defined by cm-spaced alternations of fine-grained sandy and pelitic material (Fig. 4g), by graded-bedding in coarse-grained greywacke, or by m-scale successions of

Table 1 Summary of lithologies from the different Klippen

	K1		K2		K3	K4	K5	K6		K7	K8
	Murb. S	Laut. S	Kruth	Sauwas	Thalhorn	Treh	Mark.	Arutsch	Renn.	Drumont	W-A
Sediments											
Yellow siltstone	X			X	?	X	X	X			
Red and green pelite				X		X	X				
Conglomerate	X		X		X		X	X	X	X	X
Siltstone/pelite											X
Quartz	X				X						
Gneiss	X		X		X		X		X		X
Mylonitic gneiss	X										
Amphibolite					X		X				
Gabbro	X		X		X			X	X	X	
Serpentinite					X		X			X	
Fine conglomerate, breccia			X								
Basement rocks											
Gneiss				X	X	X	X	X		(3)	
Mylonitic gneiss					X						
Amphibolite	X									(1)	
Basic and ultrabasic rocks											
Gabbro	X			X	X	(3)		X		X	
Dolerite	X				X						
Serpentinized peridotite					X	X	X		(2)	X	
Ophicalcite						X	X				
Intrusive microgranite		X	X	X	X	X		X	X		

X own observations; numbers refer to lithologies reported by (1) Delbos and Kœchlin-Schlumberger (1866), (2) De Billy, and (3) Jung (1928)
Murb. S. Murbach Sud, *Laut. S.* Lautenbach Sud, *Mark.* Markstein, *Renn.* Rennenbachfels, *W-A* Willer-Altrain

greywacke and pelite beds. Structural mapping reveals two contrasted domains (Fig. 5a). A NW–SE striking bedding is dominant both in the core of the allochtonous unit ($S0_{core}$) and in the Klippen Belt, whereas a N–S striking, mostly sub-horizontal bedding is observed at the border of the allochtonous unit and in the autochtonous unit ($S0_{border}$).

In the core of the allochtonous unit, the $S0_{core}$ bedding strikes NW–SE and variably dips either to the NE or SW. In few places, the sedimentary bedding is deformed by upright asymmetrical folds with sub-horizontal hinges and sub-vertical axial planes (Fig. 4h). In a limited area to the South of the Klippen Belt, $S0_{core}$ strikes NW–SE but consistently dips towards the NE. This orientation is similar to that observed in pelitic sediments of the Klippen Belt (Fig. 2). The northern and western boundaries of the allochtonous unit preserve a N–S striking $S0_{border}$ bedding, moderately to steeply dipping to the East or West. Towards the East of the allochtonous unit and to the South of the Klippen Belt, the $S0_{border}$ strikes N–S, but is mostly flat-lying. In this domain, a vertical section reveals that the contact between the autochtonous unit and the underlying 'Crêtes' granite is nearly horizontal (Fig. 5c). Intrusions of amphibole–biotite-bearing microgranite are common in the allochtonous unit as well as around the Klippen Belt. The orientation of the m-scale intrusions is closely linked with the orientation of the folded bedding; they are dominantly parallel to the sub-vertical NW–SE striking $S0_{core}$ bedding planes (Fig. 4f) and only rarely cross-cut the moderately dipping bedding.

The contrasted orientations of the primary bedding define a clear structural discontinuity to the South of the western Klippen Belt (Fig. 5a). It coincides with the limit between sedimentary rocks to the North and sediments with volcanic intercalations to the South. Both arguments are therefore used to redefine the boundary between the allochtonous and autochtonous units along this structural and lithological discontinuity (Fig. 5). The consistent orientation of $S0_{core}$ to the North of the boundary further suggests that the deformation was shared between the Klippen Belt and the surrounding allochtonous unit. It also implies that the Klippen Belt forms an integral, probably basal part of the allochtonous unit.

Geophysical constraints

A Bouguer anomaly map (Fig. 5b) was produced in order to evaluate the structural importance of the Klippen Belt

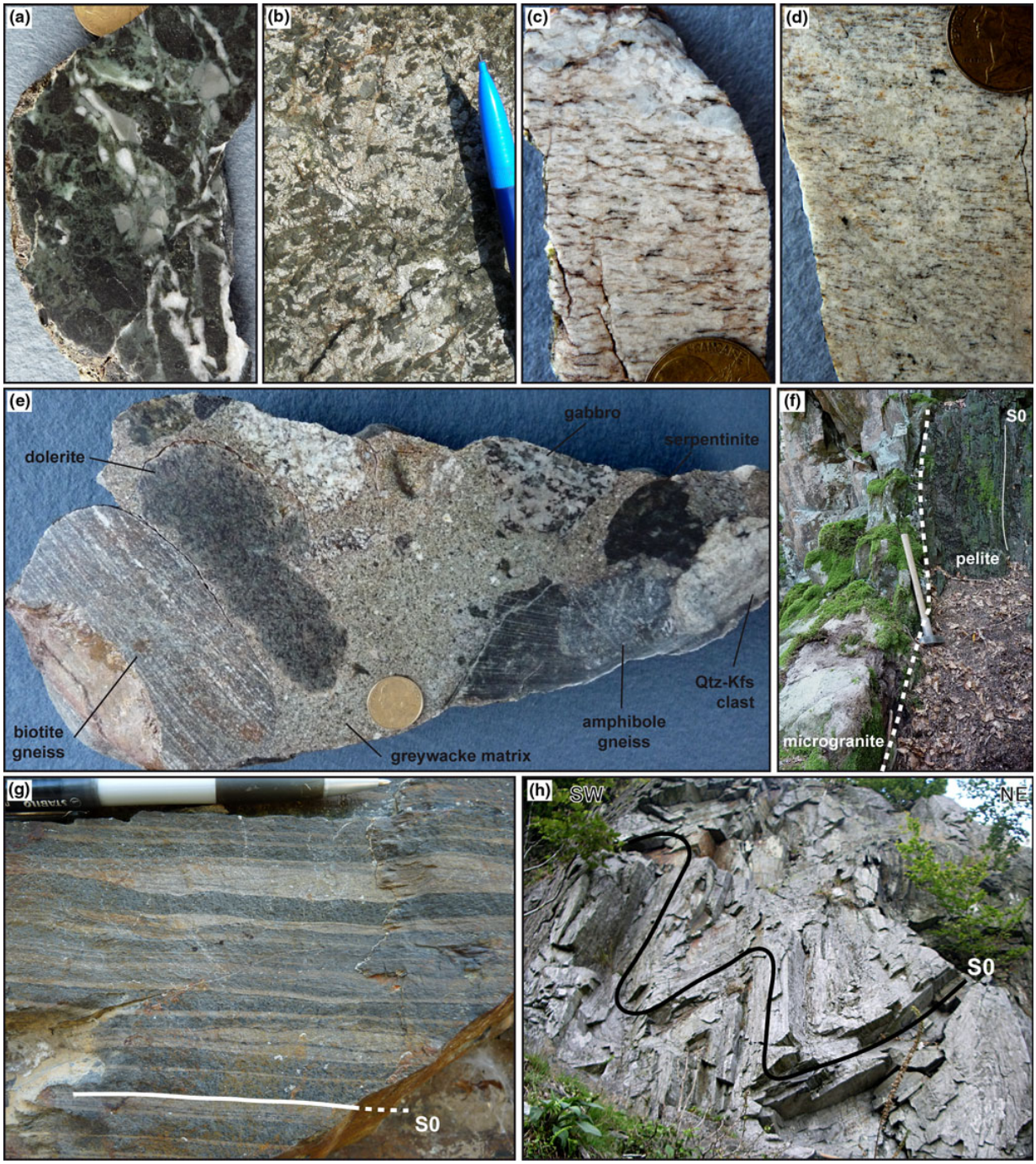

Fig. 4 Photographs illustrating the lithologies from the Vosges Klippen Belt and structures in the surrounding sediments. **a** Ophicalcite, Treh Klippe. **b** Gabbro showing a cumulative texture, **c** deformed metagranite, **d** mylonitic gneiss ('leptynite') displaying a granulitic texture, and **e** polymictic conglomerate with contrasted types and shapes of pebbles, Thalhorn Klippe. **f** Microgranite intrusion parallel to the sub-vertical bedding in the allochtonous unit. **g** Typical sedimentary bedding defined by alternating sandy and pelitic layers. Black spots in pelitic layers are due to contact metamorphism generated by the surrounding granite. **h** Upright folds affecting the bedding in the core of the allochtonous unit

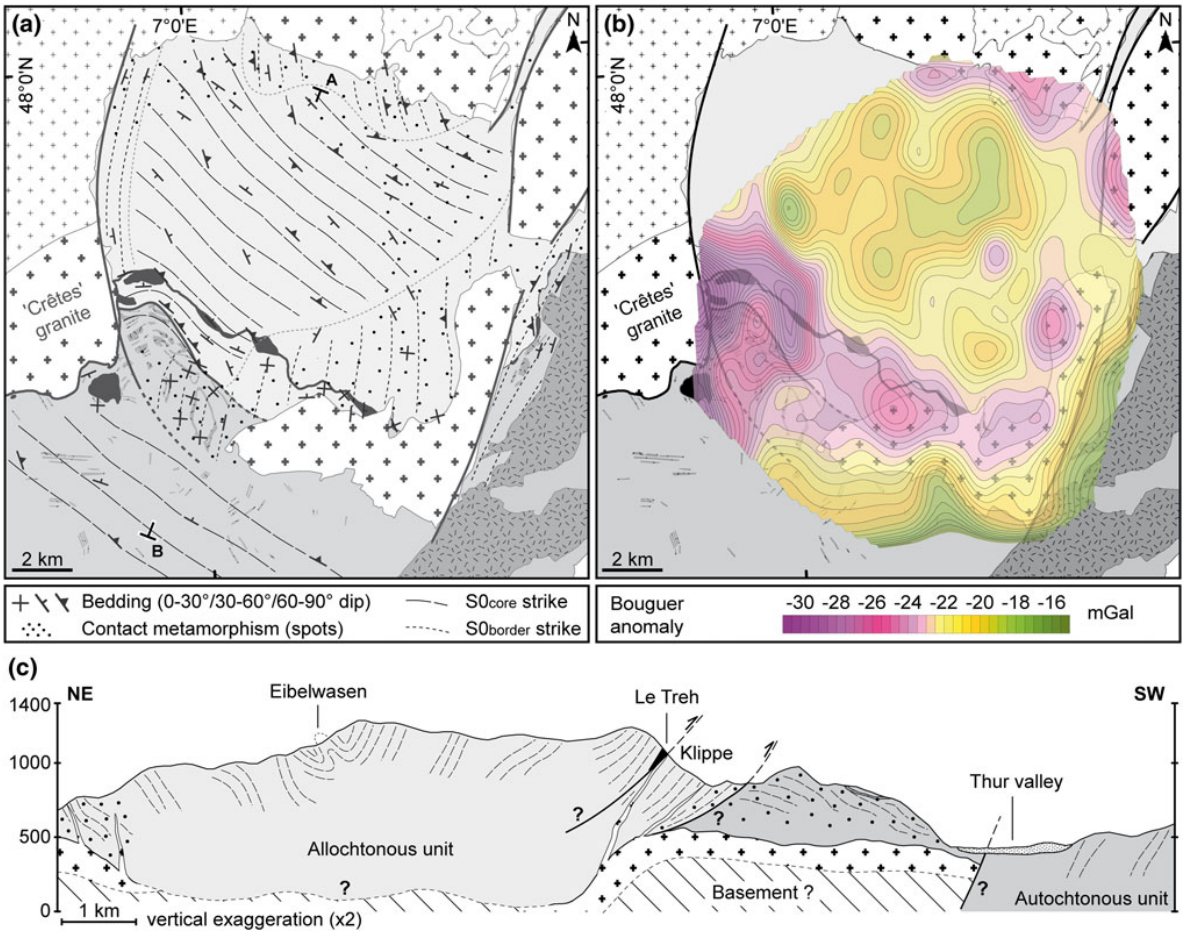

Fig. 5 **a** Structural and **b** Bouguer anomaly maps of the southern Vosges. **c** Interpretative cross-section through the Klippen Belt. The shape of the granite at depth is drawn after gravity data

lineament within the southern Vosges. Gravity measurements were performed at 238 stations with an upgraded Lacoste-Romberg gravimeter (sensibility: 2 μGal). The map was calculated using a density of 2.67 g cm^{-3} for the Bouguer corrections. Terrain correction was calculated using a digital elevation model with a grid spacing of 75 m, to a maximum radius of 22 km. The station density is about 1.2 station/km^2. The dataset was converted into the International Gravity Standardization Net 1971 (IGSN71) system.

The core of the allochtonous unit corresponds to a zone of relatively high density (Fig. 5b). It is potentially related to a thick pile of sediments. By contrast, the border of the allochtonous unit is related to zones of lower density that nearly coincide with the surface exposures of the surrounding granitic rocks (Fig. 5b). Similarly, the Klippen Belt is located on a low-density zone which can be correlated with a NW–SE trending branch of the 'Crêtes' granite. It means that a granitic ridge occurs below the Klippen Belt and that the major boundary between the granite and the allochtonous sedimentary unit is slightly shifted towards the NE with respect to the surface boundary (Fig. 5c). It is also consistent with field observations showing that the roof of the 'Crêtes' granite is sub-horizontal. A similar observation can be made for the NNE–SSW branch of the granite body. The associated gravity anomaly being shifted towards the West, it is inferred that the 'Crêtes' granite extends farther West beneath the allochtonous unit (Fig. 5b).

Petrology and geochemistry of gabbroic rocks

Analytical techniques

Detailed mapping of the various Klippen was undertaken in order to carefully collect samples for geochemical analyses.

Out of twenty four gabbro and dolerite samples, only two turned out to show fresh pyroxene in thin section (K1-30A and K2-21A). Accordingly, mineral compositions for these two gabbro samples were determined using a CAMECA SX 50 electron microprobe at BRGM Orléans, with accelerating voltage of 15 kV and beam current of 12 nA. Whole-rock compositions for six relatively fresh gabbro samples were analysed at the University of Strasbourg. Fusion technique with lithium tetraborate was used and the molten bead was then digested in a weak nitric acid solution. Major elements were analysed by inductively coupled plasma atomic emission spectrometry (ICP-AES), while trace elements were determined by ICP mass spectrometry (ICP-MS). Mineral analyses are reported in Fig. 6 and Table 2, and whole-rock data are shown in Fig. 7 and Table 3.

Mineral chemistry

Gabbro consists of approximately equal proportions of relatively fresh clinopyroxene and sericitized plagioclase. It shows an equigranular to inequigranular texture, with large (1–2 mm in size) plagioclase grains and medium to large (0.5–1.5 mm in size) clinopyroxene crystals that host some rounded plagioclase inclusions.

Clinopyroxene composition corresponds to diopside (Fig. 6a; Table 2) with a high Mg# (0.76–0.82) and does not preserve any core to rim chemical zoning. Minor element composition of clinopyroxene shows moderate Al_2O_3 (2.4–4.9 wt%; $Al^{IV} = 0.10–0.30$), moderate to low TiO_2 (0.39–1.05 wt%), and low Cr_2O_3 ($\leq$0.22 wt%) and Na_2O (0.20–0.49 wt%). Both matrix plagioclase and plagioclase inclusions have a homogenous composition (Fig. 6b; Table 2), ranging from labradorite (An_{64}) to andesine (An_{37}). Similarly to pyroxene, plagioclase crystals do not exhibit chemical zoning.

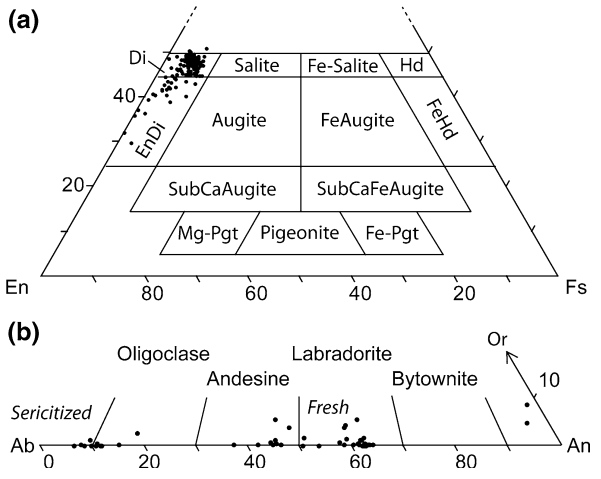

Fig. 6 Mineral chemistry of **a** pyroxene and **b** plagioclase from gabbro samples. Mineral abbreviations follow IUGS recommendations after Kretz (1983)

Whole-rock geochemistry

Major element composition of gabbro shows weak variations of SiO_2 content (48–54 wt%) and Mg# (0.69–0.76). The rare earth element (REE) patterns (Fig. 7a) normalised to chondrite (Boynton 1984) are generally characterised by Light-REE depletion ($La_N/Sm_N = 0.20–0.71$), Eu positive anomalies ($Eu/Eu^* = 1.27–1.69$) and nearly flat Heavy-REE trends ($Dy_N/Yb_N = 1.28–1.35$). Only one sample (K3-14A) differs in having high concentrations of CaO, MnO, TiO_2 and ΣREE, and low concentrations of Al_2O_3, Na_2O and Ba (Fig. 7; Table 3). This sample is also characterised by a weak negative Eu anomaly ($Eu/Eu^* = 0.82$). In primitive mantle-normalised diagrams (Sun and McDonough 1989), some samples show Th and Nb anomalies. They exhibit pronounced positive Ba and Sr anomalies, enrichment in Th, U and Eu, and depletion in Zr and Hf relative to primitive mantle (Fig. 7b).

Geochronology

U–Pb zircon dating

Approximately, 10 kg of gneiss were crushed and sieved, and the 100–315 µm fraction was processed using a Frantz magnetic separator and heavy liquids. Zircons were finally hand-picked under a binocular microscope. U–Pb zircon analyses were carried out at BRGM Orléans using a LASER ablation system coupled with a Neptune multi-collector ICP-MS (TermoFisherScientific). A new CETAC 213 nm UV laser was used allowing the U/Pb fractionation to be significantly reduced. The MC-ICP-MS was equipped with a multi-ion counting system (MIC) operating in static mode; all masses of interest were recorded simultaneously (^{202}Hg, ^{204}Pb, ^{206}Pb, ^{207}Pb, ^{208}Pb on ion counters, and ^{232}Th, ^{238}U on Faraday cup collectors). Isotope ratios were normalised using the zircon standard 91500 from Ontario (1,065 ± 1 Ma; Wiedenbeck et al. 1995). Detailed analytical conditions are described in Cocherie and Robert (2008) and Cocherie et al. (2009).

Sample K2-16B is a gneiss which was collected at the Klippe (Fig. 2c) cropping out near the locality Runsche [47°56′12.351″N; 6°58′37.17″E]. It belongs to a several m-scale block entirely surrounded by siliceous pelite and is therefore considered as representative for the continental basement found in the Klippen Belt. In thin section, coarse-grained quartz–K-feldspar–plagioclase–muscovite lenses are surrounded by brownish biotite-rich layers (Fig. 8a). Large secondary chlorite is common and small garnet is

Table 2 Representative mineral analyses of gabbro from the Vosges Klippen Belt

Mineral	Plagioclase			Clinopyroxene	
	Fresh	Fresh	Sericitized		
Sample	K2-21A	K2-21A	K2-21A	K1-30A	K2-21A
SiO_2	52.85	56.99	64.59	50.79	50.70
TiO_2	0.02	0.01	0.01	0.87	0.76
Al_2O_3	29.99	27.39	22.39	3.45	3.87
Cr_2O_3	0.00	0.06	0.00	0.01	0.10
FeO^T	0.17	0.18	0.01	6.59	6.79
MnO	0.00	0.06	0.00	0.35	0.24
MgO	0.02	0.09	0.00	14.53	14.90
CaO	13.40	9.32	3.15	24.02	23.45
Na_2O	4.41	6.30	9.93	0.35	0.37
K_2O	0.02	0.23	0.08	0.02	0.00
Total	100.90	100.60	100.20	101.00	101.20
Cations calculated of the basis of 8 O for plagioclase and 6 O for pyroxene					
Si	2.37	2.54	2.84	1.88	1.87
Ti	0.00	0.00	0.00	0.02	0.02
Al^{IV}	1.59	1.44	1.16	0.15	0.17
Cr	0.00	0.00	0.00	0.00	0.00
Fe^{2+}	0.01	0.01	0.00	0.20	0.21
Mn	0.00	0.00	0.00	0.01	0.01
Mg	0.00	0.01	0.00	0.80	0.82
Ca	0.65	0.45	0.15	0.95	0.92
Na	0.38	0.54	0.85	0.03	0.03
K	0.00	0.01	0.01	0.00	0.00
Σcations	5	5	5	4	4
Mg#				0.80	0.80
An	62.6	44.4	14.8		

FeO^T = Total Fe expressed as FeO

Mg# = moles of cations $Mg/(Mg + Fe^T)$

An = anorthite content of plagioclase (mol.%)

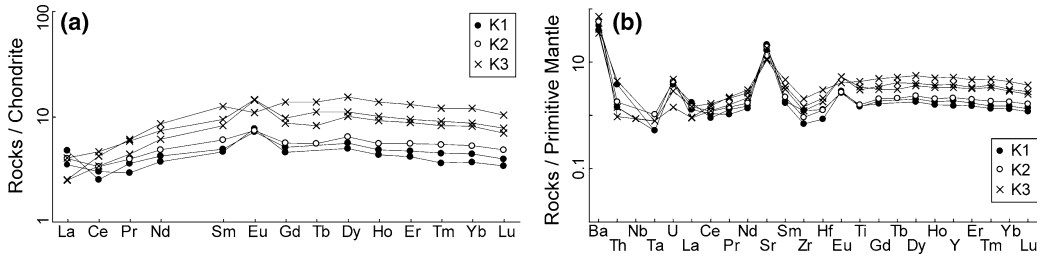

Fig. 7 Chondrite and primitive mantle-normalised trace element compositions of gabbro. Normalization after Boynton (1984) and Sun and McDonough (1989), respectively

also present. Accessory minerals include tourmaline and zircon, the latter being mostly found within the biotite-rich layers (Fig. 8a inset).

Zircon crystals extracted from this sample are clear, mostly anhedral and poorly elongated (200–250 μm in size). Prismatic faces are only rarely observed and cracks are visible in some grains. Cathodoluminescence images reveal common patchy or oscillatory zoning and some rim overgrowths (Fig. 8b). U–Pb geochronological results are listed in Table 4 and plotted in Fig. 9 using Ispolot/Ex 3.1 program (Ludwig 2004). Sixteen analyses were performed on nine zircon grains. Only one grain yielded a relatively young concordant age of 575 ± 29 Ma (Fig. 9b). Besides, several inherited ages are documented by older concordant analyses or Discordias. The oldest $^{207}Pb^*/^{206}Pb^*$ age is given by the 1.1 spot analysis at 3,206 ± 19 Ma. More importantly, analyses from grains 1 and 3 (3.2 and 3.3) define a clear trend which does not pass through the origin. The upper intercept at 3,467 ± 44 Ma (MSWD = 1.4) is interpreted as the crystallisation age of grains 1 and 3,

Table 3 Major and trace element compositions of gabbro from the Vosges Klippen Belt

Sample	K1 17D	K1 30A	K2 21A	K3 14A	K3 30A	K3 30B
Major oxides (wt%)						
SiO_2	52.00	52.20	48.40	50.80	52.60	53.90
TiO_2	0.29	0.30	0.31	0.86	0.60	0.68
Al_2O_3	17.63	20.17	16.58	10.93	13.79	15.42
$Fe_2O_3^T$	5.76	5.25	7.01	8.10	7.73	7.30
MnO	0.13	0.12	0.12	0.18	0.15	0.16
MgO	8.98	6.71	10.80	11.00	9.93	8.10
CaO	9.92	7.67	7.67	13.44	9.32	8.88
Na_2O	2.94	2.98	3.24	1.50	2.85	3.17
K_2O	0.99	1.98	0.96	1.07	0.90	1.46
P_2O_5	0.10	bd	bd	bd	bd	bd
LOI	2.15	1.99	3.03	1.29	1.41	1.53
Total	100.90	99.36	98.12	99.17	99.27	100.59
Mg#	0.76	0.72	0.75	0.73	0.72	0.69
Trace elements (ppm)						
Ba	327	260	371	226	272	464
Rb	52	100	47	68	57	89
Cs	18	29	8	56	6	39
Sr	447	355	402	238	227	382
Pb	5	7	9	7	6	9
Th	0.32	0.12	0.15	0.12	0.37	0.08
U	0.08	0.08	0.09	0.1	0.06	0.03
Zr	13	8	10	22	16	13
Nb	bd	bd	bd	bd	0.08	bd
Y	8	8	10	22	16	14
Co	33	25	38	37	35	30
V	143	109	156	360	214	241
Ni	74	71	125	81	55	44
Cr	250	430	440	1,880	560	530
Zn	60	120	70	90	60	60
Ta	0.02	0.02	0.04	0.03	0.03	0.03
Hf	0.38	0.25	0.37	0.89	0.62	0.53
REEs						
La	0.82	1.12	0.94	0.59	0.95	0.58
Ce	1.82	1.52	2.01	2.53	2.80	2.06
Pr	0.26	0.32	0.35	0.54	0.52	0.39
Nd	1.70	1.90	2.18	3.85	3.33	2.75
Sm	0.72	0.68	0.88	1.85	1.38	1.21
Eu	0.40	0.43	0.41	0.61	0.81	0.80
Gd	1.00	0.90	1.10	2.70	1.90	1.70
Tb	bd	bd	0.20	0.50	0.40	0.30
Dy	1.37	1.21	1.56	3.74	2.67	2.44
Ho	0.27	0.24	0.31	0.76	0.56	0.51
Er	0.75	0.66	0.88	2.07	1.50	1.40
Tm	0.09	0.07	0.11	0.29	0.22	0.20
Yb	0.69	0.60	0.82	1.96	1.40	1.31
Lu	0.07	0.06	0.09	0.25	0.19	0.17
La_N/Sm_N	0.71	1.03	0.67	0.20	0.43	0.30
Dy_N/Yb_N	1.33	1.35	1.27	1.28	1.28	1.25
Eu/Eu*	1.43	1.67	1.27	0.83	1.52	1.69
εNd		+12.6	+11.3			

FeO^T = Total Fe expressed as Fe_2O_3

Mg# = molar $Mg/(Mg + Fe^T)$; $Eu/Eu^* = Eu_N/(Sm_N \times Gd_N)^{0.5}$

LOI loss on ignition, *bd* below detection limit

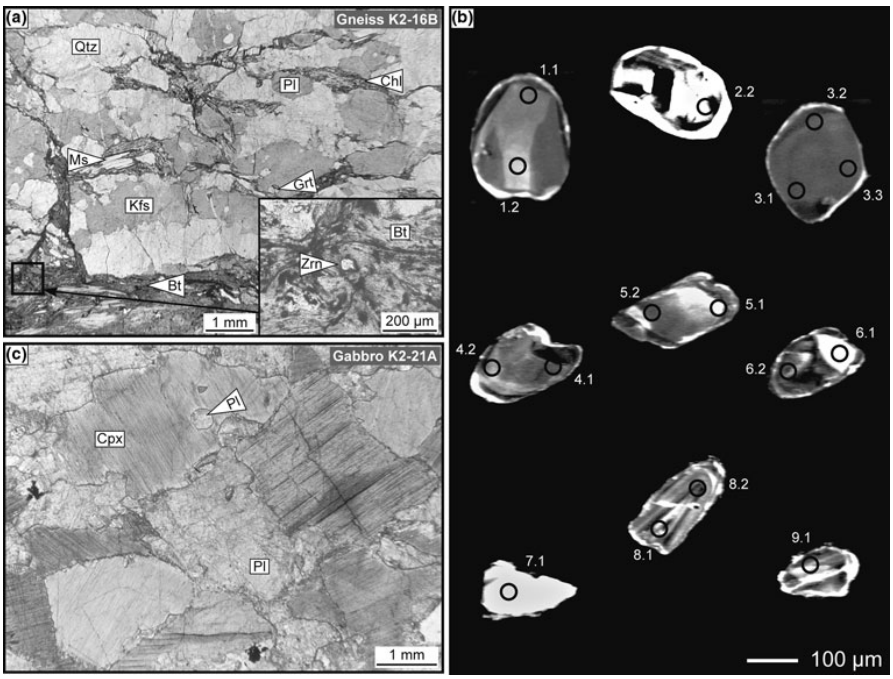

Fig. 8 Representative images of rock samples and zircon crystals used for geochronology. **a** Photomicrograph of gneiss sample K2-16B, and typical position of zircon within the matrix (inset). **b** Cathodoluminescence images of analysed zircon crystals. Spot locations refer to analyses listed in Table 4. **c** Photomicrograph of gabbro sample K2-21A showing possible plagioclase inclusions in clinopyroxene

while the lower intercept could document partial opening of the U–Pb system at 1,918 ± 38 Ma considering that the third spot analysis of grain 3 (3.1) reflects a recent slight Pb* loss (Fig. 9a). Grain 8 is younger but also of Archaean age, the 8.1 spot analysis being perfectly concordant at 2,591 ± 15 Ma (Table 4). In addition, both analyses of the same grain (8.2 and 8.1) define a lower intercept at 1,952 ± 15 Ma which could be related to the above-mentioned event at 1,918 ± 38 Ma (Fig. 9a, b). Therefore, a significant event was recorded at about 1,945 Ma. A second Palaeo-proterozoic event is also precisely defined at 2,090 ± 10 Ma by an upper intercept (MSWD = 0.74) of a Discordia anchored at the origin and derived from the sub-concordant 5.1, 5.2 and 3.1 spot analyses (Fig. 9b). The other analysed zircon grains could be of Archaean origin but are too discordant to give reliable ages.

Sm–Nd dating

Approximately, 10 kg of gabbro were crushed and sieved, and the 100–160 µm fraction was processed using a Frantz magnetic separator after removal of the magnetic fraction. Plagioclase and pyroxene concentrates were further purified by hand-picking under a binocular microscope. Approximately, 100 mg of plagioclase and pyroxene concentrates were dissolved. REE extraction and separation between Sm and Nd was performed using ion exchange columns following the method of Richard et al. (1976). Whole-rock concentrations of Sm and Nd were measured by ICP-MS at ACME Laboratories (Vancouver), and mineral concentrations were measured on a Finnigan MAT 261 mass spectrometer at BRGM Orléans. The Nd isotopic ratios were all obtained from a Finnigan MAT 262 mass spectrometer at BRGM Orléans. The decay constant used for Sm is $\lambda^{147}\mathrm{Sm} = 6.54\ 10^{-12}\ \mathrm{year}^{-1}$.

Sample K2-21A is a gabbro which was collected at the Klippe (Fig. 2c) cropping out near the locality Runsche [47°56′11.41″N; 6°59′5.64″E]. In thin section, large zones of sericitized plagioclase alternate with clinopyroxene that tends to form aggregates, and few chlorite veins occur. Rounded inclusions of plagioclase in pyroxene are observed (Fig. 8c), but small pyroxenes are also found within plagioclase crystals. This sample was selected for age dating because it does not show significant replacement of pyroxene by greenish amphibole.

The Nd isotope data are presented in Table 5 and Fig. 10. The Sm–Nd WR-mineral isochron yields an age of 372 ± 18 Ma (MSWD = 0.043) which is interpreted as the igneous cystallisation of the gabbro. The $^{143}\mathrm{Nd}/^{144}\mathrm{Nd}$ initial ratio of 0.51254 ± 29 together with the initial

Table 4 LA-MC-ICP-MS U–Pb zircon data for gneiss sample K2-16B

Grain point	U (ppm)	Th (ppm)	Th/U	$^{206}Pb^*$ (ppm)	$^{206}Pb/^{204}Pb$	$f_{206\%}$[2]	Radiogenic ratios							Age (Ma)						
							$^{206}Pb/^{238}U$	±[1]	$^{207}Pb/^{2351}$	±[1]	$^{207}Pb/^{206}Pb$	±	*r*	$^{206}Pb/^{238}U$	±[1]	$^{207}Pb/^{235}U$	±[1]	$^{207}Pb/^{206}Pb$	±[1]	Conc. %[3]
Gneiss K2-16B																				
1.1	213	17	0.08	104	17,665	0.070	0.5652	0.0046	19.745	0.199	0.2534	0.0015	0.811	2,888	19	3,079	10	3,206	9	90
1.2	104	9	0.09	47	7,681	0.160	0.5288	0.0038	17.557	0.195	0.2408	0.0020	0.653	2,736	16	2,966	11	3,125	13	88
2.2	70	19	0.27	5	–	–	0.0887	0.0006	0.724	0.007	0.0592	0.0004	0.737	548	4	553	4	575	14	95
3.1	574	8	0.01	172	12,091	0.116	0.3458	0.0039	6.176	0.090	0.1296	0.0012	0.772	1,914	19	2,001	13	2,092	16	92
3.2	446	5	0.01	145	76,246	0.018	0.3768	0.0029	7.471	0.066	0.1438	0.0006	0.882	2,061	14	2,170	8	2,273	7	91
3.3	208	3	0.01	70	–	–	0.3908	0.0045	8.745	0.112	0.1623	0.0009	0.907	2,127	21	2,312	12	2,480	9	86
4.1	324	29	0.09	120	59,769	0.024	0.4278	0.0031	9.639	0.081	0.1634	0.0007	0.856	2,296	14	2,401	8	2,491	7	92
4.2	212	24	0.11	77	10,528	0.134	0.4244	0.0042	9.823	0.123	0.1679	0.0013	0.790	2,280	19	2,418	11	2,536	13	90
5.1	81	20	0.25	27	–	–	0.3868	0.0034	6.872	0.069	0.1289	0.0006	0.874	2,108	16	2,095	9	2,082	9	101
5.2	227	74	0.33	72	–	–	0.3669	0.0032	6.569	0.063	0.1299	0.0005	0.899	2,015	15	2,055	8	2,096	7	96
6.1	102	6	0.06	37	–	–	0.4252	0.0040	9.797	0.117	0.1671	0.0012	0.797	2,284	18	2,416	11	2,529	12	90
6.2	560	17	0.03	99	23,577	0.060	0.2035	0.0084	4.250	0.183	0.1515	0.0019	0.959	1,194	45	1,684	35	2,363	21	51
7.1	35	5	0.14	13	7,356	0.191	0.4481	0.0065	9.637	0.180	0.1560	0.0018	0.775	2,387	29	2,401	17	2,412	20	99
8.1	243	28	0.11	104	–	–	0.4940	0.0042	11.811	0.112	0.1734	0.0008	0.888	2,588	18	2,590	9	2,591	7	100
8.2	242	15	0.06	88	23,891	0.059	0.4207	0.0049	8.684	0.117	0.1497	0.0010	0.871	2,263	22	2,305	12	2,343	11	97
9.1	198	28	0.14	81	20,592	0.067	0.4732	0.0047	10.826	0.127	0.1659	0.0010	0.851	2,498	21	2,508	11	2,517	10	99

[1] Uncertainties given at 1σ level

[2] $f_{206\%}$ denotes the percentage of ^{206}Pb that is common Pb, using ^{204}Pb correction (Stacey and Kramers 1975)

[3] Concordancy %, 100% denotes a concordant analysis

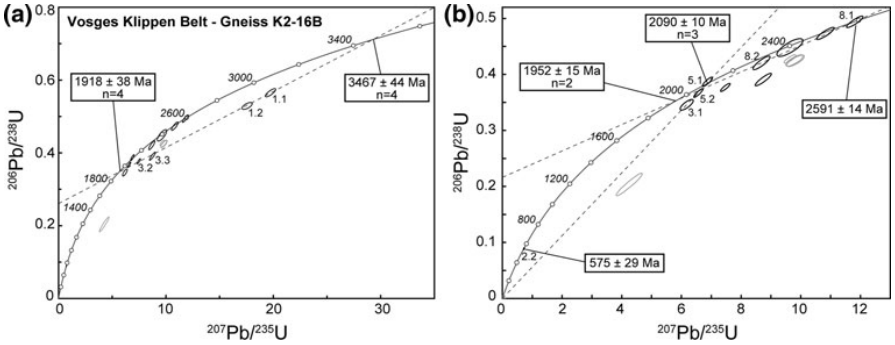

Fig. 9 **a**, **b** U–Pb Concordia diagrams with age results for gneiss sample K2-16B from the Vosges Klippen Belt. *Black ellipses* denote concordant analyses or data used for Discordia calculations. Number of analyses used for Discordia calculations are indicated. *Error ellipses* are plotted at 2σ level

Table 5 Sm and Nd concentrations, and isotopic ratios of gabbro sample K2-21A

Material	Sm (ppm)	Nd (ppm)	$^{147}Sm/^{144}Nd$	$^{143}Nd/^{144}Nd$	2σ
K2-21A					
Whole rock	0.99	2.16	0.27680	0.513220	0.000007
Plagioclase	0.17	0.59	0.17189	0.512964	0.000010
Pyroxene	1.17	2.75	0.25799	0.513173	0.000008
(Magnetic fraction)	0.89	2.34	0.23069	0.513049	0.000008

$\varepsilon_{Nd} = +11.3$ suggest that the Klippen Belt gabbro was derived from a depleted mantle source. It should be noted that the whole-rock chemical analysis does not plot between the plagioclase and pyroxene data, probably as a result of an underestimated clinopyroxene ratio (Fig. 10). It is attributed to the presence of plagioclase inclusions in clinopyroxene (Fig. 8c).

Discussion

Significance of the southern Vosges Klippen Belt

Lithological significance

Detailed mapping and petrographic observations provide constraints on the origin of the lithologies from the Klippen Belt. The occurrence of serpentinized spinel-harzburgite and of both types of ophicalcite (OC1 and OC2, Fig. 4a) points to an environment involving an altered and exhumed lithospheric mantle subsequently eroded and deposited in coarse-grained sediments. The mantle rocks are associated with a significant amount of gabbro. In addition, the observed basement lithologies (Fig. 4c, d) suggest that material from the continental crust was mixed with mafic rocks. Pebbles of oceanic and continental rocks are also found in a polymictic conglomerate (Fig. 4e), and all these lithologies are overlain by fine-grained siliceous deposits.

This lithological succession involving exhumed mantle, gabbroic intrusions and sedimentary breccias sealed by deep marine sediments is typical for Ligurian Tethys ophiolites (Lemoine et al. 1987). More generally, it could be considered to represent a slow-spreading environment known as an ocean–continent transition zone (OCT). In such a setting, the exhumed mantle is commonly brecciated and deposited in neighbouring depressions as a result of mass flows on the slopes of submarine cliffs (Tricart and Lemoine 1983). An OCT may also be characterised by the presence of allochtonous blocks of the continental upper crust over the exhumed mantle (Froitzheim and Manatschal 1996), which could explain the occurrence of large gneissic blocks in the Klippen Belt. In this view, the polymictic conglomerate could be the result of submarine erosion of the juxtaposed continental and oceanic lithologies. Additionally, some authors have demonstrated that fossil OCT-type successions can be preserved inside orogenic belts, such as in the Western Alps (e.g. Manatschal and Müntener 2009; Beltrando et al. 2010). These arguments suggest that the southern Vosges Klippen Belt may correspond to a dismembered fragment of the distal part of an OCT.

Tectonic significance

The tectonic significance of the Klippen Belt can be discussed using the distinction between the western (LK1) and the eastern (LK2) Klippen Belt already introduced by Schneider et al. (1990). The present work shows that a significant discontinuity occurs to the South of the western Klippen Belt. It marks the boundary between (1) the Klippen and the surrounding allochtonous sediments which show a folded NW–SE striking bedding, and (2) sedimentary and volcanic rocks of the autochtonous unit which

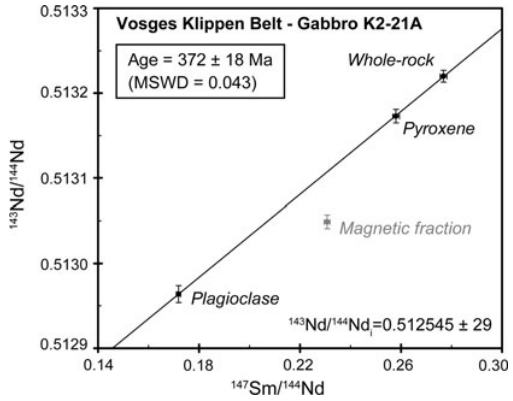

Fig. 10 Sm–Nd isochron for gabbro sample K2-21A from the Vosges Klippen Belt

preserve a flat-lying N–S striking bedding (Fig. 5a). More precisely, NW–SE trending upright folds affect the core of the allochtonous unit, whereas the Klippen Belt and the southern allochtonous sediments show consistently NE-dipping bedding planes (Fig. 5c). Several authors (Wickert and Eisbacher 1988; Schneider et al. 1990; Krecher and Behrmann 2007) have observed shear criteria indicating thrusting along these NE-dipping planes. It is therefore proposed that the discontinuity represents a thrust surface which allowed to emplace the allochtonous unit onto the autochtonous unit (Fig. 5c).

Deformation involving folding and thrusting can be observed in the allochtonous unit. In the Rhenohercynian fold and thrust belt, Oncken et al. (1999) demonstrated that contrasted deformation styles may depend, among other parameters, on the basement topography of the former sedimentary basin. In our case, gravity data suggest the presence of a NW–SE low-density ridge below the Klippen Belt (Fig. 5b). It is in line with the idea that deformation could have been controlled by the pre-existing structures. Structural and geophysical arguments therefore support a tectonic origin for the western Klippen Belt (LK1) which may represent a large-scale duplex structure (Fig. 5c). In this view, the exotic rocks do not correspond to actual Klippen, but to the discontinuous basal level of a thrust within the allochtonous unit. Only the Thalhorn body (Fig. 2b) which is entirely surrounded by sediments of the autochtonous unit would represent a true Klippe. By contrast, the eastern Klippen Belt lacks a clear lithological succession and chiefly corresponds to small lenses of conglomerate with rare exotic material. In addition, the structural pattern is similar in the eastern Klippen Belt, and in the surrounding allochtonous and autochtonous units suggesting that no structural discontinuity occurs (Fig. 2g, h). This part of the Klippen Belt (LK2) therefore better corresponds to blocks which were resedimented during the Middle to Upper Visean (Schneider 1990).

Chronological constraints on the NE–SW shortening event have already been proposed. The associated folding is thought to be nearly contemporaneous with contact metamorphism generated by the surrounding 'Crêtes' granite at 340 ± 1 Ma (Schaltegger et al. 1996; Petrini and Burg 1998). It is confirmed by the common emplacement of associated microgranite intrusions parallel to the subvertical NW–SE striking bedding (Fig. 4f). In the western Klippen Belt, these intrusions have been dated at 339.5 ± 2.5 Ma (Schaltegger et al. 1996), further supporting the idea that the dominant deformation of the allochtonous unit occurred during the Middle Visean, i.e. at ca. 340 Ma. Because the western Klippen Belt is oriented parallel to the surrounding NW–SE striking sedimentary bedding (Figs. 2, 5a), it is therefore proposed that the exhumation of the base of the allochtonous unit is related to a Middle Visean NE–SW shortening event.

Geochemical significance

Geochemical data from gabbroic rocks are used to discuss the possible geodynamic settings associated with the Vosges Klippen Belt. Major and trace element compositions of gabbro suggest that the rocks are of cumulative rather than residual origin. In addition, chondrite-normalised REE diagrams show LREE depletion followed by flat HREE profiles at 10 times chondrite values (Fig. 7a), and Nd isotope geochemistry reveals highly positive $\varepsilon_{Nd} = +11.3$ (Table 3). These observations are similar to those of typical N-MORB (Sun and McDonough 1989; Arevalo and McDonough 2010). Minor element composition of clinopyroxene and anorthite content in plagioclase (Fig. 6b) are similar to those of gabbros from the Mid-Altantic Rigde (ODP leg 153; Cannat et al. 1997) or from the Indian ridge (ODP leg 176; Niu et al. 2002). Whole-rock and isotope geochemistry is also comparable with results reported for the Early Devonian Lizard ophiolite (Davies 1984; Floyd 1984) which was interpreted as generated in a slow-spreading ridge environment (Roberts et al. 1993; Cook et al. 2002).

However, the primitive mantle-normalised trace element patterns show enrichment in Ba, Sr, Th, U and Eu (Fig. 7b). This can be explained by contamination of the mantle source by typical continental elements (e.g. Plank and Langmuir 1998), probably derived from fluids expelled from a subduction zone. Such contamination would not necessarily require significant Nb and Ta anomalies. Indeed, in western Pacific back-arc marginal basins, the geochemical influence of the subduction zone decreases with increasing distance from the subduction through, i.e. with increasing maturity of the basin. The resulting

primitive mantle-normalised trace element patterns show decreasing LREE enrichment and vanishing of the negative Nb and Ta anomalies (Auzende et al. 1990). Such basins are also characterised by isotopic compositions (ε_{Nd} and initial $^{143}Nd/^{144}Nd$ ratio) which are in the same range as those of N-MORB. According to these observations, it is proposed that gabbros from the Vosges Klippen Belt may have been emplaced in a mature spreading back-arc basin located relatively far from the subduction through.

Age significance

The Sm–Nd isochron on gabbro yields an age of 372 ± 18 Ma (Fig. 10), interpreted as its igneous crystallisation. Although more than 60 Ma can separate the opening of a basin from the age of the first sediments in an OCT (Wilson et al. 2001), the Sm–Nd age is in good agreement with the Famennian (374.5 ± 2.6–359.2 ± 2.5; Gradstein et al. 2004) record of the oldest sediments found in the southern Vosges (Maass and Stoppel 1982). This age also lies close to the $^{40}Ar/^{39}Ar$ biotite cooling age of 382 ± 20 Ma obtained on a gneiss pebble from the autochtonous unit (Boutin et al. 1995) which could indicate exhumation of the continental crust during rifting. In summary, the rifting event evidenced by OCT-type rocks of the Klippen Belt can be considered to have occurred during the Late Devonian.

Numerous large blocks of continental basement are found in the Klippen Belt. One sample has been studied in order to precise the origin of the basement and in order to evidence a possible eo-Variscan metamorphic overprint. U–Pb zircon geochronology indicates a range of Neoproterozoic to Archaean ages (Fig. 9). Because the coarse-grained texture of the gneiss sample suggests that it represents a weakly deformed metagranite, the ca. 575 Ma age is interpreted as the igneous crystallisation of the protolith. It corresponds to a well-documented episode of continental crust production across the Variscan Belt of Europe (e.g. Zeh et al. 2001). In addition, inherited ages indicate thermal events at ca. 1,950, 2,100 and 3,500 Ma (Fig. 9). Some of these ages lie close to inheritance already reported at ca. 600, 1,900 and 2,000 Ma in metamorphic rocks of the central Vosges (Schaltegger et al. 1999), and at ca. 655 and 2,120 Ma in magmatic rocks of the southern Vosges (Schaltegger et al. 1996). The similar Precambrian ages therefore suggest that the central and southern Vosges probably belonged to the same continental block which was subsequently rifted during the Late Devonian. Consequently, the basement rocks juxtaposed with the oceanic material can either correspond to a shoulder of the nearby continental rifted margin, or to allochtonous blocks that are commonly reported in OCT environments.

Geodynamic evolution of the southern Vosges Mountains

Combined lithological, geochemical and geochronological data for the Vosges Klippen Belt indicate the opening of a basin during the Late Devonian (Fig. 11a). Significant thinning of a Neoproterozoic basement resulted in the formation of a rifted margin associated with an ocean–continent transition zone towards the South. Exhumed mantle and basic magmatism point to a slow-spreading environment with probable characteristics of a back-arc setting located relatively far from the subduction zone. The southern conjugate margin of the basin could be represented by Middle to Late Devonian sediments found farther to the South. There, the presence of trilobite, crinoid and ammonoid fauna (Chevillard 1866; Asselberghs 1926) in Famennian deposits indicates a platform environment, suggesting that this part of the margin was probably much less attenuated than the northern one (Fig. 11a).

The basin was subsequently filled by thick siliciclastic turbiditic series until the Lower Visean (Fig. 11b). This episode of flysch-type sedimentation was already associated with a closure of the system, as indicated by common sedimentary instabilities (Schneider 1990). Therefore, the northern part of the basin corresponded at that time to an important topographic high developed above an already existing thickened orogenic root (Schulmann et al. 2002). In the southern part of the basin flysch sediments are interstratified with abundant volcanic rocks, whereas the northern part of the basin clearly lacks volcanic material. Both areas can be considered as the proximal and distal parts of the same basin which showed increasing volcanic activity towards the South. It is supported by the occurrence of a plutonic complex (the 'Ballons' granitoids) to the South of the autochtonous unit. Conversely, the absence of volcanic rocks in the northern part has been explained by the possible existence of a topographic high between the two basins (Schneider 1990). This could be represented by a continental block isolated during rifting (Fig. 11b), a feature called 'upper-crustal megaboudin' by Davis and Hardy (1981). Considering that the gravity anomaly map reveals the presence of a prominent low-density block beneath the Klippen Belt, the proposed geodynamic reconstruction favours the occurrence of a basement high which was subsequently accreted to the inverted rifted margin (Fig. 11).

The deformation pattern in the southern Vosges indicates folding and thrusting of the allochtonous unit over the autochtonous one. Structural observations indicate that folding of the sedimentary basins occurred during the Middle Visean (Fig. 11c) and was nearly contemporaneous with the intrusion of granitic magmas in the basement (Petrini and Burg 1998). During the dominantly NE–SW horizontal compression event, slices from deep parts of the basin were exhumed and formed the Vosges Klippen Belt.

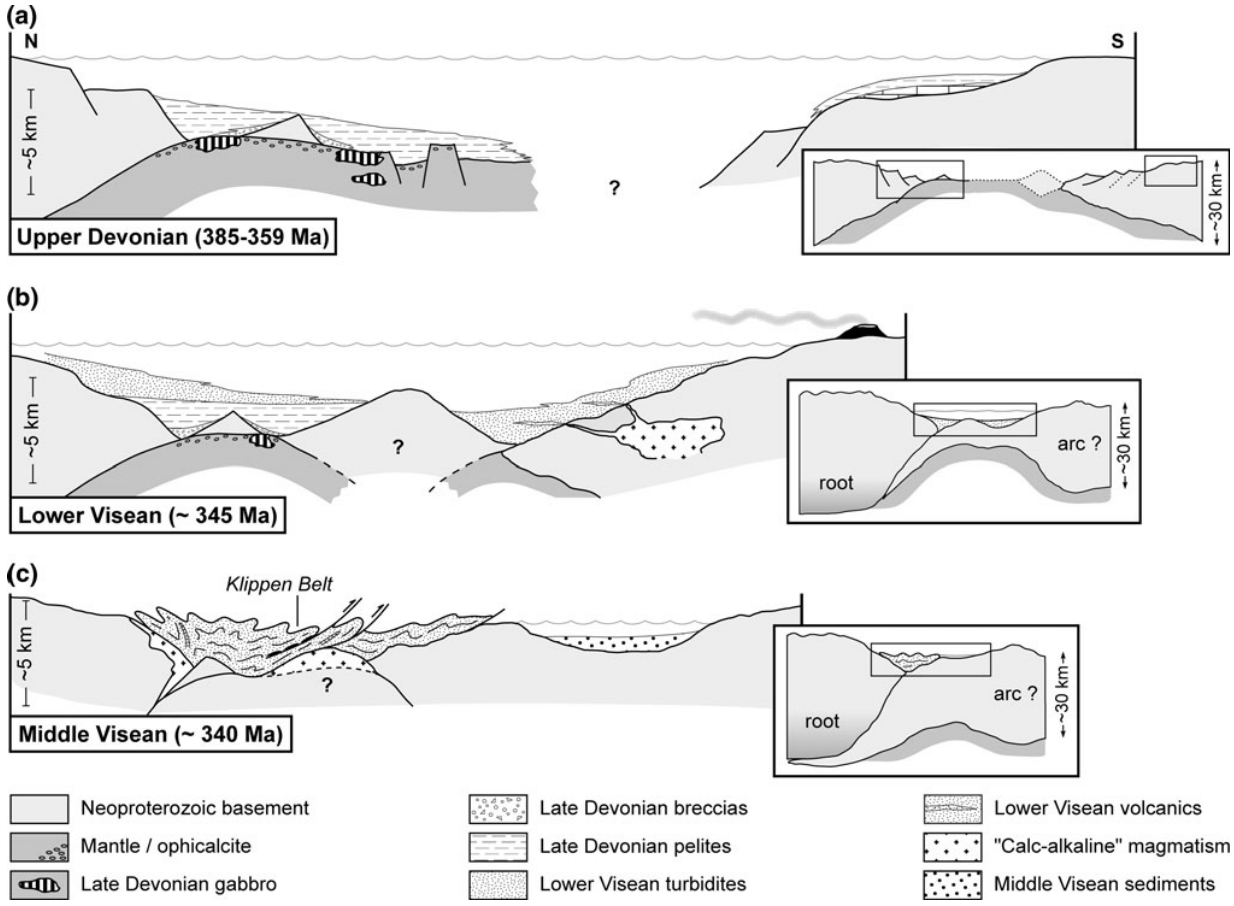

Fig. 11 A possible geodynamic scenario for the southern Vosges. **a** Late Devonian rifting and basin formation. **b** Lower Visean sedimentary (northern basin) and volcano-sedimentary (southern basin) deposits. **c** Middle Visean basin inversion, exhumation of the Klippen Belt and magmatism. Insets show the general framework from intracontinental rifting to final collision with the northern root zone

The coincidence of a gravity low with the thrust-related Klippen Belt may indicate the presence of a rigid basement obstacle at shallow depth (Fig. 11c). It is therefore proposed that the whole sedimentary basin was thrust over the rigid basement promontory, thereby producing strong deformation in the hinterland and an important deformation gradient towards the sole thrust. Because numerous microgranite sills are emplaced parallel to the folded bedding in sediments, this thrusting could have also been lubricated by syntectonic magmas (e.g. Hollister 1986).

Significance in the Variscan Belt of Europe

Origin of the southern Vosges basin

The basin evidenced in the southern Vosges could be related to several Variscan events. It could represent: (1) a late ramification of the Rhenohercynian basin or a back-arc basin related to the Rhenohercynian subduction, (2) a back-arc basin associated with the northern Saxothuringian subduction, or (3) a back-arc basin connected with the southern Palaeotethys subduction.

The suggested evolution involving inversion of Devonian–Early Carboniferous basin sequences and thrusting of allochtonous sedimentary units over autochtonous units bears similarities to a Rhenohercynian evolution (e.g. Holder and Leveridge 1986). There, Early Devonian ophiolites and sedimentary basins are inverted and covered by Middle Devonian to Early Carboniferous flysch sediments (Fig. 12). However, the geochemistry of gabbroic rocks indicates the influence of a subduction zone and probably rules out the origin of the Vosges basin as a late extension of the Rhenohercynian basin. Alternatively, because closure in the Rhenohercynian system starts in the Middle Devonian (Franke 1995), the Late Devonian Vosges basin could then be viewed as the associated back-arc system. Nevertheless, Currie et al. (2008)

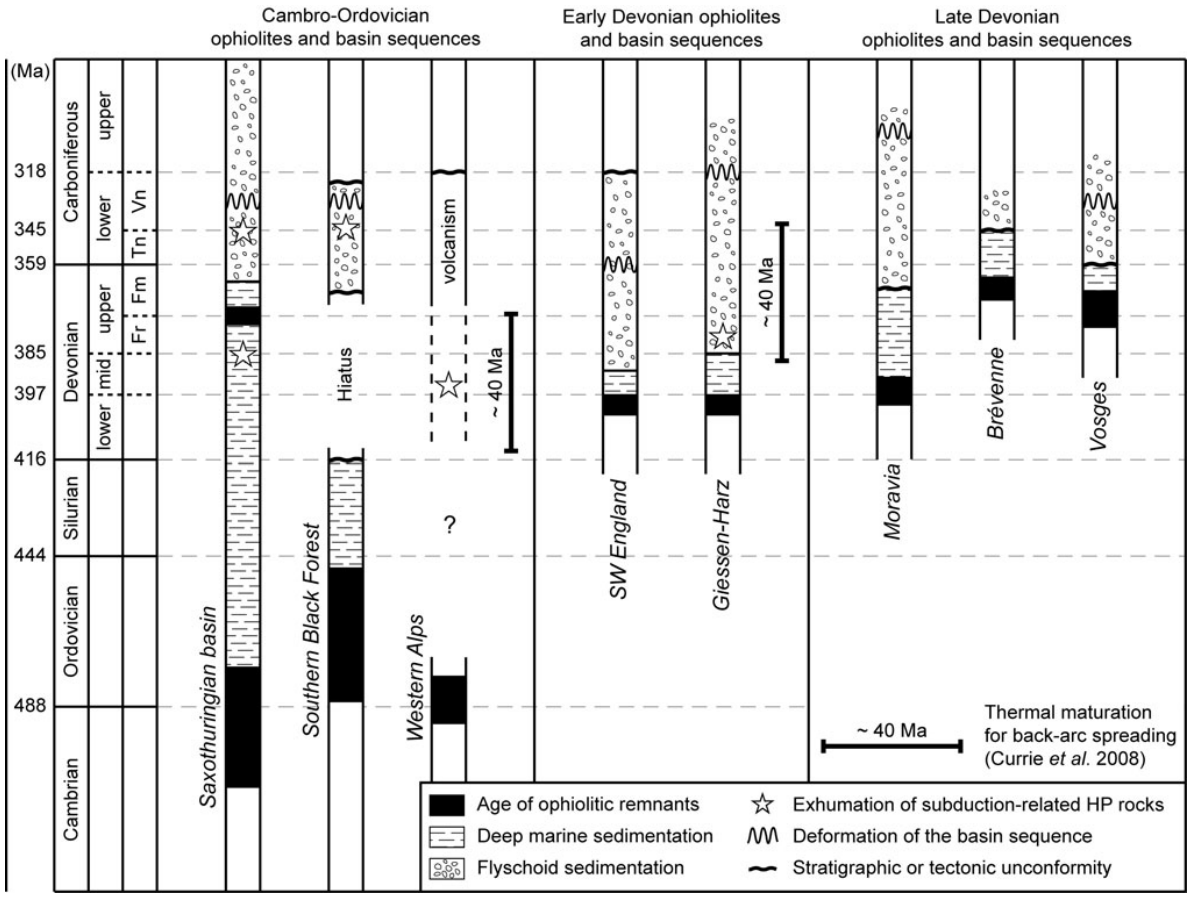

Fig. 12 Chronological relationships between the different types of Palaeozoic basin sequences. For references, see text

showed that a minimum of ~40 My is required to bring the 1,200°C isotherm to a depth of 60 km in a back-arc basin environment. A subduction of the Rhenohercynian basin is therefore more likely to trigger extension during the Carboniferous (Fig. 12). In addition, calc-alkaline magmatism at ca. 335 Ma in the northern Vosges (Altherr et al. 2000) most likely reflects the magmatic arc related to this event. The age of arc magmatism coincides with a major extension associated with partial melting and emplacement of sheeted intrusions in the southern high-grade core zone of the Vosges (Rey et al. 1992; Kratinová et al. 2007; Schulmann et al. 2009). It is therefore the central part of the Vosges Mountains that probably recorded the extensional and high temperature event associated with the southward subduction of the Rhenohercyian basin.

The timing of the northern Saxothuringian and the southern Palaeotethyan systems is markedly different from that of the Rhenohercyian one (Fig. 12). Both zones comprise Cambro-Ordovician ophiolitic remnants (e.g. Paquette et al. 1989; Bowes and Aftalion 1991; Kalt et al. 1994) covered by Ordovician to Silurian-Devonian sediments (Franke 1984; Hann and Sawatzki 1998), but also HP rocks exhumed during the Devonian (e.g. Timmermann et al. 2004; Guillot and Ménot 2009). These records indicate that Cambro-Ordovician basins started to be inverted in the Devonian (Fig. 12). Using the previously mentioned results of Currie et al. (2008), these evolutions could be concordant with the generation of back-arc basins during the Late Devonian (Fig. 12). Therefore, the southern Vosges basin probably represents a back-arc environment associated with the subduction of an Early Palaeozoic oceanic realm. It could be either the South-directed subduction of the Saxothuringian basin recognised to the North of the Vosges (Edel and Schulman 2009), or the North-directed subduction of the Palaeotethys Ocean proposed in the French Massif Central and in the Western Alps (Lardeaux et al. 2001; Guillot and Ménot 2009).

A tentative link

The present results can be compared to existing data for the Variscan massifs located to the South of the Vosges Mountains. In the Western Alps as well as in the French Massif Central (Monts du Lyonnais), Siluro-Devonian closure of an oceanic domain and HP metamorphism is documented (Lardeaux et al. 2001; Paquette et al. 1989). In addition, prolonged arc magmatism ranging from the Silurian up to the Carboniferous is proposed in the southern Black Forest (Hann et al. 2003; Hegner et al. 2001; Loeschke et al. 1998), and Late Devonian back-arc spreading is inferred from the Brévenne Séries in the NE French Massif Central (Pin and Paquette 1997; Leloix et al. 1999). Spatial, geochemical and geochronological constraints indicate that the southern Vosges fit in this geodynamic evolution, the only difference with the Brévenne Séries lying in the geochemical signature of basic rocks. Because the Brévenne Séries preserves a stronger geochemical influence of the subduction zone than the southern Vosges (Pin and Paquette 1997), the former can be considered as an incipient basin, whereas the latter may represent a mature, probably slightly older and larger basin. Consequently, the southern Vosges lithologies most likely correspond to a back-arc basin located within a continental block of Teplá-Barrandian–Moldanubian affinity, and resulting from the North-directed subduction of the Palaeotethys Ocean (e.g. Finger and Steyrer 1990).

More generally, it is proposed that Late Devonian back-arc basins which opened across Teplá-Barrandian–Moldanubian-type domains are linked with the subduction of the Palaeotethys Ocean during the general closure of the Variscan system. However, the back-arc basins recognised in Moravia (e.g. Patočka and Valenta 1996) and South Iberia (e.g. Ribeiro et al. 2010), which bears similarities to the Rhenohercynian zone, may have a different origin. Notwithstanding, the Late Devonian oceanic domains can be seen as small back-arc marginal basins which developed at the front of a large closing ocean. Such back-arc basins have also been proposed at the northern periphery of the Neotethys Ocean (e.g. Stampfli and Borel 2002). From that perspective, the Variscan system does not seem to have been much different from the more recent Neotethyan evolution.

Acknowledgments E.S. and A-S.T. kindly acknowledge funding by BRGM and Région Alsace. Field work was supported by the 'Programme de la carte géologique de France'. A. Aubert is thanked for help during zircon separation, D. Guinamant for assistance with the zircon mounts, P. Pepin for cutting large samples, M. Robert for LA-ICP-MS analyses, G. Morvan for producing CL images and G. Wille for help with the microprobe. Access to the bibliography was possible thanks to the outstanding collection held at the University of Strasbourg, and the careful work of the person in charge B. Kieffer. We are indebted to J. Honnorez for sharp comments on the manuscript. Reviews by J.R. Martínez Catalán and G. Eisbacher are greatly appreciated.

References

Altherr R, Holl A, Hegner E, Langer C, Kreuzer H (2000) High-potassium, calc-alkaline I-type plutonism in the European Variscides: northern Vosges (France) and northern Schwarzwald (Germany). Lithos 50:51–73

Arevalo RJ, McDonough WF (2010) Chemical variations and regional diversity observed in MORB. Chem Geol 271:70–85

Asselberghs E (1926) Sur l'existence du Famennien (Néodévonien) à Chagey (Belfort). Bulletin de la Société Géologique de France 26:67–74

Auzende J-M, Boespflug X, Bougault H, Dosso L, Foucher J-P, Joron J-L, Ruellan E, Sibuet J-C (1990) From intracratonic extension to mature spreading in back arc basins: examples from the Okinawa, Lau and Noth Fiji basins. Oceanol Acta 10:153–163

Azor A, Rubatto D, Simancas JF, González Lodeiro F, Martínez Poyatos D, Martín Parra LM, Matas J (2008) Rheic Ocean ophiolitic remnants in southern Iberia questioned by SHRIMP U–Pb zircon ages on the Beja-Acebuches amphibolites. Tectonics 27:TC5006

Ballèvre M, Bosse V, Ducassou C, Pitra P (2009) Palaeozoic history of the Armorican Massif: models for the tectonic evolution of the suture zones. Comptes Rendus Géoscience 341:174–201

Behr HJ, Engel W, Franke W, Giese P, Weber K (1984) The Variscan Belt in Central Europe: main structures, geodynamic implications, open questions. Tectonophysics 109:15–40

Beltrando M, Rubatto D, Manatschal G (2010) From passive margins to orogens: the link between ocean-continent transition zones and (ultra)high-pressure metamorphism. Geology 38:559–562

Boutin R, Montigny R, Thuizat R (1995) Chronologie K-Ar et $^{39}Ar/^{40}Ar$ du métamorphisme et du magmatisme des Vosges. Comparaison avec les massifs varisques avoisinants. Géologie de la France 1:3–25

Bowes DR, Aftalion M (1991) U–Pb isotopic evidence for early Ordovician and Late Proterozoic units in the Mariánské Lázně Complex, Central European Hercynides. Neues Jahrbuch für Mineralogie Abhandlungen 7:315–326

Boynton WV (1984) Cosmochemistry of the rare earth elements: meteorite studies. In: Henderson P (ed) Rare earth element geochemistry. Elsevier, Amsterdam, pp 63–114

Cannat M, Chatin F, Whitechurch H, Ceuleneer G (1997) Gabbroic rocks trapped in the upper mantle at Mid Atlantic ridge. Proc Ocean Drill Prog Sci Results 153:243–264

Chevillard MJL (1866) Trilobites du Dévonien du Mont de la Revenue, commune de Chagey, près Héricourt (Haute-Saône). Bulletin de la Société Géologique de France 24:124–129

Clark AH, Scott DJ, Sandeman HA, Bromley AV, Farrar E (1998) Siegenian generation of the Lizard ophiolite: U–Pb zircon age data for plagiogranite, Porthkerris, Cornwall. J Geol Soc Lond 155:595–598

Cocherie A, Robert M (2008) Laser ablation coupled with ICP-MS applied to U–Pb zircon geochronology: a review of recent advances. Gondwana Res 14:597–608

Cocherie A, Fanning CM, Jezequel P, Robert M (2009) LA-MC-ICPMS and multi-ion counting system, and SHRIMP U–Pb dating of complex zircons from quaternary tephras from the French Massif Central: magma residence time and geochemical implications. Geochim Cosmochim Acta 73:1095–1108

Coleman RG (1977) Ophiolites: ancient oceanic lithosphere? Springer, Berlin, p 229

Cook CA, Holdworth RE, Styles MT (2002) The emplacement of peridotites and associated oceanic rocks from the Lizard Complex, southwest England. Geol Mag 139:27–45

Corsin P, Mattauer M (1957) Quelques nouveaux gisements fossilifères du Massif des Ballons (Vosges méridionales). Comptes rendus sommaires de la Société Géologique de France 5:92–94

Corsin P, Ruhland M (1959) Les gisements à plantes du Viséen dans les Vosges méridionales. Comptes Rendus de l'Académie des Sciences 248:2145–2149

Coulon M, Fourquin C, Paicheler JC, Conil R, Lys M (1978) Stratigraphie du Viséen des Vosges méridionales et datations obtenues par l'étude de plusieurs niveaux à microfaunes et algues. Sciences Géologiques 31:77–93

Crowley QG, Floyd PA, Winchester JA, Franke W, Holland JG (2000) Early Palaeozoic rift-related magmatism in Variscan Europe: fragmentation of the Armorica Terrane Assemblage. Terra Nova 12:171–180

Currie CA, Huismans RS, Beaumont C (2008) Thinning of continental backarc lithosphere by flow-induced gravitational instability. Earth Planet Sci Lett 269:436–447

Davies GR (1984) Isotopic evolution of the lizard complex. J Geol Soc Lond 141:3–14

Davis GH, Hardy JJ (1981) The Eagle Pass detachment, southeastern Arizona: product of mid-Miocene listric normal faulting in the southern Basin and Range. Geol Soc Am Bull 92:749–762

Delbos J, Kœchlin-Schlumberger J (1866) Description géologique et minéralogique du département du Haut-Rhin, vol 1

Delesse A (1847) Mémoire sur la constitution minéralogique et chimique des roches des Vosges

Doubinger J, Ruhland M (1963) Découverte d'une faune de Chitinozoaires d'âge Dévonien au Treh (région du Markstein, Vosges méridionales). Comptes Rendus de l'Académie des Sciences 256:2894–2896

Dvořák J (1995) Moravo-Silesian Zone: Autochton—Stratigraphy. In: Dallmeyer D, Franke W, Weber K (eds) Pre-permian geology of Central and Western Europe

Edel J-B, Schulman K (2009) Geophysical constraints and model of the "Saxothuringian and Rhenohercynian subductions–magmatic arc system" in NE France and SW Germany. Bulletin de la Société Géologique de France 180:545–558

Falk F, Franke W, Kurze M (1995) Saxothuringian Basin: Autochton and Nonmetamorphic Nappe Units—stratigraphy, structure, and igneous activity. In: Dallmeyer D, Franke W, Weber K (eds) Pre-permian geology of Central and Western Europe

Finger F, Steyrer HP (1990) I-type granitoids as indicators of a late Paleozoic convergent ocean-continent margin along the southern flank of the central European Variscan orogen. Geology 18:1207–1210

Floyd PA (1984) Geochemical characteristics and comparison of the basic rocks of the Lizard Complex and the basaltic lavas within the Hercynian troughs of SW England. J Geol Soc Lond 141:61–70

Floyd PA (1995) Rhenohercynian Foldbelt: autochton and nonmetamorphic nappe units—igneous activity. In: Dallmeyer D, Franke W, Weber K (eds) Pre-permian geology of Central and Western Europe

Floyd PA SEC, Styles MT (1993) Igneous rocks of South-West England. Geological conservation review series. Chapman and Hall, London

Fluck P (1987) Apports de la "microcartographie" à divers points-clés de la géologie du socle vosgien. In: Colloque des Géologues et Géophysiciens du Socle Vosgien, Strasbourg, 7–11 October 1987, pp 11–14

Franke W (1984) Variszischer Deckenbau im Raume der Münchberger Gneismasse, abgeleitet aus der Fazies, Deformation und Metamorphose im umgebenden Paläozoikum. Geotektonische Forschungen 68:1–253

Franke W (1995) Rhenohercynian Foldbelt: autochton and nonmetamorphic nappe units—stratigraphy. In: Dallmeyer D, Franke W, Weber K (eds) Pre-permian geology of Central and Western Europe

Franke W (2000) The mid-European segment of the Variscides: tectonostratigraphic units, terrane boundaries and kinematic evolution. In: Franke W, Haak V, Oncken O, Tanner D (eds) Orogenic processes: quantification and modelling in the Variscan Belt, special publications, 179:35–63

Froitzheim N, Manatschal G (1996) Kinematics of Jurassic rifting, mantle exhumation, and passive-margin formation in the Austroalpine and Penninic nappes (eastern Switzerland). Geol Soc Am Bull 108:1120–1133

Gagny C (1962) Caractères sédimentologiques et pétrographiques des schistes et grauwackes du Culm dans les Vosges méridionales. Bulletin du Service de la Carte Géologique d'Alsace-Lorraine 15:139–160

Ganssloser M, Theye T, Wachendorf H (1996) Detrital glaucophane in graywackes of the Rhenohercynian Harz mountains and the geodynamic implications. Geol Rundsch 85:755–760

Gradstein F, Ogg J, Smith A (2004) A geologic time scale. Cambridge University Press, Cambridge

Guillot S, Ménot R-P (2009) Paleozoic evolution of the external crystalline massifs of the Western Alps. Comptes Rendus Géoscience 341:253–265

Hammel C (1996) Une faune nouvelle de trilobites (Brachymetopus, Namuropyge) dans le Viséen des Vosges du Sud. Conséquences stratigraphiques et paléoécologiques. Géobios 29:745–755

Hann HP, Sawatzki G (1998) Deckenbau und Sedimentationsalter im Grundgebirge des Südschwarzwalds/SW-Deutschland. Zeitschrift der deutschen geologischen Gesellschaft 149:183–195

Hann HP, Chen F, Zedler H, Frisch W, Loeschke J (2003) The Rand Granite in the southern Schwarzwald and its geodynamic significance in the Variscan belt of SW Germany. Int J Earth Sci 92:821–842

Hartley AJ, Otava J (2001) Sediment provenance and dispersal in a deep marine foreland basin: the Lower Carboniferous Culm Basin, Czech Republic. J Geol Soc 158:137–150

Hegner E, Chen F, Hann HP (2001) Chronology of basin closure and thrusting in the internal zone of the Variscan belt in the Schwarzwald, Germany: evidence from zircon ages, trace element geochemistry, and Nd isotopic data. Tectonophysics 332:169–184

Hladil J, Melichar R, Otava J, Galle A, Krs M, Man O, Pruner P, Cejchan P, Orel P (1999) The devonian in the Easternmost Variscides, Moravia: a holistic analysis directed towards comprehension of the original context. Abhandlungen der geologischen Bundesanstalt 54:27–47

Holder MT, Leveridge BE (1986) A model for the tectonic evolution of South Cornwall. J Geol Soc Lond 143:125–134

Hollister LH (1986) Melt-enhanced deformation: a major tectonic process. Geology 14:558–561

Janoušek V, Hanžl P, Aichler J, Pecina V, Erban V, Wilimský D, Žáček V, Mixa P, Buriánková K, Pudilová M, Chlupáčová M (2006) Contrasting petrogenesis of two volcanic suites in the devonian Vrbno group (Hrubý Jeseník Mts., Czech Republic). Geolines 20:57–59

Jung J (1928) Contribution à la géologie des Vosges hercyniennes d'Alsace. Mémoires du Service de la Carte géologique d'Alsace-Lorraine, vol 2, p 463

Kalt A, Hanel M, Schleicher H, Kramm U (1994) Petrology and geochronology of eclogites from the Variscan Schwarzwald (F.R.G.). Contrib Mineral Petrol 115:287–302

Kam M (1983) Etude pétrologique et géochimique de la «ligne des klippes» (Vosges méridionales). Mémoire de DEA, Université Louis Pasteur, Strasbourg

Kratinová Z, Schulmann K, Edel J-B, Ježek J (2007) Model of successive granite sheet emplacement in transtensional setting: integrated microstructural and anisotropy of magnetic susceptibility study. Tectonics 26:TC6003

Krecher M, Behrmann JH (2007) Tectonics of the Vosges (NE France) and the Schwarzwald (SW Germany): evidence from Devonian-Carboniferous active margin basins and their deformation. Geotectonic Res 95:61–86

Krecher M, Behrmann JH, Müller-Sigmund H (2007) Sedimentology and tectonic setting of Devonian-Carboniferous turbidites and debris flow deposits in the Variscan Vosges Mountains (Markstein Group, NE-France). Zeitschrift der Deutschen Gesellschaft für Geowissenschaften 158:1063–1087

Kretz R (1983) Symbols for rock forming minerals. Am Mineral 68:277–279

Lardeaux JM, Ledru P, Daniel I, Duchene S (2001) The Variscan French Massif Central - a new addition to the ultrahigh pressure metamorphic 'club': exhumation processes and geodynamic consequences. Tectonophysics 332:143–167

Leloix C, Faure M, Feybesse J-L (1999) Hercynian polyphase tectonics in the northeast French Massif Central: the closure of the Brévenne Devonian–Dinantian rift. Int J Earth Sci 88:409–421

Lemoine M, Tricart P, Boillot G (1987) Ultramafic and gabbroic ocean floor of the Ligurian Tethys (Alps, Corsica, Apennines): in search of a genetic model. Geology 15:622–625

Leveridge BE, Hartley AJ (2006) The Variscan Orogeny: the development and deformation of Devonian/Carboniferous basins in SW England and South Wales. In: Brenchley PJ, Rawson PF (eds) The geology of England and Wales. Geological Society, London, pp 225–255

Linck G (1892) Geognotische Beschreibung des Thalhorn im oberen Amariner Thal. Mittheilungen der geologischen Landesanstalt von Elsass—Lothringen IV:1–72

Loeschke J, Güldenpfennig M, Hann HP, Sawatzki G (1998) Die Zone von Badenweiler-Lenzkirch (Schwarzwald): Eine variskische Suturzone. Zeitschrift der deutschen geologischen Gesellschaft 149:197–212

Ludwig KR (2004) Users manual for ISOPLOT/EX, version3.1. A geochronological toolkit for Microsoft Excel. Berkeley Geochronology Center, Special Publication 4

Maass R, Stoppel D (1982) Nachweis von Oberdevon bei Markstein (Bl. Munster, Südvogesen). Zeitschrift der Deutschen Geologischen Gesellschaft 133:403–408

Manatschal G, Müntener O (2009) A type sequence across an ancient magma-poor ocean–continent transition: the example of the western Alpine Tethys ophiolites. Tectonophysics 473:4–19

Massone H, Schreyer W (1983) A new experimental phengite barometer and its application to a Variscan subduction zone at the southern margin of the Rhenohercynicum. Terra Cognita 3:197

Matte P (1986) Tectonics and plate tectonics model for the Variscan Belt of Europe. Tectonophysics 126:329–374

Matte P (1998) Continental subduction and exhumation of HP rocks in Paleozoic orogenic belts: Uralides and Variscides. Geol Soc Sweden (GFF) 120:209–222

Matte P (2001) The Variscan collage and orogeny (480–290 Ma) and the tectonic definition of the Armorica microplate: a review. Terra Nova 13:122–128

Montenari M, Leppig U, Weyer D (2002) Heterocorallia from the Early Carboniferous of the Moldanubian Southern Vosges Mountains (Alsace, France). Neues Jahrbuch für Geologie und Paläontologie Abhandlungen 224:223–254

Niu Y, Gilmore T, Mackie S, Greig A, Bach W (2002) Mineral chemistry, whole-rock compositions, and petrogenesis of Leg 176 gabbros: data and discussion. Proc Ocean Drill Prog Sci Results 176:1–56

Oncken O, von Winterfeld C, Dittmar U (1999) Accretion of a rifted passive margin: the Late Paleozoic Rhenohercynian fold and thrust belt (Middle European Variscides). Tectonics 18:75–91

Paquette J-L, Ménot R-P, Peucat J–J (1989) REE, Sm–Nd and U–Pb zircon study of eclogites from the Alpine External Massifs (Western Alps): evidence for crustal contamination. Earth Planet Sci Lett 96:181–198

Patočka F, Valenta J (1996) Geochemistry of the late Devonian intermediate to acid metavolcanic rocks from the southern part of the Vrbno Group in the Jeseníky Mts. (Moravo-Silesian Belt, Bohemian Massif, Czech Republic): paleotectonic implications. Geolines 4:42–54

Petrini K, Burg JP (1998) Relationships between deformation, plutonism and regional metamorphism in the Markstein area (southern Vosges). Géologie de la France 2:13–23

Pin C (1990) Variscan oceans: ages, origins and geodynamic implications inferred from geochemical and radiometric data. Tectonophysics 177:215–227

Pin C, Carme F (1988) Ecailles de matériaux d'origine océanique dans le charriage hercynien de la «Ligne des Klippes», Vosges méridionales (NE France). Comptes Rendus de l'Académie des Sciences 306:217–222

Pin C, Paquette J-L (1997) A mantle-derived bimodal suite in the Hercynian Belt: Nd isotope and trace element evidence for a subduction-related rift origin of the Late Devonian Brévenne metavolcanics, Massif Central (France). Contrib Mineral Petrol 129:222–238

Pin C, Fonseca PE, Paquette J-L, Castro P, Matte P (2008) The ca. 350 Ma Beja Igneous Complex: A record of transcurrent slab break-off in the Southern Iberia Variscan Belt? Tectonophysics 461:356–377

Pitra P, Ballèvre M, Ruffet G (2010) Inverted metamorphic field gradient towards a Variscan suture zone (Champtoceaux Complex, Armorican Massif, France). J Metamorph Geol 28:183–208

Plank T, Langmuir CH (1998) The chemical composition of subducting sediment and its consequences for the crust and mantle. Chem Geol 145:325–394

Rey P, Burg JP, Caron JM (1992) Middle and late carboniferous extension in the Variscan Belt: structural evidences from the Vosges massif (Eastern France). Geodin Acta 5:17–36

Ribeiro A, Munhá J, Fonseca PE, Araújo A, Pedro JC, Mateus A, Tassinari C, Machado G, Jesus A (2010) Variscan ophiolite belts in the Ossa-Morena Zone (Southwest Iberia): geological characterization and geodynamic significance. Gondwana Res 17:408–421

Richard P, Shimizu N, Allegre CJ (1976) $^{143}Nd/^{146}Nd$, a natural tracer: an application to oceanic basalts. Earth Planet Sci Lett 31:269–278

Roberts S, Andrews JR, Bull JM, Sanderson DJ (1993) Slow-spreading ridge-axis tectonics: evidence from the Lizard Complex. U K Earth Planet Sci Lett 116:101–112

Ruhland M (1958) Allure des plis et plis à axes subverticaux dans les terrains primaires des Vosges méridionales. Bulletin du Service de la Carte Géologique d'Alsace-Lorraine 11:45–50

Schaltegger U, Schneider J-L, Maurin J-C, Corfu F (1996) Precise U–Pb chronometry of 345–340 Ma old magmatism related to syn-convergence extension in the Southern Vosges (Central Variscan Belt). Earth Planet Sci Lett 144:403–419

Schaltegger U, Fanning CM, Günther D, Maurin JC, Schulmann K, Gebauer D (1999) Growth, annealing and recrystallization of zircon and preservation of monazite in high-grade metamorphism: conventional and in situ U–Pb isotope,

cathodoluminiscence and microchemical evidence. Contrib Mineral Petrol 134:186–201

Schneider J-L (1990) Enregistrement de la dynamique varisque dans les bassins volcano-sédimentaires dévono-dinantiens: exemple des Vosges du Sud (zone moldanubienne). Thèse de doctorat, Université de Strasbourg, 222 p

Schneider J-L, Hassenforder B, Paicheler J-C (1990) Une ou plusieurs «Ligne des Klippes» dans les Vosges du Sud (France)? Nouvelles données sur la nature des «klippes» et leur signification dans la dynamique varisque. Comptes Rendus de l'Académie des Sciences 311:1221–1226

Schulmann K, Schaltegger U, Ježek J, Thompson AB, Edel JB (2002) Rapid burial and exhumation during orogeny: thickening and synconvergent exhumation of thermally weakened and thinned crust (Variscan orogen in Western Europe). Am J Sci 302:856–879

Schulmann K, Edel J-B, Hasalová P, Cosgrove J, Ježek J, Lexa O (2009) Influence of melt induced mechanical anisotropy on the magnetic fabrics and rheology of deforming migmatites, Central Vosges, France. J Struct Geol 31:1223–1237

Shail RK, Leveridge BE (2009) The Rhenohercynian passive margin of SW England: development, inversion and extensional reactivation. Comptes Rendus Géoscience 341:140–155

Stacey JS, Kramers JD (1975) Approximation of terrestrial lead isotope evolution by a two-stage model. Earth Planet Sci Lett 26:207–221

Stampfli GM, Borel GD (2002) A plate tectonic model for the Paleozoic and Mesozoic constrained by dynamic plate boundaries and restored synthetic oceanic isochrons. Earth Planet Sci Lett 196:17–33

Sun SS, McDonough WF (1989) Chemical and isotopic systematics of oceanic basalts: implications for mantle composition and processes. In: Saunders AD, Norry M (eds) Magmatism in the ocean basins, vol 42. Geological Society Special Publications, London, pp 313–345

Tait J, Schätz M, Bachtadse V, Soffel H (2000) Paleomagnetism and Palaeozoic palaeogeography of Gondwana and European terranes. In: Franke W, Haak V, Oncken O, Tanner D (eds) Orogenic processes: quantification and Modelling in the Variscan Belt, special publications, vol 179, pp 21–34

Timmermann H, Štědrá V, Gerdes A, Noble SR, Parrish RR, Dörr W (2004) The problem of dating high-pressure metamorphism: a U–Pb isotope and geochemical study on eclogites and related rocks of the Mariánské Lázně Complex, Czech Republic. J Petrol 45:1311–1338

Tricart P, Lemoine M (1983) Serpentinite oceanic bottom in South Queyras ophiolites (French western Alps): record of the incipient oceanic opening of the Mesozoic Ligurian Tethys. Eclogae Geologicae Helvetiae 76:611–629

Vogt C (1981) Benthonische Klein-Foraminiferen aus dem Unter-Karbon der Südvogesen. Neues Jahrbuch für Geologie und Paläontologie Monatshefte 6:363–384

von Raumer JF, Stampfli GM (2008) The birth of the Rheic Ocean—early palaeozoic subsidence patterns and subsequent tectonic plate scenarios. Tectonophysics 461:9–20

von Seidlitz W (1914) Leitlinien varistischer Tektonik im Schwarzwald und in den Vogesen. Zeitschrift der Deutschen Geologischen Gesellschaft 66:100–124

Weigand B (1875) Die Serpentine der Vogesen. Mineralogische Mittheilungen 3:183–206

Wickert F, Eisbacher GH (1988) Two-sided Variscan thrust tectonics in the Vosges Mountains, northeastern France. Geodinamica Acta 2:101–120

Wiedenbeck M, Allé P, Corfu F, Griffin WL, Meier M, Oberli F, von Quadt A, Roddick JC, Spiegel W (1995) Three natural zircon standards for U-Th-Pb, Lu-Hf, trace element and REE analyses. Geostandards Newslett 19:1–23

Wilson RCL, Manatschal G, Wise S (2001) Rifting along non-volcanic passive margins: stratigraphic and seismic evidence from the Mesozoic successions of the Alps and western Iberia. In: Wilson RCL, Whitmarsh RB, Taylor B, Froitzheim N (eds) Non-volcanic rifting of continental margins: a comparison of evidence from land and sea. Geological Society Special Publications, vol 187, pp 429–452

Zeh A, Brätz H, Millar IL, Williams IS (2001) A combined zircon SHRIMP and SmNd isotope study of high-grade paragneisses from the Mid-German Crystalline Rise: evidence for norther Gondwanan and Greenvillian provenance. J Geol Soc Lond 158:983–994

Ziegler PA (1986) Geodynamic model for the palaeozoic crustal consolidation of Western and Central Europe. Tectonophysics 126:303–328

Chapitre 3 : le magmatisme des Vosges moyennes et méridionales : Pétrologie - Géochimie - Géochronologie

Dans ce chapitre, nous traitons des évènements magmatiques affectant les Vosges moyennes et méridionales (anciennement Granite des Crêtes, des Ballons et son volcanisme associé et Granite Fondamental). L'objectif est de caractériser par des analyses pétrologiques, géochimiques, isotopiques et géochronologiques les différents évènements magmatiques afin de relier le Massif des Vosges aux autres massifs de la chaine varisque et de proposer un modèle d'évolution et de développement de la croûte continentale du massif vosgien moyen et méridional.

L'étude s'appuie sur un échantillonnage sur le terrain tous les 2km dans les différentes unités magmatiques définies par les différents auteurs. J'ai effectué la préparation des échantillons pour les analyses. Les poudres ont été envoyées à ACME Labs (Vancouver, Canada) pour les analyses en éléments majeurs et traces et au BRGM pour les analyses isotopiques (Catherine Guerrot). J'ai complété ces données par des analyses minéralogiques faites à la microsonde au BRGM (encadrée par Guillaume Wille) ainsi que par des nouvelles datations U-Pb sur zircons et monazites où j'ai effectué les séparations des minéraux, préparé les plots (encadrée par Jérémie Melleton, BRGM) et effectué les analyses au laboratoire Magmas et Volcans de Clermont-Ferrand (encadrée par Jean-Louis Paquette).

L'ensemble de ces données nous a permis de distinguer deux principaux évènements magmatiques affectant les Vosges moyennes et méridionales.

Le premier évènement daté à 345-335 Ma est constitué de deux types d'un magmatisme dit « magnésio-potassique Mg-K » résultant d'un mélange de magmas d'origine crustale et mantellique. Nous avons mis en évidence que la différence qu'il existe entre ces deux types provient de protolithe crustaux différents impliqués dans la fusion grâce à l'analyse des éléments en trace (anomalie en Sr ou en P sur les profils normalisés au manteau primitif), à l'analyse isotopique (deux groupes bien distincts) et à l'âge des zircons hérités (jusqu'au Protérozoïque pour l'un et Cambro-Ordovicien pour l'autre). Nous avons interprété ce magmatisme comme résultant de la fusion partielle (par apport de chaleur radiogénique), d'une part, de la croûte continentale Saxothuringienne subductée sous la croûte continentale Moldanubienne et de l'autre part, du manteau lithosphérique enrichi et métasomatisé.

Le second évènement, daté à 330-320 Ma, est aussi constitué de deux ensembles de roches plutoniques péralumineuses (anomalie en Sr ou P, deux groupes distincts pour les rapports isotopiques du Sr et Nd). Nous avons montré que cet évènement magmatique présente des caractéristiques géochimiques et isotopiques proches de celle du magmatisme Mg-K. Grâce à une modélisation de l'apport de chaleur par désintégration radiogénique du magmatisme Mg-K ainsi que par l'étude des zircons hérités, nous avons montré que la genèse des magmas de ce second évènement magmatique provient d'un mélange entre un magma Mg-K et de la fusion de la croûte moyenne gneissique pour l'un et des magmas issus de la fusion de la croûte supérieure sédimentaire pour l'autre.

L'article qui constitue ce chapitre de thèse sera soumis à la revue *Journal of Petrology*.

Chronology, petrogenesis and heat sources for successive Carboniferous magmatic events in the Variscan Vosges Mts (NE France).

Anne-Sophie Tabaud[1]*, Philippe Rossi[2], Hubert Whitechurch[1], Etienne Skrzypek[1], Karel Schulmann[1], Catherine Guerrot[2] and Jean-Louis Paquette[3]

[1]Ecole et Observatoire des Sciences de la Terre UMR 7516, Université de Strasbourg, 1, rue Blessig, 67084 Strasbourg, France

[2]BRGM, 3 avenue Claude Guillemin, BP 36009, Orléans cedex 02, France

[3]Laboratoire Magmas et Volcans UMR 6524, CNRS and Université Blaise Pascal, 5, rue Kessler, 63038 Clermont-Ferrand cedex, France

*Corresponding author: Anne-Sophie Tabaud, Ecole et Observatoire des Sciences de la Terre UMR 7516, Université de Strasbourg, 1, rue Blessig, 67084 Strasbourg, France

Tel : +33 3 68 85 04 47; Fax : +33 3 68 85 04 02; e-mail: as.tabaud@unistra.fr

1. Introduction

The final convergence stage of the Variscan Orogeny was characterized by the formation of sedimentary basins, HP-HT metamorphism and intrusion of granitoids (Finger & Clemens, 1995; Schaltegger et al., 1996; Kröner et al., 1998). During a very short episode dated at about 340 Ma, Mg-K magma was emplaced in a rather narrow discontinuous N-S ribbon over about 1500 km within the internal "Moldanubian" zone of the European Variscan Belt. These rocks range from the Bohemian Massif (Holub, 1997; Janoušek et al., 1995, 2000; Janoušek & Holub, 2007), to the Black Forest (Hann et al, 2003), Vosges Mountains, some External Crystalline massifs of the Alps (Banzet, 1987; Schaltegger et al, 1991; Debon et al., 1998; Debon & Lemmet, 1999) and the Corsica Batholith (Rossi & Cocherie, 1991; Cocherie et al., 1994). This magmatism is restricted to the internal zone of the Variscan orogeny and was considered as an indicator of a Late Paleozoic convergent ocean-continent margin (Finger & Steyrer, 1990).

During the Variscan orogeny, the Central and Southern Vosges Mountains (CVM and SVM) in northeastern France were part of the Moldanubian zone, characterized by Visean sedimentary and volcano-sedimentary basins (the Markstein and Oderen units, respectively; Stussi, 1970; Fluck et al., 1989, 1991; Schneider, 1990) and by HP-HT metamorphic formations (granulite and gneiss) whose peak was dated at 350-340 Ma (Schaltegger et al., 1999; Skrzypek, 2011). These formations were affected by large intrusions, including: i) the so-called "Crêtes" granite (Gagny, 1968) now referred to as Central Vosges Mg-K; ii) the "Ballons" granite (Pagel & Leterrier, 1980) now referred to as South Vosges Mg-K; and iii) the "Fundamental" granite (Hameurt, 1967; von Eller, 1961), a huge area of peraluminous "S-type" granite now referred to as Central Vosges Granite (CVG).

The aim of this paper is to better define the magmatism of the Vosgian Massif in order to bridge the gap between the Vosges and surrounding massifs. New field work and petrographic, whole-rock major- and trace-element geochemistry, and geochronological data associated with recent structural results (Skrzypek, 2011; Kratinová et al., 2007, 2012; Schulmann et al., 2009a) are combined to better constrain the Variscan geodynamics of the Moldanubian Variscan Internal Zone.

2. Geological setting and background

Across Europe, the exposed remnants of the Variscan orogenic belt commonly host abundant Early Carboniferous magmatic rocks (Fig. 1a). Similarly, the Palaeozoic basement of the Vosges Mountains (NE France) is dominantly composed of granitoids which can be observed in the Saxothuringian part to the N as well as in the Moldanubian part to the S (Kossmat, 1927). The present study will only focus on magmatic units that can be found in the Moldanubian part, i.e. in the Central and Southern Vosges Mountains (Fig. 1b).

The Central and Southern Vosges Mts are characterized by abundant magmatic rocks intruding Visean sedimentary or volcanosedimentary deposits to the S (*Markstein* and *Oderen* units; Stussi, 1970; Schneider, 1990), and medium- to high-grade metamorphic units to the N (*Sainte-Marie-aux-Mines* units; von Eller, 1961; Fluck, 1980). According to their petrography the magmatic rocks have long been divided into distinct groups, and it is presently proposed to distinguish between: (1) the "*Crêtes*" granite ("*Kammgranit*" of the German authors; Groth, 1877) revisited hereafter as the Central Vosges Mg-K association (CVMg-K), (2) the "*Ballons*" plutonic complex (Michel-Levy, 1910) revisited hereafter as the Southern Vosges Mg-K association (SVMg-K), and (3) the "*Fondamental"* granite (Hameurt, 1967) revisited hereafter as the Central Vosges Granite (CVG):

i) The CVMg-K association (180 km²) is composed of several bodies corresponding to amphibole−biotite porphyritic monzonite or granite (*"Crêtes"* granite). It can be subdivided into three distinct types: (1) the CVMg-K durbachite (termed after a similar lithology described by Sauer (1893) in the neighbouring Black Forest) which appears as small intrusions within the metamorphic units to the N of the Central Vosges Mts, (2) the CVMg-K dark granitoids and (3) the CVMg-K light granitoids corresponding to the black and blue-grey facies recognized by Gagny (1968) to the S of the Central Vosges Mts (Fig. 1b).

ii) The SVMg-K association (260 km²) encompasses a large plutonic complex as well as some volcanic rocks which crop out in the Southern Vosges Mts (e.g. Pagel & Leterrier, 1980). There, it is commonly possible to distinguish between (1) the dominant SVMg-K amphibole−biotite porphyritic granite (*"Ballons"* granite), (2) the SVMg-K fine-grained granite (*"Corravillers"* granite) observed to the W of the complex, (3) various SVMg-K mafic rocks forming a discontinuous belt of gabbro, diorite, syenite and monzonite along the margin of the plutonic complex, and (4) SVMg-K volcanic rocks (*"Molkenrain"* volcanism) found in volcanosedimentary units towards the E (Fig. 1b).

iii) The CVG corresponds to a wide area (860 km²) of biotite and biotite−muscovite granite that occupies the major part of the Central Vosges Mts. It is separated into a western (Western-CVG) and eastern (Eastern-CVG) part by the NE-SW striking Sainte-Marie-aux-Mines Fault

and E-W Blistein fault (Fig. 1b). Field observations and petrographic studies reveal that the CVG is heterogeneous; the Western-CVG exhibits either a coarse-grained isotropic texture or a weak gneissosity (Hameurt, 1967), whereas the Eastern-CVG is characterized by the presence of numerous xenoliths of CVMg-K granitoid, gneiss and sedimentary rocks (von Eller, 1961).

Previous geochemical works proposed different hypotheses for the origin of Mg-K magmas: Gagny (1968; for CVMg-K) and Pagel & Leterrier (1980; for SVMg-K) related them to hyperpotassic or shoshonitic series and proposed that magma might have originated from the partial melting of lithospheric mantle enriched in incompatible elements above a subduction zone, with crustal contamination of the magma during ascent. André (1983) suggested that the basic end-member rocks of the northern margin of the Ballons plutons (SVMg-K) were derived by fractional crystallization of a tholeiitic basaltic magma. Based on geochemical work, Lefèvre et al. (1994) deduced that the volcanic rock presents overprints of earlier subduction as well as mantle and crustal affinities. On the basis of Sr-isotopic geochemistry, Pagel (1981) favoured the hypothesis that the crustal components implied in the genesis of the two associations were mostly amphibolitic for the Ballons plutons (SVMg-K) and mostly granulitic for the Crêtes plutons (CVMg-K). Fluck et al. (1991) proposed, for the whole Mg-K magmatism, a gabbroic mantle origin that suffered hybridization in shallow crustal levels in the case of Ballons plutons and in deeper levels for the Crêtes plutons.

Previous geochronological data indicate that the intrusion of CVMg-K and SVMg-K associations took place at 345-335 Ma. U-Pb results point to an emplacement age of 332 ± 3 Ma for the CVMg-K durbachite (Schulmann et al., 2002), and of *ca.* 340 Ma for CVMg-K granite and microgranite intrusions (Schaltegger et al., 1996). Zircon analyses reveal an inherited Pb component of Proterozoic age (2.12 ± 0.02 Ga; Schaltegger et al., 1996). There is no indication of younger inheritance age for this association. For the SVMg-K association, mafic rocks dated at 356 ± 2 Ma (Ar-Ar on amphibole, Boutin et al., 1995) and 342 ± 1 (U-Pb on zircon, Schaltegger et al., 1996) seem to be older than the porphyrictic granite and rhyolitic volcanism estimated at 339 ± 2 Ma and 340 ± 2 Ma, respectively (Schaltegger et al., 1996). The oldest inherited Pb component for this association reveal Cadomian age (between 670 and 655 Ma; Schaltegger et al., 1996). In both Mg-K associations, Ar-Ar ages on biotite reflect cooling at 335−330 Ma (Boutin et al., 1995). Geoghronological data for the CVG indicate continuous plutonic activity from *ca.* 330 to 325 Ma. It is exemplified by U-Pb ages of 329 ± 2 Ma (*"Brézouard"* granite; Schulmann et al., 2002) and 326 ± 1 Ma (*"Thannenkirch"* granite; Kratinová et al., 2007) in the W-CVG. The E-CVG gives U-Pb ages of 328 ± 5 Ma (*"Trois Epis"* metatexite; Schaltegger et al, 1999) and 326 ± 5 Ma ("*Kasersberg*" granite; Schaltegger et al., 1999). Across the whole CVG, Ar-Ar cooling ages cluster at 325-320 Ma (Boutin et al, 1995).

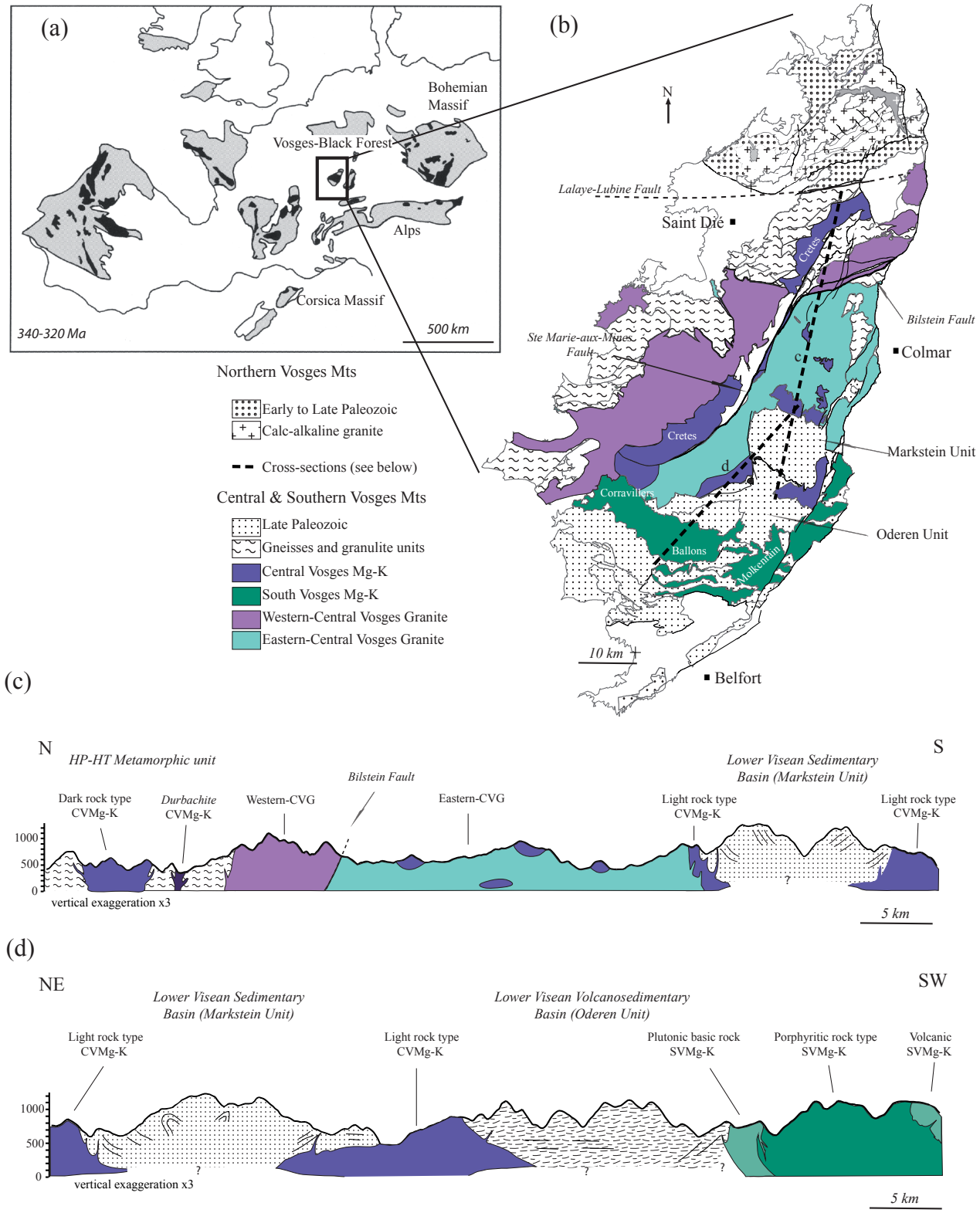

Figure 1: (a) Distribution of granitic rocks of the Variscan orogeny with intrusion ages between 340 and 320 Ma (after Franke (1989), Martinez et al. (1990), Neubauer & von Raumer (1993), Carron et al. (1994) and Ledru et al. (1994)) and position of the Vosges Mountains within the European Variscan Belt (black square). (b) Geological map of the Vosges Mts (modified after Fluck et al., 1989). (c) Schematic cross-section of line «c» through the Vosges Mts. (d) Schematic cross-section of line «d» through the Vosges Mts.

3. Field relationships

Field evidences indicate that the CVMg-K association intruded different crustal levels. To the N of the Central Vosges Mountains, sheets of CVMg-K durbachite as well as a large body of dark granitoid are intrusive in amphibolite- or granulite-facies metamorphic units (Fig. 1c). These intrusions are elongated and lie parallel to the NE-SW subvertical metamorphic fabric which is dominant in the orogenic lower crust. Farther to the S, an elongated body of CVMg-K light granitoid is entirely surrounded by the CVG and points to a shallower emplacement level. The CVMg-K magmatism also generates contact metamorphism in upper crustal sedimentary units to the S of the Central Vosges Mts. There, granitoid stocks show clear intrusive contacts with Visean sediments and host numerous xenoliths of sedimentary host rocks. In addition, small syn-tectonic sills of fine-grained granite are emplaced parallel to the NW-SE subvertical bedding (Fig. 1c).

The SVMg-K plutonic complex forms an E-W striking body which occupies a large part of the Southern Vosges Mts. Although relationships between SVMg-K mafic rocks and surrounding sediments remain unclear, several observations indicate that the whole complex intruded only the upper orogenic crust. The porphyritic granite evolves to a fine-grained type towards the W and shows granophyric margins at the contact with Visean volcanosedimentary sequences to the E (Fig. 1d). The SVMg-K magmatic episode even evolves to aerial volcanism as exemplified by SVMg-K volcanic rocks found within volcanosedimentary units to the E (Fig. 1d).

Petrological and textural arguments suggest that the emplacement of the CVG is syn- to post-tectonic (Kratinová et al., 2007; 2012). It is indicated by subhorizontal ductile to solid-state fabrics and by the shape of granitic bodies ("*Bilstein-Brézouard-Thannenkirch*" granites) in the Western-CVG (Fig. 1c). Towards the S, the Eastern-CVG contains numerous xenoliths of CVMg-K magmatic rocks and the contact between its roof and the overlying sedimentary units is flat-lying (Fig. 1d). These observations suggest that the CVG corresponds to a subhorizontal granitic sheet which was emplaced after the CVMg-K magmatic event.

4. Analytical methods

4.1. Microprobe

Chemical mineral analyses of rocks from the successive magmatic events were determined using a CAMECA SX 50 electron microprobe at BRGM Orléans, equipped with five wavelength-dispersive spectrometers (two PET, two TAP and one LIF) with an accelerating voltage of 15 kV and a beam current of 12 nA (Tables of mineral chemistry are in "*Annexe: CVMg-K, SVMg-K & CVG*").

4.2. U-Th-Pb zircon and monazite ages

The U-Th-Pb zircon and monazite ages were determined by laser ablation inductively coupled plasma spectrometry (LA-ICPMS) at the Laboratoire Magmas et Volcans, Clermont-Ferrand (France). The analyses involve the ablation of minerals with a Resonetics Resolution M-50 powered by an ultra-short pulse (< 4 ns) ATL Atlex Excimer laser system operating at a wavelength of 193 nm (detailed description in Müller et al., 2009). A spot diameter of 26 μm associated with 3 Hz repetition rates and a laser energy of 4 mJ producing a fluence of 9.5 J/cm^2 were used for zircon dating, and a spot diameter of 7 μm associated with 3 Hz repetition rates and a laser energy of 6 mJ for monazite dating. The ablated material was carried into helium, and then mixed with nitrogen and argon, before injection into a plasma source of an Agilent 7500 cs ICP-MS equipped with a dual pumping system to enhance the sensitivity.

Data were corrected for U-Th-Pb fractionation occurring during laser sampling and for instrumental mass discrimination (mass bias) by standard bracketing with repeated measurements of a GJ-1 zircon standard (Jackson et al., 2004). At the beginning and end of every run, repeated analyses of a 91500 zircon standard (Wiedenbeck et al., 1995), treated as unknowns, independently controlled the reproducibility and accuracy of the corrections. Data reduction was carried out with the GLITTER® software package from Macquarie Research Ltd (van Achterbergh et al., 2001; Jackson et al., 2004). For each analysis, the time-resolved signal of single isotopes and isotope ratios was monitored and carefully inspected to verify the presence of perturbations related to inclusions, fractures, mixing of different age domains, or common Pb. Calculated ratios were exported and Concordia ages and diagrams were generated using the Isoplot/Ex v. 2.49 software package (Ludwig, 2001).The concentrations in U-Th-Pb were calibrated relative to the certified contents of a GJ-1 zircon standard (Jackson et al., 2004). The zircon analyses were projected on $^{207}Pb/^{206}Pb$ *vs.* $^{238}U/^{206}Pb$ diagrams (Tera & Wasserburg, 1972), where the analytical points plot along a mixing line between the common Pb composition at the upper intercept and the zircon age at the lower intercept. This method is commonly used to date Phanerozoic zircons using *in situ* methods (Claoué-Long et al., 1995; Jackson et al., 2004). Tables of zircon analyses are in "*Annexe: CVMg-K, SVMg-K & CVG*"

4.3. Major- and trace-element whole-rock geochemistry

About 140 samples (5 to 10 kg of fresh material) were sampled over an about 4 km² grid (40 CVMg-K rocks, 30 SVMg-K rocks and 70 CVG samples). The size of the samples was adapted to account for the presence of K-feldspar megacrysts. After crushing and splitting, samples were ground in agate mills to fine powder. Major- and most trace-elements analyses (Data in *"Annexe: CVMg-K, SVMg-K & CVG"*) were performed in AcmeLabs™, Vancouver, by ICP-emission spectrometry following lithium metaborate/tetraborate fusion and dilute nitric digestion of a 0.2 g sample. REE and refractory elements were determined in the same laboratory by ICP mass spectrometry. The geochemical data were plotted with the R software package *GCDkit* (Janoušek et al., 2003).

4.4. Nd-Sr isotopic composition

Sr and Nd isotope data for 13 samples of Mg-K associations (7 for SVMg-K and 6 for CVMg-K) and 10 CVG samples (6 samples for the eastern part and 4 for the western part) were determined at BRGM Orléans. External reproducibility is given by the results of repeated analyses of the La Jolla [$^{143}Nd/^{144}Nd$ = 0.511869±8 (2σ) n = 4 and $^{143}Nd/^{144}Nd$ = 0.511878±13 (2σ) n = 13] and NBS 987 [$^{87}Sr/^{86}Sr$ = 0.710247±9 (2σ) n = 12 and $^{87}Sr/^{86}Sr$ = 0.710245±12 (2σ) n=12] isotopic standards.

5. Petrology

5.1. The Central Vosges Mg-K association

The most mafic end-member of this group of plutons (corresponding mostly to the so-called "Crêtes" granite) is an amphibole-biotite-bearing syenite previously known as "Durbachite*"* (Sauer, 1893). The rock of intermediaire composition, located in the northern part of the "Crêtes" granite, is an amphibole-biotite quartz melasyenite and melagranite [Gagny's (1968) so-called "dark or black facies"] (Fig.2). A porphyritic amphibole-biotite to biotite granite is the lighter rock type, which is located in the southern part of the Crêtes granite [Gagny's (1968) so-called "light facies" or "blue facies"] (Fig. 2). Amphibole-biotite-bearing syenite is poor in SiO_2 and rich in MgO, FeO, CaO, TiO_2 and P_2O_5. The rocks of this association are usually coarsely porphyritic with abundant K-feldspar phenocrysts (10-20 mm) in a dark to light grain matrix. The matrix is composed of abundant biotite, amphibole, K-feldspar, plagioclase and quartz. Clinopyroxene commonly occurs as relics within amphibole crystals in the basic end-member, but locally can still be present in the felsic rock. Accessory minerals include apatite, zircon, allanite, and titanite, whereas opaque minerals (magnetite, sulphides and thorite) occur mostly in the darkest rock types. Clinopyroxene composition ranges from diopside in the mafic member to augite in the felsic end-member. Its Al_2O_3 and TiO_2 are negligible (Al^{VI} = 0) whereas CaO content is very high (as much as 23%). Plagioclase is weakly zoned and the composition ranges from An_{40-30} in syenite to An_{30-15} in quartz melasyenite up to An_{15-5} in monzogranite. K-feldspar

occurs as abundant, large crystals with inverse Ba zoning (core about 0.5% and rim up to 2%). Mg-amphibole shows a weak pleochroism and its composition ranges from actinolitic hornblende to actinolite, poor in Al_{tot} (<0.7) and rich in Mg with mg# (0.70-0.75) mostly constant even with decreasing SiO_2 content. Amphibole and brown biotite commonly cluster into small aggregates clots. In every rock type of the Mg-K association, biotite crystals show a strong pleochroism. The biotite composition varies little regardless the rock type and, plotted in an AFM diagram (Fig.3), displays a cloud where X_{Mg} ranges from 0.60 to 0.65. The FeO/MgO ratio falls between 0.9 and 1.10, and Ti (0.18-0.28 a.p.f.u.) decreases weakly with increasing Si (2.8-3.0 a.p.f.u.). This, according to Robert (1976), suggests a slow decrease of the temperature during crystallization.

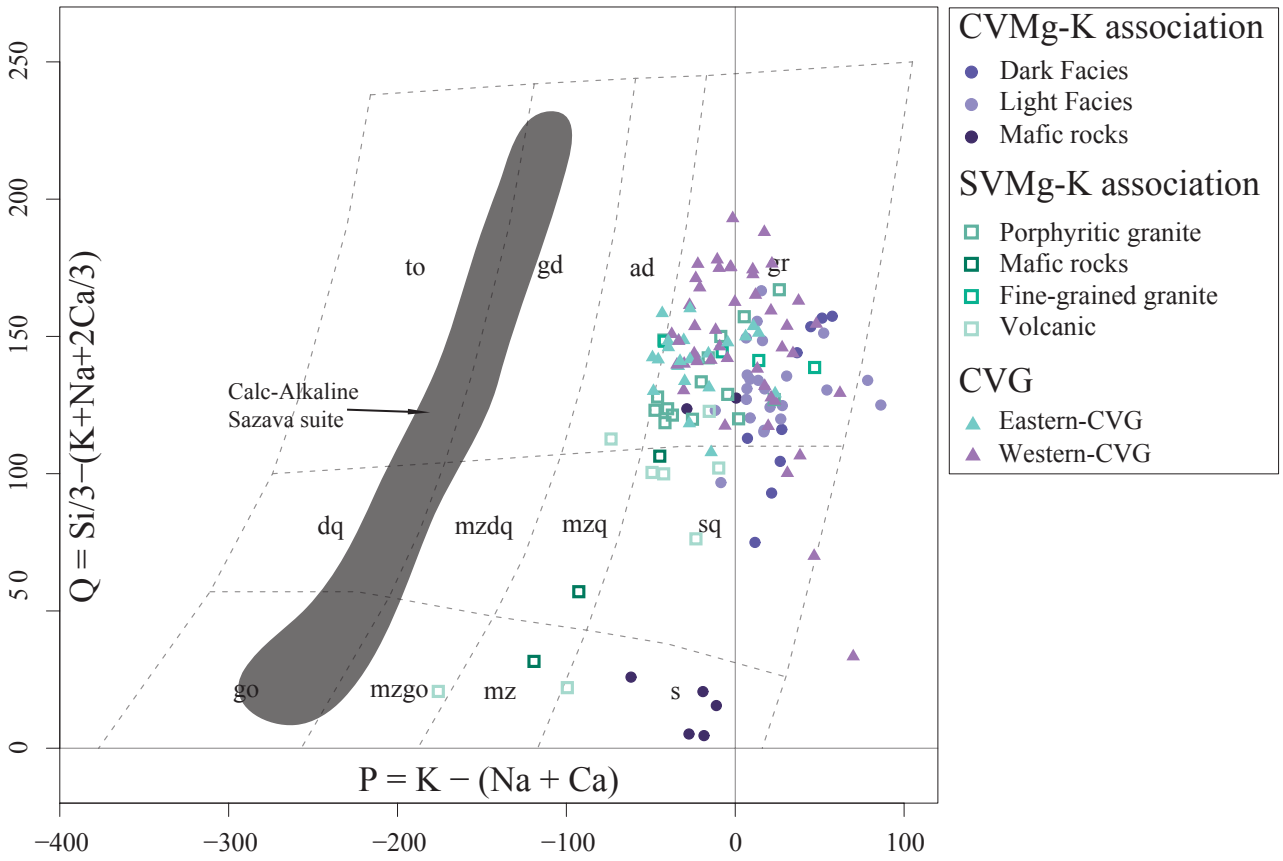

Figure 2: Multicationic P-Q plot (Debon & Le Fort, 1983) for granitoids of Vosges Mts; P represents the proportion of K-feldspar to plagioclase and Q the quartz content. The calc-alkaline Sázava suite from Bohemia (Janoušek et al., 2000) is plotted for comparison.

5.2. The South Vosges Mg-K association

The northern margin of the plutonic massif (the "Ballons" granite) is formed by an amphibole-biotite monzonite to quartz monzonite (Fig. 2), the mafic end member. The most common rock is a porphyritic granite-monzogranite with large (up to 50 mm) pinkish K-feldspar phenocrysts (Fig. 2). The "Corravillers*"* granite located west of the "Ballons" granite displays a fine-grained type that could indicate a high-level of emplacement. Mg-K volcanic rocks are exposed south and east of the main pluton and were known as the "Molkenrain" rhyolite (Coulon, 1977, 1979); their composition ranges from andesite to trachyte and rhyolite. As in the CVMg-K, plutonic rocks are composed of the same mineral association: amphibole, biotite, plagioclase, K-feldspar and quartz with apatite, zircon, titanite, thorite, magnetite and sulphides as accessory phases. The Ca content in plagioclase decreases from An_{60-50} in monzonite and quartz monzonite to An_{35-20} in porphyritic facies and to An_{15-5} in volcanic and some fine-grained rocks. K-feldspar is less abundant than in the CVMg-K association, but occurs as larger sized-crystals. Green Mg amphibole shows a strong pleochroism, and its composition ranges from magnesium- to actinolitic hornblende; the Al_{tot} content varies between 0.7 and 1.4, the Mg content is rather high and mg# mostly constant with increasing SiO_2 (0.70 to 0.75). Brown biotite composition is mostly independent of the host rock SiO_2 content: X_{Mg} = 0.50-0.60. FeO/MgO = 1.1 to 1.7 and on the AFM diagram (Fig. 3) it clusters within the same narrow area as the CVMg-K intrusions. Ti (0.13-0.28 a.p.f.u.) decreases with increasing Si (2.7-3.7 a.p.f.u.). The volcanic rocks are also composed of some coarse-grained green Mg amphibole, brown biotite, plagioclase and K-feldspar into a fine-grained quartz-feldspar matrix.

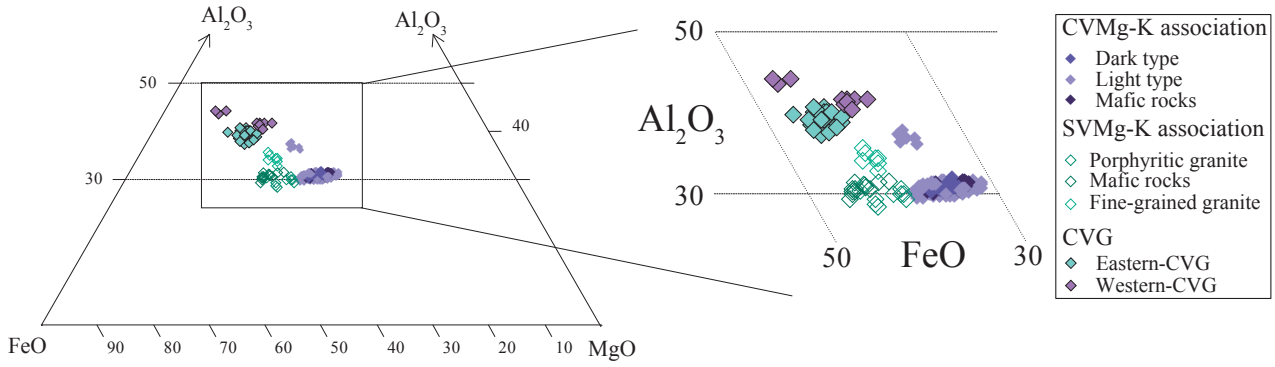

Figure 3: Biotite compositions from CVMg-K, SVMg-K and CVG in AFM diagram.

5.3. The Central Vosges Granite

The CVG has been divided into two parts located on each side of the Ste Marie-aux-Mines - Bilstein fault zone. SiO_2 content in every rock type remains > 65 wt%. The Eastern-CVG comprise biotite to biotite-muscovite granite-monzogranite. The Western-CVG is composed of biotite to biotite-muscovite quartz syenite and granite (Fig. 2). Accessory minerals are apatite, monazite, zircon and magnetite. Ca content in plagioclase ranges from An_{25} to An_0 and is weakly zoned. K-feldspar occurs as small crystals (< 10 mm). Ba content in plagioclase and K-feldspar never exceeds 1%; it decreases from core to rim in K-feldspar crystals and decreases with increasing host rock SiO_2 content. X_{Mg} in foxy-red-biotite decreases with increasing host-rock SiO_2 content from 0.60 to 0.40. FeO and Al_2O_3 contents increase with increasing whole-rock SiO_2 content whereas MgO decreases (Fig. 3)

6. Geochronology of CVM and SVM intrusions

For a good understanding of the mechanism and succession of emplacement of the granitic intrusions in the Vosges, it is important to constrain the crystallization and emplacement ages of the successive pulses in both Mg-K and CVG. Crystallization ages of some rock types of Mg-K or CVG (Table 1) were established in previous studies using K-Ar and Ar-Ar techniques (Boutin, 1995) and conventional U-Pb dating on zircon (Schaltegger et al., 1996, 1999; Schulmann et al., 2002; Kratinová et al., 2007).

Table 1: Summary table of geochronological data. The new U-Th-Pb zircon and monazite ages (in bold italic) are included.

Method	CVMg-K association			SVMg-K association				CVG	
	Mafic rocks	Dark type	Light type	Mafic rocks	Porphyritic granite	Fine-grained granite	Volcanism	Eastern part	Western part
U-Pb zircon	332 +3/-2 Ma		340 ± 1 Ma	342 ± 1 Ma	340 +4/-2 Ma		345 ± 2 Ma 336 +3/-5 Ma 340 ± 2 Ma	326 ± 4.8 Ma	326 ± 1 Ma 329 ± 2 Ma
		337 ± 2 Ma	***337 ± 3 Ma***	***345 ± 3 Ma***	***336 ± 4 Ma***	***336 ± 3 Ma***	***346 ± 2 Ma***		***319 ± 6 Ma***
U-Th-Pb monazite									***324 ± 4 Ma***
K-Ar				337 ± 19 Ma amphibole	335 ± 13 Ma amphibole		337 ± 11 Ma amphibole	336 ± 11 Ma biotite	330 ± 10 Ma biotite 334 ± 11 Ma biotite
Ar-Ar			333 ± 1 Ma biotite			331 ± 5 Ma biotite	335 ± 3 Ma amphibole		331 ± 5 Ma biotite

From Boutin, 1995; Schaltegger et al., 1996, 1999; Schulmann et al., 2002; Kratinová et al., 2007

New U-Pb age determinations of the different rock types of CVMg-K and SVMg-K and of the western part of the CVG were carried out on zircons and (for CVG only) monazite. Three representative samples were analysed for CVMg-K, four representative samples for SVMg-K and two representative samples for CVG. For each sample, 50 to 70 zircons (50-250 μm) were generally mounted. The results of the analyses are shown on Figs. 4, 5 and 6.

6.1. Age of the Central Vosges Mg-K association

Three representative samples from different magmatic bodies of the CVMg-K association were analysed for age dating. Sample CN6 is a dark granitoid which was collected in the northernmost CVMg-K magmatic body. Zircon grains from this sample are either prismatic or anhedral, but always show a uniform dark CL pattern. Several discordant analyses point to the presence of common lead, but seven analyses on six prismatic zircons can be used to calculate a lower intercept age of 337 ± 2 Ma which is interpreted as the age of igneous crystallization (Fig. 4a). However, three analyses on three rounded zircon crystals yield a lower intercept age of 353 ± 5 Ma and point to slightly older inheritance (Fig. 4a).

Sample CS1 corresponds to a light granite from the southern CVMg-K magmatic body. It mostly contains prismatic zircons which show a uniform dark CL patterns. Like in the dark granitoid, two distinct age populations are observed (Fig. 4b). Together with numerous discordant data, eight analyses on eight prismatic zircons define a lower intercept age of 337 ± 3 Ma regarded as the crystallisation age of the granite. In addition, two spot analyses suggest a possible inheritance at 351 ± 5 Ma, this lower intercept age being only indicative (Fig. 4b).

Sample BR14 belongs to a small body of CVMg-K light granite located in the southern part of the Central Vosges Mts. Zircons are mainly prismatic with uniform dark CL patterns. In addition to several discordant analyses due to the presence of common lead, two concordant spots yield a lower intercept age of 337 ± 4 Ma (Fig. 4c). This age is consistent with previous estimates for other CVMg-K granites and is similarly thought to reflect the igneous crystallization.

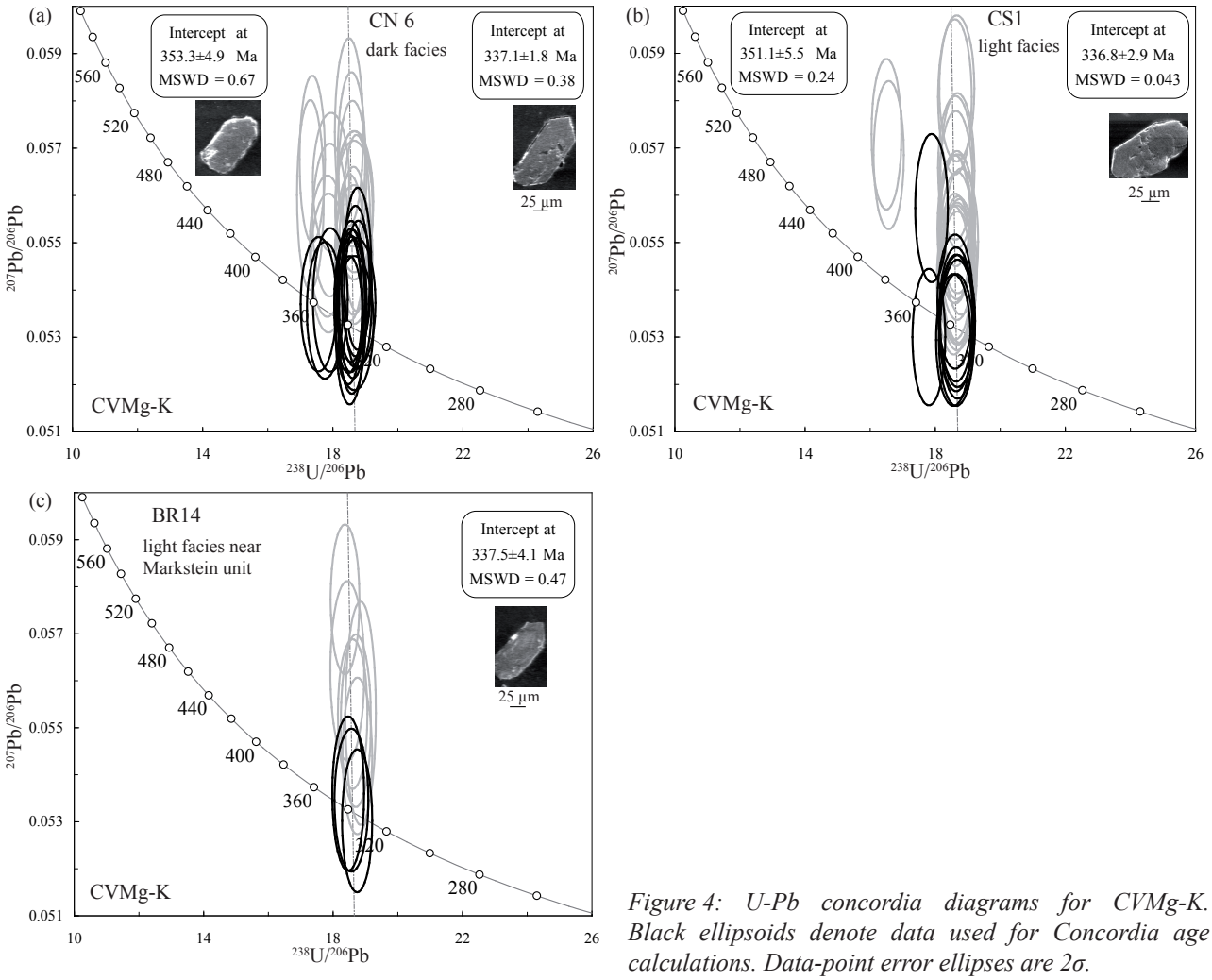

Figure 4: U-Pb concordia diagrams for CVMg-K. Black ellipsoids denote data used for Concordia age calculations. Data-point error ellipses are 2σ.

6.2. Age of the Southern Vosges Mg-K association

Within the SVMg-K plutonic complex, four representative samples were collected in order to constrain the age of mafic rocks, porphyritic granite and fine-grained granite. Sample BA11 represents a typical porphyritic granite which is dominant in the central and eastern parts of the SVMg-K plutonic complex. It contains prismatic zircon grains with frequent inclusions and slightly disturbed dark CL patterns. A large number of analyses are discordant due to the presence of common lead, but five analyses on five zircons yield a lower intercept age of 336 ± 4 Ma which is considered as the crystallization age of the porphyritic granite (Fig. 5a).

Sample CO1 corresponds to a SVMg-K fine-grained granite occurring to the West of the plutonic complex. It shows subhedral zircon grains with few prismatic faces and more common rounded boundaries. The zircon crystals frequently host inclusions and have uniform CL patterns. Although almost all analyses point to a contribution of common Pb, a lower intercept age based on three spots on three zircons yields a 336 ± 3 Ma age which documents the crystallization of the fine-grained granite (Fig. 5b).

Sample BAB4 is a monzonite which was collected at the northern margin of the SVMg-K plutonic complex. It chiefly preserves prismatic zircon grains with slightly rounded tips and uniformly dark CL patterns. U-Pb data are mostly concordant and six analyses on six prismatic zircons yield a lower intercept age of 345 ± 3 Ma (Fig. 5c) interpreted as the igneous crystallization of the monzonite.

Sample BAB5 corresponds to quartz monzonite from the southern margin SVMg-K plutonic complex. In this sample clean zircon crystals are euhedral or rounded, and show a dark and uniform CL pattern. Several analyses show a slight contribution of common lead, but fifteen spots on twelve zircons can be used to calculate a lower intercept age of 346 ± 2 Ma (Fig. 5d). Like for the diorite of the northern margin of the complex, this estimate is thought to reflect the age of igneous crystallization.

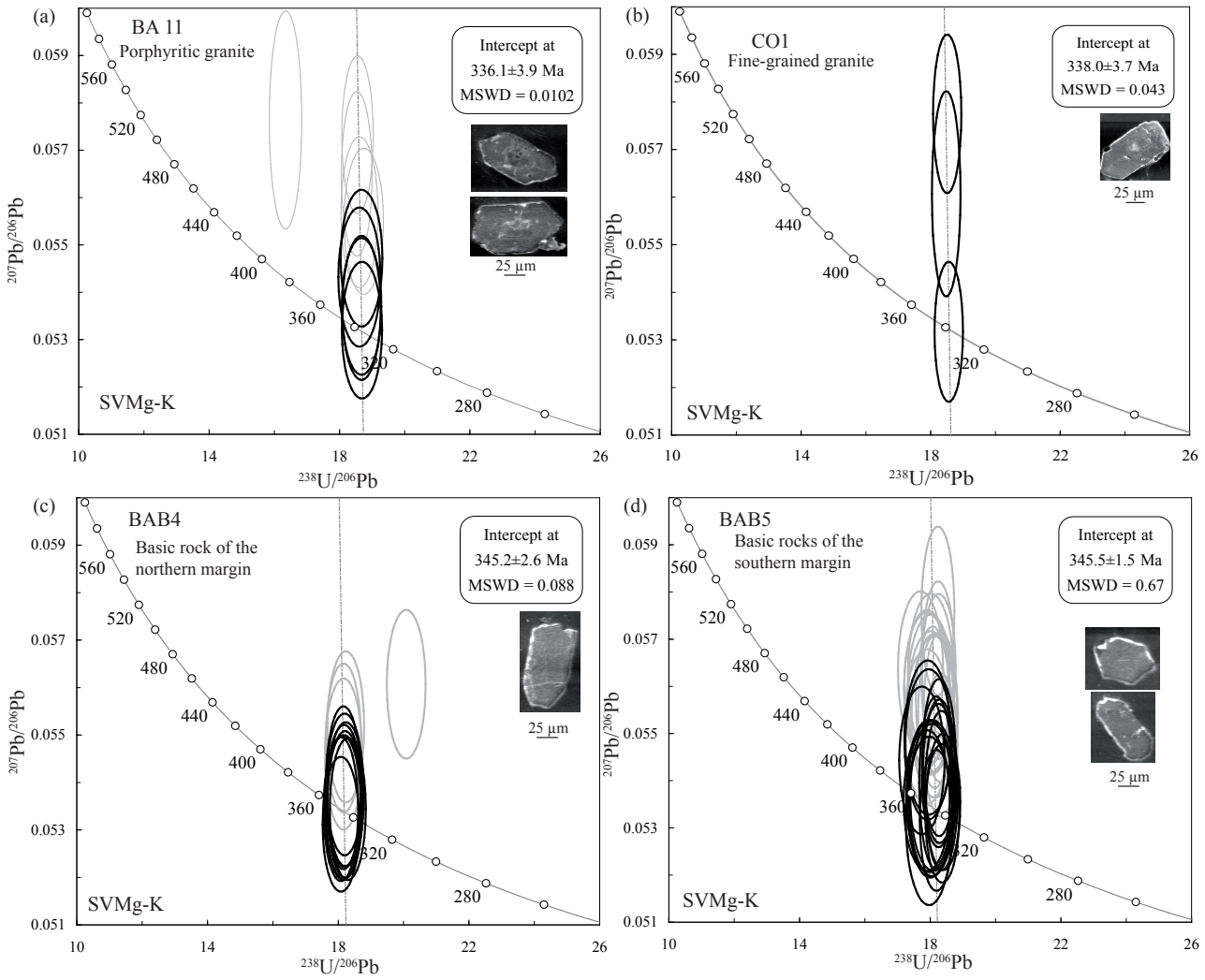

Figure 5: U-Pb concordia diagrams for SVMg-K.

6.3. Age of the Central Vosges Granite

Zircon and monazite dating were performed on two samples from the Western-CVG in order to constrain the magmatic age of this granitic body and to explore possible inheritance. Sample G-G4 is weak gneissify biotite-bearing granite. It contains subhedral zircon grains with well-developped prismatic faces but also slightly rounded tips. CL images reveal two distinct populations; some zircons show a uniform dark pattern, whereas numerous crystals preserve an oscillatory zoning pattern in the core surrounded by a tiny CL-dark rim (Fig. 6a). Four analyses on four prismatic zircons with dark CL patterns define a lower intercept age of 319 ± 6 Ma which is correlated with the igneous crystallization of the granite. By contrast, zircons showing an oscillatory zoning pattern yield a continuous array of concordant ages between *c.* 510 Ma and 390 Ma and point to Ordovician inheritance (Fig. 6a).

Sample G1-3 corresponds to biotite-bearing granite which was collected in the centre of the Western-CVG. Seven analyses on four monazite grains (50 µm) constrain a mean $^{238}Pb/^{232}Th$ age of 324 ± 4 Ma (Fig. 6b). This estimate overlaps within error with the zircon age of 319 ± 6 Ma obtained for sample G-G4 and indicates that the Western-CVG most likely crystallized at *c.* 322 Ma.

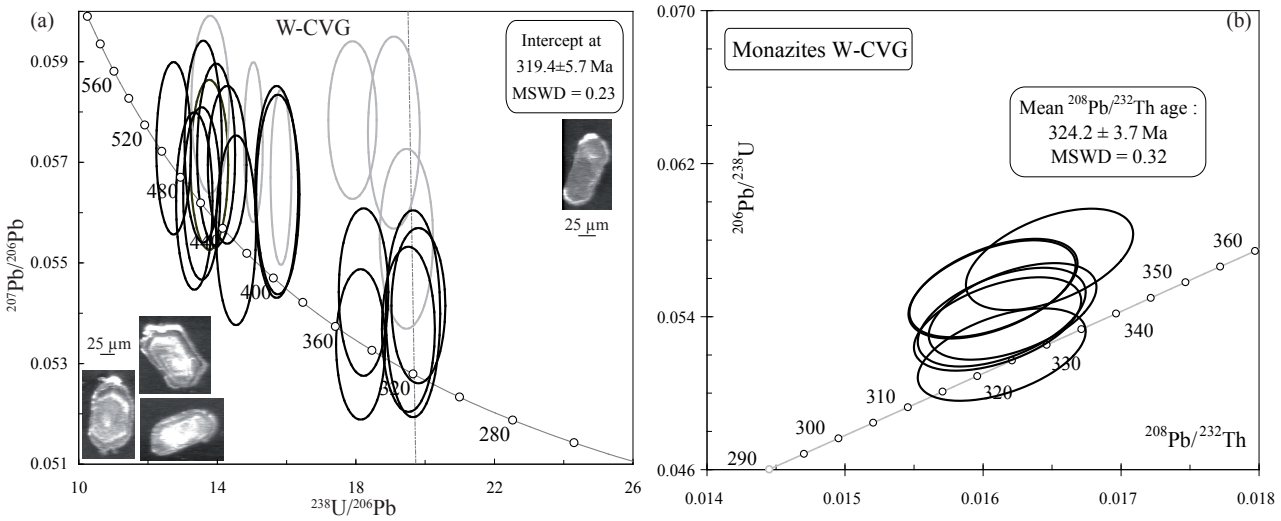

Figure 6: U-Th-Pb concordia diagrams for Western-CVG.

7. Whole-rock geochemistry

7.1. Central and South Vosges Mg-K associations (CVMg-K and SVMg-K)

7.1.1 Major elements

CVMg-K and SVMg-K are mostly composed of metaluminous rocks (A/CNK = 0.7 to 1.2). Plots of CaO, MgO and total alkalis *vs*. SiO_2 of the CVMg-K and SVMg-K are shown in Fig. 7. Typical compositions are characterized by a rather high MgO (9 to 2 wt%) and high K_2O (~8 wt%) contents. Mg-K magmatic rocks define linear trends that display decreasing MgO and CaO (also the case for FeO_t, TiO_2 and P_2O_5) and constant total alkalis as a function of SiO_2. The gap in intermediate compositions between 50 and 55 wt% SiO_2 was also observed in Mg-K intrusions in the Corsican Batholith (Cocherie et al., 1994) and the Bohemian Massif (Holub, 1997) where it was suggested that this might indicate that the mafic and felsic end members had a different origin.

The Vosgian Mg-K rock compositions range from syenite to granite. According to Peacock's (1931) discriminant and evolution trend of these associations (Figs. 7 and 8), none of these magmatic events conform to a calcalkaline suite. Although CaO decreases with SiO_2 from 6 to 1 wt%, total alkalis stay rather constant (about 8 wt%). This reinforces the use of Mg-K for qualifying the Vosgian magmatism as was done earlier for similar rocks elsewhere (Banzet, 1987; Rossi & Cocherie, 1991; Holub, 1997).

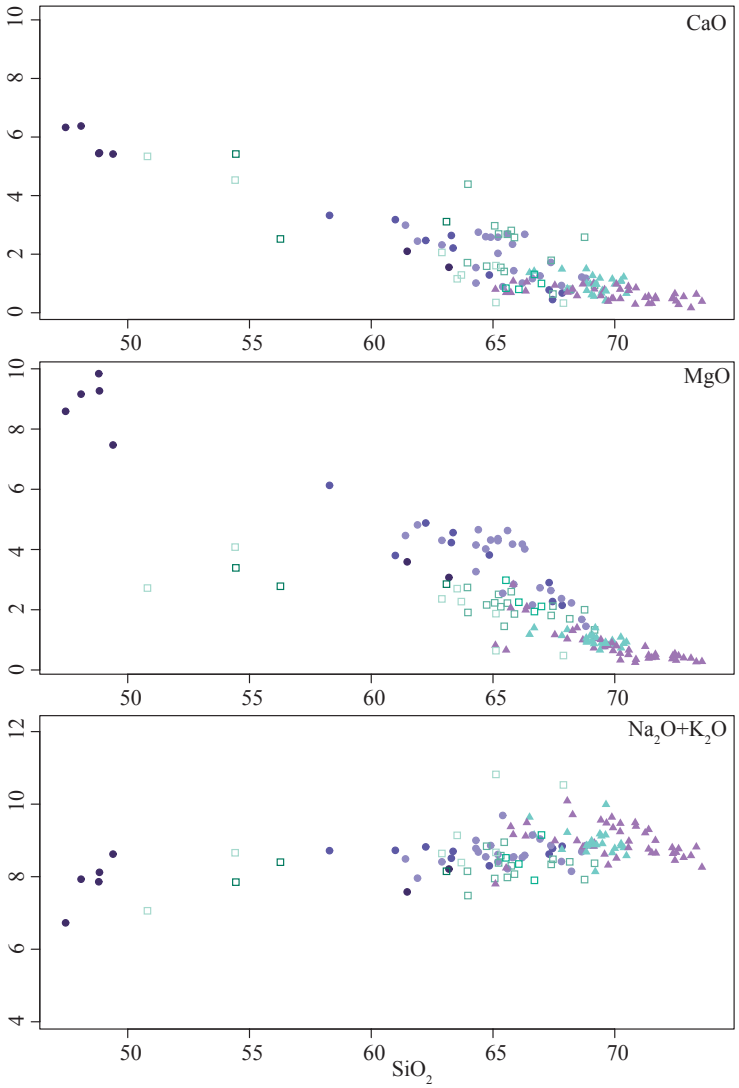

Figure 7: Variation diagram of CaO, MgO and total alkalis vs. SiO_2 (wt%) for whole-rock samples from CVMg-K, SVMg-K, Eastern- and Western-CVG. Same legend as Fig. 2

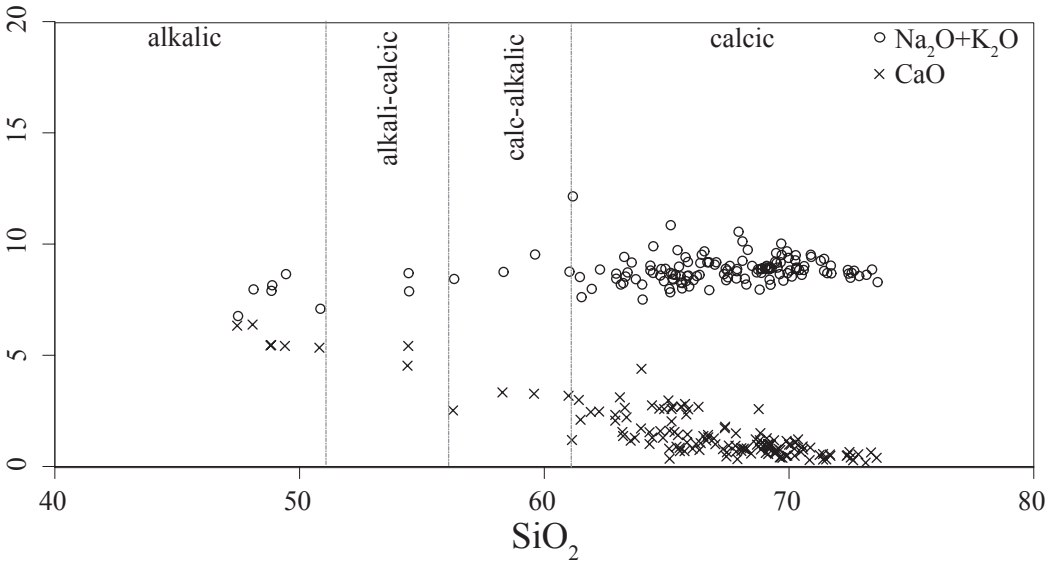

Figure 8: Variations of CaO wt% and $Na_2O + K_2O$ vs. SiO_2 wt% for Vosgian rocks. Original named fields within SiO_2 wt% ranges are Peacock (1931) and are applied to suites whose oxide variation trends intersect within a given field.

7.1.2 Trace elements

Regarding trace-elements, the Mg-K plutonism is characterized by enrichment in Cr and Ni (>80 ppm and >15 ppm, respectively) as well as in many incompatible elements (Th = 20-80 ppm; U = 5-25 ppm). Primitive mantle-normalized plots of representative samples are given in Fig. 9a. Rocks of the Mg-K association show enrichment of LILE (Large Ion Lithophile Elements: Cs, Rb, Ba) as well as high contents of K, U and Th (except for rocks with SiO_2 <50% in the CVMg-K association). Weakly positive Zr and Hf anomalies are observed in the SVMg-K association. The CVMg-K association is characterized by a negative Sr anomaly whereas the SVMg-K association shows a negative P anomaly. All the patterns display weak negative Nb, Ta and Ti anomalies that are generally considered to reveal a genesis by subduction-related processes (Thompson et al., 1984).

Chondrite-normalized REE patterns are illustrated in Fig. 9b. All Mg-K samples display a strong enrichment in LREE with Ce_N/Yb_N about 13 to 30 (CVMg-K) and about 9 to 15 (SVMg-K). Mg-K rocks are characterized by a sizeable negative Eu anomaly: Eu/Eu*= 0.6 for the CVMg-K association and Eu/Eu*= 0.7 for the SVMg-K association. The magnitude of the negative Eu anomaly remains nearly constant even with increasing silica content. The total REE contents are generally high and decrease from basic to acidic rocks (450 ppm to 180 ppm for CVMg-K; 300 ppm to 120 ppm for SVMg-K). A constant Eu anomaly and a decreasing REE content with increasing host rock SiO_2 are typical characteristics of Mg-K magmatism.

7.1.3 Isotopic composition

Sr-Nd whole-rock isotope data are listed in Table 2. Initial ratios were calculated using a mean age of 340 Ma for Mg-K associations. These results were plotted onto a $(^{87}Sr/^{86}Sr)_i$ *vs.* ε_{Ndi} diagram (Fig. 10a). Each of the Mg-K associations defines a well-defined cluster of restricted Sr-Nd isotopic composition. Apart from some mafic members of SVMg-K, none of the analysed rocks had positive ε_{Nd} values. In the SVMg-K association, $(^{87}Sr/^{86}Sr)_i$ ratios are bracketed between 0.705 and 0.708 and ε_{Nd} between +1.4 and -4.8. Rocks of the CVMg-K association have significantly higher $(^{87}Sr/^{86}Sr)_i$ of 0.710-0.714 and lower ε_{Nd} values than those of the SVMg-K associations; ε_{Ndi} values remain mostly constant for all rocks of CVMg-K association as -5.0 to -6.7.

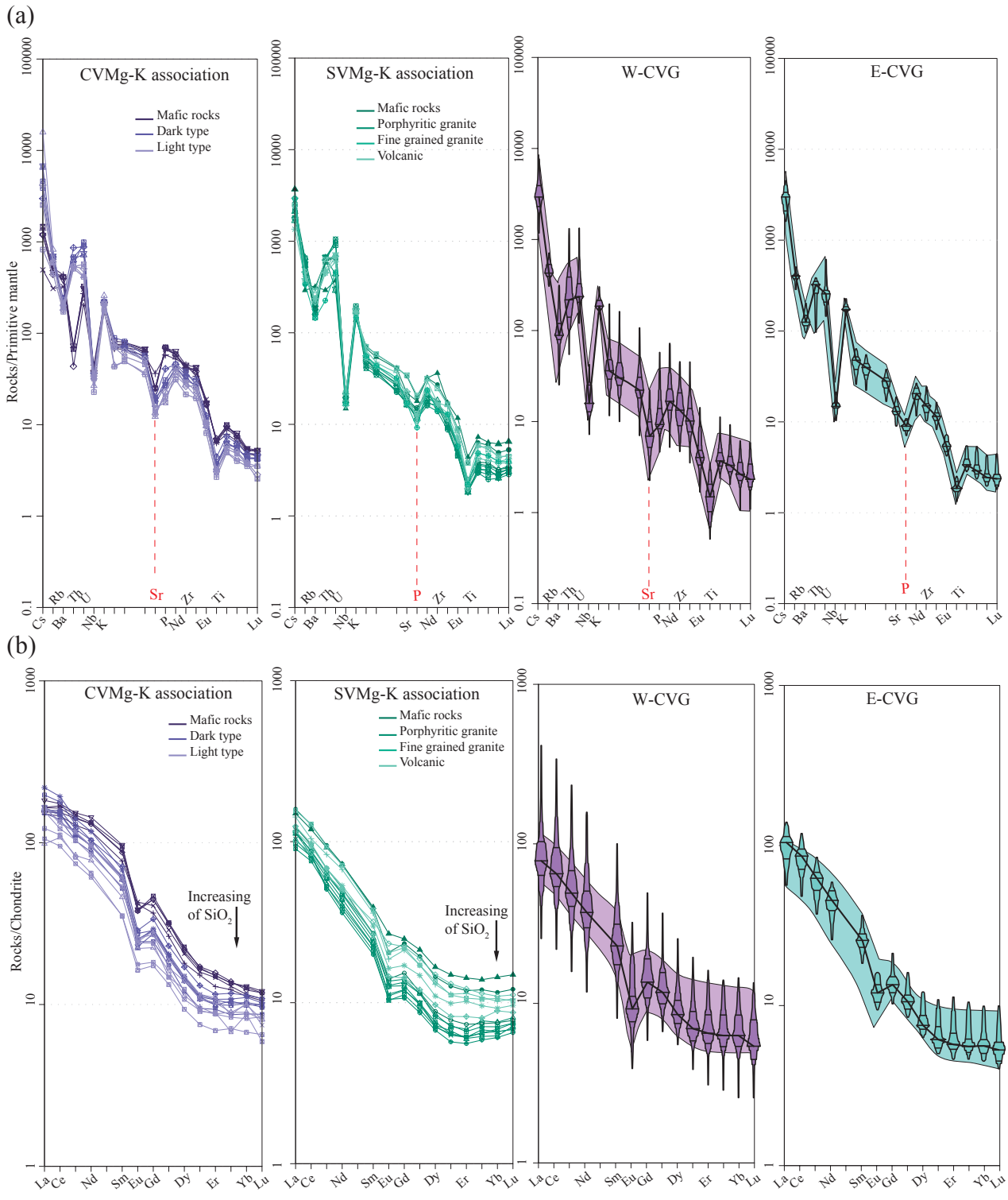

Figure 9: (a) Primitive mantle-normalized spider plots for W-CVG, E-CVG, CVMg-K and SVMg-K associations (after Sun & McDonough, 1989). (b) Chondrite-normalized REE diagram for representative analyses from the four CVM and SVM associations; normalizing values from Boynton (1984), "spider box and percentile plots" for CVG.

7.2. The Central Vosges Granite

7.2.1 Major elements

The Eastern and Western CVG are composed of peraluminous rocks (A/CNK >1.1). Plots of CaO, MgO and total alkalis *vs*. SiO_2 are shown on Fig. 7. SiO_2 contents in all rock types exceeded 65 wt%. The CVG defines linear trends with decreasing MgO and CaO (also the case for FeO_t, TiO_2 and P_2O_5) and constant total alkalis as a function of SiO_2.

7.2.2 Trace elements

In contrast to Mg-K associations in the CVG, Ni and Cr contents never exceed 10 ppm and 50 ppm, respectively. Primitive mantle-normalized plots of the CVG association (Fig. 9a) are rather similar to those of Mg-K associations, though with lower LILE and U and Th contents for a similar SiO_2 content. The Eastern part of the CVG is characterized by a strong negative P anomaly and a positive Zr and Hf anomalies, whereas the Western part shows a more pronounced negative Sr anomaly.

Chondrite-normalized REE patterns (Fig. 9b) display the same strong enrichment in LREE as in the Vosgian Mg-K associations and a strong fractionation (Ce_N/Yb_N ~ 4.0 to 30.0). The sum of REE is about 130 to 150 ppm for all rocks and lower than in Mg-K. Moreover, CVG is characterized by a significant negative Eu anomaly (Eu/Eu* between 0.30 to 0.70 for the western and 0.55 to 0.7 for the Eastern part).

7.2.3 Isotopic composition

Sr-Nd whole-rock isotope data are listed in Table 2 and plotted onto a ($^{87}Sr/^{86}Sr$) *vs.* ε_{Nd} diagram (Fig. 10b). Initial ratios were calculated using a mean age of 320 Ma for CVG. CVG displays a ribbon of isotopic composition bridging SVMg-K values with those of the "Moldanubian" continental crust (Gorokhov et al., 1977; Köhler & Müller-Sohnius, 1980; Liew & Hofmann, 1988; Scharbert & Veselà; 1990). The CVG isotopic values are ($^{87}Sr/^{86}Sr$) = 0.709 to 0.712 and ε_{Nd} = -4.1 to -5.4 for the Eastern part and ($^{87}Sr/^{86}Sr$) = 0.715 to 0.720 and ε_{Nd} = -6.1 to -6.8 for the Western part (Fig. 10b). Isotopic data of the Eastern CVG are bracketed between SVMg-K and CVMg-K isotopic values whereas Western CVG rocks show the highest ($^{87}Sr/^{86}Sr$) values of CVM and SVM granitoids and the same ε_{Nd} values as CVMg-K.

Table 2: Sr-Nd isotopic data for rocks of the Central and Southern Vosges Mts.

	Sample	Rb (ppm)	Sr (ppm)	$^{87}Rb/^{86}Sr$	$^{87}Sr/^{86}Sr$	2σ(m)	$(^{87}Sr/^{86}Sr)_{340}$	Sm (ppm)	Nd (ppm)	$^{147}Sm/^{144}Nd$	$^{143}Nd/^{144}Nd$	2σ(m)	ε^{340}_{Nd}	T^{Nd}_{DM} (Ga)
CVMg-K														
Mafic rocks	EV 382N	294.5	488.2	1.7449	0.72213	0.000008	0.71369	18.89	86.2	0.1325	0.512189	0.000006	-6.0	1.80
Dark facies	CN 7	341.1	352.7	2.7974	0.72532	0.000006	0.71178	10.17	52.6	0.1169	0.512150	0.000004	-6.1	1.57
Light facies	CS 3	360.0	310.0	3.3590	0.72733	0.000008	0.71107	11.98	56.5	0.1282	0.512177	0.000006	-6.1	1.73
	CS 21	340.0	249.0	3.9496	0.72950	0.000007	0.71039	12.02	57.9	0.1254	0.512141	0.000009	-6.7	1.74
	ME 1	359.8	326.4	3.1885	0.72683	0.000006	0.71140	10.27	51.2	0.1213	0.512202	0.000004	-5.3	1.56
	BR 14	299.6	413.0	2.0983	0.71983	0.000006	0.70968	13.86	61.1	0.1371	0.512162	0.000005	-6.7	1.96
SVMg-K														
Mafic rocks	BAB 5	287.1	374.3	2.2186	0.71587	0.000006	0.70514	5.21	31.0	0.1016	0.512307	0.000004	-2.4	1.15
	BAB 3	184.8	464.8	1.1500	0.71043	0.000007	0.70486	7.64	43.4	0.1064	0.512511	0.000004	1.4	0.91
Porphyry granite	BA 8	336.1	413.0	2.3539	0.71747	0.000006	0.70608	5.63	30.9	0.1102	0.512307	0.000006	-2.7	1.24
	BA 16	360.7	335.5	3.1098	0.72349	0.000006	0.70844	4.71	26.6	0.1071	0.512300	0.000007	-2.7	1.21
Fine-grained granite	CO 3	479.8	332.2	4.1777	0.72760	0.000009	0.70738	10.56	49.4	0.1292	0.512245	0.000003	-4.8	1.63
Volcanism	VOS 4	84.1	971.2	0.2505	0.70766	0.000006	0.70644	6.22	29.9	0.1258	0.512532	0.000007	1.0	1.07
	VOS 8	292.9	479.2	1.7680	0.71503	0.000007	0.70648	5.14	30.6	0.1016	0.512210	0.000004	-4.3	1.28

	Sample	Rb (ppm)	Sr (ppm)	$^{87}Rb/^{86}Sr$	$^{87}Sr/^{86}Sr$	2σ(m)	$(^{87}Sr/^{86}Sr)_{320}$	Sm (ppm)	Nd (ppm)	$^{147}Sm/^{144}Nd$	$^{143}Nd/^{144}Nd$	2σ(m)	ε^{320}_{Nd}	T^{Nd}_{DM} (Ga)
Eastern-CVG														
	CO 4	337.2	350.8	2.7804	0.72306	0.000006	0.71040	9.59	46.8	0.1239	0.512219	0.000005	-5.2	1.58
	LV 8	269.8	249.2	3.1316	0.72358	0.000006	0.70931	5.12	27.2	0.1138	0.512241	0.000005	-4.4	1.39
	TF 1	240.3	303.8	2.2879	0.71980	0.000006	0.70938	4.74	25.8	0.1111	0.512250	0.000004	-4.1	1.33
	FU 2	299.5	278.9	3.1061	0.72571	0.000006	0.71157	9.29	44.0	0.1277	0.512218	0.000004	-5.4	1.65
	WI 10	253.4	250.8	2.9225	0.72499	0.000008	0.71168	4.54	23.9	0.1148	0.512217	0.000005	-4.9	1.44
	BR 4	237.9	294.5	2.3366	0.71957	0.000008	0.70893	5.44	29.8	0.1104	0.512239	0.000006	-4.3	1.34
Western-CVG														
	GG 4	192.5	98.8	5.6357	0.74548	0.000007	0.71981	4.38	20.1	0.1317	0.512158	0.000005	-6.8	1.84
	GG 9	259.6	287.9	2.6082	0.72709	0.000007	0.71521	12.69	97.0	0.0791	0.512053	0.000006	-6.6	1.24
	RE 11	243.3	111.8	6.2947	0.74699	0.00001	0.71832	3.53	19.3	0.1106	0.512145	0.000006	-6.1	1.48
	G1 3	376.1	216.6	5.0225	0.73889	0.000008	0.71601	5.80	34.6	0.1013	0.512113	0.000006	-6.4	1.40

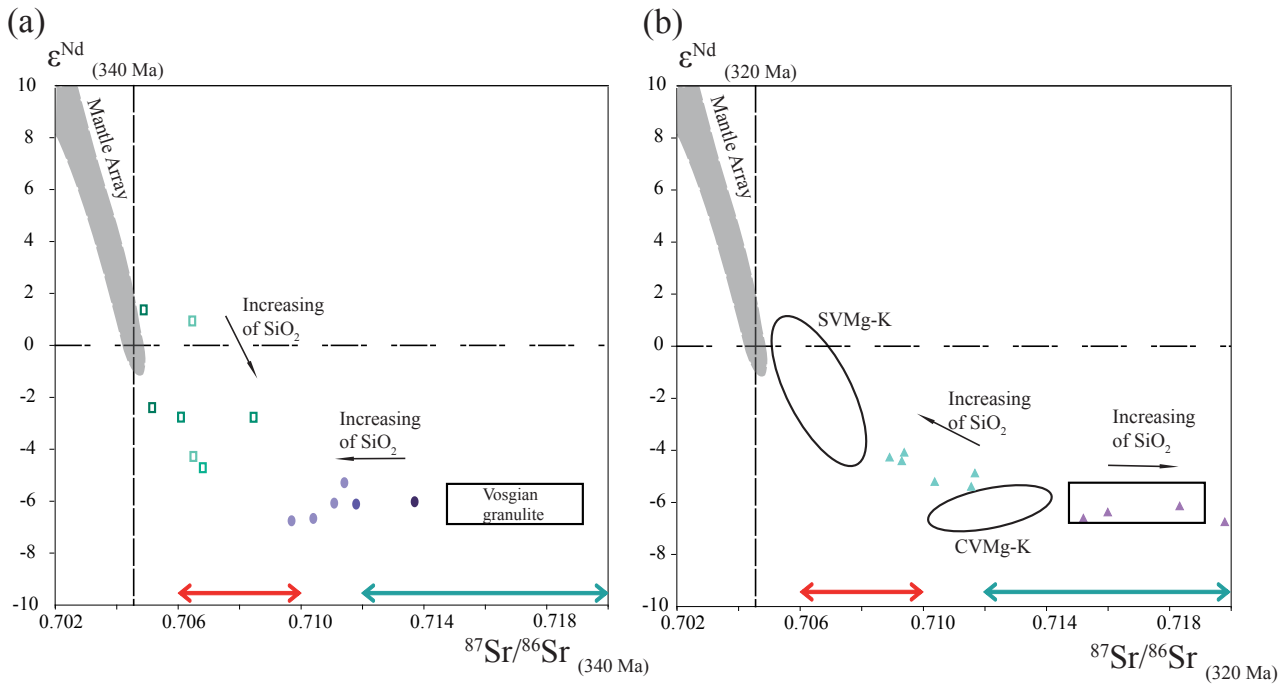

Figure 10: (a) $(^{87}Sr/^{86}Sr)_{340}$ vs. ε^{Nd}_{340} plot for SVMg-K and CVMg-K. Arrows show trend from mafic to felsic end-members for the two associations. (b) $(^{87}Sr/^{86}Sr)_{320}$ vs. ε^{Nd}_{320} plot for W-CVG and E-CVG; CVMg-K and SVMg-K fields are indicated for comparison. Red arrow represents $^{87}Sr/^{86}Sr$ of Vosgian orthogneiss (Bonhomme & Fluck, 1981) and green arrow represents $^{87}Sr/^{86}Sr$ of Vosgian granulite and paragneiss recalculated at 340 Ma. Black rectangle represents isotopic composition of Vosgian granulite (Skrzypek, 2011). Same legend as Fig. 2.

8. Discussion

8.1. Chronology of intrusions in light of new data

New U-Th-Pb zircon and monazite age data together with existing geochronological works reveal that two major magmatic pulses occurred in the Central and Southern Vosges Mts. (Table 1). The first event corresponds to the intrusion of the CVMg-K and SVMg-K associations at 345-335 Ma. The oldest magmatic bodies are the SVMg-K mafic rocks emplaced at *ca.* 345 Ma. Although Schaltegger et al. (1996) proposed that the mafic intrusions are contemporaneous with granitic magmatism, the present study reveals that an interval of 5-10 Ma separates the mafic magmas from the porphyritic and fine-grained granites emplaced from *ca.* 340 Ma (Schaltegger et al., 1996) to 336 ± 4 Ma. In the light of these data, the SVMg-K granites appear to be contemporaneous with the CVMg-K granitoids showing a crystallization ages ranging from *ca.* 340 Ma (Schaltegger et al., 1996) to 337 ± 3 Ma. The SVMg-K rhyolitic volcanism dated at 340 ± 2 Ma is also coeval with acid plutonism.

The second magmatic event is distinctly younger and corresponds to the emplacement of the voluminous CVG association. Previous results indicate that the plutonic activity lasted from 330 to 325 Ma in the E-CVG. New zircon and monazite ages ranging from 324 ± 4 Ma to 319 ± 6 Ma show that a similar evolution is recorded in the W-CVG. In addition, W-CVG rocks yielded inherited ages between 510 and 390 Ma (Fig. 6a). These Ordovician bear similarities to inherited U-Pb zircon ages found in the Central Vosges metamorphic units, and especially in the granulite-facies varied or monotonous gneiss unit (Skrzypek et al., submitted). It is therefore very likely that the W-CVG partly reflects magmatic recycling of metasedimentary protoliths.

8.2. Origin of the Mg-K magmas

Mg-K associations emplaced between 345 and 335 Ma are characterized by high contents of Mg, Cr and Ni, strong REE fractionation with a constant Eu anomaly, and a high LILE content. The decrease in REE content correlates with increasing silica content, but the chemical composition of the minerals remains rather constant. These observations indicate a genetic link between mafic and felsic rocks of the Mg-K associations. While a decreasing REE content with an increase in silica content is due to fractional crystallization of accessories minerals (apatite, zircon, allanite), co-variation diagrams for some major and primitive mantle-normalized trace element patterns (Figs. 7 and 9) favour the main role of mixing processes in the generation of Mg-K magmas.

8.2.1 Petrogenesis

The origin of the Mg-K magmatism has been debated during the last decades (e.g. Rossi & Cocherie, 1991; Holub et al., 1997). Although a high Cr and Ni content and Mg# should point to a derivation from a mantle source, the high concentration of U, Th, LREE and LILE, and the depletion in Ti, Nb and Ta and the Sr-Nd isotopic composition resembles that of the continental crust. Hypotheses for the origin of this type of magmatism were diverse: in the Bohemian Massif, Holub (1997) considered that the Mg-K association of mafic and felsic compositions resulted from mixing between two geochemically contrasting magmas: a basic one that could correspond to enriched mantle-derived melts and a felsic crustal melt of leucogranitic composition. Given the high degree of homogenization, mixing processes had to occur in the lower crust under granulite-facies conditions (Rossi & Cocherie, 1991; Holub, 1997). More recently, Janoušek & Holub (2007) suggested that the very common spatial and temporal link of this Mg-K magmatism with HP-HT granulites might indicate that the magmas are the result of partial melting of a lithospheric mantle contaminated and metasomatized by mature crustal material. Mantle domains were presumably melted by heat advected from the rising asthenospheric mantle, shortly after slab break off.

Thus, the particular geochemical variation and isotopic composition of the studied Mg-K rocks were very probably acquired at an early stage of crustal melting. The differences in $^{87}Sr/^{86}Sr$ and ε_{Nd} ratios coupled with different geochemical patterns (Fig. 9 & 10a) point to different mantle and crustal sources for the two Mg-K associations. In the case of SVMg-K, isotopic ratios $^{87}Sr/^{86}Sr$, high ε^{Nd} and negative phosphorus anomaly argue for a mantle source contaminated and metasomatized by juvenile (Cambro-Ordovician) crustal material or by rocks with low $^{87}Sr/^{86}Sr$ and high ε_{Nd} isotopic compositions (see isotopic data from Canigó Massif; Navidad et al.; 2010; and orthogneiss from Black Forest, Chen et al., 2000). This juvenile material can correspond to early Paleozoic metasediments (Varied gneiss) found in the central Vosges which reveal Late Ordovician maximum sedimentation U-Pb zircon ages (Skrzypek et al., submitted). CVMg-K rocks are, in contrast, characterized by high $^{87}Sr/^{86}Sr$, low ε_{Nd} and a strontium anomaly, which strongly argues for a mature crustal material contamination. The mature crustal material can correspond to the slightly older Cambro-Ordovician U-Pb zircon protolith ages of the felsic granulites (Skrzypek et al., submitted) or to possible Neo-Proterozoic basement which has been found in southern Vosges Klippen belt (Skrzypek et al., 2012). The inherited zircon population agrees with these considerations. Analysed CVMg-K zircons reveal Early Proterozoic component (2.12 ± 0.02 Ga) with no indication of a younger inheritance, whereas SVMg-K zircons do not show any inherited component older than Pan-African ("Cadomian"; Schaltegger et al., 1996). The evolution of isotopic composition trends for these two Mg-K associations tends toward a common isotopic composition reflecting a metasedimentary Moldanubian middle-to-upper crust.

8.2.2 Heat Sources

Janoušek & Holub (2007) proposed that Mg-K magmas of Bohemian massif were generated shortly after slab break-off during the southeastward subduction of the Saxothuringian ocean floor, by partial melting of contaminated and metasomatized lithospheric mantle due to upwelling of asthenospheric mantle material. The same geodynamic scenario is proposed for generation of the Mg-K magmas of the External Crystalline massifs of the Alps and Corsica Batholith (Rossi et al., 2009; Guillot & Ménot, 2009; Giacomini et al, 2006; von Raumer et al., 2002, 2003, 2009), but involving a north-directed subduction of the Paleotethys ocean. Recently, Lexa et al. (2011) modelled the influence of radiogenic heat production of subducted and underplated Saxothuringian rocks at Moho depth under a thickened Moldanubian continental crust in the Bohemian massif. They proposed that subducted continental crust produced fluids that contaminated and enriched the lithospheric mantle by adding lithophile elements and removing radiogenic elements (U, Th and K) with a thermal incubation of 10-15 Ma. This process generated high temperature metamorphism transforming Saxothuringian Ordovician protoliths into HP granulite via dehydratation melting and, at the same time, heated the metasomatized lithospheric mantle producing Mg-K magmas. The existence of both types of Mg-K magma a few kilometres apart in the Vosges Mountains suggests that involvement of synchronous slab-break off of two subduction zones in each part of the Variscan internal zone seems unrealistic. We thus prefer to adopt the geodynamic scenario of Lexa et al. (2011) for explaining the generation of Mg-K magmas. The source for radiogenic heat production is evidenced by trace-element patterns showing U, Th and Cs enrichment in Mg-K rocks, as for contemporaneous and chemically identical granitoids in the Bohemian Massif (Fig 11)**.** In the case of the Vosges the material Saxothuringian affinity (varied gneiss and felsic granulite) was relaminated underneath Early Paleozoic metasediments (Monotonous gneiss) of the Moldanubian domain (Fig. 17).

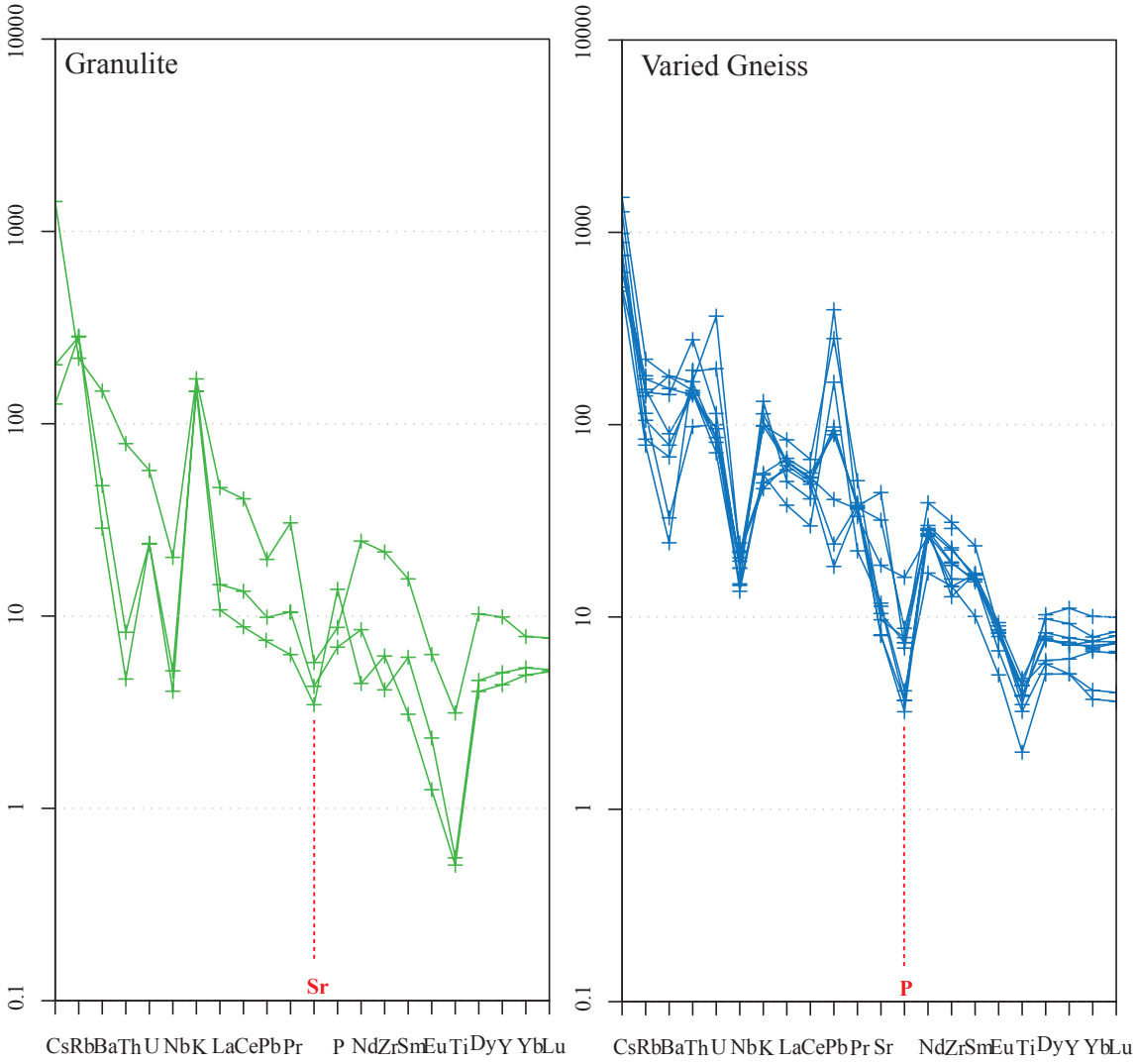

Figure 11:Primitive mantle-normalized spider plots (after Sun & McDonough, 1989) for Vosgian granulite and varied gneiss (Data from Skrzypek, 2011). Patterns show similarities and are complementary with Mg-K patterns.

8.3. Origin of the CVG magmas

The CVG rocks are 15 to 20 Ma younger than the Mg-K associations, but they are also characterized by a high LILE content and a high REE fractionation. Trace-element patterns (Figs. 9) as well as mineral chemical composition point to a strong influence of assimilation and fractional crystallization processes (AFC). The AFC process is also supported by the trend of CVG rocks in the La/Yb – Eu/Yb correlation plot and Ce/Yb - Ce plot which show straight line (Fig. 12). Common characteristics (high LILE and incompatible elements contents and strong REE fractionation) of both Mg-K associations and CVG suggest similar source compositions characterized by LREE, LILE and incompatible-elements enrichment. Moreover, presence of xenoliths of different composition in the CVG suggests a variety of sources involved in magma generation.

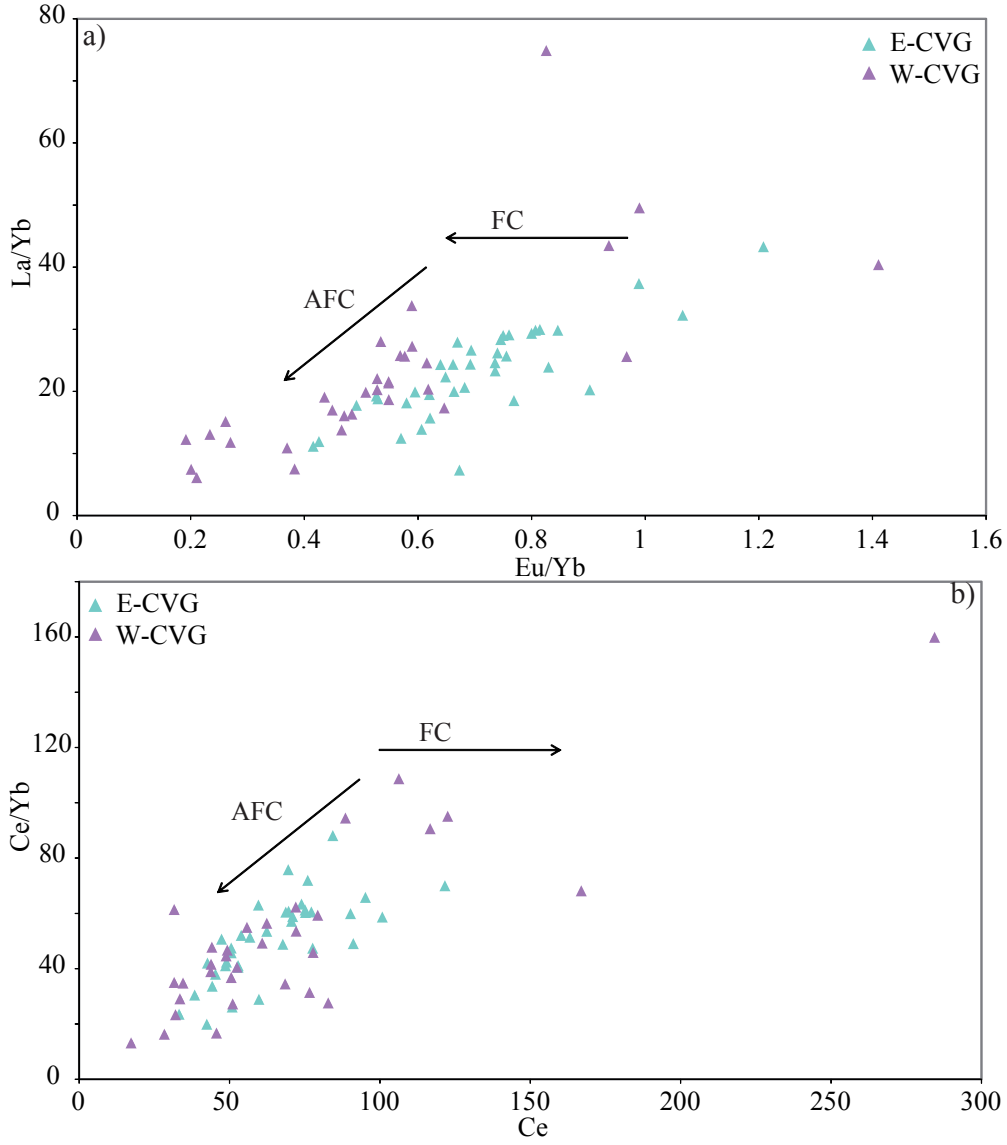

Figure 12: (a) La/Yb vs. Eu/Yb and (b) Ce/Yb vs. Ce diagrams for CVG rocks. The arrows correspond to the evolution trends in assimilation and fractional crystallization process (AFC) and fractional crystallization process only (FC).

8.3.1 Petrogenesis

Isotopic CVG data (Fig. 10b) bridge compositions between felsic SVMg-K and CVMg-K associations in the Eastern-CVG part and have similar $^{87}Sr/^{86}Sr$ ratios as Vosgian amphibolite (0.706-0.709; Bonhomme & Fluck, 1981). The Western part has an intermediate isotopic composition between the mafic CVMg-K association and felsic granulite and gneisses of Vosges Mts ($^{87}Sr/^{86}Sr$ ratios between 0.710 and 0.720; Bonhomme & Fluck, 1981 and this study and ε_{Nd} values around -7; this study). These differences in isotopic composition and in geochemical patterns (Fig. 9 & 10b) point to different crustal sources for the two part of CVG. In the case of E-CVG, isotopic ratios $^{87}Sr/^{86}Sr$, ε^{Nd} values and negative phosphorus anomaly argue for juvenile crustal material derived from igneous protolith or juvenile metasedimentary rocks involved in sources. This crustal material can correspond to amphibolite found in the central Vosges Mts or metasedimentary Moldanubian middle

to upper crust. Contamination by the Moldanubian upper crust is also precluded by the decrease of initial Sr ratios with increasing of silica content.

The W-CVG is, in contrast, characterized by high $^{87}Sr/^{86}Sr$, low ε_{Nd} and a strontium anomaly, which strongly argue for a mature crustal material involved in sources. The mature crustal material can correspond to granulite or gneisses found in the Vosges Mts. Inherited zircons of the Western-CVG part show ages similar to than of varied and monotonous gneissic units (450 to 550 Ma; Skrzypek, 2011) whereas the Eastern-CVG does not contain any inheritance (Schaltegger et al., 1999). These observations and the presence of xenoliths of CVMg-K, gneiss and sedimentary rock suggest that: i) the Western-CVG magma derived from melting of a source composed of a mixture of CVMg-K and varied gneisses and ii) the Eastern-CVG magma derived from amphibolite or the metasedimentary Moldanubian middle-to-upper crust.

8.3.2 Heat source

However, this raises the question about the potential heat sources required for generating the CVG magmas. Henk et al. (2000) discussed different possible geodynamic scenarios for such heat-producing processes during the final stage of Variscan Belt, i.e. i) lithospheric mantle delamination, ii) the ascent of a mantle plume, and iii) radiogenic heat production. Gerdes et al. (2000) concluded, through modelling of radiogenic heat production from rocks with an average heat production of about 2 μWm^{-3}, that such internal radiogenic heat production within thickened crust is the essential source for heat required to form widespread the 330-320 Ma granite.

The evolution of the crustal geotherm was modelled to evaluate the thermal influence of Mg-K granitoids emplaced at *ca.* 340 Ma. Using the finite-difference method, the model solves the one-dimensional heat flow equation simplified to:

$$\frac{\partial T}{\partial t} = \kappa \frac{\partial^2 T}{\partial z^2} + \frac{A_{rad}}{\rho c}$$

where T is temperature, t is time, κ is thermal diffusivity ($1e^{-6}$ $m^2.s^{-1}$), z is depth, ρ is density (2.7 $g.cm^{-3}$), c is the specific heat capacity (1 $kJ.kg^{-1}.K^{-1}$), and A_{rad} is the heat production per unit volume by radioactive decay. The model setup involves a thickened felsic crust for which a mean radiogenic heat production of 2 $\mu W.m^{-3}$ has been prescribed down to 50 km depth, and subject to a basal mantle heat flow Q_m=30 $mW.m^{-2}$ (Fig. 13). A layer of Mg-K granitoid of variable thickness (2-10 km) and radiogenic heat production (0-8 $\mu W.m^{-3}$) is introduced at 20 km depth, and its intrusion temperature is set at 900 °C. The initial geotherm was calibrated according to P-T conditions of ~9 kbar/700 °C and ~15 kbar/900 °C inferred for gneiss and granulite of the Central Vosges, respectively (Skrzypek, 2011).

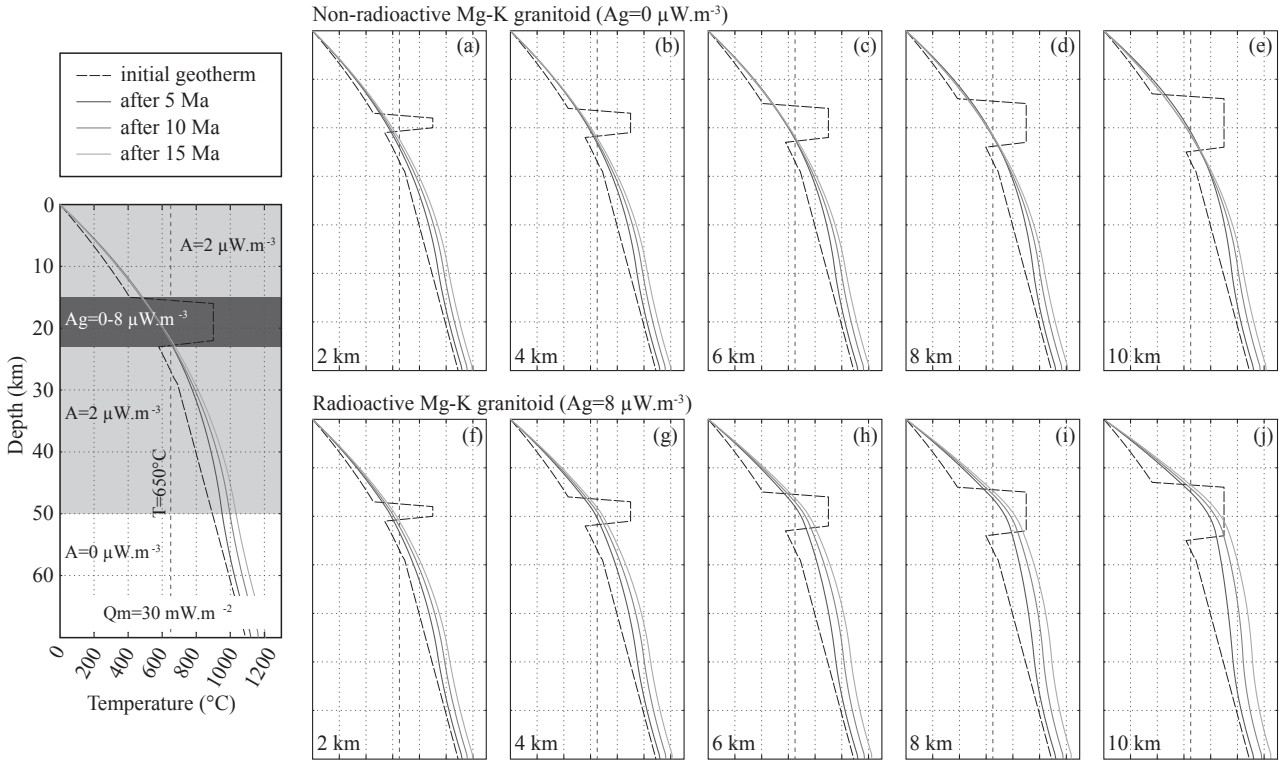

Figure 13: Results of 1D thermal models to compare geotherm evolution controlled by different radiogenic heat production and variable thickness of Mg-K intrusions at 20 km depth.

Fig. 13 presents the evolution of the geotherm during 15 Ma, at 5 Ma intervals, for both a non-radioactive (0 µW.m^{-3}) and radioactive (8 µW.m^{-3}) Mg-K layer. It shows that, regardless of the thickness of the Mg-K intrusion, the 650 °C isotherm is never crossed above 20 km depth in the case of a non-radioactive body (Fig. 13 a-e). On the other hand, temperatures above 650 °C are achieved at depths of 14-19 km after 10 Ma and for Mg-K layers thicker than 4 km (Fig. 13 f-j). The depth at which the 650 °C isotherm is crossed slightly rises to 13 km for a longer period of 15 Ma. Thermal modelling therefore shows that partial melting in the upper crust can occur if a relatively hot (900 °C), radioactive (8 µW.m^{-3}) and thick (4-10 km) Mg-K granitoid is emplaced deep enough within the crust. Calculations involving shallow intrusions and radiogenic heat production only down to 15 km depth turned out to show no significant perturbation of the geotherm.

Average heat production of the CV- and SV-Mg-K associations varies from 4 to 8 µWm^{-3} (Table 3) and is sufficient to melt the varied gneisses unit and metasedimentary Moldanubian middle-to-upper crust, producing enough magma volume to generate the CVG without involving heat from the lithospheric mantle. The lack of mafic enclaves within the CVG is in agreement with this hypothesis.

Table 3: Average K, Th and U contents, and estimation of heat production (A; microwatt per cubic meter; Kramers et al., 2001) of CVMg-K and SVMg-K rock types.where t represents age in Ga, ρ is density and K, U, Th are concentrations in ppm.

Rock type	Concentrations (ppm)			A (μWm^{-3})	
	K	Th	U	Present	at 340 Ma
CVMg-K association:					
Mafic rocks	48552	20.5	5.7	3.43	3.65
Dark facies	53471	54.7	14.7	8.28	8.71
Light facies	50960	41.6	12.8	6.83	7.21
SVMg-K association:					
Mafic rocks	29941	30.0	8.2	4.59	4.83
Porphyry granite	44313	57.2	18.2	9.32	9.80
Fine-grained granite	45555	37.3	10.1	5.76	6.07

$$A\left[\mu Wm^{-3}\right] = \rho\left[\begin{array}{l} K\left(3.45.10^{-6}/e^{-0.554t}\right) + Th\left(2.638.10^{-2}/e^{-0.0495t}\right) \\ + U\left(\left(4.03777.10^{-3}/e^{-0.985t}\right) + \left(9.396852.10^{-2}/e^{-0.1551t}\right)\right)\end{array}\right]$$

8.4. Link with the Corsican, Alpine, Black Forest and Bohemian massifs for the ca. 340 Ma Mg-K associations

Many other Mg-K intrusions occur in the Moldanubian zone of the European Variscan Belt. Data from Holub (1997), Holub & Janoušek (2003), Janoušek et al. (1995, 2000) for the Bohemian massif; Schaltegger et al. (1991), Debon & Lemmet (1999), Debon et al.(1998) for the External Crystalline Massifs of the Alps; Hann (2003) and Schaltegger (2000) for the Black Forest, and Rossi & Cocherie (1991) and Cocherie et al. (1994) for the Corsica Batholith will be used hereafter for comparison with the Mg-K magmatism of the Vosges Massif. The Čertovo Břemeno suite of Bohemian Massif was dated (U-Pb/zircon) between 343 and 336 Ma (Holub et al., 1997). Mg-K rocks of Alps were dated (U-Pb/zircon) between 343 and 332 Ma from Argentera (Malinvern-Argentera metamonzonite, Lombardo et al., 1997), the Pelvoux Massif (Rochail monzogranite, Guerrot, 1998), the Belledonne Massif (Saint Colomban, la Lauzière and Sept Laux granites, Debon et al., 1998), the Aiguilles Rouges Massif (Pormenaz monzonite, Bussy et al., 1998) and the Aar Massif (Giuv syenite and Punteglias granite, Schaltegger & Corfu, 1992, 1995). Similar ages (U-Pb/zircon) from 347 to 336 Ma were found for the Corsica Batholith (Paquette et al., 2003). Ages of Mg-K granite (U-Pb/zircon) from the Black Forest range from 342 to 332 Ma (Schaltegger, 2000). In the classification diagram of Debon and Le Fort (1983; Fig. 14), the evolution trend of Mg-K rocks from the Alps, Corsica and the Black Forest follows the same trend as the SVMg-K association from monzonite to granite-adamellite, whereas Mg-K rocks from the Bohemian Massif and the CVMg-K association show a similar trend. Major- and trace-element compositions are similar for all these massifs; while by MgO varies from 10 to 2 wt% and CaO ranges from 5 to 2 wt%, the total alkalis remain constant at about 8 wt% (Fig. 15).

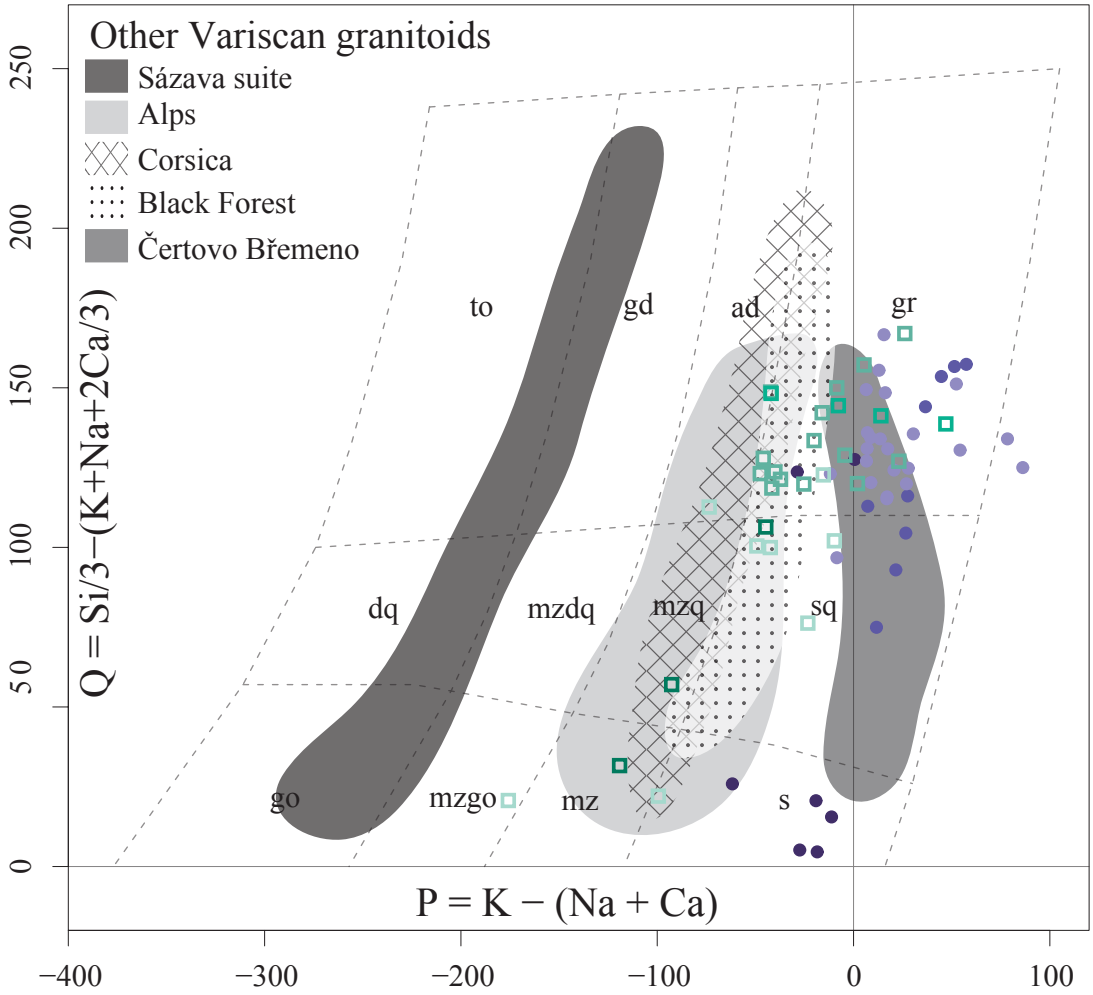

Figure 14: Multicationic P-Q plot (Debon & Le Fort, 1983) for other Mg-K Variscan plutons. Data from Holub, 1997 and Janoušek et al., 2000 for Bohemian massif, Schaltegger et al., 1991, Debon and Lemmet, 1999 and Debon et al., 1998 for External Crystalline massifs of the Alps, Hann, 2003 and Schaltegger, 2000 for Black Forest, and Rossi & Cocherie, 1991 and Cocherie et al., 1994 for Corsica Batholith. Parameter P provides the proportion between K-feldspar and plagioclase and Q the quartz content in the rock. The calc-alkaline Sazava suite and Mg-K Vosgian samples are plotted for comparison (Same legend as Fig. 2).

Enrichment in Cr (50-600 ppm), Ni (10-180 ppm), Th (20-50 ppm) and U (5-30 ppm) is a common feature throughout the different Variscan Mg-K intrusions. These are also characterized by a similar mineral composition and nature of the accessory phases. CVMg-K and Bohemia's Čertovo Břemeno rocks as well as SVMg-K and U1 Corsica rocks have an identical biotite chemical composition. Moreover, Sr-Nd isotopic compositions (Fig. 16) follow the same pattern: initial $^{87}Sr/^{86}Sr$ and ε_{Nd} ratios from Corsica ($^{87}Sr/^{86}Sr$ = 0.704-0.708 and ε_{Nd} = +1 to -5) and the Black Forest ($^{87}Sr/^{86}Sr$ about 0.708 and ε_{Nd} = -4 to -5) fall in the range of the SVMg-K association, whereas those of Čertovo Břemeno ($^{87}Sr/^{86}Sr$ = 0.710-0.712 and ε_{Nd} = -6.3 to -7.8) and the CVMg-K association are similar.

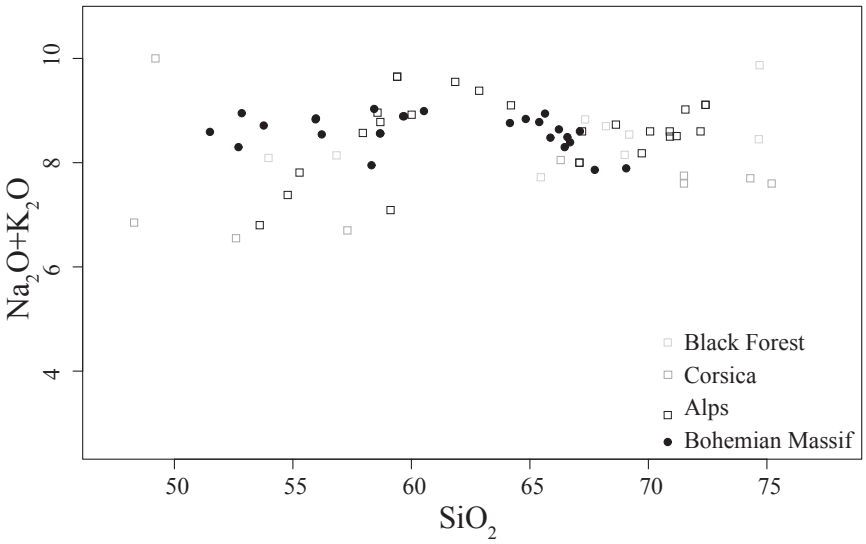

Figure 15: Variation diagram of total alkali (wt%) vs. SiO_2 (wt%) for Mg-K whole-rock samples from Bohemian Massif, Alps, Corsica Batholith and Black Forest. Data from Holub, 1997 and Janoušek et al., 2000 for Bohemian Massif, Schaltegger et al., 1991, Debon and Lemmet, 1999 and Debon et al., 1998 for External Crystalline Massifs of the Alps, Hann, 2003 and Schaltegger, 2000 for Black Forest and Rossi & Cocherie, 1991 and Cocherie et al., 1994 for Corsica Batholith.

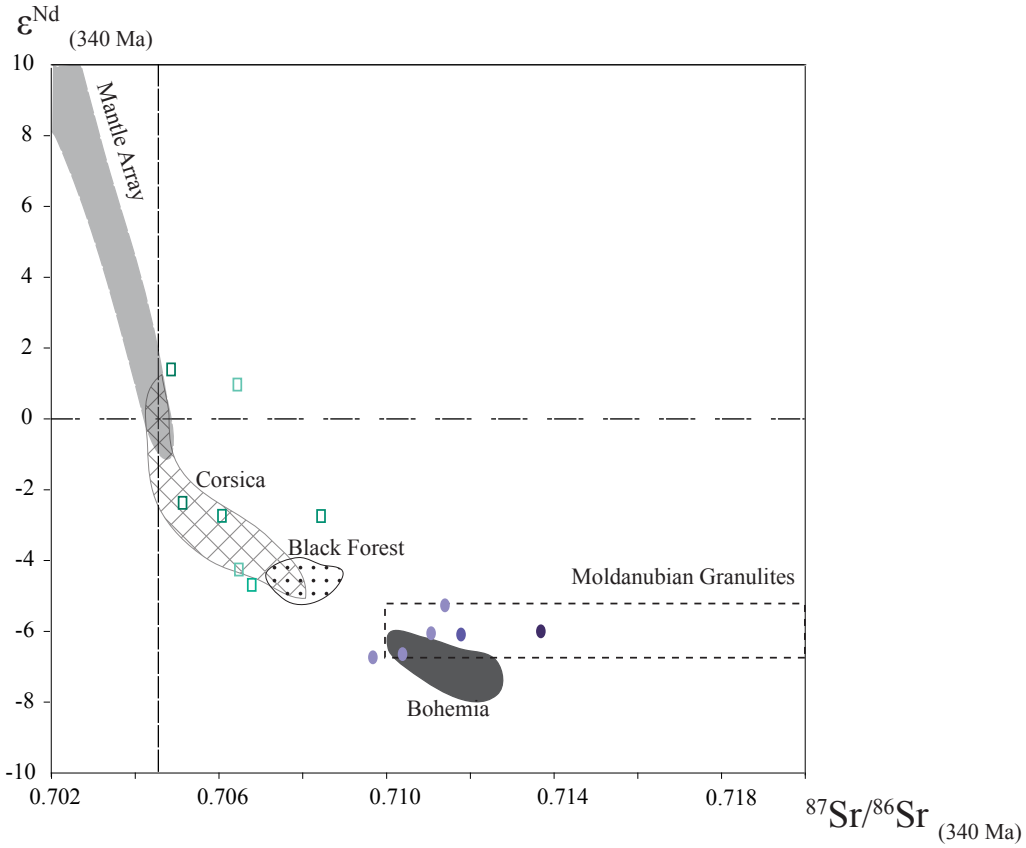

Figure 16: $(^{87}Sr/^{86}Sr)_{340}$ vs. ε^{Nd}_{340} plot for other Mg-K Variscan plutons. Data from Janoušek et al., 1995 and Holub and Janoušek, 2003 for Bohemian Massif, Schaltegger et al., 1991, Debon and Lemmet, 1999 and Debon et al., 1998 for External Crystalline Massifs of the Alps, Hann, 2003 and Schaltegger, 2000 for Black Forest and Rossi & Cocherie, 1991 and Cocherie et al., 1994 for Corsica Batholith. Mg-K Vosgian samples are plotted for comparison. Corsica, CVMg-K and Black Forest data as well as CVMg-K and Bohemia data are arranged in two independent clouds, suggesting a genesis from different protoliths. Same legend as Fig. 10.

These observations underline that the Mg-K magmatism was a characteristic feature of the Moldanubian zone and point to two homogeneous Mg-K magmatic associations. The northern part of the Moldanubian was intruded by the CVMg-K –type, oriented NE-SW from the Bohemian Massif to the Black Forest to the Vosges Mountains, and the southwestern part of the European Moldanubian zone is characterized by an E-W trending SVMg-K type recognized in the Corsica Batholith, in some External Crystalline massifs of the Alps, and in the southern part of the Black Forest and Vosges.

8.5. Geodynamic significance

Janoušek & Holub (2007) proposed that Mg-K magmas of Bohemian Massif were generated shortly after slab break-off during the southeastward subduction of the Saxothuringian Oceanic crust, by partial melting of contaminated and metasomatized lithospheric mantle due to upwelling of asthenosphere. The same geodynamic scenario was proposed for generation of the Mg-K magmas of the External Crystalline massifs of the Alps and Corsica Batholith (Rossi et al., 2009; Guillot & Ménot, 2009; Giacomini et al, 2006; von Raumer et al., 2002, 2003, 2009), but involving a north-directed subduction of the Paleotethys Ocean. Recently, Lexa et al. (2011) modelled the influence of radiogenic heat production of subducted and underplated felsic Saxothuringian metaigneous rocks at Moho depth under a thickened Moldanubian continental crust in the Bohemian Massif. They proposed that subducted continental crust produced fluids that contaminated and enriched the lithospheric mantle by adding lithophile elements with a thermal incubation of 10-15 Ma. This process converted the Saxothuringian rocks into granulite via dehydratation melting, switched off the heat source by removing radiogenic elements (U, Th) and, at the same time, heated the metasomatized lithospheric mantle producing Mg-K magmas. The existence of both types of Mg-K magma a few kilometres apart in the Vosges Mountains suggests that involvement of synchronous slab-break off of two subduction zones in each part of the Variscan internal zone seems unrealistic. We thus prefer to adopt the geodynamic scenario of Lexa et al. (2011) for explaining the generation of Mg-K magmas. Proterozoic to Neoproterozoic felsic rock underlies Early Paleozoic mafic (magmatic-arc) rock in the Saxothuringian continental crust (Fig. 17; Schulmann et al., 2009b; Lexa et al., 2011). The petrological, geochemical and isotopic differences of these two groups of Mg-K intrusions could be explained by separately melting each of these rock types on the top of the metasomatized lithospheric mantle (Fig. 17).

Intrusion of Mg-K magma in the middle crust at about 20 km depth could have occurred shortly after the partial melting of surrounding country rocks caused by radiogenic heat production and may have formed the CVG magma at *ca.* 330 Ma. Exhumation of the lower and middle crust could have been accelerated by the Ste-Marie-aux-Mines and Bilstein fault zones (Fig. 17). This would imply that these fault zones can be considered as a detachment fault (Skrzypek, 2011), and thus as a first-order structural element of the Vosges.

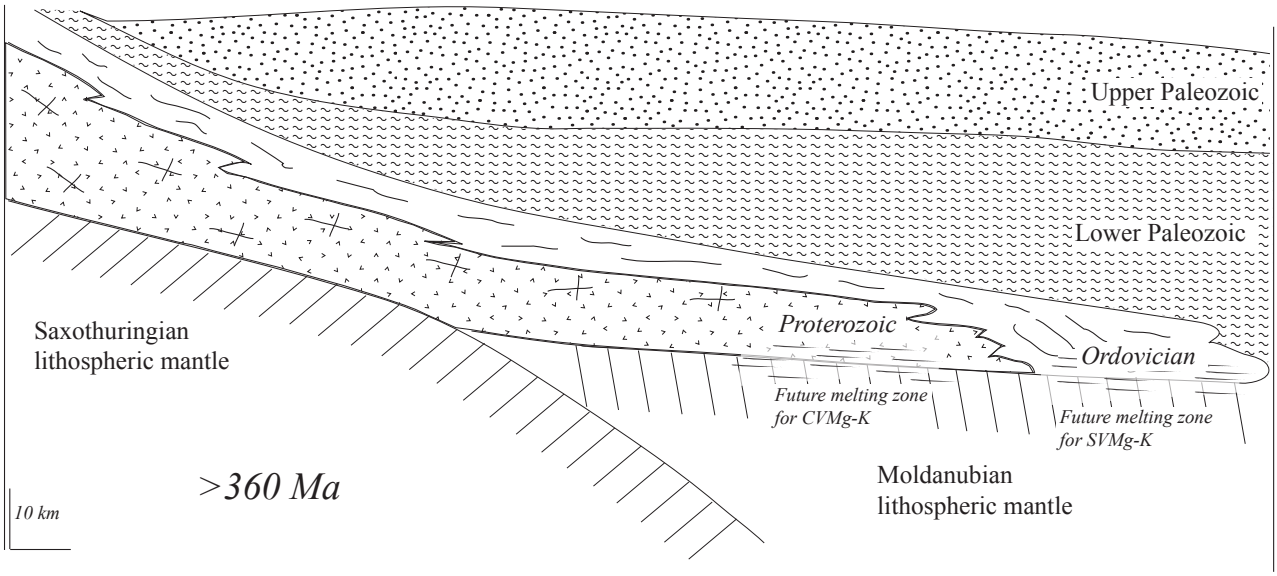
Upper Paleozoic
Lower Paleozoic
Saxothuringian
lithospheric mantle
Proterozoic
Ordovician
Future melting zone
for CVMg-K
Future melting zone
for SVMg-K
Moldanubian
lithospheric mantle
>360 Ma
10 km

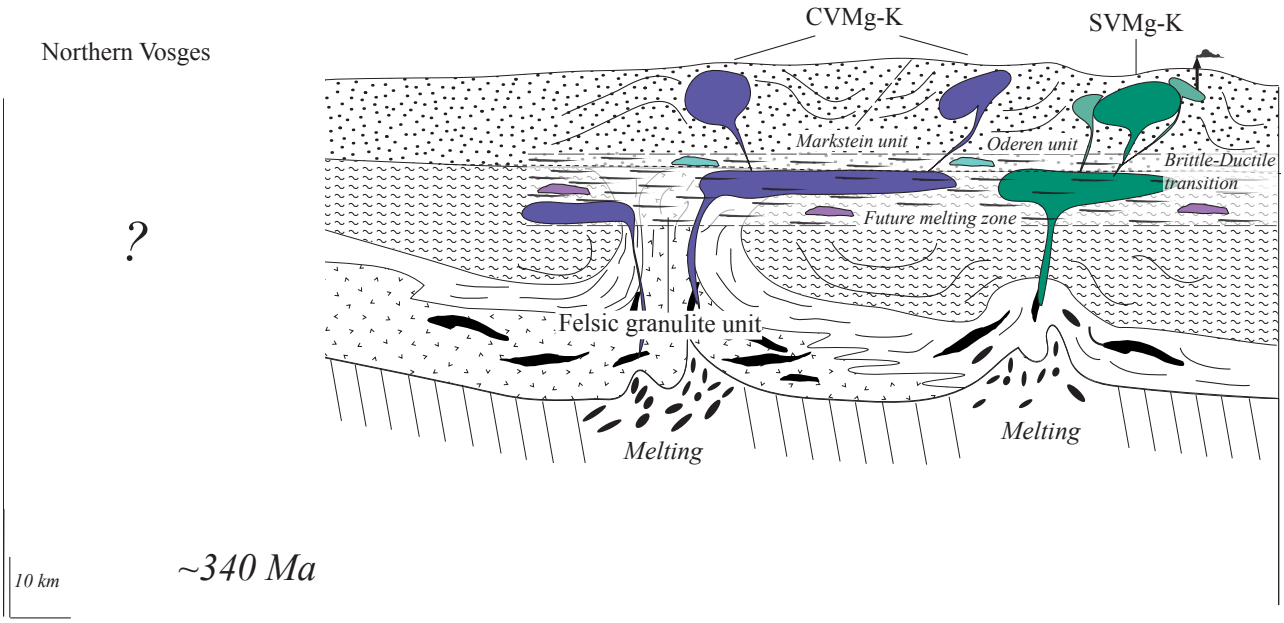
Northern Vosges
CVMg-K
SVMg-K
Markstein unit
Oderen unit
Brittle-Ductile
transition
Future melting zone
?
Felsic granulite unit
Melting
Melting
10 km
~340 Ma

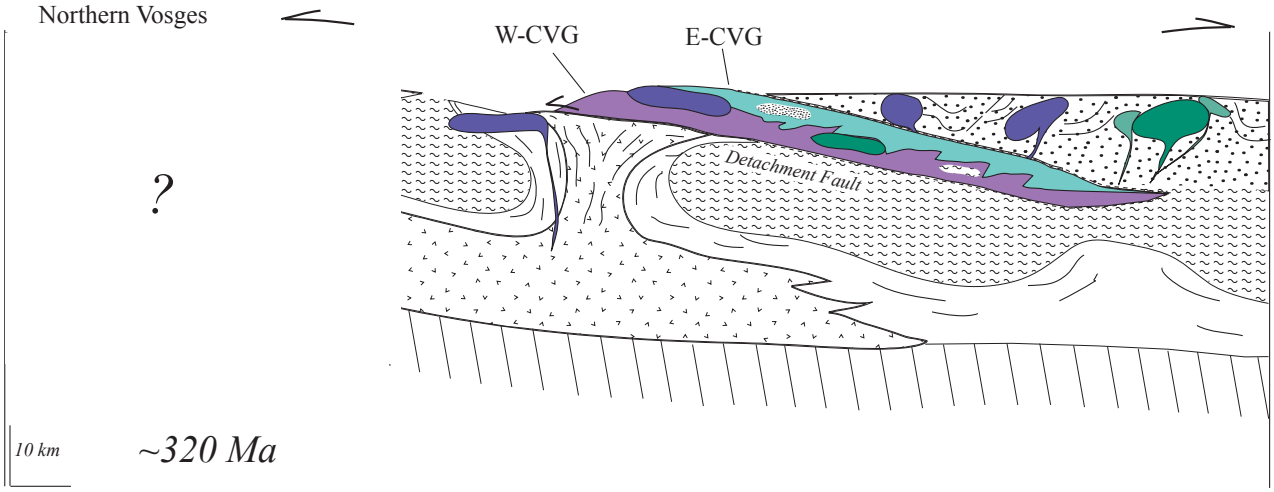
Northern Vosges
W-CVG
E-CVG
Detachment Fault
?
10 km
~320 Ma

9. Conclusions

The Early- to Middle-Carboniferous magmatism of the Vosges Massif (NE France) provides a powerful key for reconstructing the palinspastic spatial organization of the different sources involved in Variscan crustal growth. According to geochemical and isotopic data, the synchronous emplacement of CVMg-K and SVMg-K associations was the result of a mixing of enriched mantle-derived melts contaminated by mature crustal material for the CVMg-K or by juvenile crustal material for the SVMg-K. Based on correlations with other Mg-K plutons in the Variscan Belt of Europe, the involvement of two subduction zones with synchronous slab break-off on either side of the Variscan internal zone seems unrealistic. For this reason, we explain the generation and the petrological, geochemical and isotopic differences of these two groups of Mg-K intrusions by means of a geodynamic scenario (Lexa et al., 2011), which involves radiogenic-heat production from subducted Saxothuringian continental crust under Moldanubian continental crust. Shortly after this Mg-K magmatism, the emplacement of the peraluminous S-type granite may have derived from the mixing of Mg-K magma with partially molten Vosgian gneisses as well as with Moldanubian upper crust, thanks to the radiogenic heat produced by the earlier intrusion of Mg-K magmas..

Figure 17: Sketch of the geotectonic scenario for the development of magmatic intrusions during late stages of the Variscan Orogeny. See text for discussion. Figure previous page.

REFERENCES CITED

André, F. (1983). Pétrologie structurale et pétrogenèse des formations plutoniques septentrionales du Massif des Ballons (Vosges, France). Ph.D. thesis, University of Nancy, 247 p.

Banzet, G. (1987). Intéractions croûte-manteau et genèse du plutonisme subalcalin du Haut-Dauphiné Occidental (massifs cristallins externes, Alpes) : vaugnérites, durbachites et granitoïdes magnésio-potassiques. *Géologie alpine,* **63**, 95-117.

Bonhomme, M. & Fluck, P. (1981). Nouvelles données isotopiques Rb-Sr obtenues sur les granulites des Vosges. Age protérozoïque terminal de la série volcanique calco-alcaline et âge acadien du métamorphisme régional. *Comptes Rendus de l'Académie des Sciences*, **293**, 771-774.

Boutin, R., Montigny, R. & Thuizat, R. (1995). Chronologie K-Ar et $^{39}Ar/^{40}Ar$ du métamorphisme et du magmatisme des Vosges. Comparaison avec les massifs varisques avoisinants. *Géologie de la France*, **1**, 3–25.

Boynton, W. V. (1984). Cosmochemistry of the rare earth elements meteoritic studies. In: Henderson, P. (ed.) *Rare Earth Elements Geochemistry*. *Amsterdam: Elsevier*, 63–114.

Bussy, F., Delitroz, D., Fellay, R. & Hernandez, J. (1998). The Pormenaz monzonite (Aiguilles-Rouges, Western Alps): an additional evidence for a 330 Ma-old magnesio-potassic magmatic suite in the Variscan Alps. *Schweizerische Mineralogische und Petrographische Mitteilungen,* **78**, 193–194.

Carron, J. P., LeGuen de Kerneizon, M. & Nachit, H. (1994). Variscan granites from Brittany. In: Keppie, J. D. (ed.) *Pre-Mesozoic Geology in France and Related Areas*. Springer, Berlin, 231-239.

Chen, F., Hegner, E. & Todt, W. (2000). Zircon ages and Nd isotopic and chemical compositions of orthogneisses from Black Forest, Germany: evidence for a Cambrian magmatic arc. *International Journal of Earth Sciences,* **88**, 791-802.

Claoué-Long, J., Compston, W., Roberts, J. & Fanning, C. M. (1995). Two Carboniferous ages: a comparison of SHRIMP zircon dating with conventional zircon ages and $^{40}Ar/^{39}Ar$ analysis, In: Berggren, W. A., Kent, D. V., Aubry, M. P., Hardenbol, J. (eds) *Geochronology, Time Scales and Stratigraphic Correlation, SEPM Special Publication,* **54**, 1-22.

Cocherie, A., Rossi, P., Fouillac, A. M. & Vidal, P. (1994). Crust and mantle contributions to granite genesis – An example from the Variscan batholith of Corsica, France, studied by trace-element and Nd-Sr-O-isotope systematics. *Chemical Geology,* **115**, 173-211.

Coulon, M., Fourquin, C. & Paicheler, J. C. (1979). Contribution à la connaissance du tectorogène Varisque dans les Vosges méridionales : III-Le Culm entre Bourbach-le-Haut et le Molkenrain (Vosges méridionales). *Bulletin de la Société Géologique de France,* **32**, 117-129.

Coulon, M. (1977). Evolution du Viséen entre les vallées du Rahin et de l'Ognon (Vosges méridionales). Existence d'une zone à comportement de linéament. *Bulletin de la Société Géologique de France,* **30**, 79-89.

Debon, F. & Lemmet, M. (1999). Evolution of Mg/Fe Ratios in Late Variscan Plutonic Rocks from the External Crystalline Massifs of the Alps (France, Italy, Switzerland). *Journal of Petrology,* **40**, 1151-1185.

Debon, F., Guerrot, C., Ménot, R. P., Vivier, G. & Cocherie, A. (1998). Late Variscan granites of the Belledonne massif (French Western Alps): an Early Visean magnesian plutonism. *Schweizerische Mineralogische und Petrographische Mitteilungen,* **78**, 67–85.

Debon F. & Le Fort, P. (1983). A chemical–mineralogical classification of common plutonic rocks and associations. *Transactions of the Royal Society of Edinburgh, Earth Sciences,* **73**, 135–149.

Finger, F. & Clemens, J. D. (1995). Migmatization and "secondary" granitic magmas: effects of emplacement and crystallization of "primary" granitoids in Southern Bohemia, Austria. *Contributions to Mineralogy and Petrology,* **120**, 311-326.

Finger, F. & Steyrer, H. P. (1990). I-type granitoids as indicators of a Late Paleozoic convergent ocean–continent margin along the southern flank of the central European Variscan orogen. *Geology,* **18**, 1207–1210.

Fluck, P., Piqué, A., Schneider, J. L. & Whitechurch, H. (1991). Le socle vosgien. *Sciences Géologiques Bulletin,* **44**, 207-235.

Fluck, P., Edel, J. B., Gagny, C., Montigny, R., Piqué, A., Schneider, J. L. & Whitechurch, H. (1989). Carte synthétique et géotraverse N-S de la chaine varisque des Vosges (France). Synthèse des travaux effectués depuis deux décennies. *Comptes-rendus de l'Académie des Sciences, Série II,* **309**, 907-912.

Fluck, P. (1980). Métamorphisme et magmatisme dans les Vosges moyennes d'Alsace. Contribution à l'histoire de la chaine Varisque. *Mémoires des Sciences Géologiques*, **62**, 248 p.

Franke, W. (1989). Tectonostratigraphic units in the Variscan belt of central Europe. In: Dallmeyer, R. D. (ed.) *Terranes in the Circum-Atlantic Palaeozoic Orogens. Geological Society of America, Special Papers,* **230**, 67-90.

Gagny, C. (1968). Pétrogenèse du granite des Crêtes, Vosges meridionales, France. Ph.D. thesis, University of Nantes, 515 p.

Gerdes, A., Wörner, G. & Henk, A. (2000). Post-collisional granite generation and HT-HP metamorphism by radiogenic heating: the Variscan South Bohemian Batholith. *Journal of the Geological Society, London,* **157**, 577-587.

Giacomini, F., Bomparola, R. M., Ghezzo, C. & Guldbransen, H. (2006). The geodynamic evolution of the Southern European Variscides: constraints from the U/Pb geochronology and geochemistry of the lower Palaeozoic magmatic-sedimentary sequences of Sardinia (Italy). *Contributions to Mineralogy and Petrology,* **152**, 19-42.

Gorokhov, I. M., Losert, I., Varshavskaya, E. S., Kutyavin, E. P., Mel'nikov, N. N. & Czekupayev, V. P. (1977). Rb-Sr geochronology of the metamorphic rocks of the eastern part of the Bohemian Massif (region of the Zelezné Hory Mts. and adjacent Czech-Moravian Uplands). In: Afanasjev, G. D. (ed) *An Attempt on Corakia and Some Regions of the USSR*. Nauka, Moscow, 81-92.

Groth, P. (1877). Das Gneissgebiet von Markirch im Oberelsass. *Abhandlungen zur geologishen Spezialkarte Elsass-Lothringen*, **1**, 395-488.

Guerrot, C. (1998). Résultats de datation U–Pb par dissolution sur zircons pour deux échantillons du massif du Pelvoux, Alpes. Massif du Rochail (RO 1)-Massif de Turbat-Lauranoure (TL 1). Rapport SMN/PEA/ISO 146/98 CG/NB. Orléans: Bureau de Recherches Géologiques et Minières, 6 p.

Guillot, S. & Ménot, R. P. (2009). Paleozoic evolution of the external crystalline massifs of the Western Alps. *Comptes Rendus Géoscience,* **341**, 253–265.

Hameurt, J. (1967). Les terrains cristallins et cristallophylliens du versant occidental des Vosges moyennes. Ph.D. thesis, University of Strasbourg, 402 p.

Hann, H. P., Chen, F., Zedler, H., Frisch, W. & Loeschke, J. (2003). The Rand Granite in the southern Schwarzwald and its geodynamic significance in the Variscan belt of SW Germany. *International Journal of Earth Sciences,* **92**, 821–842.

Henk, A., von Blanckenburg, F., Finger, F. Schaltegger, U. & G. Zulauf (2000). Syn-convergent high-temperature metamorphism and magmatism in the Variscides: a discussion of potential heat sources. *The Geological Society of London, Special publication,* **179**, 387-399.

Holub, F. V. & Janoušek, V. (2003). Geochemical and Sr-Nd isotopic constraints on the genesis of ultrapotassic plutonic rocks from the Moldanubian zone of the Bohemian Massif. *Journal of Czech Geological Society,* **48**, 1-2, 61-62.

Holub, F. V., Cocherie, A. & Rossi, P. (1997). Radiometric dating of granitic rocks from the Central Bohemian Plutonic Complex (Czech Republic): constraints on the chronology of the thermal and tectonic events along the Moldanubian–Barrandian boundary. *Comptes Rendus de l'Académie des Sciences, Series IIA, Earth and Planetary Sciences,* **325**, 19–26.

Holub, F. V. (1997). Ultrapotassic plutonic rocks of the durbachite series in the Bohemian Massif: petrology, geochemistry and petrogenetic interpretation. *Sborník geologických ved, Lozisková geologie–mineralogie,* **31**, 5–26.

Jackson, S. E., Pearson, N. J., Griffin, W. L. & Belousova, E. A. (2004). The application of laser ablation-inductively coupled plasma-mass spectrometry to in situ U–Pb zircon geochronology. *Chemical Geology,* **211**, 47-69.

Janoušek, V. & Holub, F. V. (2007). The causal link between HP-HT metamorphism and ultrapotassic magmatism in collisional orogens: case study from the Moldanubian Zone of the Bohemian Massif. *Proceedings of the Geologists' Association,* **118**, 75-86.

Janoušek, V., Farrow, C. M. & Erban, V. (2003). GCDkit: new PC software for interpretation of whole-rock geochemical data from igneous rocks. *Geochimica et Cosmochimica Acta,* **A67**, 186.

Janoušek, V., Bowes, D. R., Rogers, G., Farrow, C. M. & Jelínek, E. (2000). Modelling diverse processes in the petrogenesis of a composite batholith: the Central Bohemian Pluton, Central European Hercynides. *Journal of Petrology,* **41**, 511-543.

Janoušek, V., Rogers, G. & Bowes, D. R. (1995). Sr–Nd isotopic constraints on the petrogenesis of the Central Bohemian Pluton, Czech Republic. *Geologische Rundschau,* **84**, 520–534.

Köhler, H. & Müller-Schnius, D. (1980). Rb-Sr systematics on paragneiss series from the Bavarian Moldanubicum. *Contributions to Mineralogy and Petrology,* **71**, 387-392.

Kossmat, F. (1927). Gliederung der varistischen Gebirgsbaues. *Abhandlungen des Sächsischen geologischen Landesamts,* **1**, 1-39.

Kramers, J., Kreissig, K. & Jones, M. (2001). Crustal heat production and style of metamorphism: a comparison between two Archean high grade provinces in the Limpopo Belt, southern Africa. *Precambrian research*, **112**, 149-163.

Kratinová, Z., Schulmann, K., Edel, J. B. & Tabaud, A. S. (2012). AMS record of brittle dilation, viscous-stretching and gravity-driven magma ascent in area of magma-rich crustal extension (Vosges Mts., NE France). *International Journal of Earth Sciences*, **101**, 803-817.

Kratinová, Z., Schulmann, K., Edel, J. B., Ježek, J. & Schaltegger, U. (2007). Model of successive granite sheet emplacement in transtensional setting: Integrated microstructural and anisotropy of magnetic susceptibility study. *Tectonics,* **26**, TC6003.

Kröner, A., Jaeckel, P., Reischmann, T. & Kroner, U. (1998). Further evidence for an early Carboniferous (340 Ma) age of high-grade metamorphism in the Saxonian granulite complex. *Geologische Rundschau,* **86,** 751-766.

Ledru, P. Costa, S. & Echtler, H. (1994). Structure. In: Keppie, J. D. (ed.) *Pre-Mesozoic Geology in France and Related Areas. Springer, Berlin*, 305-323.

Lefèvre, C., Lakhrissi, M. & Schneider, J. L. (1994). Les affinités magmatiques du volcanisme dinantien des Vosges méridionales (France) ; approche géochimique et interprétation. *Comptes Rendus de l'Académie des Sciences, Series II*, **319**, 79-86.

Lexa, O., Schulmann, K., Janoušek, V., Štípská, P., Guy, A. & Racek, M., 2011. Heat sources and trigger mechanisms of exhumation of HP granulites in Variscan orogenic root. *Journal of Metamorphic Geology*, **29**, 79-102.

Liew, T. C. & Hofmann, A. W. (1988). Precambrian crustal components, plutonic associations, plate environment of the Hercynian Fold Belt of central Europe: indications from a Nd and Sr isotopic study. *Contributions to Mineralogy and Petrology,* **98**, 129-138.

Lombardo, B., Rubatto, D., Colombo, F. & Compagnoni, R. (1997). Variscan eclogites and HP granulites in the Malinvern–Argentera Complex (Argentera massif, Western Alps): PT estimations and U–Pb zircon ages. *Terra Nova,* **9**, 18–19.

Ludwig, K. R. (2001). Isoplot/Ex version 2.49, a geochronological toolkit for Microsoft Excel. Berkeley: Berkeley Geochronology Center.

Martinez, F. J., Corretge, L. G. & Suarez, O. (1990). Distribution, characteristics and evolution of metamorphism. In: Dallmeyer, R. D. & Martinez Garcia, E. (eds) *Pre-Mesozoic Geology of Iberia. Springer, Berlin*, 207-211.

Michel-Levy, A. (1910). Analogie des terrains primaires du Sud des Vosges et de ceux du Morvan. *Bulletin de la Société géologique de France*, **10**, 816-828.

Müller, W., Shelley, M., Miller, P. & Broude, S. (2009). Initial performance metrics of a new custom-designed ArF excimer LA-ICPMS system coupled to a two-volume laser-ablation cell. *Journal of Analytical Atomic Spectrometry,* **24**, 209-214.

Navidad, M., Castiñeiras, P., Casas, J. M., Liesa, M., Suárez, J. F., Barnolas, A., Carreras, J. & Gil-Peña, I. (2010). Geochemical characterization and isotopic age of Caradocian magmatism in the northeastern Iberian Peninsula: Insights into the Late Ordovician evolution of the northern Gondwana margin. *Gondwana Research,* **17**, 325-337.

Neubauer, F. & von Raumer, J. (1993). The Alpine Basement – linkage between Variscides and east-Mediterranean mountain belts. In: von Raumer, J. & Neubauer, F. (eds) *Pre-Mesozoic Geology in the Alps. Springer, Berlin*, 641-663.

Pagel, M. (1981). Facteurs de distribution et de concentration de l'uranium et du thorium dans quelques granites de la chaîne hercynienne d'Europe. Thèse Sciences C.R.P.G. et C.R.E.G.U., I.N.P.L., Nancy, 566 p.

Pagel, M. & Leterrier, J. (1980). The subalkaline potassic magmatism of the Ballons massif (Southern Vosges, France): shoshonitic affinity. *Lithos,* **13**, 1-10.

Paquette, J. L., Ménot, R. P., Pin, C. & Orsini, J. B. (2003). Episodic and short-lived granitic pulses in a post-collisional setting: evidence from U-Pb zircon dating through a crustal cross-section in Corsica. *Chemical Geology,* **198**, 1-20.

Peacock, M. A. (1931). Classification of igneous rock series. *Journal of Geology,* **39**, 54–67.

Petrini, K. & Burg, J. P. (1998). Relationship between deformation, plutonism and regional metamorphism in the Markstein area (southern Vosges). *Géologie de la France,* **2**, 13-23.

Robert, J. L. (1976). Titanium solubility in synthetic phlogopite solid solutions. *Chemical Geology,* **17**, 213-227.

Rossi, P., Oggiano, G. & Cocherie, A. (2009). A restored section of the "Southern Variscan realm" across the Corsica-Sardinia microcontinent. *Comptes-Rendus Géoscience,* **341**, 224-238.

Rossi, P. & Cocherie, A. (1991). Genesis of a Variscan batholith: field, petrological and mineralogical evidence from the Corsica–Sardinia batholith. *Tectonophysics,* **195**, 319–346.

Sauer, A. (1893). Der Granitit von Durbach im nördlichen Schwarzwald un seine Grenzfacies von Glimmersyenit (Durbachit). *Mitteilungsblatt der Badischen Geologischen Landesanstalt,* **2**, 233-276.

Schaltegger, U. (2000). U-Pb geochronology of the Southern Black Forest Batholith (Central Variscan Belt): timing of exhumation and granite emplacement. *International Journal of Earth Sciences,* **88**, 814-828.

Schaltegger, U., Fanning, C. M., Günther, D., Maurin, J. C., Schulmann, K. & Gebauer, D. (1999). Growth, annealing and recrystallization of zircon and preservation of monazite in high-grade metamorphism: conventional and in situ U–Pb isotope cathodoluminescence and microchemical evidence. *Contributions to Mineralogy and Petrology,* **134**, 186–201.

Schaltegger, U., Schneider, J. L., Maurin, J. C. & Corfu, F. (1996). Precise U–Pb chronometry of 345–340 Ma old magmatism related to syn-convergence extension in the Southern Vosges (Central Variscan Belt). *Earth and Planetary Science Letters,* **144**, 403–419.

Schaltegger, U. & Corfu, F. (1995). Late Variscan 'Basin and Range' magmatism and tectonics in the Central Alps: evidence from U–Pb geochronology. *Geodinamica Acta,* **8**, 82–98.

Schaltegger, U. & Corfu, F. (1992). The age and source of late Hercynian magmatism in the central Alps: evidence from precise U–Pb ages and initial Hf isotopes. *Contributions to Mineralogy and Petrology,* **111**, 329–344.

Schaltegger, U., Gnos, E., Küpfer, T. & Labhart, T. P. (1991). Geochemistry and tectonic significance of Late Hercynian potassic and ultrapotassic magmatism in the Aar Massif (Central Alps). *Schweizerische Mineralogische und Petrographische Mitteilungen,* **71**, 391–403.

Scharbert, S. & Veselá, M. (1990). Rb-Sr systematics of intrusive rocks from the Moldanubian around Jihlava. In: Minařiková, D. & Lobitzer, H. (eds) *Thirty Years of Geological Cooperation between Austria and Czechoslovakia. Czech Geological Survey*, *Prague*, p.262-271.

Schneider J. L. (1990). Enregistrement de la dynamique varisque dans les bassins volcano-sédimentaires dévono-dinantiens: exemple des Vosges du Sud (zone moldanubienne). Ph.D. thesis, University of Strasbourg, 222 p.

Schulmann, K., Edel, J. B., Hasalová, P., Cosgrove, J. Ježek, J. & Lexa, O. (2009a). Influence of melt-induced mechanical anisotropy on the magnetic fabrics and rheology of deforming migmatites, Central Vosges, France. *Journal of Structural Geology,* **31**, 1223-1237.

Schulmann, K., Konopásek, J., Janoušek, V. et al., (2009b). An Andean type Palaeozoic convergence in the Bohemian Massif. *Comptes Rendus-Géoscience,* **341**, 266–286.

Schulmann, K., Schaltegger, U. Ježek, J., Thompson, A. L. & Edel, J. B. (2002). Rapid burial and exhumation during orogeny: thickening and synconvergent exhumation of thermally weakened and thinned crust (Varican orogen in Western Europe). *American Journal of Science,* **302**, 856-879.

Skrzypek, E., Štipská, P. & Cocherie, A. (*submitted*). The origin of zircon and the significance of U-Pb ages in high-grade metamorphic rocks: a case study from the Variscan orogenic root (Vosges Mountains, NE France). *Contributions to Mineralogy and Petrology*.

Skrzypek, E., Tabaud, A. S., Edel, J. B., Schulmann, K., Cocherie, A., Guerrot, C. & Rossi, P. (2012). The significance of Late Devonian ophiolites in the Variscan orogen: a record from the Vosges Klippen Belt. *International Journal of Earth Sciences*, **101**, 951-972.

Skrzypek, E. (2011). Contribution structurale, pétrologique et géochronologique à la tectonique intracontinentale de la chaîne hercynienne d'Europe (Sudètes, Vosges). Ph.D. thesis, University of Strasbourg, 381 p.

Stussi, J. M. (1970). Le volcanisme associé au Culm des Vosges méridionales: Tendances évolutives générales et géochimie de l'uranium et thorium. Ph.D. thesis, University of Nancy, 383 p.

Sun, S. S. & McDonough, W. F. (1989). Chemical and isotopic systematics of oceanic basalts: implications for mantle composition and processes. In: Saunders, A. D. & Norry, M. (eds) *Magmatism in the Ocean Basins. Geological Society, London, Special Publication,* **42**, 313–345.

Tera, F. & Wasserburg, G. (1972). U-Th-Pb systematics in three Apollo 14 basalts and the problem of initial Pb in lunar rocks. *Earth and Planetary Science Letters,* **14**, 281-304.

Thompson, R. N., Morrison, M. A., Hendry, G. L. & Parry, S. J. (1984). An assessment of the relative roles of crust and mantle in magma genesis an elemental approach. *Philosophical Transactions of the Royal Society,* **310**, 549-590.

van Achterbergh, E., Ryan, C. G., Jackson, S. E. & Griffin, W. (2001). Data reduction software for LA-ICP-MS. In: Sylvester, P. (ed) *Laser ablation-ICPMS in the earth science. Mineralogical Association of Canada,* **29**, 239-243.

von Eller, J. P. (1961). Les gneiss de Sainte Marie-aux-Mines et les séries voisines des Vosges moyennes. *Mémoire du service de la Carte Géologique d'Alsace et Lorraine Strasbourg,* **19**, 160 p.

von Raumer, J. F., Bussy, F. & Stampfli, G. M. (2009). The Variscan evolution in the External massifs of the Alps and place in their Variscan framework. *Comptes Rendus Géoscience,* **341**, 239-252.

von Raumer, J. F., Stampfli, G. M. & Bussy, F. (2003). Gondwana-derived microcontinents-the constituents of the Variscan and Alpine collisional orogens. *Tectonophysics,* **365**, 7-22.

von Raumer, J. F., Stampfli, G. M., Borel, G. & Bussy, F. (2002). The organization of pre-Variscan basement areas at the north-Gondwanan margin. *International Journal of Earth Sciences,* **91**, 35-52.

Wiedenbeck, M., Allé, P., Corfu, F., Griffin, W. L., Meier, M., Oberli, F., von Quadt, A., Roddick, J. C. & Spiegel, W. (1995). Three natural zircon standards for U-Th-Pb, Lu-Hf, trace element and REE analyses. *Geostandards Newsletter,* **19/1**, 1-23.

Chapitre 4 : le magmatisme des Vosges moyennes et méridionales : Anisotropie de la Susceptibilité Magnétique (ASM)

Ce chapitre est en continuité avec le Chapitre 3 sur le magmatisme des Vosges moyennes et méridionales. Il présente les données de l'Anisotropie de la Susceptibilité Magnétique (ASM) réalisées sur l'ensemble du massif vosgien moyen et méridional afin de déterminer les contraintes de mise en place des granites et celles affectant les différents niveaux de la croûte continentale lors de la mise en place de ces phases magmatiques.

L'étude s'appuie sur une étude de terrain avec un échantillonnage tous les kilomètres. La prise des échantillons par forage avec une carotteuse portative ainsi que les mesures des foliations magmatiques ont été effectuées avec l'aide d'Etienne Skrzypek et Ludovic Jeanniot. Les mesures des échantillons ont été effectuées par Etienne Skrzypek pour le S-CVMg-K à Brno, par Tsvetomila Mateeva pour le W-CVG à l'IPG Strabourg (encadré par Jean-Bernard Edel) et par moi-même au Département Géosciences et Environnement, Université de Cergy-Pontoise pour le reste du massif ainsi que pour la détermination de la minéralogie magnétique.

L'ensemble de ces données (foliations magmatiques, données ASM) associées aux données structurales des roches métamorphiques et sédimentaires environnantes (Skrzypek, 2011), nous a permis de montrer la complexité des données magnétiques enregistrées par les granitoids vosgiens et de mettre en évidence les phénomènes de surimpression dus aux différentes déformations successives. Nous proposons un modèle d'évolution des fabriques magnétiques où nous interprétons les fabriques verticales comme étant les fabriques originelles de la mise en place de ces granitoids (corrélation avec les interprétations géochimiques) qui sont plus ou moins retravaillées par les déformations consécutives (aplatissement vertical et cisaillement simple vers le sud) qui peuvent être liées à la mise en place du Granite Central Vosgien (CVG).

1. Introduction

Anisotropy of magnetic susceptibility (AMS) is a popular petrophysical method applied in structural geology to study fabrics of granitoids, volcanic and sedimentary rocks (Borradaile, 1994; Borradaile & Jackson, 2004). In particular, this method is successfully applied to determine emplacement fabrics of plutonic rocks (Bouchez, 2000) and to derive tectonic regimes related to magma flow and its deformation (de Saint Blanquat et al., 2001). Because the magma flow is intrinsically related to geometrical boundary conditions and dynamics of fluid flow, the technique is traditionally used to determine relations between internal structure of plutonic bodies, its host rock and regional deformation (e.g. Bouchez and Gleizes, 1995). The quantification of mineral fabrics, in particular in case of paramagnetic granites is now possible thanks to numerical and analogue models allowing to simulate mineral preferred orientation for complex flow geometries (Ježek et al., 1994; 1996; Arbaret et al., 2000). The AMS technique thus became a first order tool supporting links between regional deformation and syn-tectonic magma emplacement at various tectonic regimes ranging from compression, transpression or (trans) tension (Gleizes et al., 1998a; Bouchez – for Pyrenees, Žák et al., 2005; Kratinová et al., 2007).

To date, the studies of magmatic fabrics using AMS mapping are applied to single plutonic bodies and relatively simple tectonic histories (e.g. Gleizes et al., 1998b; Žák et al., 2007). It is supposed that magmatic and therefore AMS fabrics record deformation related to simple flow geometry. However, recently an effort is made to understand AMS fabrics resulting from multiple deformation overprints related to complex and polyphase ascent and emplacement magmatic histories (e.g. Kratinová et al., 2010). The modelling of polyphase magmatic fabrics shows a range of possible fabrics in a single magmatic body related to a variety of emplacement scenarios (Schulmann & Ježek, 2012). The advances in fabric modelling allow to study complex and polyphase magmatic histories related to prolonged orogenic evolution and magmatism.

Vosges Mountains represent an ideal example where at least two chronologically distinct magmatic and tectonic cycles can be studied (Schulmann et al., 2002; Tabaud et al., submitted). An early magmatic event is related to building of thick orogenic root and exhumation of deep crust to shallow crustal level associated with major pulse of Mg-K magmatism. The Mg-K magmatism is intruding all crustal levels from deep granulitic crust to supracrustal sedimentary sequences in a very short time frame (~342 – 338 Ma). The second magmatic event developed ten millions years later, affected exclusively the mid-crustal level and separated deep crustal and shallow crustal orogenic edifice by a sub-horizontal magma rich zone ca. 5 – 10 km wide. This magmatic event is marked by production of large quantity of anatectic melts which reworks previously intruded magmas.

It is the complex orogenic magma emplacement history which makes the Vosges Mountains particularly attractive for quantitative structural research. Therefore, an orogenic-scale AMS study was performed to provide a picture of complex intrusion of magma at different crustal levels and later magmatic-deformation recycling. As a result, a complex structural overprint can be studied by means of AMS technique giving an insight in complexity of AMS fabrics studied in orogenic scale.

2. Geological setting

2.1. Regional geological framework

The Vosges Mountains are divided into three major domains (Fluck, 1980; Schulmann et al., 2002). The Northern Paleozoic low-grade metamorphic unit traditionally interpreted as a westernmost extension of the Saxothuringian zone, limited from the south by the dextral shear Lalaye-Lubine zone (Kossmat, 1927) and, the Central high-grade gneissic unit correlated with the Moldanubian zone of the Bohemian Massif (Kossmat, 1927), recently interpreted as a remnant of deeply eroded Variscan orogenic root (Schulmann et al., 2002), and the Southern Paleozoic basin (Fig.1).

The Central high-grade gneissic unit is cross-cut by the NE-SW trending Ste-Marie-aux-Mines fault zone and E-W Bilstein shear zone (Fig.1). In the north, it is composed of felsic granulitic unit (T = ~750°C, P = 9-11kbar; Rey et al., 1992; Skrzypek et al., submitted) including lenses of peridotites, granulite and amphibolite (Fluck, 1980) facies, varied unit (Skrzypek et al., submitted) and medium grade monotonous unit (T = ~650°C, P = 6kbar; Latouche et al., 1992) and in the south by large migmatitic domain occurred in amphibolite facies conditions (T = ~700°C, P = 3kbar; Rey et al., 1992). The whole high grade core of the Vosges Mts. is characterized by polyphase deformation marked by NE-SW trending subvertical foliation subsequently transposed into subhorizontal foliation interpreted as a result of vertical extrusion of orogenic lower crust over mid-crustal rocks (Kratinová et al., 2007).

The whole metamorphic complex is intruded by two generations of magmatic rocks which occupy three main regions. The first magmatic event occurred at about 340 Ma and is characterized by emplacement at deep crustal level in the Central and shallow crustal level in the Southern Vosges Mts (Fig.1) of two associations of Mg-K intrusions (Tabaud et al., submitted): the Central Vosges Mg-K (CVMg-K) and the Southern Vosges Mg-K (SVMg-K) plutonic groups, respectively.

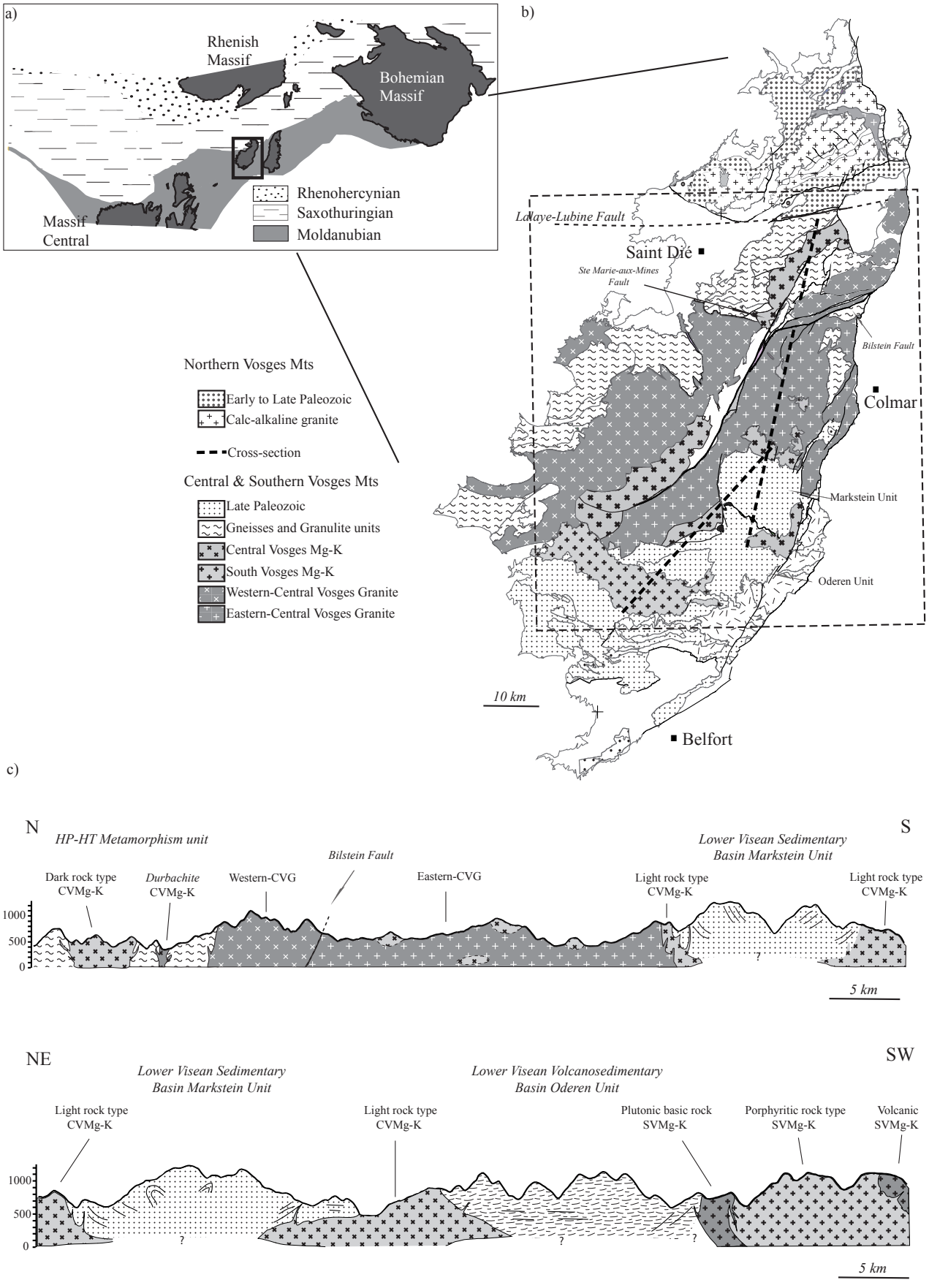

Figure 1: (a) Location of the study area in the framework of the European Variscides (black square marks the Vosges Mountains), modified after Edel and Weber (1995). (b) Geological map of the Vosges Mts (modified after Fluck et al., 1989) with region of interest indicated within the black rectangle. (c) Schematic cross-sections through the Vosges Mts.

i) CVMg-K (180 km²) outcrops in two principal bodies (Northern-CVMg-K and Southern-CVMg-K) and in some stocks (Eastern-CVMg-K) in the north and along southern margin of Lower Visean sedimentary Markstein basin in the south (Fig. 1 & 2). The northern part of the CVMg-K pluton (N-CVMg-K) forms elongated NE-SW trending body intrusive in amphibolite or granulite-facies metamorphic units (Fig.1 & 2). The southern part of CVMg-K (S-CVMg-K) is an NE-SW elongated body along Ste-Marie-aux-Mines fault zone and entirely surrounded by the CVG (Fig.1 & 2). The eastern part of CVMg-K (E-CVMg-K) divided into two small stocks along margin of Markstein basin, shows clear intrusive contact with this Visean sediments Unit and host numerous xenoliths of sedimentary host rocks (Fig.1 & 2). In addition, small syn-tectonic sills of fine-grained granite are emplaced parallel to the NW-SE trending subvertical bedding.

ii) SVMg-K (260 km²) occurs in the southern part as an E-W striking body which occupies a large part of the southern Vosges Mountains (Fig.1 & 2). This porphyric granite evolves to a fine-grained high plutonic type towards the west and show granophyric margins at the contact with Visean volcanosedimentary sequences and volcanic rocks to the East.

In a previous work focused on petrological, geochemical and isotopic data, Tabaud et al., (submitted) shown that CVMg-K intrusive association comprises rocks ranging from amphibole-biotite-bearing syenite to amphibole-biotite granite and SVMg-K association comprises amphibole-biotite monzonite to monzogranite. We interpreted this type of magmatism as a result of magma mixing at deep crustal level of Saxothuringian basement derived crustal and metasomatized lithospheric mantle components. This magmatic event is spatially and genetically associated with development of granulite facies metamorphism of the granulitic and varied units and with structures related to juxtaposition of orogenic lower and middle crust.

The second magmatic event occurred at about 325 Ma in the Central Vosges Mts (Fig.1) with intrusion (860 km²) of the two types of Central Vosges Granite (Eastern-CVG and Western-CVG; Tabaud et al., submitted) which comprises biotite to biotite-muscovite granite-monzogranite and covers the central Vosgian domain. This intrusion is bordered in the north by migmatitic domain and varied and monotonous gneissic unit, in the east by the sedimentary Markstein unit and small stocks of CVMg-K and in the south by the volcanosedimentary basin and the SVMg-K intrusion (Fig.1 & 2). This magmatic event shows geochemical features roughly similar to the Mg-K magmatism. We interpreted these intrusions (Tabaud et al., submitted) as a result of mid-crustal level mixing of Mg-K granitoids with anatectic melts derived from mid- and upper Moldanubian continental crust. This magmatic event is associated with an N-S extensional event characterized by migmatitic foliation which generally dips to the W or SW at moderate angle (Rey et al., 1992).

2.2. Geochronology

For a good understanding of the mechanism of evolution and development of moldanubian continental crust in the Vosges Mts, it is important to constrain the crystallization, emplacement ages of the successive pulses for either Mg-K or CVG. Ages were established in previous studies using K-Ar and Ar-Ar (Boutin, 1995) and U-Pb on zircon (Schaltegger et al., 1996, 1999; Schulmann et al., 2002; Kratinová et al., 2007; Tabaud et al., submitted) and are summarized in Table 1.

The CVMg-K yields age between 337 ± 2 Ma and 340 ± 1 Ma (U-Pb on zircon; Tabaud et al., submitted; Schaltegger et al., 1996; respectively) and the SVMg-K is constrained by the U-Pb between 336 ± 4 Ma and 340 +4/-2 Ma (Tabaud et al., submitted; Schaltegger et al., 1996; respectively). These ages are contemporaneous with age of 335 ± 1 Ma of granulite facies metamorphism (Schaltegger et al, 1999)

The CVG shows ages between 326 ± 1 Ma and 329 ± 2 Ma (U-Pb on zircon; Schaltegger et al., 1999; Kratinová et al., 2007; Schulmann et al., 2002) for the north-eastern part and between 319 ± 6 Ma (U-Pb on zircon; Tabaud et al., submitted) and 324 ± 4 Ma (Th-Pb on monazite; for the southwestern part (Tabaud et al., submitted). These ages are similar with age of 328 ± 4 Ma of the amphibolite-facies retrograde metamorphism (Schaltegger et al., 1999).

Table 1: Summary table of published geochronological data.

Method	CVMg-K association			SVMg-K association				CVG	
	Mafic rocks	Dark type	Light type	Mafic rocks	Phophyry granite	Fine-grained granite	Volcanism	Eastern part	Western part
U-Pb zircon	332+3/-2 Ma		340 ± 1 Ma	342 ± 1 Ma	340+4/-2 Ma		345 ± 2 Ma 336+3/-5 Ma 340 ± 2 Ma	326 ± 4.8 Ma	326 ± 1 Ma 329± 2 Ma
U-Th-Pb monazite		337 ± 2 Ma	337 ± 3 Ma	345 ± 3 Ma	336 ± 4 Ma	336 ± 3 Ma	346 ± 2 Ma		319 ± 6 Ma 324 ± 4 Ma
K-Ar				337± 19 Ma amphibole	335± 13 Ma amphibole		337± 11 Ma amphibole	336± 11 Ma biotite	330± 10 Ma biotite 334± 11 Ma biotite
Ar-Ar			333± 1 Ma biotite			331± 5 Ma biotite	335± 3 Ma amphibole		331±5 Ma biotite

2.3. Whole-rock geochemistry of granitoids

Major and trace-elements geochemistry of Mg-K magmatic associations show that these rocks are mostly metaluminous and characterized by high content of MgO, K_2O, enrichment in Cr, Ni, incompatible elements (U, Th) and lithophile elements (Ba, Rb, Cs). Isotopic compositions and inherited zircons of CVMg-K argue for a mantle source contaminated and metasomatized by mature crustal material (Proterozoic). For SVMg-K, isotopic compositions and inherited zircons point to juvenile crustal material contamination (Cambro-Ordovician). These crustal components imply that

magma sources are generally deeply subducted crustal rocks of Saxothuringian provenance which produced fluids that contaminated and triggered melting of the lithospheric mantle (Tabaud et al., submitted).

The CVG is composed of peraluminous rocks characterized by high enrichment in LILE, LREE and incompatible elements (U, Th, K). Isotopic compositions of E-CVG bridge compositions between the two Mg-K associations whereas W-CVG has intermediate isotopic compositions between CVMg-K and Vosgian metamorphic rocks. According to inherited zircons, magma sources of CVG reflect a mixing between Mg-K rocks and anatectic melts derived from gneissic Moldanubian middle crust for W-CVG and a mixing between Mg-K rocks and products of melting of sedimentary Moldanubian upper-crust for E-CVG. Partial melting of mid- and upper Moldanubian crust is most likely caused by radiogenic heat produced by intrusion of Mg-K magma, rich in radiogenic elements, at about 20 km depth (Tabaud et al., submitted).

2.4. Fabrics pattern of surrounding metamorphic and sedimentary unit

Structural record of the surrounding metamorphic and sedimentary units of the Central Vosges domain exhibit four successive deformation events. The first deformation event is characterized by NE-SW subvertical foliation observed in gneisses of varied, montonous and granulite units (Fig.2). This deformation is followed by the second deformation event which tranposes subvertical foliation into a flat-lying fabric (Skrzypek, 2011). The two set of fabrics is interpreted as a result of vertical juxtaposition of orogenic lower and middle crust by vertical extrusion mechanism (Schulmann et al., 2008). The third deformation event is developed during a NW-SE compression as indicated by NW-SE trending upright folds in sedimentary Markstein unit and metamorphic units are preserved the original E-W compressional fabrics (Fig.2). This deformation event is affected only the upper crust and the deepest part of the crust is not experienced this compression and is acted as rigid blocks (Skrzypek, 2011).

In the sedimentary Oderen Unit in the Southern Vosges domain the structural record is less clear. In the south the bedding strikes NW-SE and dips mostly to the NE at moderate to steep angle which may result from NW-SE compression like in the northerly Markstein unit. Closed to SVMg-K intrusion, sedimentary beds strike N-S and dip to the E (Fig.2; Krecher, 2005). Finally, the latest deformation is affecting the whole migmatitic and CVG region being characterized by sub-horizontal fabrics as indicated by previous AMS works on the NE quarter of the studied area (Fig.2; Schulmann et al., 2009; Kratinová et al., 2012). This deformation is associated with N-S extension that developed during crustal anatexis (Rey et al., 1992).

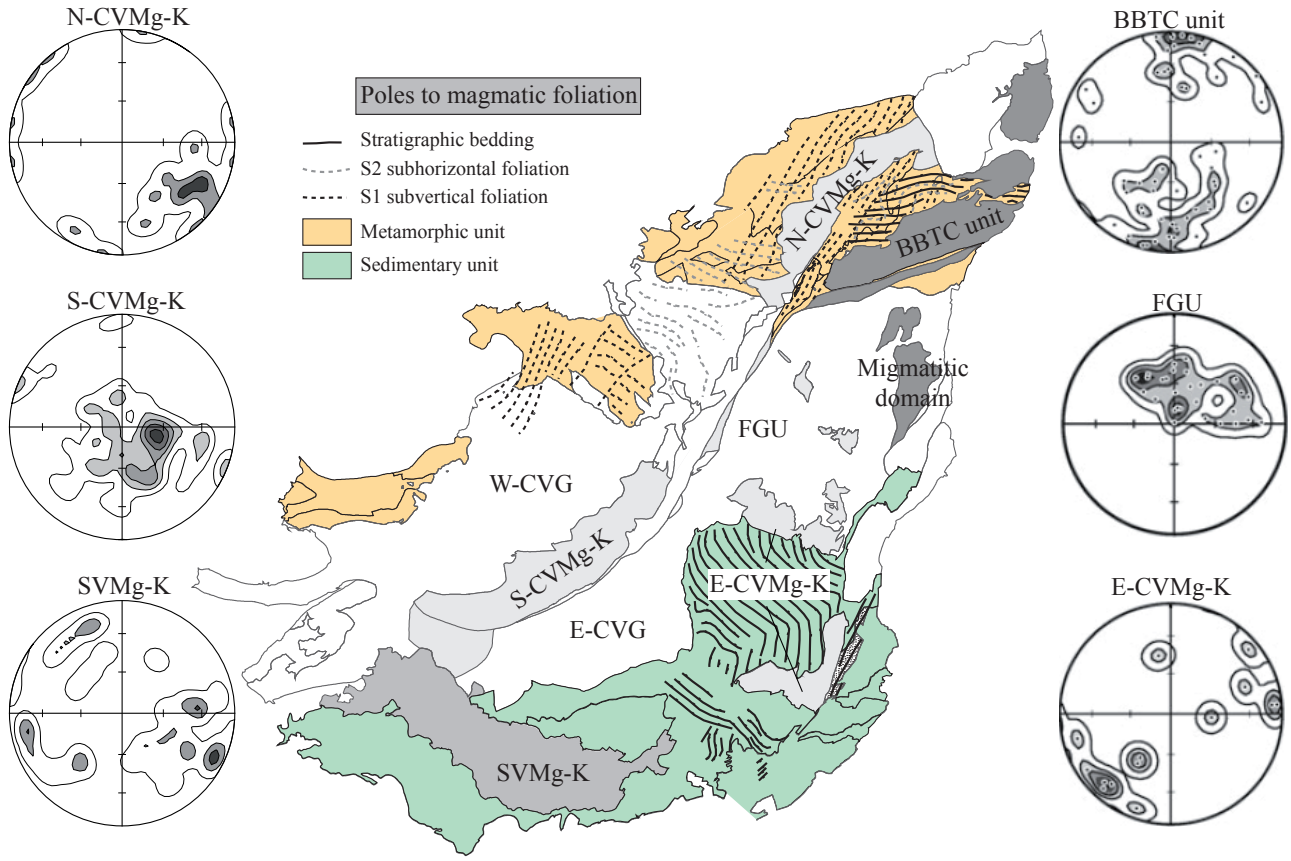

Figure 2: Map of the studied area showing structural data of metamorphic and sedimentary units of the Vosges Mts (Rey et al., 1992; Skrzypek, 2011) with contoured stereogram (equal-area lower hemisphere projection) of poles to field magmatic foliation planes defined by the preferred orientation of K-feldspars. Contoured stereograms of the BBTC and FGU units are from Kratinová et al. (2012).

3. Fabric pattern of the granitoids

3.1. Macroscopic structures

The N-CVMg-K intrusion shows magmatic to solid state foliation pattern which is defined by the preferred orientation of K-feldspar phenocrysts parallel to host rock metamorphic fabric (Fig.2 & 3.b). Magmatic foliation pattern of S-CVMg-K defined by preferred orientation of K-feldspar phenocrysts (Fig.2 & 3.c) is mostly subhorizontal and dips to the NE or E. Further to the south, between S-CVMg-K and SVMG-K plutonic bodies, a small stock of CVMg-K shows sub-vertical magmatic foliation. In the E-CVMg-K, the fabric intensity of K-feldspar phenocrysts is variable and could not be determined in many places. In some cases, magmatic foliation is subvertical and trending NW-SE (Fig.2). Dominant magmatic fabric of SVMg-K defined by preferred orientation of K-Feldspar phenocrysts is marked by subvertical N-S foliations (Fig.2 & 3.d).Both parts of the CVG (E-CVG and W-CVG) show only exceptionally planar and linear structures (Fig.2 & 3.a) but in general, structural data cannot be obtained by field measurements.

Figure 3: Field photographs of main textural types of vosgian granitoids. a) Textural type of CVG showing the difficulty to obtain structural data by field measurements b) Macroscopic magmatic foliation defined by the preferred orientation of K-feldspar in N-CVMg-K. c) Macroscopic magmatic foliation defined by the preferred orientation of K-feldspar in S-CVMg-K. d) Macroscopic magmatic foliation defined by the preferred orientation of K-feldspar in SVMg-K.

3.2. Petrography and microstructures of principal granitoids

CVMg-K association represents dark (N-CVMg-K) to light (S- and E-CVMg-K) coarse-grained rocks characterized by idiomorphic K-feldspar and plagioclase ranging from andesine (An_{40-30}) to albite (An_{15-5}), quartz, brown biotite and pale green Mg-amphibole (actinolitic hornblende). Zircon, allanite, apatite, thorite and magnetite are present as accessory phases (Fig.4.b, c, d). Absence of plagioclase zoning suggests slow crystallisation. Quartz occurs in form of large grains with lobate boundaries. Biotite (X_{Mg}= 60-65) and amphibole are arranged into large grains aggregates or are elongated along adjacent grains boundaries which exibit corroded shape. Ti content of biotite (0.18-0.28 a.p.f.u) decreases weakly with increasing of Si content which also suggests slow decrease of the temperature during crystallisation of CVMg-K rocks (Robert, 1976).

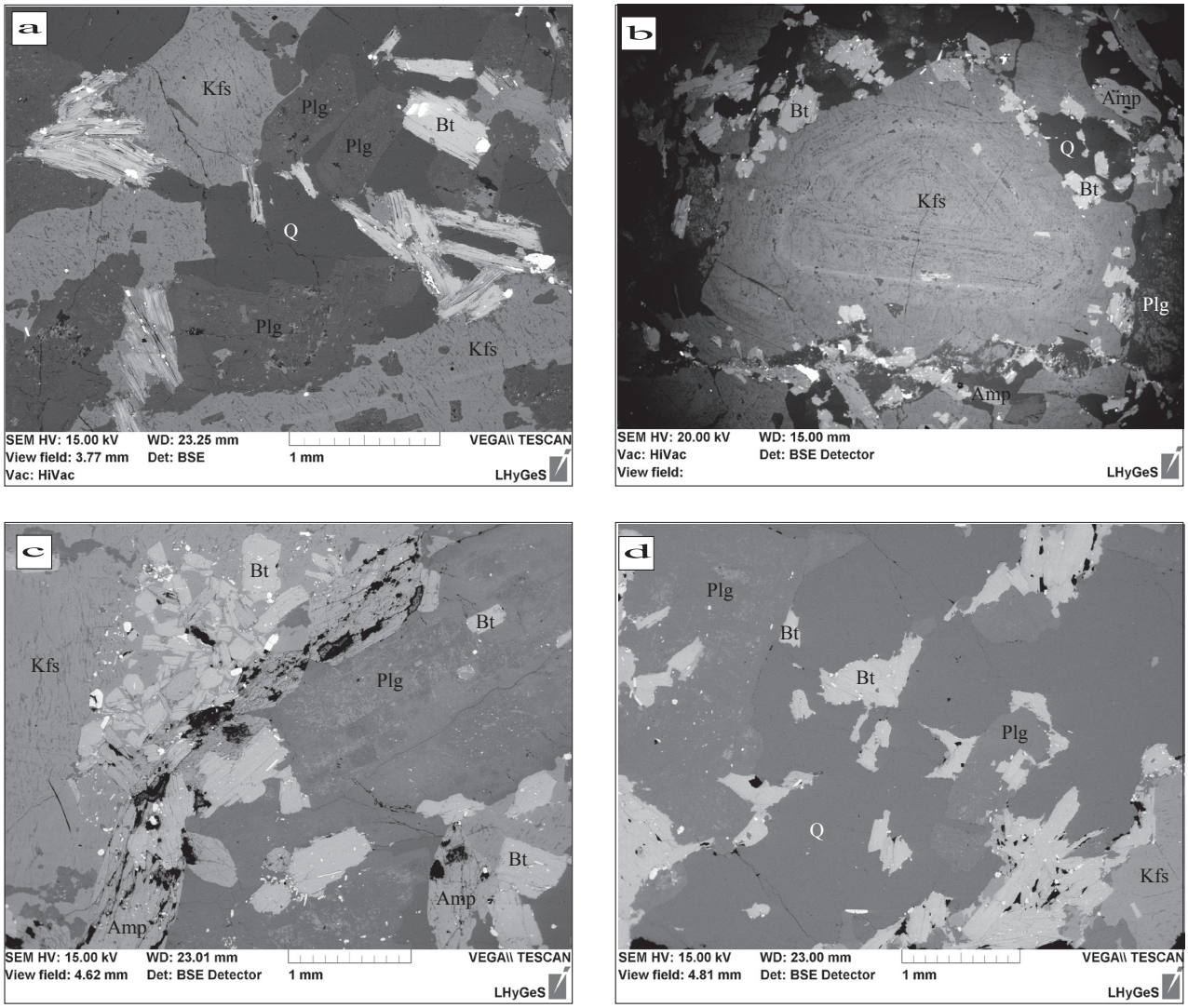

Figure 4: Principal microtextures of the rock types. a) W-CVG. b) N-CVMg-K. c) S-CVMg-K. d) E-CVMg-K. (Mineral abbreviations after Kretz 1983).

The small stock of CVMg-K shows alignment of minerals (Fig.5.d). Plagioclase and K-feldspar grains have lobate boundaries. This alignment suggests that minerals crystallized during magma flow.

SVMg-K association consists essentially of coarse to medium-grained rocks formed by idiomorphic plagioclase ranging from labradorite (An_{60-50}) to albite (An_{15-5}) and K-feldspar, large quartz with lobate boundaries, brown biotite, green Mg-amphibole (magnesio to actinolitic hornblende) and accessory zircon, thorite, apatite, Ti-oxides and magnetite (Fig.5.c). Biotite (X_{Mg}= 0.50-0.60) and amphibole are arranged into large grains aggregates with accessory phases. In the same way as CVMg-K, Ti content of biotite (0.13-0.28 a.p.f.u.) decreases weakly with increasing of Si content.

CVG medium-grained biotite to biotite-muscovite granite contains weakly zoned plagioclase ranging from oligoclase to albite (An_{25-0}), corroded K-feldspar and accessory minerals like apatite, monazite, zircon and magnetite (Fig.4.a & 5.a). Biotite is arranged into elongated aggregates or is elongated along K-feldspar boundaries.

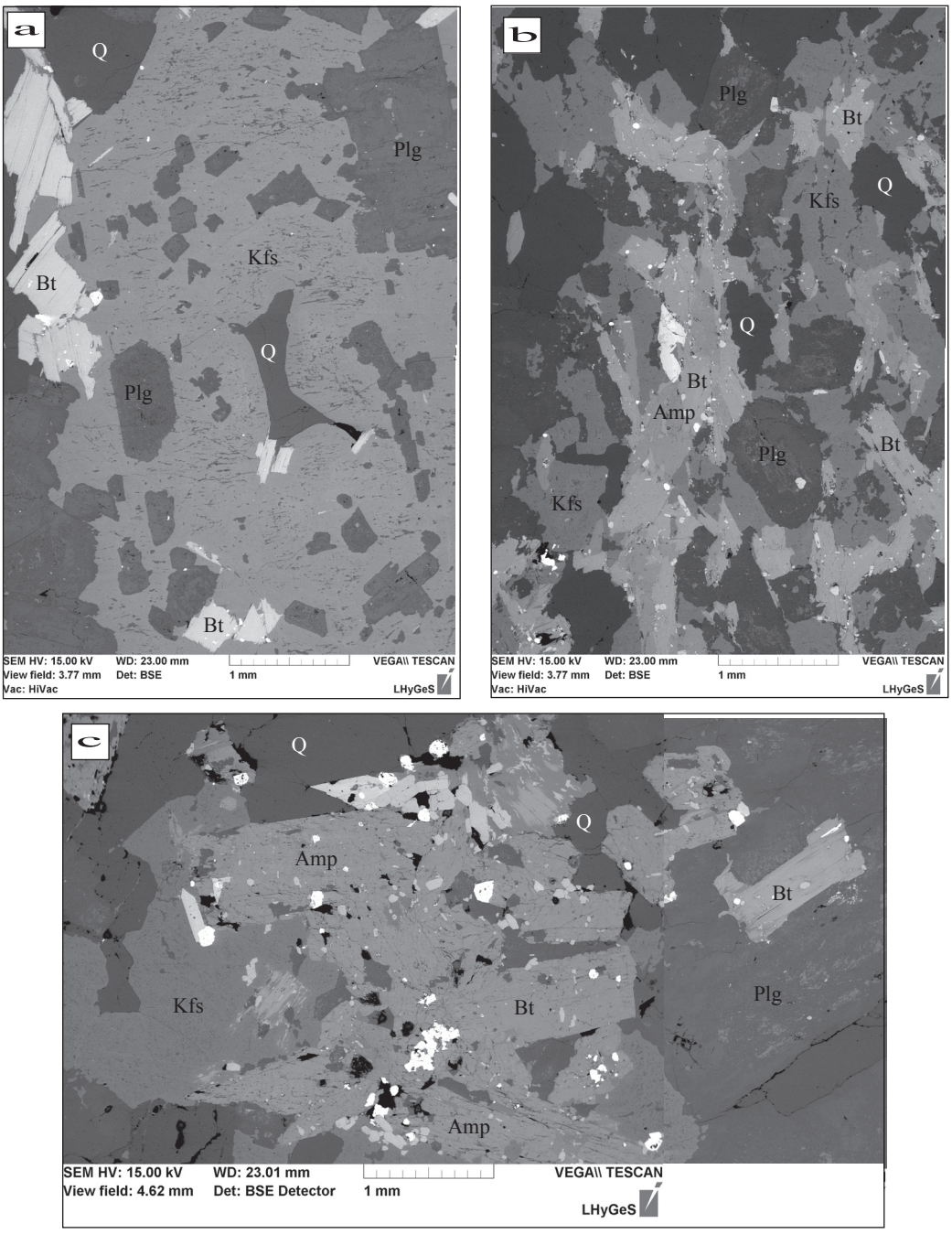

Figure 5: Principal microtextures of the rock types. a) E-CVG. b) CVMg-K (small stock). c) SVMg-K. (Mineral abbreviations after Kretz 1983)

4. Anistropy of magnetic susceptibility

Samples were drilled with a portable drilling machine. The low-field AMS was measured with KLY-3S Kappabridge (Jelinek & Pokorny, 1997) and with DIGICO instruments in Ecole et Observatoire des Sciences de la Terre, Strasbourg. The data were statistically evaluated using the ANISOFT package of programs (Hrouda et al., 1990; Jelinek, 1978). In order to characterized the intensity and shape of the magnetic fabric ellipsoid, two parameters were calculated (Jelinek, 1978): the degree of anisotropy P=k1/k3, and the shape factor T= 2ln(k2/k3)/ln(k1/k3)-1, where $-1<T<0$ indicates prolate and $0<T<1$ oblate shapes of magnetic susceptibility ellipsoids. Measurement of the bulk magnetic susceptibility and of the anisotropy of magnetic susceptibility was performed on 2900 specimens from 210 localities (2.25 cm length, 2.5 cm diameter) distributed according to a grid allowing a spacing of ~1 km between localities.

4.1. Magnetic mineralogy

The magnetic mineralogy was established by thermal demagnetization of three axes IRM, as proposed by Lowrie (1990) using a pulse Magnetizer (ASC Scientific Model IM-10) and a thermal demagnetizer in Département Géosciences et Environnement, Université de Cergy-Pontoise. The saturation for each axes was 1.2, 0.5, 0.15 T.

The bulk magnetic susceptibility (Km) of CVMg-K granitoids is ranging from 80.10-6 to 370.10-6 (SI). Rocks of SVMg-K show highest values of Km (60.10-6 to 2500.10-6 SI). Km data for CVG between 10.10-6 and 240.10-6, are the lowest values of all studied granitoids (Fig. 6).

Thermomagnetic curves of all granitoids of the studied area reveal hyperbolic courses which indicate the importance of a paramagnetic phase as carriers of magnetization but high values of Km suggest also the presence of ferromagnetic phases.

The thermomagnetic curves of CVMg-K (Fig.7.b) show a decrease between 320°C and 400°C and at 500°C which suggests minor presence of pyrrhotite or maghemite or titano-magnetite. Samples of SVMg-K display thermomagnetic curve (Fig.7.a) which show a decrease at 580°C and/or at 680°C. These temperatures (580°C and 680°C) are Curie temperature of magnetite and hematite, respectively. Thermomagnetic curves for CVG (Fig.7.c) are mostly hyperbolic with exception of few samples where a small drop occurs at 580°C or 680°C which indicates presence of small amount of magnetite and hematite.

Measurement of bulk magnetic susceptibility after each heating step reveals for most of the samples a slight decrease before 450°C which is typical of the paramagnetic behaviour of biotite.

Samples which display a decrease at 580°C and 680°C show a weak to strong (up to 4 times) increase of bulk susceptibility above 500°C. This increase of Km above 500°C is attributed to early formation of magnetite or hematization of preexisting magnetite during heating (Trindade et al., 2001).

Thermomagnetic investigations of granitoids suggest that paramagnetic phases, such as biotite and amphibole for Mg-K intrusions and only biotite for CVG intrusion, are dominant with small contribution of ferromagnetic phases (magnetite) which occur in inclusion in biotite crystals for SVMg-K.

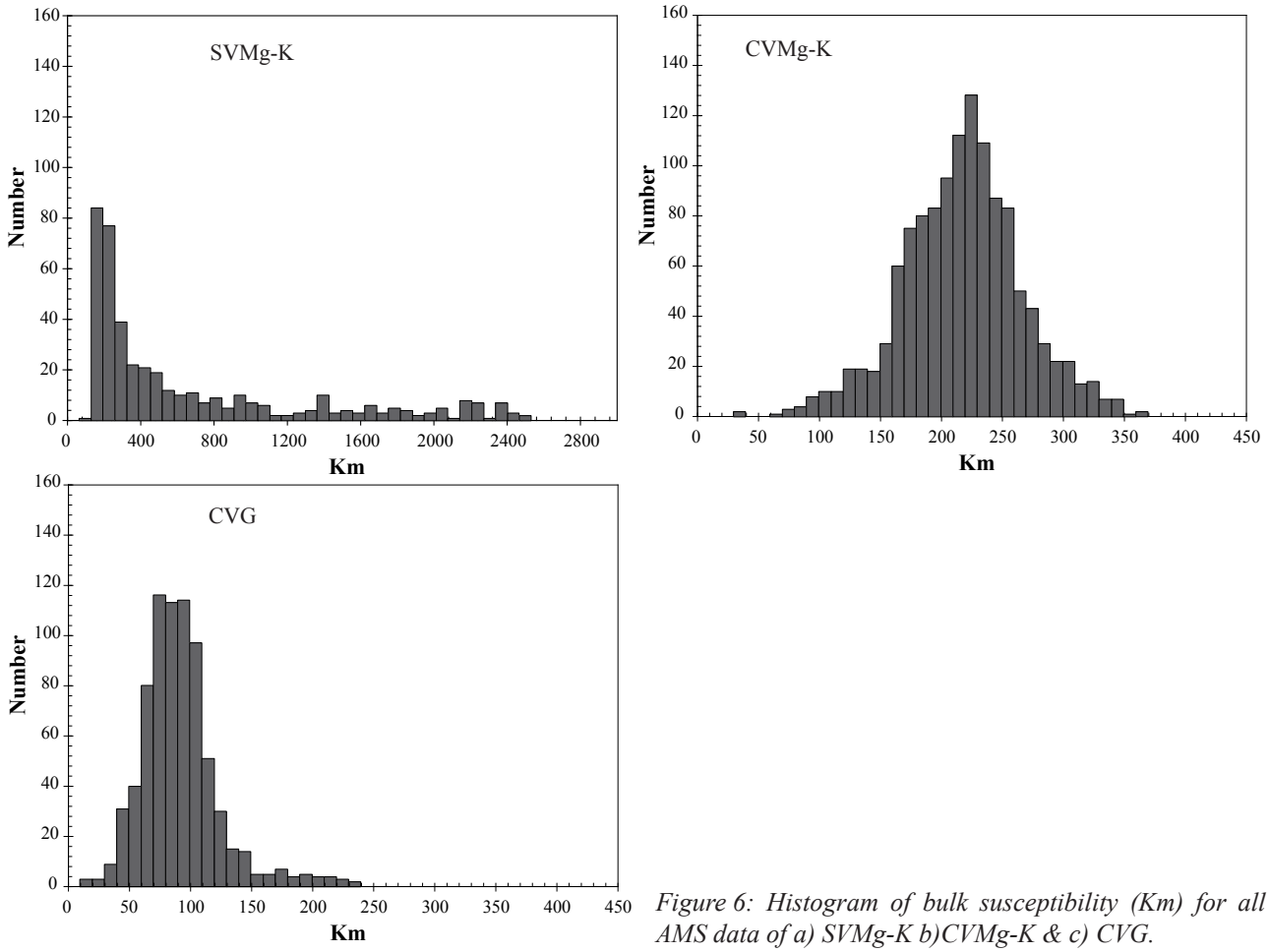

Figure 6: Histogram of bulk susceptibility (Km) for all AMS data of a) SVMg-K b)CVMg-K & c) CVG.

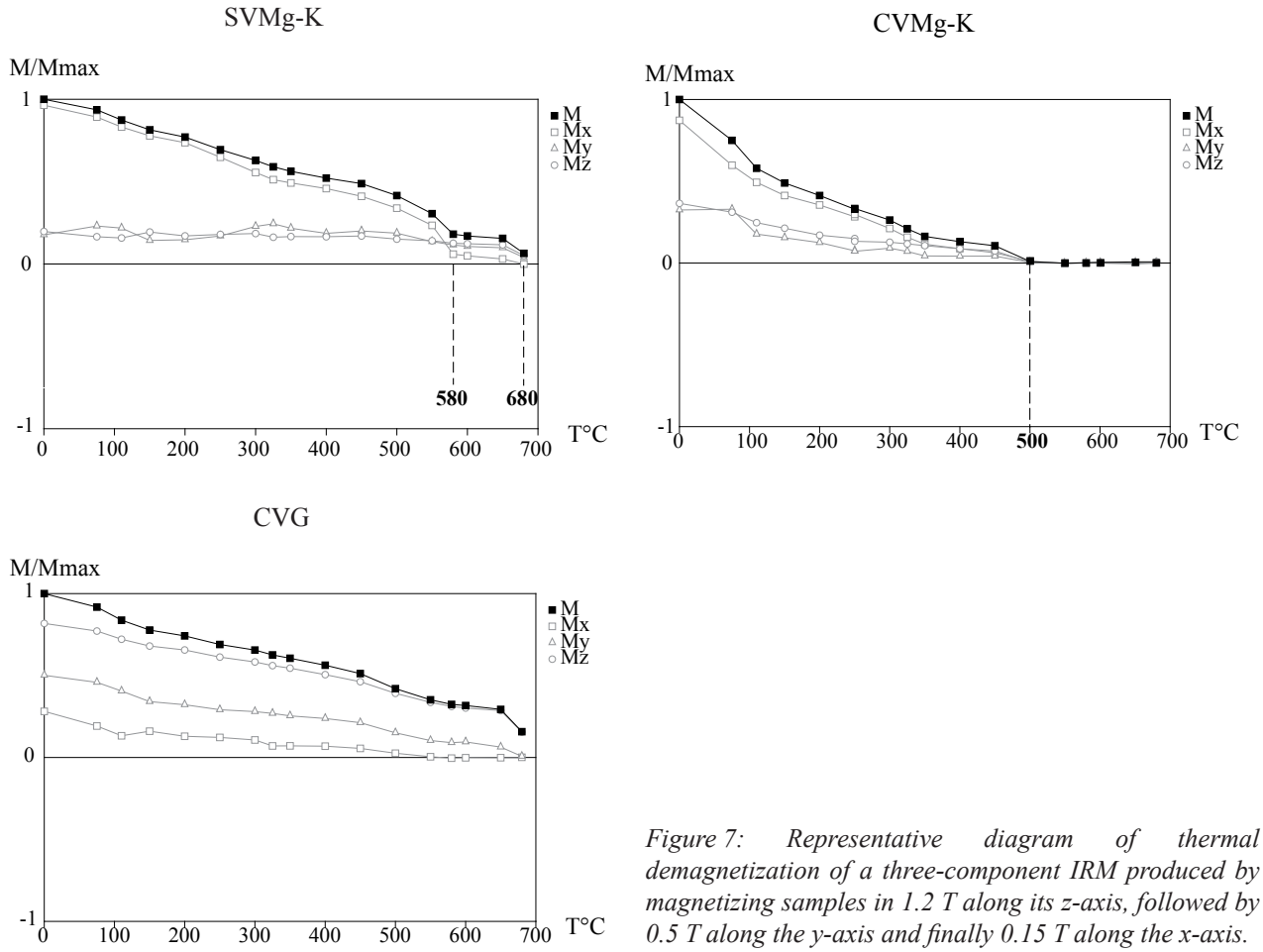

Figure 7: Representative diagram of thermal demagnetization of a three-component IRM produced by magnetizing samples in 1.2 T along its z-axis, followed by 0.5 T along the y-axis and finally 0.15 T along the x-axis.

4.2. Magnetic fabric

Magnetic fabric of igneous rocks is characterized by the magnetic lineation K1 and the magnetic foliation, perpendicular to K3 (Hrouda, 1982; Borradaile, 1988; Bouchez, 1997; 2000). According to the shapes of K3 and K1 distributions, four types of fabrics can be distinguished i)Type I - K3 cluster ii) Type II - K3 girdle iii) Type III - incomplete K3 girdle and iv) Type IV - K1 girdle.

The N-CVMg-K yields a incomplete girdle-Type III fabric (Fig.8 & 9) marked by magnetic foliations generally dipping to the SW with moderate to gentle angles and E-W subhorizontal magnetic lineations evolving towards SW direction. Magnetic ellipsoids vary from oblate to prolate shapes and degree of anisotropy is generally low (P = 1 to 1.08; Fig.10).

The S-CVMg-K shows a Type IV pattern (Fig.8 & 9) marked by a strong maximum of magnetic foliations which are moderately dipping to the NNW and SW. Magnetic lineations are subhorizontal and are distributed along NW and SE quarters of pole figure with a maximum NW direction. Magnetic ellipsoids vary from oblate to prolate to neutral shapes and show weak degree of anisotropy (P < 1.05; Fig.10).

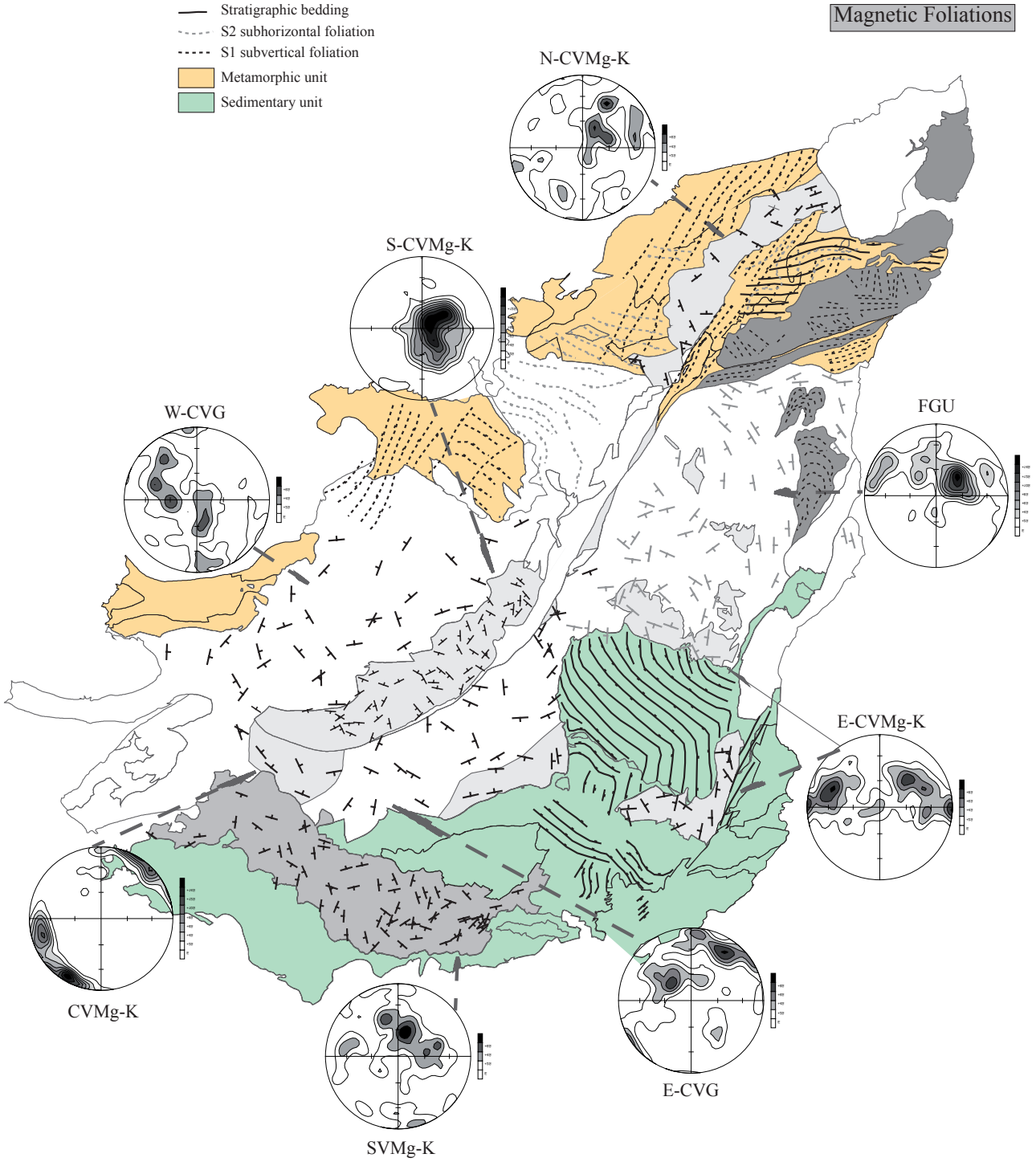

Figure 8: Magnetic foliations. Contoured stereonets of poles to magnetic foliation (k3 direction) show the distribution of k3 for all bodies of granitoids; see discussion in the text (equal area, lower hemisphere projection, contoured at multiples of uniform distribution). Data in grey after Kratinová et al. (2012). Foliations trend in migmatitic domain after Schulmann et al., 2009 and foliations trend in BBTC unit after Kratinová et al. (2007). Structural data of metamorphic and sedimentary units after Rey et al., 1992 and Skrzypek (2011).

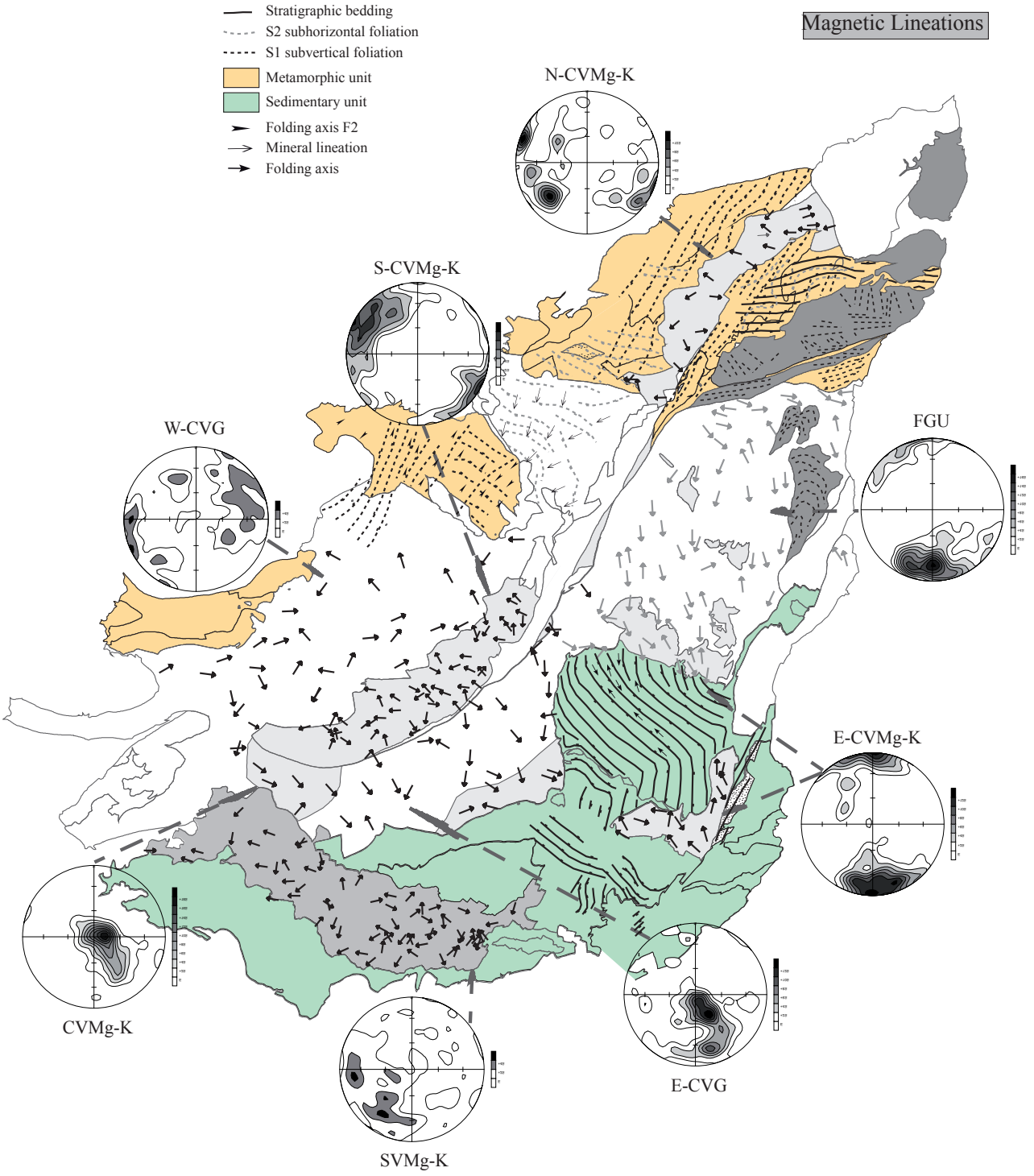

Figure 9: Magnetic lineations (k1 direction). Contoured stereonets of magnetic lineations are shown for all bodies of granitoids; for the detailed discussion see the text (equal area, lower hemisphere projection, contoured at multiples of uniform distribution). Data in grey after Kratinová et al. (2012). Lineations trend in migmatitic domain after Schulmann et al., 2009 and lineations trend in BBTC unit after Kratinová et al. (2007). Structural data of metamorphic and sedimentary units after Rey et al., 1992 and Skrzypek (2011).

The small stock further to the south shows a Type I fabric marked by a strong subvertical to moderate SE plunging magnetic lineations and NW-SE direction of magnetic foliations (Fig.8 & 9). Magnetic ellipsoids have oblate to neutral shapes and degree of anisotropy is higher compared to other CVMg-K intrusions (P = 1.02 to 1.12; Fig.10).

In the southern part of the E-CVMg-K, new AMS data are consistent with previous AMS study of its northern part (Fig.8 & 9; Kratinová et al., 2012) with a Type II fabric marked by N-S trending magnetic foliation with moderate to steep dip angles and subhorizontal N-S-trending magnetic lineations. Magnetic ellipsoids vary from neutral to weakly oblate and degree of anisotropy ranges between 1.0 and 1.1 with some samples reaching higher P values (until 1.2; Fig.10).

The SVMg-K intrusion shows mainly incomplete girdle-Type III fabric similar to N-CVMg-K (Fig.8 & 9) associated with magnetic foliations gently dipping either to the S or to the E. In the western part of SVMg-K pluton, magnetic lineations plunge mostly to the E at moderate angles whereas in the central and eastern part, magnetic lineations plunges SW. Magnetic ellipsoids vary from oblate to prolate with degree of anisotropy between 1.0 and 1.1 (Fig.10).

The W-CVG yields a Type II fabric marked by NNW-SSE striking magnetic foliations and NE-SW trending variably plunging magnetic lineations (Fig.8 & 9). The degree of anisotropy is between 1.0 and 1.1 and shapes of their magnetic ellipsoids vary from oblate to neutral (Fig.10).

The E-CVG displays also a girdle Type II fabric but poles of magnetic foliations are distributed along a NE-SW oriented girdle (Fig.8 & 9). The magnetic lineations plunge mostly to the SE and S at steep to moderate angles. The shapes of the magnetic ellipsoids vary from oblate to neutral with degree of anisotropy between 1.0 and 1.1 (Fig.10). In a previous AMS work on the E-CVG (FGU), Kratinová et al (2012) shows N-S orientation of foliation trends which dip predominantly to the W at moderate to steep angles in the northern part. This fabric pattern is in clear continuity with foliation trends of migmatitic unit (Fig.8). The southernmost part of granite, adjacent to E-CVMg-K intrusions, shows foliations dipping at moderate to shallow angles to the south.

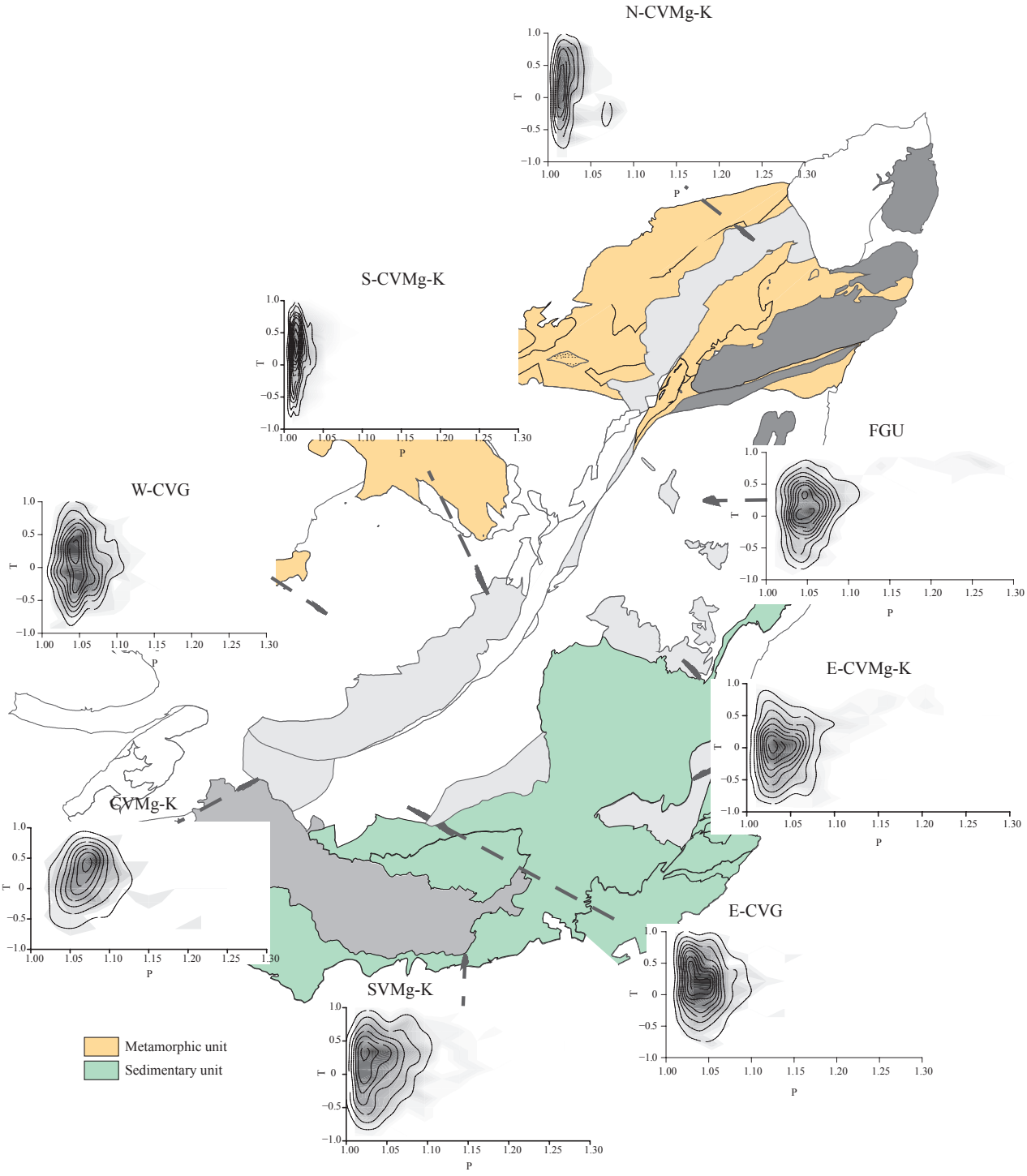

Figure 10: Map showing the P-T diagrams for all bodies of granitoids (contoured at multiples of uniform distribution). P = degree of anisotropy, T = shape of ellipsoid (see text for parameter definition).

5. Discussion

Critical aspect for interpretation of magmatic fabrics in granitoids is the understanding of their emplacement history in relation of regional deformation. When geometrical and temporal relationships between individual magmatic and tectonic events are established the model of magmatic/magnetic fabric evolution can be proposed.

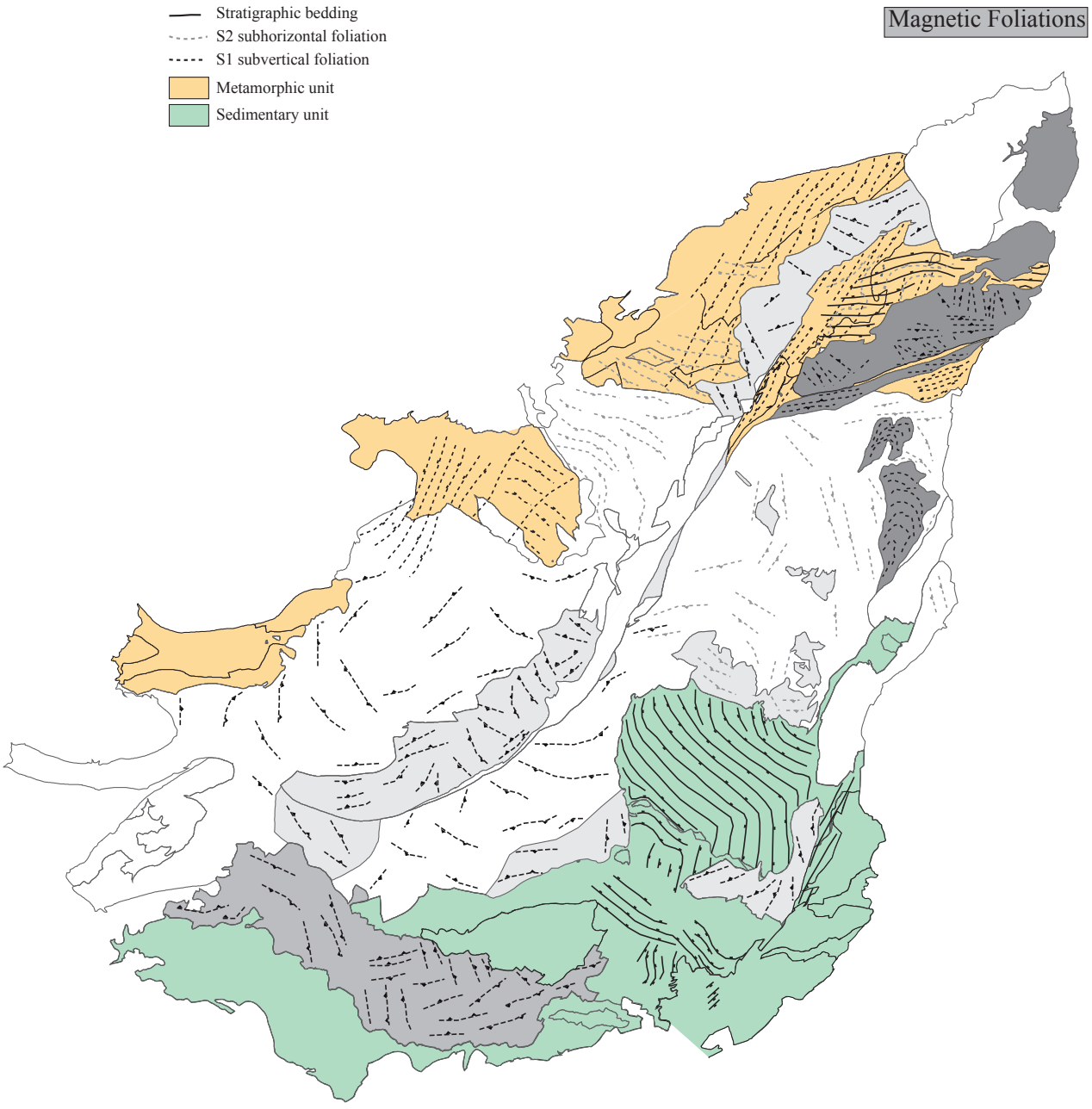

Figure 11: Interpretative map of distribution of AMS foliation in the different plutonic bodies. Data in grey after Kratinová et al. (2012). Foliations trend in migmatitic domain after Schulmann et al., 2009 and foliations trend in BBTC unit after Kratinová et al. (2007). Structural data of metamorphic and sedimentary units after Rey et al., 1992 and Skrzypek (2011).

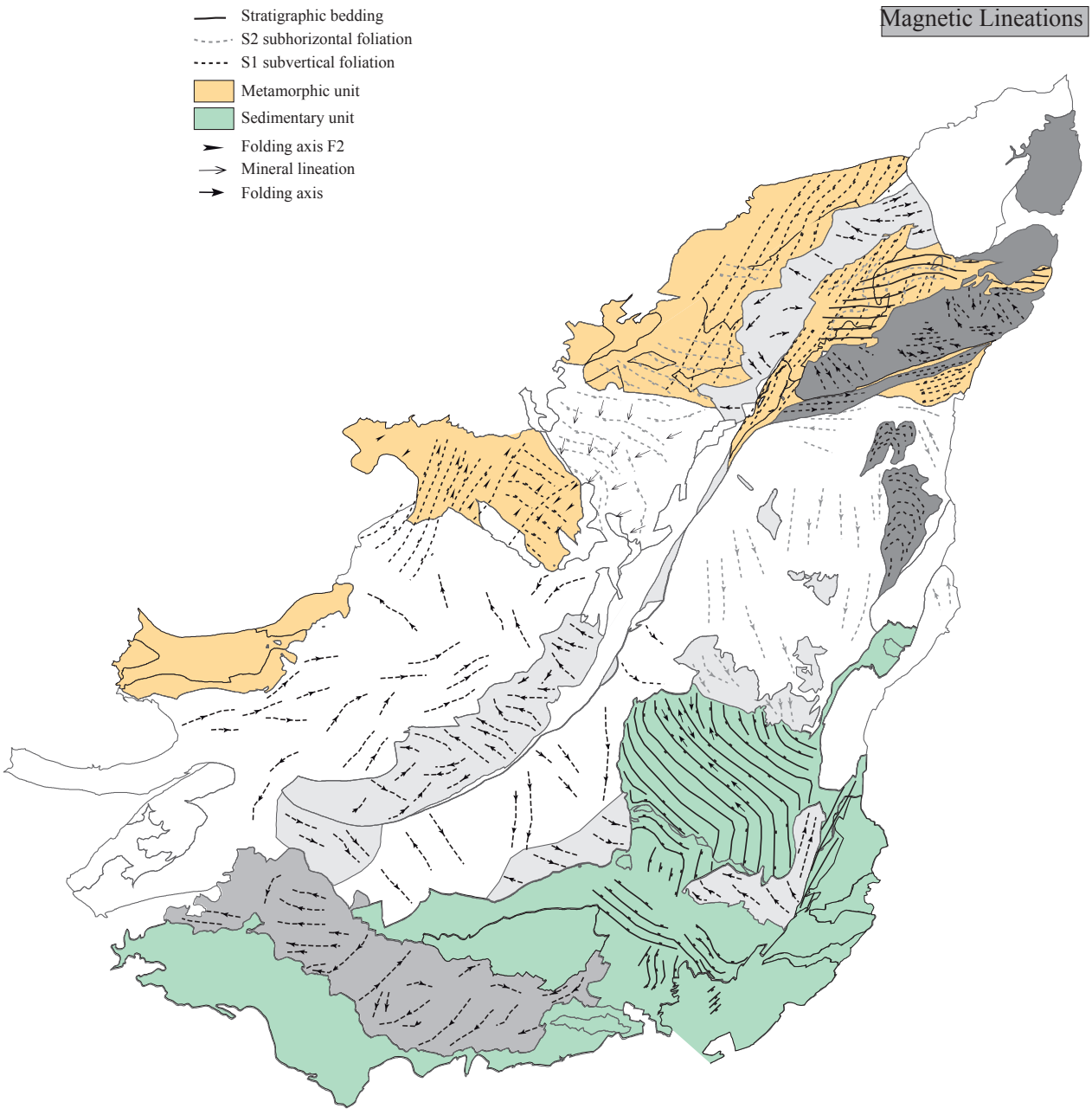

Figure 12: Interpretative map of distribution of AMS lineation in the different plutonic bodies. Data in grey after Kratinová et al. (2012). Lineations trend in migmatitic domain after Schulmann et al., 2009 and lineations trend in BBTC unit after Kratinová et al. (2007). Structural data of metamorphic and sedimentary units after Rey et al., 1992 and Skrzypek (2011).

5.1. Correlation of magnetic and macroscopic granitoid fabrics

The magnetic fabric of studied granitoids is in agreement with magmatic fabrics defined by preferred orientation of feldspar phenocrysts measured in the field except for N-CVMg-K and SVMg-K plutons at the N and S boundaries of the studied area, respectively. Magmatic and magnetic fabrics of both plutons exhibit orthogonal directions of planar fabrics suggesting complex emplacement and deformation history (Kratinová et al., 2010). As confirmed by microstructural observations, the magmatic fabric of both intrusions defined by feldspar preferred orientation is not reworked by visible solid-state deformation. This observation suggests that the magnetic fabric carried by biotite is acquired later than K-feldspar phenocryst preferred orientation and probably still in magmatic state. Previous studies of granitoids marked by deformation of highly crystallized suspensions represented by high proportion of crystallized feldspars and low proportion of interstitial melt (Borradaile & Kehlenbeck, 1996; Barros et al., 2001; Paterson et al., 2003; Žák et al., 2005; Žák et al., 2007) suggested a possibility to record successive deformation events. These intrusions show fabrics defined by rigid framework of K-feldspar phenocrysts which is not necessarily the same as that defined by inter-phenocryst melt-bearing matrix (Žák et al., 2008; Kratinová et al., 2010). In these cases the AMS data could reflect late overprinting strains which are not recorded by the K-feldspar phenocryst.

5.2. Correlation of magnetic and country rocks fabrics

All fabrics of the granitoids are more or less coherent with host rock fabrics. Only magnetic fabrics of E-CVG are only partly recorded in adjacent metamorphic and sedimentary units. The magnetic fabrics of N-CVMg-K (Fig.11 & 12) generally consistent with the NE-SW S1 and S2 foliations recorded in northern metamorphic units (Skrzypek, 2011). These metamorphic foliations are the result of vertical exhumation of the lower crust at mid-crustal level (S1) subsequently followed by a localised flattening (S2; Skrzypek, 2011). Magnetic fabrics of S-CVMg-K and W-CVG (Fig.11 & 12) are subparallel to foliation and mineral lineation of the migmatitic domain in the western part of the Vosges Mts (Rey et al., 1992). Foliations recorded in this migmatitic domain are compatible with W to SW-directed extension (Rey et al., 1992). In contrast, the magnetic fabrics of E-CVMg-K and FGU (Fig.11 & 12) are consistent with the bedding dipping either to the N or to the S in the sedimentary Markstein unit and with axial planes and upright folds affecting metamorphic rocks (Skrzypek, 2011). These structures recorded in both sedimentary and metamorphic units are interpreted as the result of N-S shortening affected only upper crustal lithologies. S1 subvertical foliation recorded in granulites and gneisses (Skrzypek, 2011) is well represented in the small stock of CVMg-K (Fig.11 & 12) and in the same way as N-CVMg-K, this S1 subvertical foliation is the result of vertical exhumation of the lower crust (granulite and amphibolite). This is in agreement with geochemistry study where we demonstrated the particular link between granulite and Mg-K magmatism.

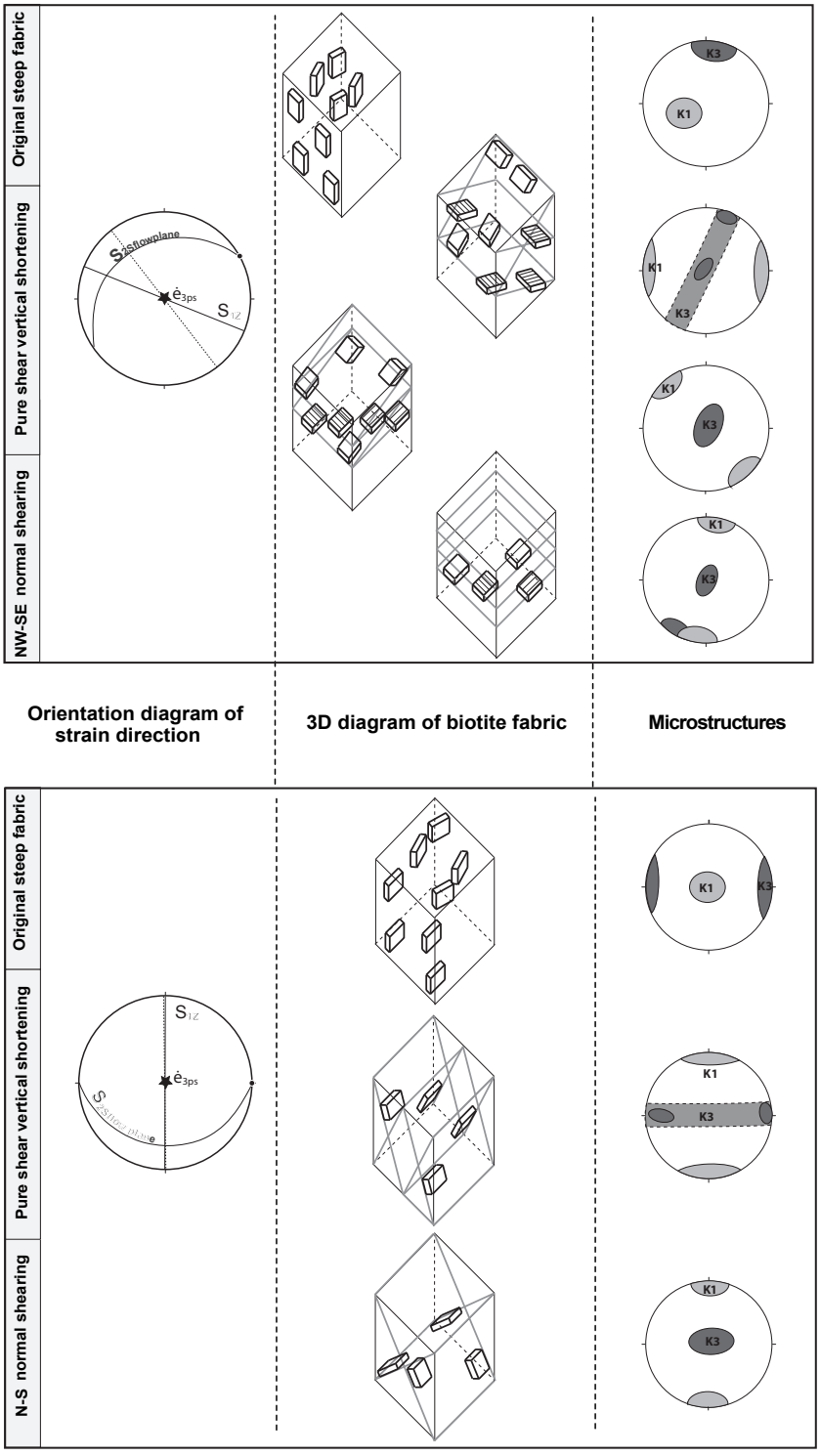

Figure 13: Summary diagram of the evolution through time for two orthogonal steep fabrics (a) the CVMg-K and (b) the E-CVMg-K. The figures show orientation diagram illustrating mechanisms of emplacement, 3D idealized diagram of biotite fabric, and resulting stereograms of microstructures.

5.3. Fabric-forming processes in Central and Southern Vosgian granitoids

The preserved steep fabrics in small stock of CVMg-K is interpreted to reflect vertical emplacement of magmas and it is assumed that it is not reworked by subsequent deformation. According to field relationship, geochemical characteristics (Tabaud et al., submitted) and overprinting relationships between successive deformation events affecting differently various crustal levels, a relative timing relationships for each type of fabrics could be proposed and is summarized in Fig.13.

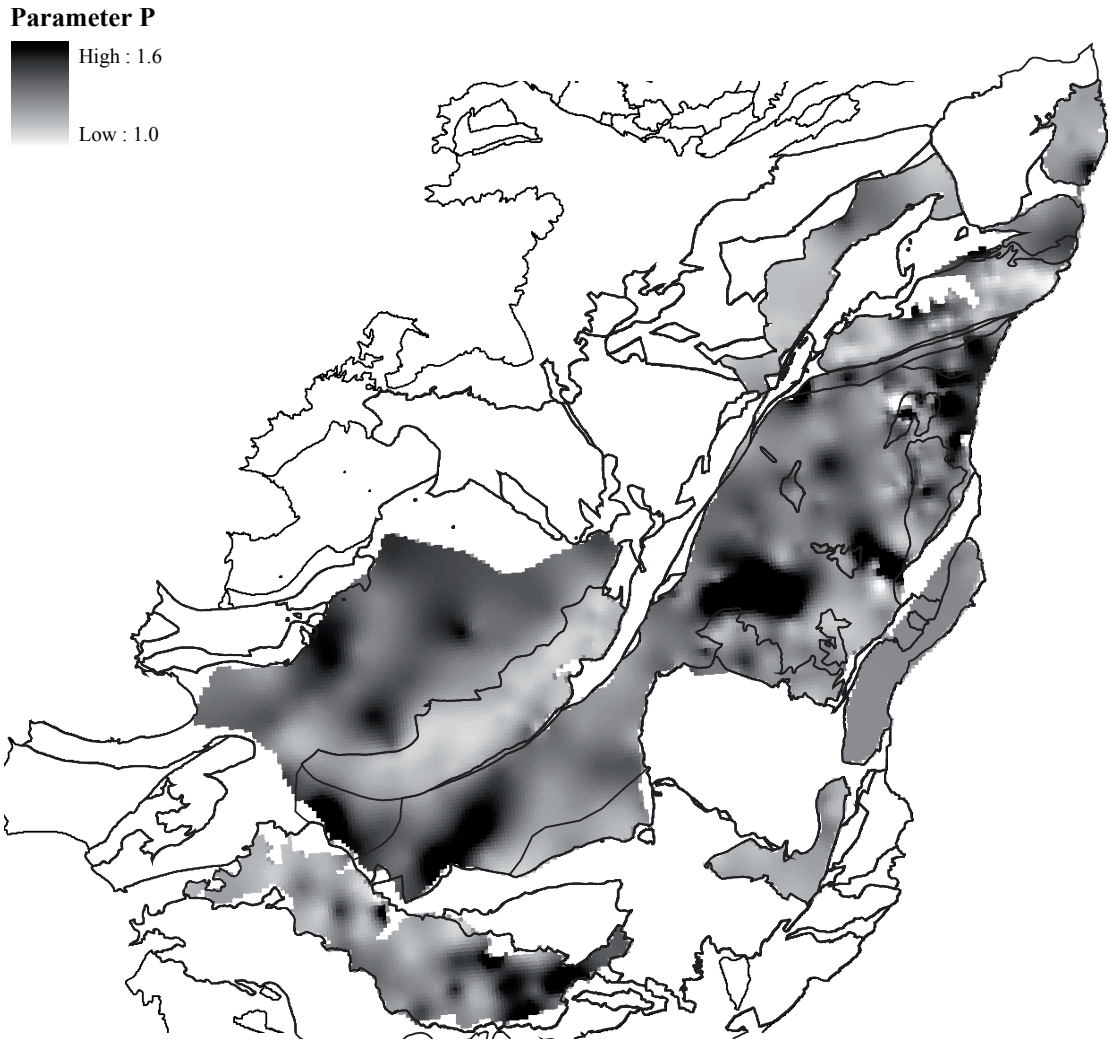

Figure 14: Contoured map of P parameter for all granitoids of Central and Southern Vosges Mts. Data from Kratinová et al. (2007); Schulmann et al., 2009; Kratinová et al. (2012) and this study.

Type I fabric, corresponding to original steep fabric, occurs namely in the E-CVMg-K and CVMg-K intrusions. These two fabrics are orthogonal and result from D1 and D2 deformation events, respectively (Skrzypek, 2011). The two deformation events are well developed in all structural levels. The last large deformation event D4 separates the deep orogenic rocks from shallow crustal superstructure represented by metasedimentary units. The deformation coincides with large scale detachment associated with large magmatic activity and emplacement of anatectic magmas. The AMS fabrics of studied plutons can be therefore regarded as a result of overprint of two vertical fabrics by horizontal shearing resulting from mid-crustal detachment.

In this light two end member fabrics can be defined: 1) The relics of early steep fabrics unaffected or weakly reworked by D4 detachment represented by fabric CVMg-K and E-CVG. 2) The fabrics resulting from southward flow marked by subhorizontal foliation and south-plunging magnetic lineation represented by FGU and partly by N-CVMg-K and W-CVG patterns. 3) An intermediate fabrics represented by E-CVMg-K, S-CVMg-K and SVMg-K plutons. These evolutions follow theoretical model predictions proposed by Schulmann and Ježek (2012). According to this model, a vertical NW-SE trending fabric CVMg-K when affected by vertical shortening and south directed horizontal flow (mixed fabric of Ježek et al., 1996) will result in horizontal foliation and E-W trending intersection lineation. Similarly, the NNE-SSW trending vertical fabric reworked by vertical shortening and south directed simple shear will result in vertical to horizontal foliation represented by FGU, SVMg-K and E-CVMg-K patterns and N-S lineation. All three transitional fabrics tend to show neutral to constrictional shapes of AMS ellipsoids which is in agreement with theoretical models proposed by Schulmann et al., (2009) and Schulmann and Ježek (2012). The FGU, N-CVMg-K and SVMg-K show fabric types typical for high degree of orthogonal reworking i.e. sub-horizontal foliation, predominantly lineation in the direction of flow and dominantly oblate strain ellipsoid shapes. All together, the fabric pattern of Vosges granitoids can be explained by magmatic overprints resulting from three major tectonic events: 1) two deformations resulting in vertical orthogonal fabrics, 2) successively reworked by south-directed horizontal shearing combined with vertical shortening. The variations in fabrics shapes and orientations of K1, K3 directions and degree of magnetic susceptibility can be explained by various degree of fabric overprint and various strength of original fabric (Kratinová et al., 2010). The deformation overprint model is supported well by map of degree of magnetic susceptibility (Fig.14) showing high anisotropy in regions of perfectly preserved early vertical fabric (CVMg-K and SVMg-K) and low anistropy in regions of major subhorizontal reworking by D4 strain (E-CVMg-K). It is noticeable that all three bodies reflect also highest degree of mean magnetic susceptibility showing common origin of these intrusions (Fig.15). In detail, the same relationships can be followed in the E-CVMg-K and FGU bodies where important relics of Mg-K granitoids reworked by later CVG melting occur.

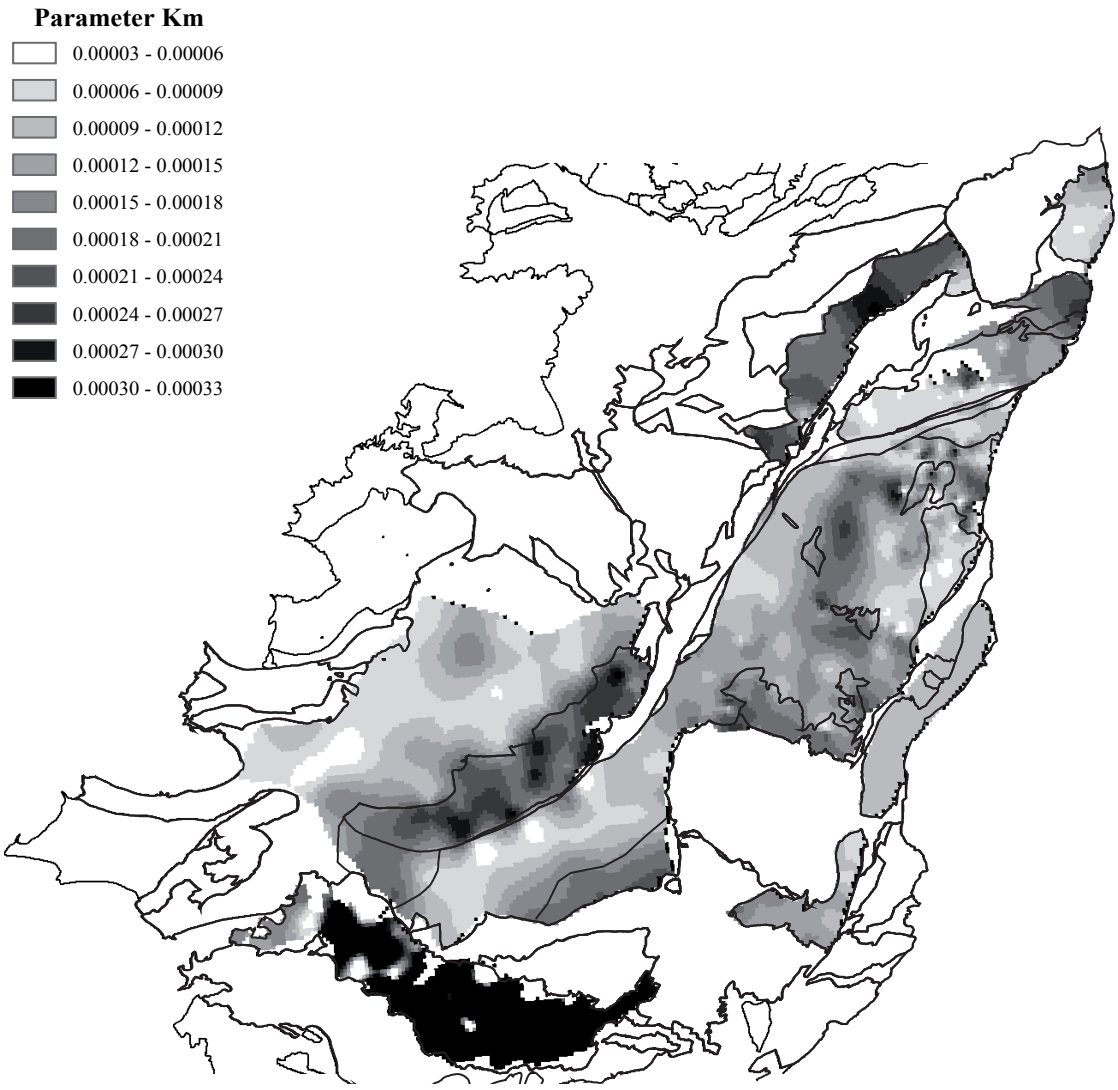

Figure 15: Contoured map of Km for all granitoids of Central and Southern Vosges Mts. Data from Kratinová et al. (2007); Schulmann et al., 2009; Kratinová et al. (2012) and this study.

5.4. Fabric inheritance in granitoids

Fundamental question in granitoids is what is the fabric related to magma emplacement and to subsequent deformation and/or remelting. These questions were so far not addressed by structural geologists and the Vosges magmatic system offers an insight to this important issue. This work shows that the Mg-K magma was emplaced along vertical paths, probably syntectonically in coherence with vertical fabrics of host rocks. The magma exploited vertical anisotropies of rocks in any crustal levels. Ten millions years after this major magmatic pulse a new event occurred resulting in emplacement of large proportion of magma along a mid-crustal detachment zone ca. 5 – 10 km wide. Here, the original vertical fabrics of Mg-K plutons became reworked leading to formation of complex fabrics. We note that magmatic fabrics in thermally and deformationally reworked Mg-K magmas record a memory of original fabric and that this information can be depicted by detailed AMS study. Existing numerical modelling studies suggest that resulting magmatic fabrics can be decomposed in two major events and the tectonic history restored similarly as it is done in metamorphic and sedimentary rocks.

6. Conclusion

Our orogenic scale AMS study reveals the complexity of AMS fabrics recorded by magmatic intrusions which are the result of polyphase magmatic histories occurring between 340 Ma and 320 Ma. Detailed analysis of K-feldspar, microstructural and AMS data indicate that each fabric of the different plutonic bodies which intruded different crustal level reflects more or less the different subsequent deformation affecting the crust during and after their emplacement. We propose a model of fabric evolution for the Central and Southern Vosgian granitoids where the two orthogonal end member original steep fabrics interpreted to reflect vertical emplacement of Mg-K magmas, are subsequently more or less reworked by a vertical shortening and a south-directed simple shear which both could occur during emplacement of CVG magmas.

Collaborators: Karel Schulmann, Etienne Skrzypek, Jean-Bernard Edel

REFERENCES CITED

Arbaret, L., Fernandez, A., Ježek, J., Ildefonse, B., Launeau, P. & Diot, H. (2000). Analogue and numerical modelling of shape fabrics: application to strain and flow determination in magmas. *Transactions of the Royal Society of Edinburgh, Earth Sciences*, **90**, 97–109.

Barros, C. E. M., Barbey, P. & Boullier, A. M. (2001). Role of magma pressure, tectonic stress and crystallization progress in the emplacement of syntectonic granites. The A-type Estrela Granite Complex (Carajás Mineral Province, Brazil). *Tectonophysics*, **343**, 93–109.

Borradaile, G. J. & M. Jackson (2004). Anisotropy of magnetic susceptibility (AMS): Magnetic petrofabrics of deformed rocks. *Geological Society Special Publication*, p. 299.

Borradaile, G. J. & Kehlenbeck, M. M. (1996). Possible Crypto tectonic magnetic fabrics in "Posttectonic" granitoid plutons of the Canadian Shield. *Earth and Planetary Science Letters*, **137**, 119–127.

Borradaile, G. J. (1994). Paleomagnetism carried by crystal inclusions: the effect of preferred crystallographic orientations. *Earth and Planetary Science Letters*, **126**, 171-182.

Borradaile, G. J. (1988). Magnetic susceptibility, petrofabrics and strain. *Tectonophysics*, **156**, 1-20.

Bouchez, J. L. (2000). Magnetic susceptibility anisotropy and fabrics in granites. *Comptes Rendus de l'Académie des Sciences, Series IIA, Earth and Planetary Sciences* **330**, 1–14.

Bouchez, J. L. (1997). Granite is never isotropic: an introduction to AMS studies of granitic rocks. In: J.L. Bouchez, D.H.W. Hutton & W.E. Stephens (Eds) *Granite: from segregation of melt to emplacement fabrics*. *Kluwer academic Publishers*, 95-112.

Bouchez, J. L. & Gleizes, G. (1995). Two-stage deformation of the Mont-Louis-Andorra granite pluton (Variscan Pyrenees) inferred from magnetic susceptibility anisotropy. *Journal Geological Society London*, **152**, 669–679.

Boutin, R., Montigny, R. & Thuizat, R. (1995). Chronologie K-Ar et 39Ar/40Ar du métamorphisme et du magmatisme des Vosges. Comparaison avec les massifs varisques avoisinants. *Géologie de la France*, **1**, 3–25.

de Saint Blanquat, M., Law, R. D., Bouchez, J. L. & Morgan, S. S. (2001). Internal structure and emplacement of the Papoose Flat pluton: An integrated structural, petrographic, and magnetic susceptibility study. *Geological Society of America Bulletin*, **113**, 976-995.

Edel, J. B. & Weber, K. (1995). Cadomian terranes, wrench faulting and thrusting in the central Europe Variscides: Geophysical and geological evidence. *Geologische Rundschau*, **84**, 412-432.

Fluck, P., Edel, J. B., Gagny, C., Montigny, R., Piqué, A., Schneider, J. L. & Whitechurch, H. (1989). Carte synthétique et géotraverse N-S de la chaine varisque des Vosges (France). Synthèse des travaux effectués depuis deux décennies. *Comptes-rendus de l'Académie des Sciences, Série II,* **309**, 907-912.

Fluck, P. (1980). Métamorphisme et magmatisme dans les Vosges moyennes d'Alsace. Contribution à l'histoire de la chaine Varisque. *Mémoires des Sciences Géologiques*, **62**, 248 p.

Gleizes, G., Leblanc, D., Santana, V., Olivier, P. & Bouchez, J. L. (1998b). Sigmoidal structures featuring dextral shear during emplacement of the Hercynian granite complex of Cauterets-Panticosa (Pyrenees). *Journal of Structural Geology*, **20**, 1229-1245.

Gleizes, G., Leblanc, D. & Bouchez, J. L. (1998a). The main phase of the Hercynian orogeny in the Pyrenees is a dextral transpression. In: Holdsworth, R. E., Strachan, R. A. & Dewey, J. F. (eds.) *Continental transpression and transtensional tectonics, Geological Society Special Publication, London*, **135**, 267-273.

Hrouda, F., Jelínek, V. & Hrušková, L. (1990). A package of programs for statistical evaluation of magnatic data using IBM-PC computers. *EOS Transactions, American Geophysical Union, San Francisco*, 1289.

Hrouda, F. (1982). Magnetic anisotropy of rocks and its application in geology and geophysics. *Geophysical surveys*, **5**, 37-82.

Jelínek, V. & Pokorný, J. (1997). Some new concepts in technology of transformer bridges for measuring susceptibility anisotropy of rocks. *Physics of the Earth and Planetary Interiors*, **22**, 179-181.

Jelínek, V. (1978). Statistical processing of anisotropy of magnetic susceptibility measured on groups of specimens. *Studia Geophysica et Geodaetica*, **22**, 50-62.

Ježek, J., Schulmann, K. & Segeth, K. (1996). Fabric evolution of rigid inclusions during mixed coaxial and simple shear flows. *Tectonophysics*, **257**, 203-221.

Ježek, J., Melka, R., Schulmann, K. & Venera, Z. (1994). The behaviour of rigid triaxial ellipsoidal particles in viscous flows—Modelling of fabric evolution in a multiparticle system. *Tectonophysics*, **229**, 165–180.

Kossmat, F. (1927). Gliederung der varistischen Gebirgsbaues. *Abhandlungen des Sächsischen geologischen Landesamts* **1**, 1-39.

Kratinová, Z., Schulmann, K., Edel, J. B. & Tabaud, A. S. (2012). AMS record of brittle dilation, viscous-stretching and gravity-driven magma ascent in area of magma-rich crustal extension (Vosges Mts., NE France). *International Journal of Earth Sciences*, **101**, 803-817.

Kratinová, Z., Ježek, J., Schulmann, K., Hrouda, F., Shail, R. K. & Lexa, O. (2010). Noncoaxial K-feldspar and AMS subfabrics in the Land's End granite, Cornwall: Evidence of magmatic fabric decoupling during late deformation and matrix crystallisation. Journal of Geophysical Research, 115, B09104, doi: 10.1029/2009JB006714.

Kratinová, Z., Schulmann, K., Edel, J. B., Ježek, J. & Schaltegger, U. (2007). Model of successive granite sheet emplacement in transtensional setting: Integrated microstructural and anisotropy of magnetic susceptibility study. *Tectonics,* **26**, TC6003.

Krecher, M. (2005). Die Turbiditsandstein-Komplexe der devono-karbonischen Markstein Gruppe im Oberelsass (NE-Frankreich) und ihre Beziehungen zu den moldanubischen Gesteinseinheiten von Schwarzwald und Vogesen. Dissertation, Albert-Ludwigs-Universität, Freiburg im Breisgau, 386 p.

Kretz, R. (1983). Symbols for rock-forming minerals. *American Mineralogist*, **68**, 277 – 279.

Latouche, L., Fabries, J. & Guiraud, M. (1992). Retrograde evolution in the Central Vosges mountains (north-eastern France): implications for the metamorphic history of high-grade rocks during the Variscan orogeny. *Tectonophysics*, **205**, 387–407

Lowrie, W. (1990). Identification of ferromagnetic minerals in a rock by coercivity and unblocking temperature properties. *Geophysical Research Letters*, **17**, 159-162.

Paterson, S. R., Onezime, J., Teruya, L. & Žák, J. (2003). Quadruple-pronged enclaves: Their significance for the interpretation of multiple magmatic fabrics in plutons. *Journal of the Virtual Explorer, Electronic Edition, General Contributions 2003,* **10**, paper 2.

Rey, P., Burg, J. P. & Caron, J. M. (1992). Middle and Late Carboniferous extension in the Variscan Belt: structural evidences from the Vosges massif (Eastern France). *Geodinamica Acta*, **5**, 17-36.

Robert, J. L. (1976). Titanium solubility in synthetic phlogopite solid solutions. *Chemical Geology,* **17**, 213-227.

Schaltegger, U., Fanning, C. M., Günther, D., Maurin, J. C., Schulmann, K. & Gebauer, D. (1999). Growth, annealing and recrystallization of zircon and preservation of monazite in high-grade metamorphism: conventional and in situ U–Pb isotope cathodoluminescence and microchemical evidence. *Contributions to Mineralogy and Petrology,* **134**, 186–201.

Schaltegger, U., Schneider, J. L., Maurin, J. C. & Corfu, F. (1996). Precise U–Pb chronometry of 345–340 Ma old magmatism related to syn-convergence extension in the Southern Vosges (Central Variscan Belt). *Earth and Planetary Science Letters,* **144**, 403–419.

Schulmann, K. & Ježek, J. (2012). Some remarks on fabric overprints and constructional AMS fabrics in igneous rocks. *International Journal of Earth Sciences*, **101**, 705-714.

Schulmann, K., Edel, J. B., Hasalová, P., Cosgrove, J. Ježek, J. & Lexa, O. (2009). Influence of melt-induced mechanical anisotropy on the magnetic fabrics and rheology of deforming migmatites, Central Vosges, France. *Journal of Structural Geology,* **31**, 1223-1237.

Schulmann, K., Schaltegger, U. Ježek, J., Thompson, A. L. & Edel, J. B. (2002). Rapid burial and exhumation during orogeny: thickening and synconvergent exhumation of thermally weakened and thinned crust (Varican orogen in Western Europe). *American Journal of Science,* **302**, 856-879.

Skrzypek, E., Štípská, P. & Cocherie, A. (*submitted*). The origin of zircon and the significance of U-Pb ages in high-grade metamorphic rocks: a case study from the Variscan orogenic root (Vosges Mountains, NE France). *Contributions to Mineralogy and Petrology*.

Skrzypek, E. (2011). Contribution structurale, pétrologique et géochronologique à la tectonique intracontinentale de la chaîne hercynienne d'Europe (Sudètes, Vosges). Ph.D. thesis, University of Strasbourg, 381 p.

Tabaud, A. S., Rossi, P., Whitechurch, H., Skrzypek, E., Schulmann, K., Guerrot, C. & Paquette, J. L. (*submitted*). Chronology, petrogenesis and heat sources for successive Carboniferous magmatic events in the Variscan Vosges Mts (NE France).

Trindade, R. I. F., Mintsa Mi Nguema, T. & Bouchez, J. L. (2001). Thermally enhanced mimetic fabric of magnetite in a biotite granite. *Geophysical Research Letters*, **28**, 2687-2690.

Žák, J., Verner, K. & Týcová, P. (2008). Multiple magmatic fabrics in plutons: an overlooked tool for exploring interactions between magmatic processes and regional deformation? *Geological Magazine*, **145**, 537-551.

Žák, J., Paterson, S. R. & Memeti, V. (2007). Four magmatic fabrics in the Tuolumne batholith, central Sierra Nevada, California (USA): Implications for interpreting fabric patterns in plutons and evolution of magma chambers in the upper crust. *Geological Society of America Bulletin*, **119**, 184-201.

Žák, J., Schulmann, K. & Hrouda, F. (2005). Multiple magmatic fabrics in the Sázava pluton (Bohemian Massif, Czech Republic): A result of superposition of wrench-dominated regional transpression on final emplacement. *Journal of Structural Geology*, **27**, 805–822.

Chapitre 5 : le magmatisme des Vosges septentrionales : Pétrologie - Géochimie - Géochronologie

Dans ce chapitre, nous traitons les évènements magmatiques affectant les Vosges septentrionales : le volcanisme du Dévonien supérieur du Massif de Schirmeck et du Massif de Rabodeau, le plutonisme du Champ du Feu et le volcanisme permien du Nideck. L'objectif est de caractériser par des analyses pétrologiques, géochimiques, isotopiques et géochronologiques ces successions d'évènements dans le temps dans un espace restreint afin de proposer un modèle d'évolution et de développement de la croûte continentale du massif vosgien septentrional.

L'étude s'appuie sur un échantillonnage effectué sur le terrain de roches des différentes unités définies par les géologues vosgiens ainsi que sur les données préexistantes. J'ai effectué la préparation des échantillons pour les analyses. Les poudres ont été envoyées à ACME Labs (Vancouver, Canada) pour les analyses en éléments majeurs et traces et au BRGM pour les analyses isotopiques (Catherine Guerrot). Les nouvelles datations U-Pb ont été effectuées par Alain Cocherie (BRGM).

L'ensemble de ces données nous a permis de distinguer plusieurs évènements magmatiques et de déterminer les sources impliquées et les contextes géodynamiques associés à ces différents évènements évoluant des tholéiites continentales (Massif de Schirmeck-Rabodeau) vers un volcanisme et plutonisme calco-alcalin (Bande médiane et partie sud du Champ du Feu) suivi par un plutonisme dit calco-alcalin riche en potassium (partie nord du Champ du Feu) suivi par un magmatisme Mg-K (granite de Senones, Natzwiller et Andlau) et enfin par un volcanisme et plutonisme de type-S (granite de Kagenfels et massif du Nideck). Nous montrons que le processus principal de cette évolution restreinte dans l'espace est la progression de la croûte continentale rhénohercynienne subduite sous la croûte continentale Saxothuringienne.

Ce chapitre de thèse sera soumis dans la revue « *International Journal of Earth Sciences* » ou dans la revue « *Société Géologique de France* » pour une publication spéciale à l'issu du congrès sur la Chaine Varisque à Sassari (Sardaigne).

1. Introduction

During orogenic processes, the continental crust commonly experiences significant partial melting and intense magmatic activity at depth. This is revealed by the development of large anatectic domains deep within recent mountain belts (e.g., Owens & Zandt, 1997; Oncken et al, 2003) or by the occurrence of vast plutonic complexes in exposed parts of ancient orogens. Repeated thermal pulses can even cause multiple anatectic events that will result in the juxtaposition of magmatic suites of contrasting geochemical signatures, reflecting their variable sources and conditions of melting. This clearly indicates the persistence of a relatively hot thermal regime, melt mobility (e.g. Sawyer, 1994) and magma emplacement at different levels of the crust. Nevertheless, key questions arise regarding (1) the chronology of intrusions, (2) the origin of magmas and (3) the nature of heat sources. In deeply evoded older orogens where crosscutting relationships among magmatic bodies can be observed, these major issues need to be addressed using a combination of field, geochronological, petrological and geochemical data.

Across Europe, the outcropping remnants of the Variscan orogenic belt commonly host abundant Early Carboniferous magmatic rocks (Didier, 1991; Sabatier, 1991; Holub et al., 1995; Finger et al., 1997; Schaltegger, 1997). Among them, the Palaeozoic basement of the Vosges Mountains (NE France) is dominantly composed of granitoids which can be observed in the Saxothuringian domain to the North as well as in the Moldanubian domain to the South (Kossmat, 1927). These two domains are separated by the Lalaye-Lubine line thought to have acted during Late Carboniferous as a dextral shear zone (Fluck, 1980; Fluck et al., 1989; Wickert & Eisbacher, 1988). The present study will mainly focus on magmatic units that can be found in the Saxothuringian part. The aims are to characterize each magmatic pulse where new field, petrographical, geochemical and geochronological investigations, associated with previous results (von Eller, 1964, 1970; de la Roche & von Eller, 1969; Geldron, 1986; Deschamps, 1995; Altherr et al., 2000; Edel et al., submitted), and to propose a geodynamic scenario for the evolution and the development of the Northern Vosges continental crust.

2. Geological setting

The Northern Vosges Mts are characterized, from North to South by: i) a Devonian to Early Carboniferous volcanic and sedimentary formation (*The Bruche Unit*; Juteau, 1971; Wickert & Eisbacher, 1988; Rizki & Baroz, 1988) and ii) an Ordovician to Silurian NE-SW trending belt of low-grade metamorphic metapelites rests (*The Steige Unit*) deposited in a shallow marine environment (Tobschall, 1974). The laster unit unconformably upon the Late Cambrian to Early Ordovician greenschist-facies metapelitic and metapsammitic schists and quartzite (*The Villé Unit*; Doubinger & von Eller, 1963a; Ross, 1964; Reitz & Wickert, 1989). All these formations constituted the upper part of the basement which was intruded by the Variscan magmatic units.

The range of compositions and magmatic affinities of the Northern Vosges magmatism are very varied: they change from basic to acidic rocks, and from tholeiitic, to calc-alkaline, to high-K and to ultrapotassic.

The first and oldest magmatic episode occurred from Devonian to Visean (Ikenne, 1986) according to paleontological data (Benecke & Bücking, 1898) on interbedded sediments of the Bruche unit. This magmatic unit is exposed in two massifs: Schirmeck (48 km²) and Rabodeau (21 km²) (Fig.1). Rocks were previously characterized, using major-element geochemistry, as the products of a tholeiitic magmatism which "evolved" to a calc-alkaline magmatism in the Rabodeau Massif (Rizki and Baroz, 1988). This magmatic "evolution" has been considered to characterize a convergent domain (Ikenne et al., 1991).

The second important igneous association is exposed in the so-called "*Champ du Feu Massif*" (von Eller, 1964, 1965, 1968, 1969; von Eller et al., 1970, 1971a,b; de Béthune et al.,1968; de la Roche and von Eller, 1969; Hahn-Weinheimer et al., 1971; Leterrier, 1978). Altherr et al. (2000) divided the "*Champ du Feu Massif*", combining crosscutting field relations, geochronology, mineralogical and geochemical analyses, into five intrusive "suites". As "suites" could refer to series of cogenetic batches, we will refer hereafter to five intrusive groups (Fig.1).

i) Early mafic magmas (diorite of Neuntelstein & Muckenbach and volcanic rocks of the "*Bande Médiane*";

ii) Granodioritic units of Hohwald;

iii) "Older Granite" "I-type" intrusion of Northern CDF (Belmont granite);

iv) "Younger Granites": Andlau, Natzwiller and Senones;

v) Peraluminous alkalic "S-type" granites (Kagenfels, Kreuzweg, Grendelbruch).

Figure 1: (a) Geological map of the plutonic Champ du Feu massif. (b) geological section A-B (after Edel et al. submitted). Figure next page.

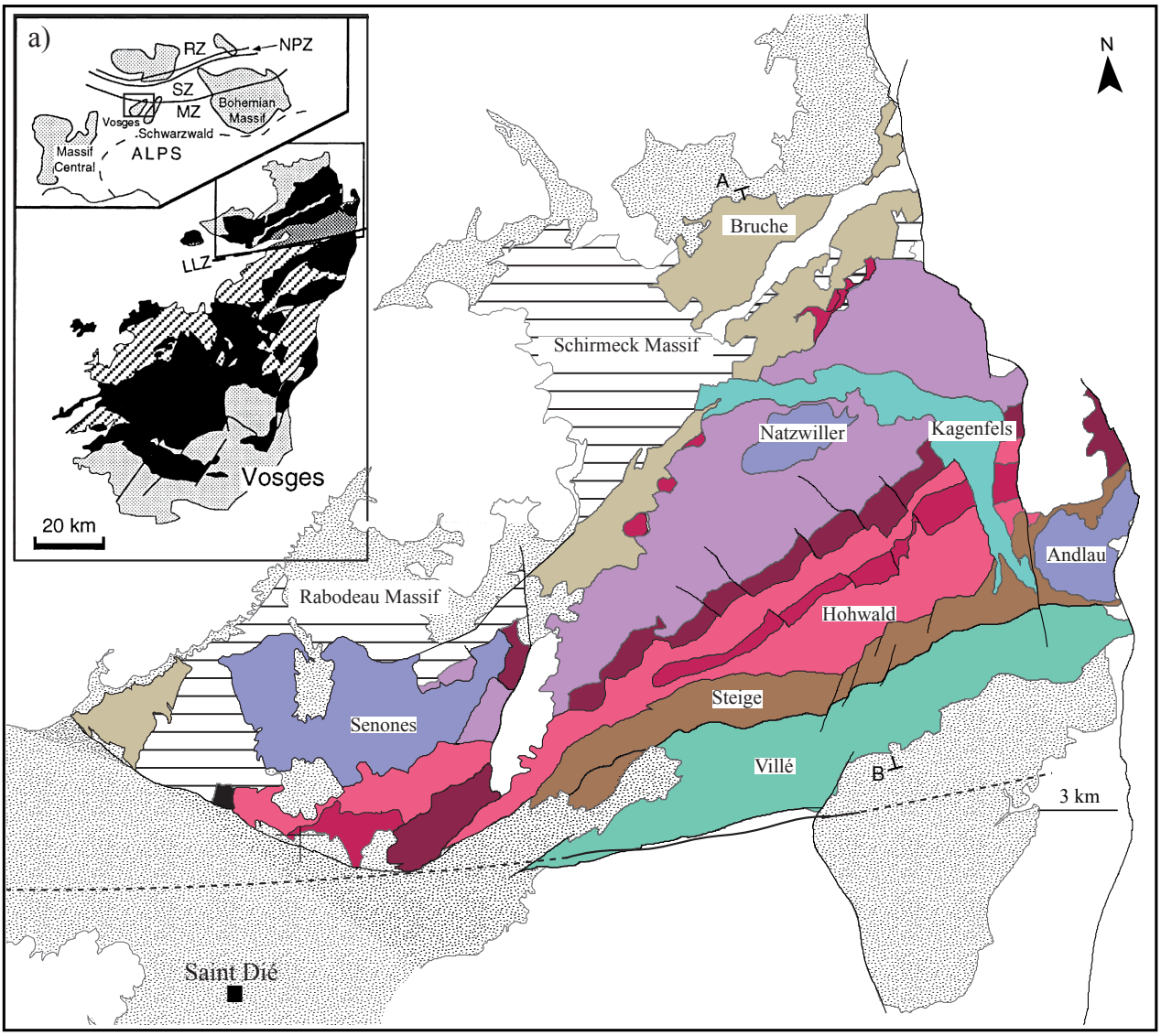
a)
RZ
NPZ
SZ
MZ
Bohemian Massif
Vosges
Schwarzwald
Massif Central
ALPS
LLZ
Vosges
20 km
N
A
B
Bruche
Schirmeck Massif
Natzwiller
Kagenfels
Andlau
Rabodeau Massif
Hohwald
Steige
Senones
Villé
3 km
Saint Dié
Permian
Villé unit
Steige unit
Bruche unit
Devonian volcanic
Volcanic of the «Bande Mediane»
Diorite
Granodiorite
Older granite
Younger granite
S-type granite

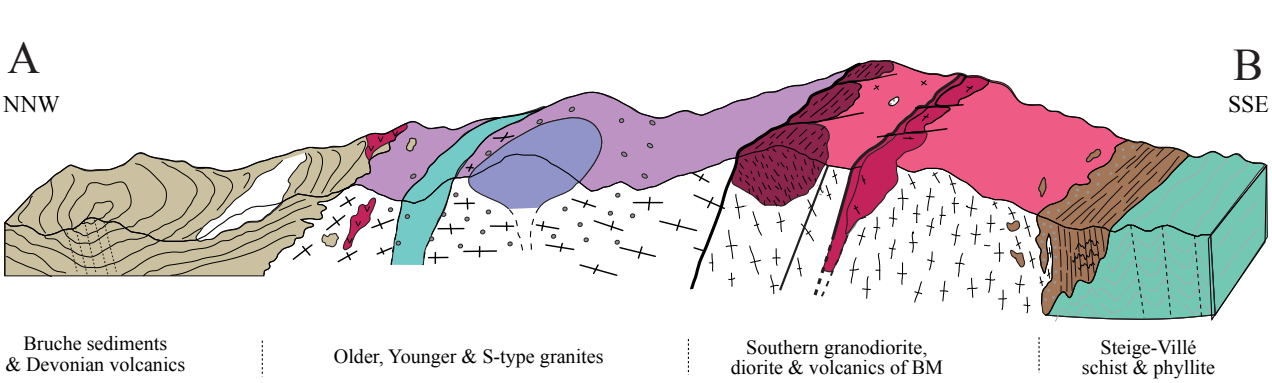
b)
A
NNW
B
SSE
Bruche sediments & Devonian volcanics
Older, Younger & S-type granites
Southern granodiorite, diorite & volcanics of BM
Steige-Villé schist & phyllite

Fields observations reveal that all these intrusive groups are organized according various shaped- and sized- extrusions/intrusions e.g respectively: NE-SW elongated bodies for the volcanic rocks of the "*Bande Médiane*", diorite, granodiorite and Older Granite to roughly ellipsoid for Younger Granites which could result from tectonic and erosion interaction.

Magmatic events in the Northern part of the Vosges Mts ended with emplacement of Permian volcanic in the Nideck-Donon Massif and the Villé Basin (Carasco, 1987). Laubacher & von Eller (1966) proposed that this volcanism was related to the emplacement of Kagenfels leucogranite and was cogenetic with the subvolcanic facies at the margin of this plutonic body.

A diagram displaying their relative chronology of emplacement, based on field evidence, has been established for the main magmatic units (Fig.2).

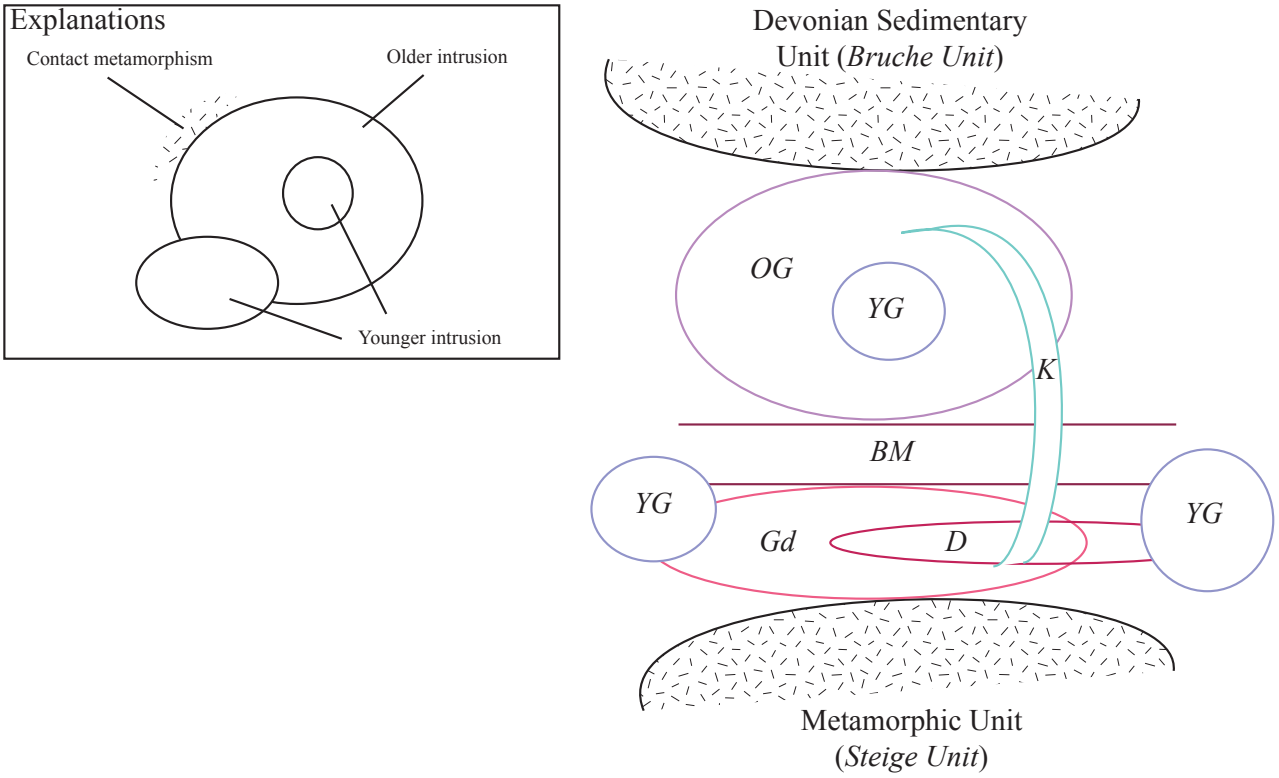

Figure 2: Diagrammatic representation of field relationship of the different intrusions of the Northern Vosges Mts. BM= «Bande Médiane»; D= Diorite; Gd= Granodiorite; OG= Older Granite (Belmont granite); YG= Younger Granite; K= Kagenfels granite.

3. Geochronology

3.1. Calc-Alkaline suite

According to Altherr et al. (2000): (i) the volcanic rocks of the "*Bande Médiane*" and diorite, (ii) granodiorite and (iii) Older Granite are members of a calc-alkaline suite. We will revisit hereafter the geochemical characteristics of the magmatic products of this group in order to better examine if they define a real suite and before to conclude will write suite between comas.

i) Volcanic rocks (ignimbrite) were dated at 334 ± 4 Ma (U-Pb on zircon; Edel et al., submitted) with Neoproterozoic and Lower Cambrian inheritance (530 & 620 Ma). The cooling of dioritic intrusion falls between 331 Ma and 326 Ma (K-Ar & Ar-Ar on hornblende; Edel et al., 1986; Boutin et al., 1995 and Altherr et al., 2000).

ii) Conventional K-Ar and Ar-Ar on hornblende ages of 325 and 330 Ma were reported by Boutin et al. (1995) and Altherr et al. (2000) for the Hohwald granodioritic intrusion. U-Pb on zircon dating of the Hohwald granodiorite (Edel et al., submitted) gave an age of 329 ± 2Ma (with inherited age of Lower Carboniferous at 347 ± 3 Ma).

iii) Older Granite (Belmont granite) has been dated at 329 ± 4 Ma (K-Ar & Ar-Ar on hornblende; Altherr et al., 2000) and 335 ± 4 Ma (K-Ar on biotite; Altherr et al., 2000).

3.2. Younger Granites

Three plutons define the Younger Granites Group, from West to East:

- the "*Senones granite*" was dated by conventional K-Ar and Ar-Ar on hornblende at 325 ± 4 Ma and 328 ± 4 Ma respectively (Altherr et al., 2000);

- the "*Natzwiller granite*" was dated by K-Ar and Rb–Sr methods on biotite and muscovite at 332 and 338 Ma (recalculated with new constants after Faul & Jäger, 1963). Altherr et al. (2000) also obtained, by K-Ar method, a comparable age on biotite at 330 ± 4 Ma but a relatively old conventional K-Ar age on biotite at 351 ± 12 Ma was reported by Edel et al. (1986) and Boutin et al., (1995).

- the "*Andlau granite"* for which a conventional K-Ar on biotite age of 328 ± 4 Ma was reported by Altherr et al. (2000). All these ages, taking into account the uncertainties, roughly fit with the relative chronology deduced from field data.

3.3. S-Type Granite

Obvious, field evidences led first authors like Laubacher & von Eller (1966) or von Eller et al., (1970) to propose that the "*Kagenfels*" subvolcanic-leucogranite was the youngest intrusion of the Northern Vosges area. However, geochronological measurements have given ages at 331 ± 5 Ma (K-Ar, Ar-Ar on biotite and Pb-Pb evaporation on zircon; Hess et al., 1995), moreover an Ar-Ar on biotite age of 329 ± 2 Ma was also published (Boutin et al., 1995). These are almost identical to ages for the other intrusions even though the Kagenfels granite crosscut them.

3.4. Permian volcanism

Permian volcanism of the Nideck-Donon Massif was dated at 299 ± 7 Ma (Rb-Sr on whole rock; Hess & Lippolt, 1986). This age is in agreement with field observations as the volcanics are interbedded with Permian detrital sediments (Laubacher & von Eller, 1966).

4. Analytical techniques

4.1. Mineral chemistry

Mineral compositions for rocks of the individual magmatic associations were determined at BRGM Orléans using a CAMECA SX 50 electron microprobe equipped with five wavelength-dispersive spectrometers (two PET, two TAP and one LIF), and under 15 kV accelerating voltage and 12 nA beam current (Tables of mineral chemistry are in "*Annexe: Northern Vosges*").

4.2. U-Pb Laser-Neptune

Due to the high probability of heterogeneous U-enriched phases suitable for geochronology, in situ technique were selected. Zircon grains were dated using laser ablation coupled with MC-ICP-MS at BRGM Orléans (Cocherie A. & Robert M., 2008). Chemical dating was applied for monazite and xenotime (EPMA, electron probe microanalysis) accordingly to the method of data reduction (Cocherie A. & Albarède F., 2001; Cocherie A. & Legendre O., 2007). Data error ellipses for U-Pb zircon analyses were drawn at the 1σ level in order to facilitate reading of the geochronological diagrams, but all calculations were done at the 2σ level using Isoplot (Ludwig K.R., 2003). Tables of zircon analyses are in "*Annexe: Northern Vosges*").

4.3. Major and trace elements

About 30 samples were collected according to a grid allowing a maximal spacing of ~4 km between localities. The sample size (5 to 10 kg of fresh material) also took into account the texture and the presence of K-feldspar phenocrysts. The samples were crushed and later ground in agate mills to get fine powder. Major- and trace-element analyses were performed at AcmeLabs™, Vancouver,

by ICP emission spectrometry following a lithium metaborate/tetraborate fusion and dilute nitric digestion of a 0.2 g sample. REE and refractory elements were determined at the same laboratory by ICP mass spectrometry. This database is supplemented by previously published analyses of Northern Vosges granitoids (von Eller, 1964, 1970; La Roche & von Eller, 1969; Geldron, 1986; Deschamps, 1995; Altherr et al., 2000). Representative analyses (Table of major and trace elements analyses is in "*Annexe: Northern Vosges*") are plotted using *GCDkit* software (Janoušek et al., 2003).

4.4. Nd−Sr isotopic compositions

Sr and Nd isotopic compositions of 2 samples of volcanic rocks (samples VON1 from Rabodeau Massif & VON11 from Schirmeck Massif) were determined at BRGM Orléans. The external reproducibility is given by the results of repeated analyses of the La Jolla ($^{143}Nd/^{144}Nd$=0.511878±13 (2σ) n=13) and NBS 987 ($^{87}Sr/^{86}Sr$=0.710245±12 (2σ) n=12) isotopic standards.

5. Petrology

5.1. Devonian volcanism

Composition of Devonian volcanic rocks ranges from basalt to trondhjemite (Fig.3) formed by K-feldspar, idiomorphic plagioclase and quartz in a fine-grained matrix for all volcanic rocks with some altered phenocrysts (plagioclase and K-feldspar) for trondjemite.

5.2. Calc-Alkaline "suite"

The composition of the calc-alkaline magmatic rocks varies from basalt to rhyodacite for volcanic rocks of the "*Bande Mediane*", and from fine- to medium-grained diorite, through medium-grained granodiorite to porphyritic monzogranite in plutonic members (Older Granite, Altherr et al., 2000) (Fig.3). The calc-alkaline plutonic rocks are characterized by idiomorphic K-feldspar and plagioclase, quartz, green Mg-amphibole and light brown biotite; accessory minerals being apatite, zircon and Ti-oxides. Ca content in plagioclase decreases from diorite (An_{48-56}) to granodiorite (An_{35-45}) to monzogranite where plagioclase crystals are discontinuously zoned (core An_{40-30} and rim An_{10}). Mg-amphibole composition ranges from tschermakite to magnesio-hornblende (Fig.4b). Amphibole is rich in Al_{tot} (>1.2%) and Mg content increases according to SiO_2. X_{Mg} in light brown biotite decreases from 0.55 to 0.3, Fe/Mg ratio increases from 1.5 to 3.5 with rising SiO_2 content in host rocks. On the other hand, Ti content remains fairly constant between 0.20 and 0.25 a.p.f.u.. In AFM diagram (Fig.4a), chemical composition of biotite displays a linear trend with increasing Al_2O_3 from diorite to monzogranite. These observations suggest that the evolution trend of calc-alkaline rocks was dominated by fractional crystallisation. Moreover, Altherr et al. (2000) using the Al-in-hornblende barometer (Schmidt, 1992) concluded that diorite intruded at about 10 km and depth of intrusion became less from diorite through granodiorite to monzogranite..

5.3. Younger Granites

Characteristic rock type is a porphyritic quartz monzonite-monzogranite (Fig.3) with large sized (up to 50 mm) pinkish K-feldspar, idiomorphic plagioclase, brown biotite, ± Mg green-amphibole, rounded quartz and Ti-oxide; apatite, zircon and monazite are accessory phases. Plagioclase is weakly zoned and composition ranges from An_{30} to An_5 with increasing host-rock silica content. Green Mg-amphibole shows a strong pleochroism and is poor in Al_{tot} (<1 %). Composition ranges from magnesiohornblende to actinolite (Fig.4b). Chemical composition of brown biotite is mostly constant with X_{Mg} (0.55-0.60) regardless the host-rock SiO_2 contents and plot clusters in a narrow area of the AFM plot (Fig.4a). Fe/Mg ratio of the biotite is nearly constant (0.9-1.2) and Ti content (0.24-0.30 a.p.f.u.) weakly decreases with Si (2.8-3.0 a.p.f.u.). This suggests a slow decrease in the temperature during crystallization (Robert, 1976).

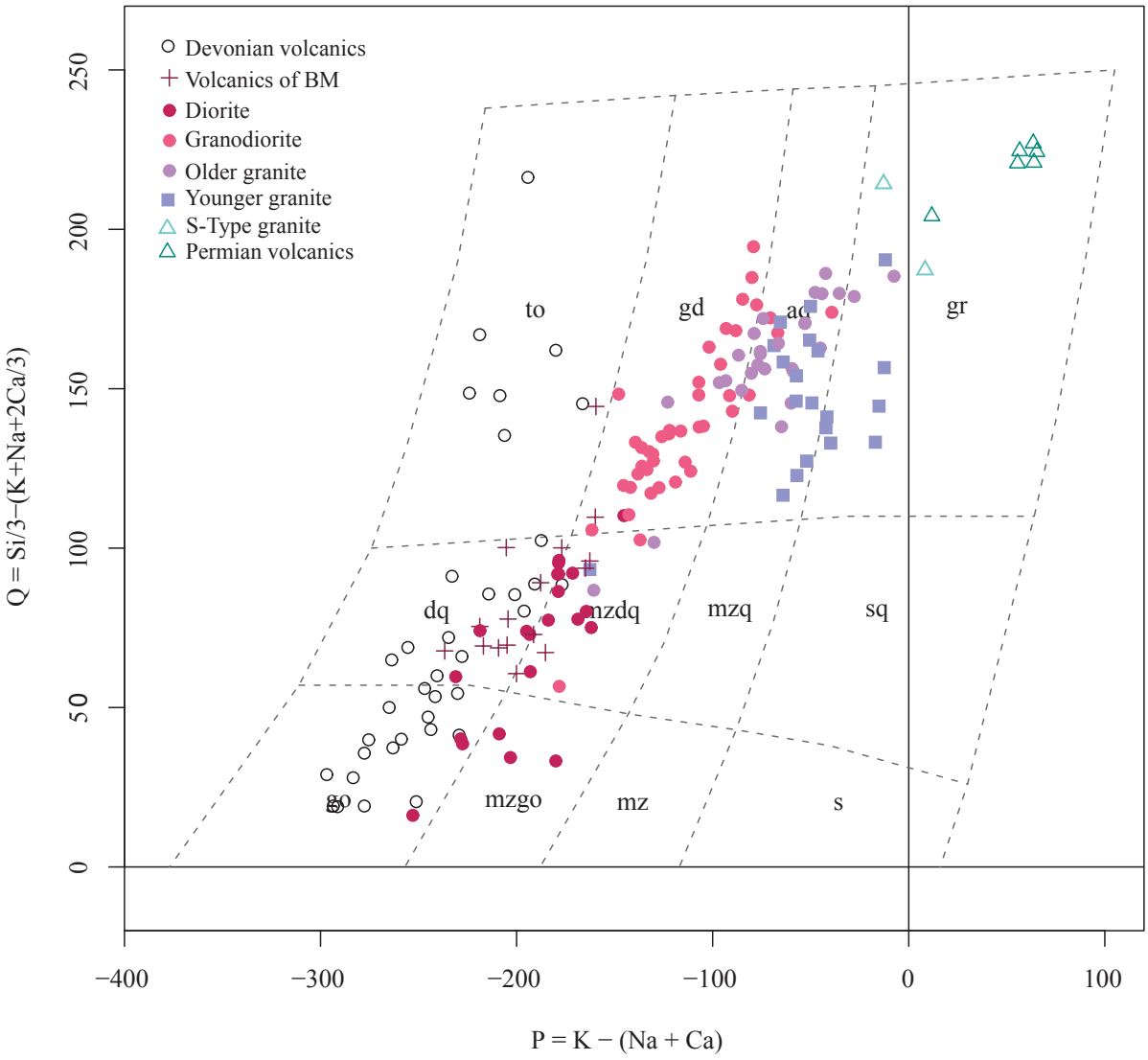

Figure 3: Multicationic P-Q plot (Debon & Le Fort, 1983) for granitoids of Northern Vosges Mts; P represents the proportion of K-feldspar to plagioclase and Q the quartz content.

5.4. S-type granite

In a previous work on Kagenfels granite (Fig.3), Hahn-Weinheimer et al. (1971) have distinguished four different rock types: 1) a fine-grained porphyric type at northern borders; 2) a medium-grained granitic type occurring in the centre; 3) a rhyolitic type at the southern part and 4) a granophyric type occurring at the transition between rhyolitic and granitic types. All these rock types are characterized by quartz, plagioclase, K-feldspar and a few biotite and muscovite, zircon and apatite remaining present as accessory phases.

5.5. Permian volcanism

Permian volcanic rocks are fine-grained rhyolite (Fig.3) composed of K-feldspar, idiomorphic plagioclase and quartz in a fine-grained matrix.

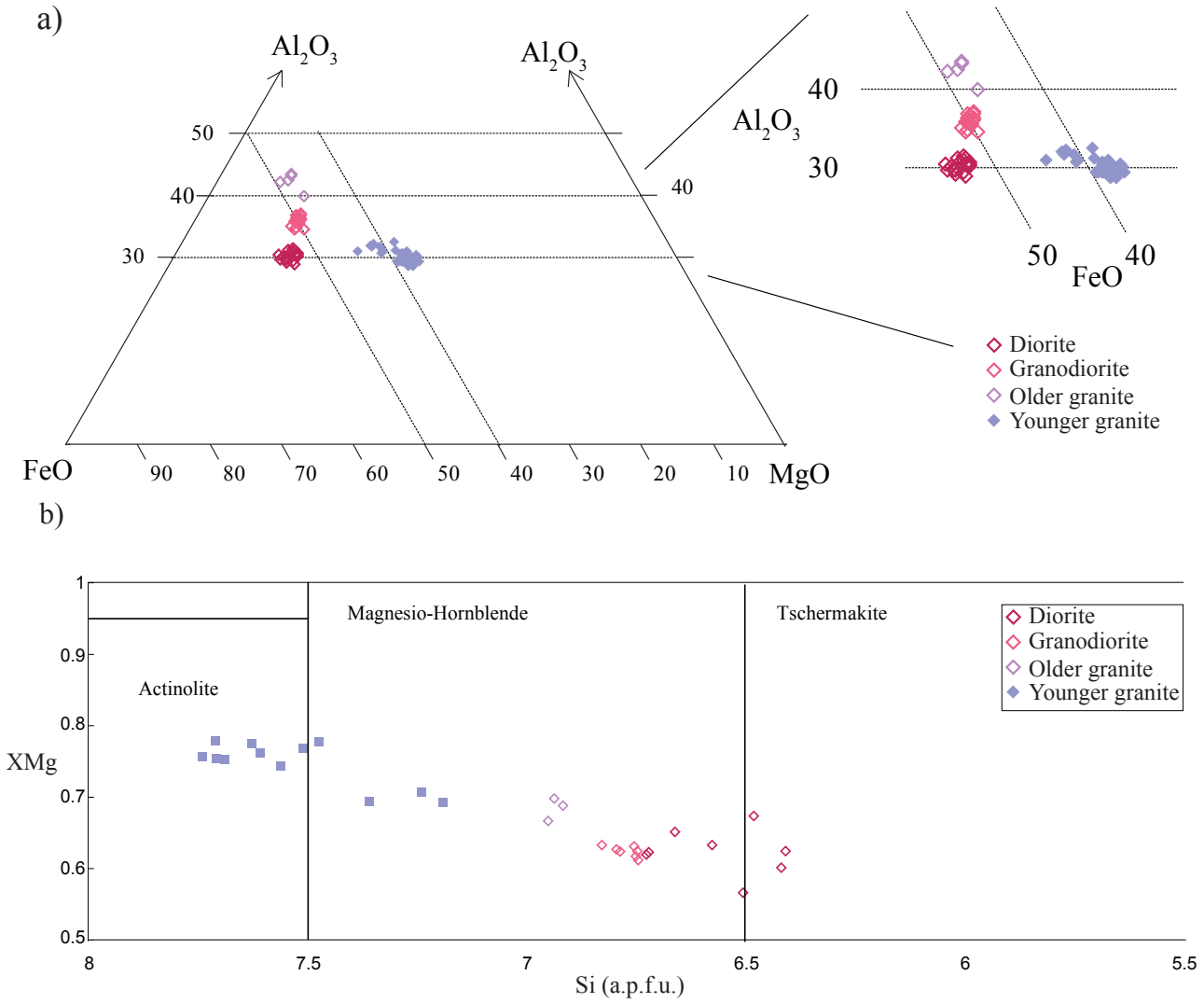

Figure 4: (a) Biotite compositions from granitoids of Northern Vosges Mts in AFM diagram. (b) Amphibole compositions of calc-alkaline "suite" and "younger granite" in XMg vs Si (a.p.f.u.) diagram (after Leake et al., 1997).

6. New geochronological data

In order to better constrain dating of successive magmatic events in the Northern Vosges, two key samples were chosen among plutonic massifs whose relative chronology was clear based on field observations. The emplacement of the first post-tectonic intrusion was dated by the sample SL3 from the Belmont Granite (Older granite) and the age of "Younger Granites" by the sample EV 159 of the Natzwiller Granite.

6.1. The Belmont granite (SL3)

Zircons of this rock are homogeneous and large (~ 500 μm). They are generally clear, but contain numerous inclusions, cracks and fractures. There is a fairly wide dispersion into Pupin (1980)'s morphologic diagram where the majority of the population plots around high temperature S17-S18 types, some grains were identified as P1 characteristic of zircons crystallized at low temperature.

The direct plot of the 22 analyses onto Tera-Wasserburg diagram reveals a dispersion of points between 380 and 300 Ma. The analysis 20.1 has to be discarded because it contains a significant content in common Pb and, moreover, a strong uncertainty. The statistical distribution of plots highlights inherited ages at 340, 360 and 380 Ma. The 18 remaining analyses are arranged according to 2 groups. A core group of 12 homogeneous analyses plot at 319 Ma (Fig.5a) whereas further 6 analyses would be shifted (not represented in Fig.5a) towards younger ages. This latter group is interpreted as the result of radiogenic Pb loss. The straight line of mixing passing through the composition of common Pb at 320 Ma and the 12 for common Pb uncorrected analyses is drawn on the Tera-Wasserburg's diagram (Fig.5a). Its intersection with the Concordia provides the age of crystallization of zircons at 318 ± 3 Ma (2(σ). The MSWD = 2.3 is compatible with a single population. This datum is interpreted as the emplacement age of the Belmont granite, being significantly younger than dioritic and granodioritic intrusion, and fits with field evidence.

6.2. The Natzwiller granite (EV159)

Zircons of this granite are numerous and well crystallized. Their size ranges between 200 and 500 μm. They frequently display micro-chanels and are micro-cracked. Plotted onto the Pupin (1980)'s diagram, 60% of the population is clustered around the S25-S23 types characteristic of zircons crystallized at high temperature.

Eighteen analyses were performed on 17 different grains. Eight aof them were excluded in the calculation of the average $^{206}Pb/^{238}U$ age because of a slight loss Pb. The 10 remaining analyses give an age of 312 ± 2 Ma (Fig.5b).

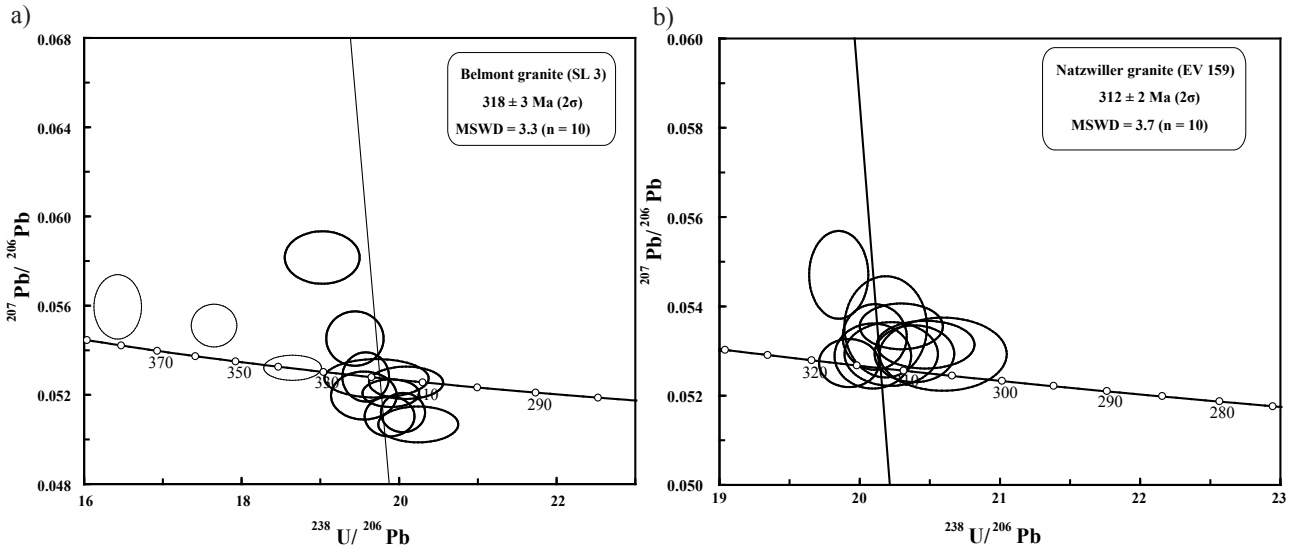

Figure 5: Tera-Wasserburg diagrams with U-Pb radiometric datations (a) of Belmont Granite (SL3; "older granite") and (b) of the Natzwiller granite (EV159; "younger granite"). Data-point error ellipses are 1σ.

These geochronological results are in full agreement with field data and the results of Edel et al. (submitted) and provide a realistic timing of emplacement of the main magmatic events, milestones of the Hercynian geodynamics.

In summary, the activity of the igneous arc that postdated the subduction is dated by volcanic of "*Bande Mediane*" at 334 ± 4 Ma (Edel et al., submitted); the age of early post collision magmatism (granodiorite of Hohwald; Edel et al., submitted) at 329 ± 2 Ma; the first post-tectonic intrusion (older granite) is dated at 318 ± 3 Ma and "Younger Granites" are dated at 312 ± 2 Ma. Following these results and field evidences the ^{207}Pb-^{206}Pb evaporation age on zircon for the Kagenfels granite of 331 ± 5 Ma (Hess et al., 1995) is clearly not the emplacement age but that of inherited zircons. Ar-Ar and K-Ar systems have to be reassessed to better understand the bias providing the too 'old' ages. It could be the same mechanism that causes the 'old' K-Ar age on biotite (351 ± 12 Ma) for the Natzwiller granite (Edel et al., 1986 and Boutin et al., 1995) dated (this study) by U-Pb on zircon at 312 ± 2 Ma.

7. Geochemistry

7.1. The Devonian volcanism

7.1.1 Major elements

Devonian volcanic products are composed of metaluminous rocks (A/CNK = 0.6 – 1.0). Plots of CaO, MgO and total alkali vs. SiO_2 are represented in Fig.6. Volcanic-rock analyses define linear trends that display decreasing of MgO (9-0.1 wt %) and CaO (12-0.25 wt %) (this is also the case for FeO_t, TiO_2 and P_2O_5) and increasing of total alkali (4-9 wt %) according to SiO_2.

7.1.2 Trace elements

Among trace-elements, volcanic rocks are characterized by low contents of Cr (27-20 ppm), Ni (< 25 ppm), Ti (< 2 wt %), LILE (Large Ion Lithophile Elements; Ba < 500 ppm, Rb < 100 ppm) and incompatible elements (U < 4 ppm and Th < 20 ppm) which remain roughly constant according to increase of SiO_2.

Primitive mantle-normalized multi-elementary plots of samples are given in Fig.7b. Multi-element patterns are characterized by a weak negative slope with depletion in Ba, Nb, Ti and P and a weak enrichment in U, Th and K.

Chondrite-normalized REE patterns (Fig.7a) show a weak fractionation of LREE (Light Rare Earth Elements) with $2 < Ce_N/Yb_N < 7$ and are characterized by a sizeable negative Eu anomaly ($Eu/Eu^* = 0.60 – 0.65$). The total REE contents of 120 to 150 ppm remain nearly constant even with increasing host-rock silica content.

7.1.3 Isotopic composition

The results of Sr-Nd whole-rock analyses are listed in Table 1. Initial ratios have been calculated using a mean age of 330 Ma according to geochronological investigations. These results were plotted onto ($^{87}Sr/^{86}Sr$) versus ε_{Nd} diagram (Fig.12). The isotopic composition of volcanic rocks are ($^{87}Sr/^{86}Sr$) =0.704 to 0.706 and ε_{Nd} = +5 to +3 and are similar to isotopic values of continental tholeiite (Holm, 1985; Carlson 1984).

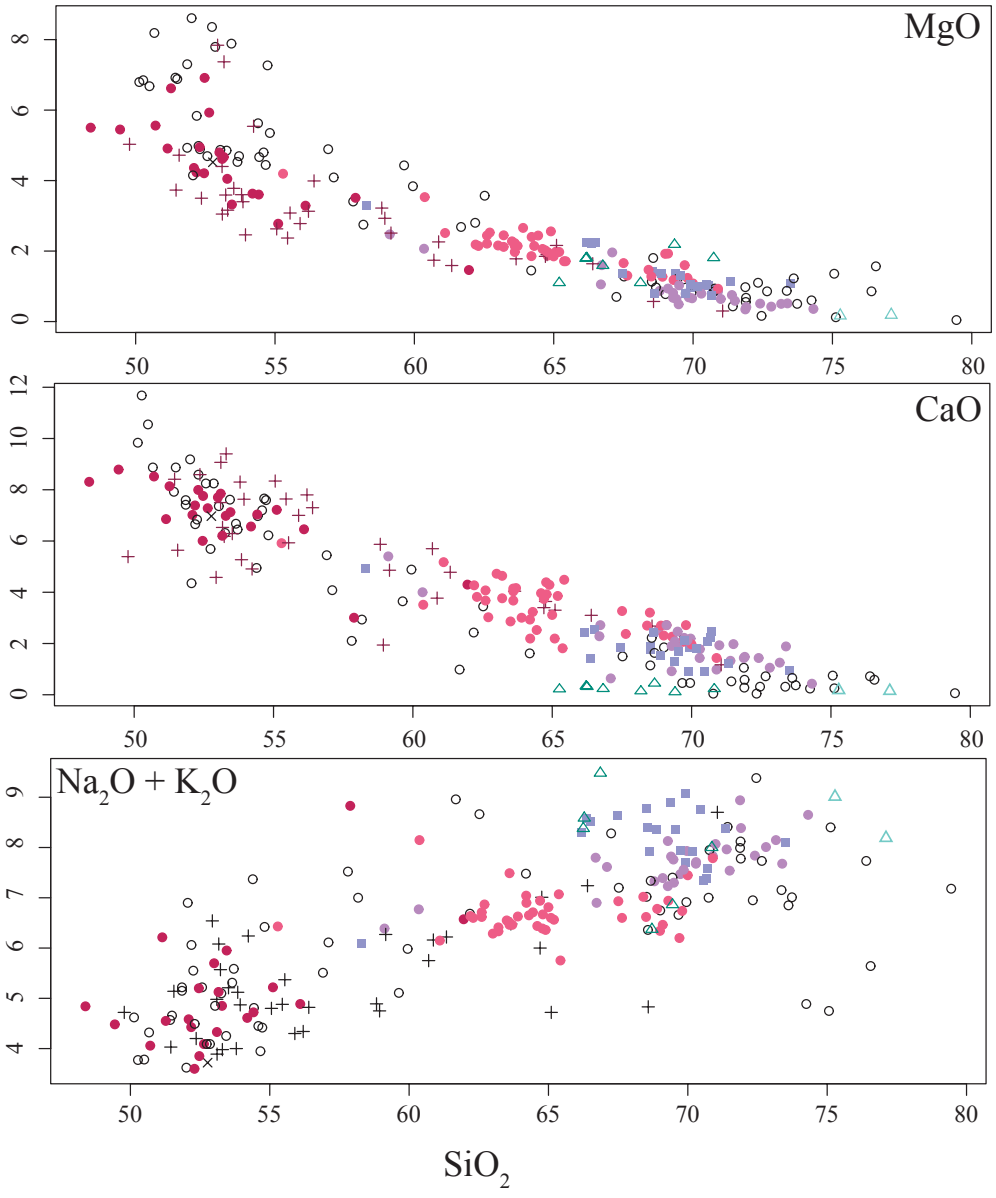

Figure 6: Variation diagram of CaO, MgO and total alkali (wt %) vs. SiO2 (wt %) for whole-rock samples from Devonian volcanics, Calc-alkaline "suite", Younger granite, S-type granite and Permian volcanics. Same legend as Fig.3.

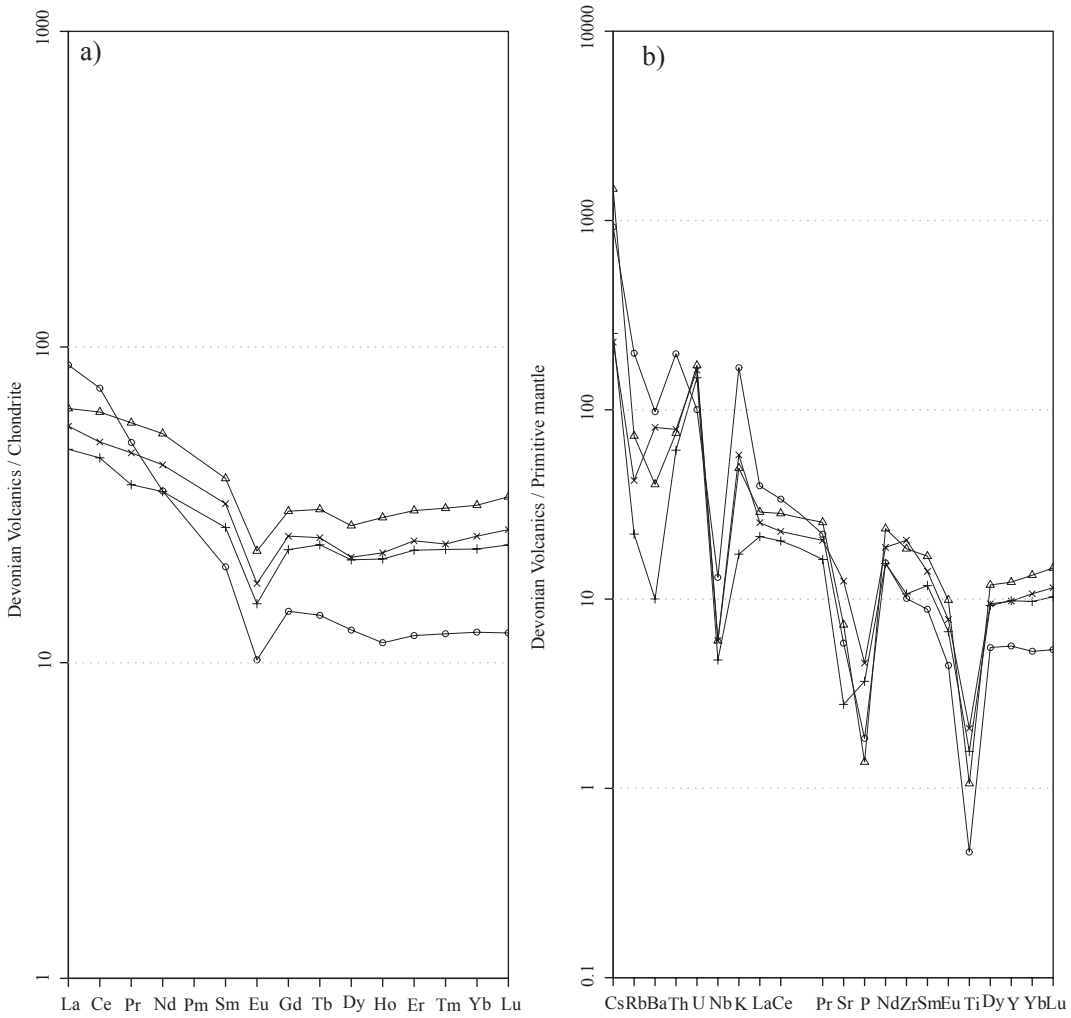

Figure 7: (a) Chondrite-normalized REE diagram for the Devonian volcanics; normalizing values from Boynton (1984). (b) Primitive mantle-normalized spider plots for the Devonian volcanics (after Sun & McDonough, 1989).

7.2. Calc-Alkaline "suite"

7.2.1 Major elements

Calc-alkline "suite" is mostly metaluminous with minor peraluminous compositions (A/CNK= 0.7 - 1.3). Plots of CaO, MgO and total alkali vs. SiO_2 are reported on Fig.6. Calc-alkaline "suite" shows linear trends that display decreasing of MgO (6 - 0.5 wt %), CaO (9 -0.5 wt %) (also the case for FeO_t (10 – 2 wt %) and TiO_2 (< 1 wt %)) and increasing of total alkali (4-8 wt %) according to SiO_2 increase. P_2O_5 content increases from 0.15 to 0.3 wt% according to SiO_2 content up to 55 wt% and then decreases until 0.05 wt% when SiO_2 content is over 55 wt%. According to Peacock (1931)'s discriminant diagram (Fig.8a), this "suite" conforms to a calc-alkalic trend.

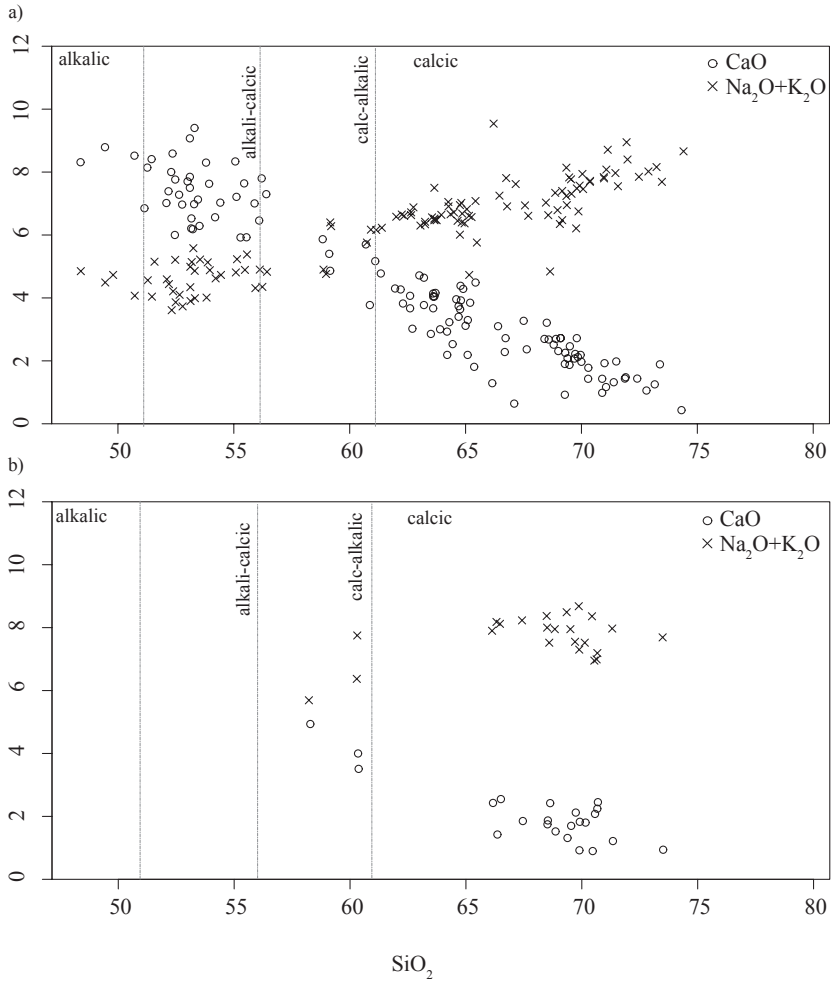

Figure 8: Variations of CaO wt% and $Na_2O + K_2O$ vs. SiO_2 wt% for (a) Calc-alkaline "suite" and (b) Younger granite. Original named fields within SiO_2 wt% ranges are Peacock (1931) and are applied to suites whose oxide variation trends intersect within a given field.

7.2.2 Trace elements

Calc-alkaline "suite" is characterized by low content of Cr (~20 ppm) and Ni (<10 ppm). The degree of LILE enrichment (Ba = 400-1000ppm; Rb = 50-200ppm) and incompatible elements (U = 2-5ppm and Th = 5-18ppm) increase with increasing SiO_2.

Primitive mantle-normalized plots (Fig.9b) exhibit enrichment in LILE (Cs, Rb, Ba) and depletion in Nb, Ta, Sr, Ti and P. The depletion in Sr, P and Ti is more pronounced from volcanic to monzogranite whereas depletion in Nb and Ta is less pronounced. Only monzogranitic rocks display weak positive U and Th anomalies. Negative Nb, Ta, Sr and Ti anomalies are generally considered to reveal genesis of the host rocks by subduction-related processes (Thompson et al., 1984).

Chondrite-normalized REE patterns (Fig.9a) show enrichment in LREE which increases with rising silica (Ce_N/Yb_N ~ 4 for volcanic rocks and diorite and ~ 9 for monzogranite). Rocks of the calc-alkaline "suite" are also characterized by a weak negative Eu anomaly which remains roughly constant (Eu/Eu* = 0.8) but then increases with silica content for monzogranite (Eu/Eu* = 0.75-0.4). Total content of REE (100-150ppm) increases also with whole-rock SiO_2.

7.2.3 Isotopic composition

Isotopic data of calc-alkaline "suite" has been previously analysed by Altherr et al. (2000) and were recalculated in this study at 330 Ma (Table 1). Initial ε_{Nd} values for diorite and granodiorite are slightly positive to negative (+0.4 to -3) and $^{87}Sr/^{86}Sr$ ratios are comprised between 0.705 and 0.706 and remain close to isotopic values of Bulk Earth for diorite and granodiorite (Fig.12). Monzogranite shows initial ε_{Nd} values about -2.5 and $^{87}Sr/^{86}Sr$ ratios about 0.706.

7.3. Younger Granites

7.3.1 Major elements

Younger Granites are mostly metaluminous, A/CNK ratio varies between 0.9 and 1.1. Plots of MgO, CaO and total alkali vs. SiO_2 are reported on Fig.6. Younger Granites are characterized by linear trends that display decreasing of MgO (4-1 wt %), CaO (5-1 wt %), FeO_t (7-2 wt %), TiO_2 (1-0.4 wt %) and P_2O_5 (0.3-0.15 wt %) according to SiO_2. Total alkali remains fairly constant at 7-9 wt% for any SiO_2 content. According to Peacock's discriminant diagram (Fig.8b), this association does not conform to calc-alkaline suite.

7.3.2 Trace elements

In contrast to calc-alkaline "suite", Younger Granites are characterized by high content of Cr (>30 ppm) and Ni (>10 ppm) as well as many incompatible elements and LILE (Ba > 500 ppm, Rb > 200 ppm, U > 4 ppm, Th >20 ppm).

Primitive mantle normalized multi-elementary plots of Younger Granites (Fig.10b) show strong enrichment in LILE (Cs, Rb, Ba) as well as high contents of U, Th and K. All patterns displays weak negative Nb, Ta, Sr and Ti anomalies and depletion in P. As for calc-alkaline "suite", these anomalies reveal that the genesis of these rocks underwent in subduction-related processes (Thompson et al., 1984).

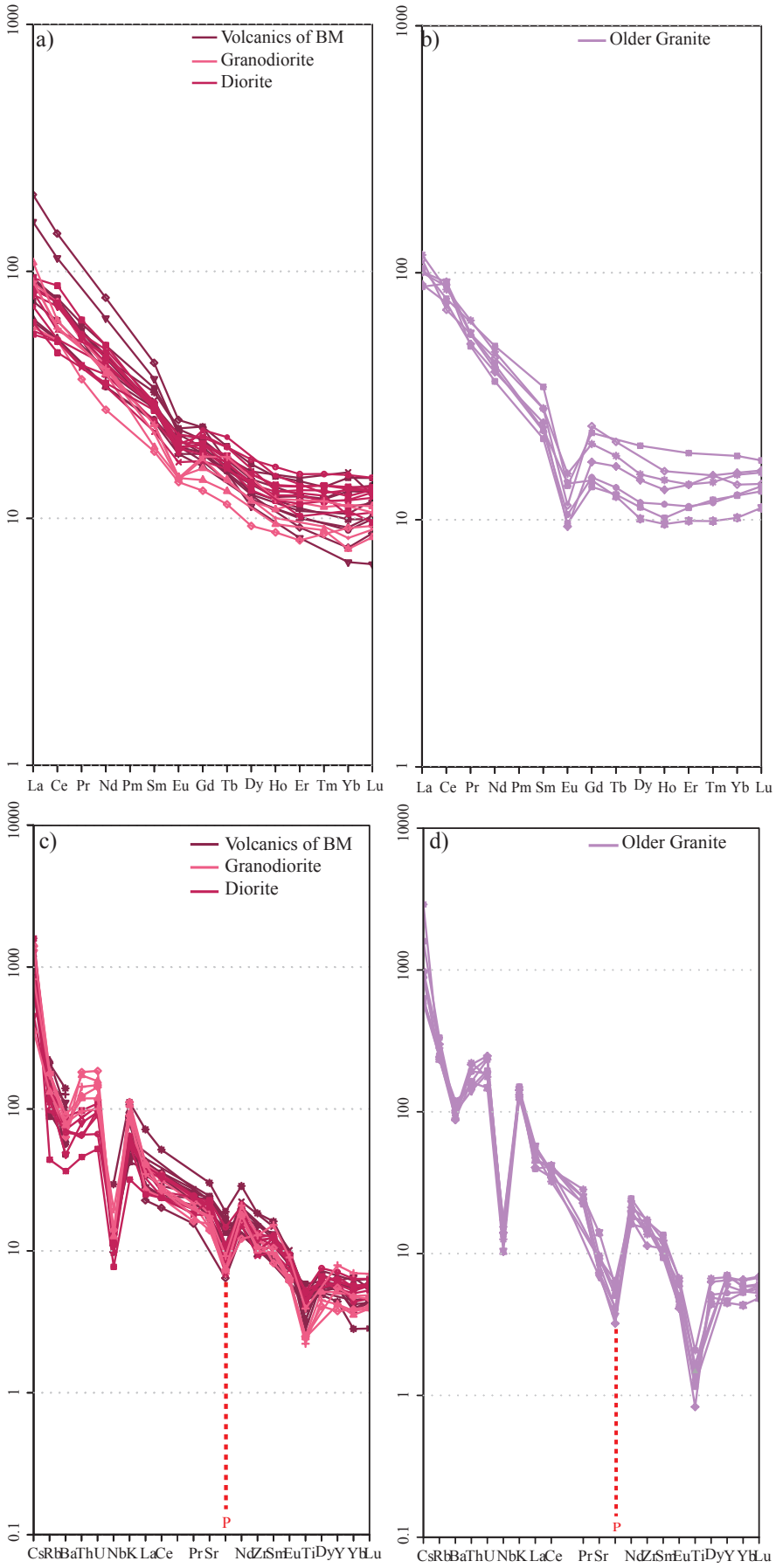

Figure 9: (a) and (b) Chondrite-normalized REE diagram for calc-alkaline "suite"; normalizing values from Boynton (1984). (c) and (d) Primitive mantle-normalized spider plots for calc-alkaline "suite" (after Sun & McDonough, 1989).

Chondrite-normalized REE patterns are reported on Fig.10a. Younger Granites display a strong enrichment in LREE $25 < Ce_N/Yb_N < 39$ higher than in calc-alkaline "suite", moreover these rocks are characterized by a weak Eu anomaly. The Eu anomaly (Eu/Eu* = 0.75-0.80) remains rather constant whatever silica content, revealing the absence of plagioclase fractionation in the melt. Total content of REE is high (400-200 ppm) and generally decreases with increasing of SiO_2 content coupled with the decrease of the volume of accessory minerals towards the most felsic rocks. Constant Eu anomaly and decreasing of REE content according to SiO_2 increase in host rock are typical characteristics of Mg-K magmatism (Tabaud et al. submitted).

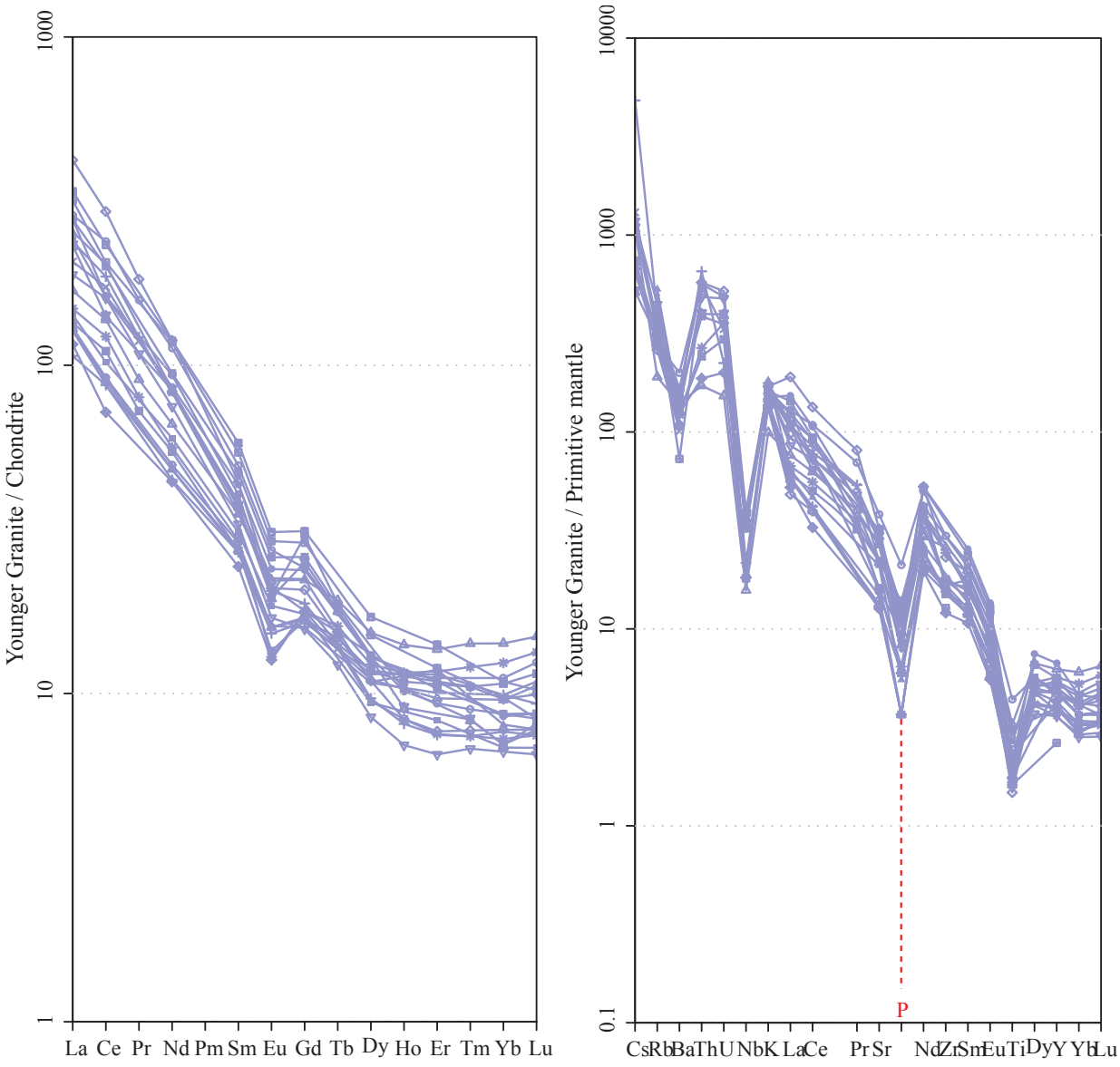

Figure 10: (a) Chondrite-normalized REE diagram for Younger granite; normalizing values from Boynton (1984). (b) Primitive mantle-normalized spider plots for Younger granite (after Sun & McDonough, 1989).

7.3.3 Isotopic composition

Isotopic data of Younger Granites previously published (Altherr et al., 2000) were recalculated at 330 Ma (Table 1 & Fig.12). Initial $0.705 < {}^{87}Sr/{}^{86}Sr < 0.706$ ratio values are in the same range as those of the calc-alkaline "suite" and initial $-3,5 < \varepsilon_{Nd} < -2$ ratio values are slightly lower than those of calc-alkaline suite but are in the same range as those of the South Vosges Mg-K granites (Tabaud et al, submitted).

7.4. S-type granite and Permian volcanism

7.4.1 Major elements

S-type "Kagenfels" leucogranite and Permian volcanic rocks display the same peraluminous composition (A/CNK > 1.1). Plots of CaO, MgO and total alkali vs. SiO_2 are reported on Fig.6. In Harker's diagram for volcanic rocks a plot analyses of MgO (2-0.1 wt %) and total alkali (10-7 wt %) vs. SiO_2 define a decreasing linear trend whereas in the same representation CaO (~0.2 wt %) content remains fairly constant (it is also the case for FeO_t, TiO_2 and P_2O_5) according to increase of SiO_2.

7.4.2 Trace elements

Among trace-element content, S-type granite and Permian volcanic rocks are characterized by a low content of Cr (30-15 ppm), Ni (< 10 ppm) and are mostly enriched in LILE (Ba =400-100 ppm, Rb ~ 250 ppm) and in incompatible elements (U = 3-6 ppm and Th < 20 ppm).

Primitive mantle-normalized multi-elementary plots analyses are reported on Fig.11b. Trace-element patterns show a strong enrichment in Cs, Rb, U, Th and K, and a depletion in Sr and P for rocks where the silica content > 70 wt % and a weak depletion in Zr and Ti most pronounced for rocks where SiO_2 > 70 wt %). These trace-elements patterns of S-type granite and Permian volcanic rocks reveal a strong geochemical fingerprint of a continental crust component.

Chondrite-normalized REE patterns reported on Fig.11a show a very strong fractionation of LREE ($5 < Ce_N/Yb_N < 18$) and are characterized by i) a deep negative Eu anomaly ($0.10 < Eu/Eu^* < 0.60$) which increases according to silica content and ii) a total content in REE between 100 and 200 ppm.

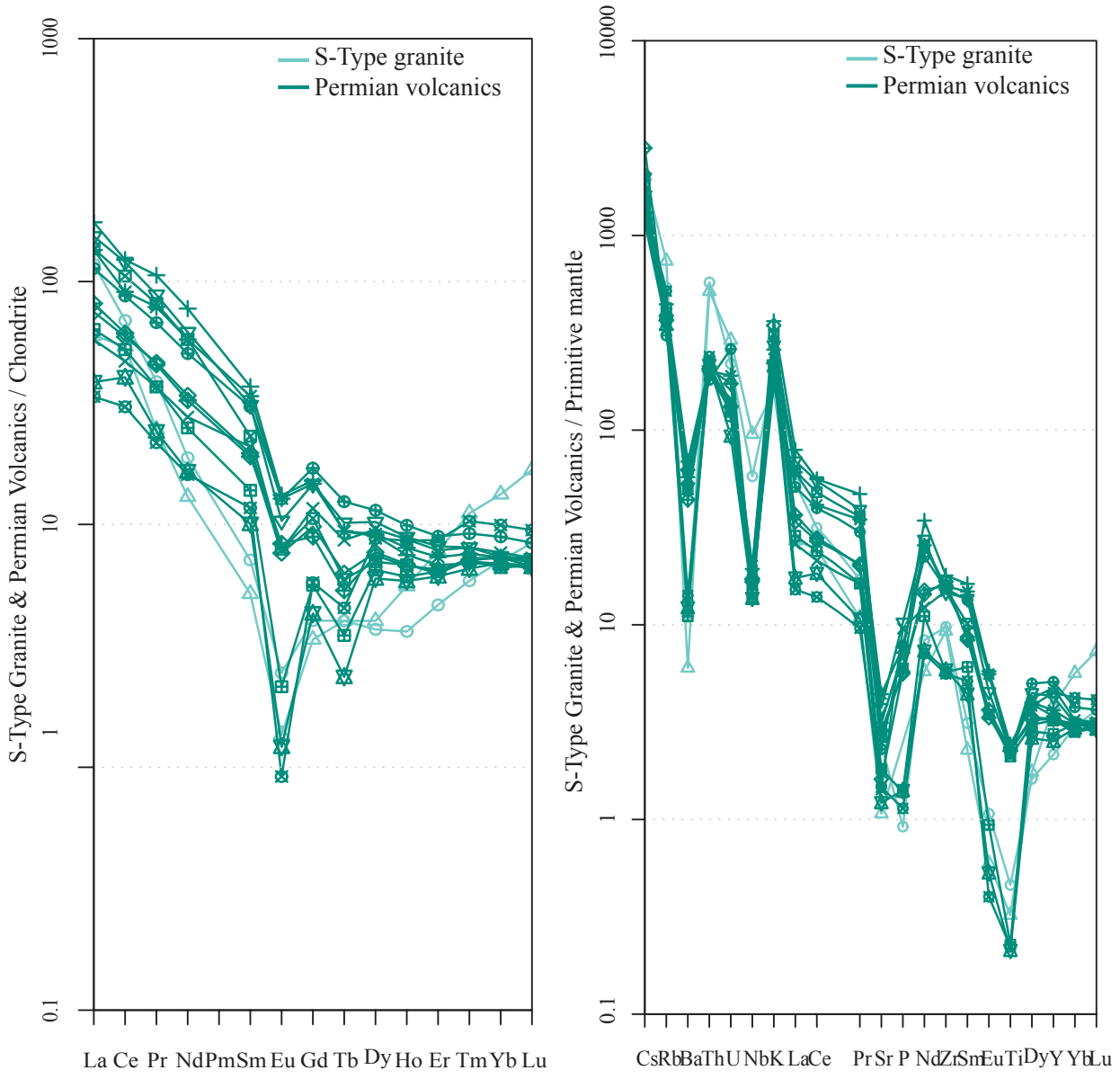

Figure 11: (a) Chondrite-normalized REE diagram for S-type and Permian volcanics; normalizing values from Boynton (1984). (b) Primitive mantle-normalized spider plots for S-type and Permian volcanics (after Sun & McDonough, 1989).

8. Discussion

8.1. Evolution trends of Northern Vosges magmatism

Devonian to Visean volcanic rocks are characterized by low content of Cr, Ni, LILE, weak REE fractionation with Eu anomaly and total REE content mostly constant (Fig.7). The volcanic rocks, from the East (Schirmeck Massif) to the West (Rabodeau Massif) display changes from tholeiitic to calc-alkaline serial character (Rizki and Baroz, 1988).

This early magmatism was followed by the volcanism of the "*Bande Médiane*", diorite intrusion and, 10 Ma later (334 - 329 Ma), by intrusion of granodiorite in the Southern part of "*Champ du Feu massif*". All these rocks are characterized by a decreasing content of Mg and Ca (Fig.6) and low contents of Cr and Ni, weak fractionation of REE with Eu anomaly roughly constant and increasing of total REE with SiO_2 that could support their cogenetism (Fig.9). The monzogranite emplaced 10 Ma latter, shows similar chemical characteristics to the previous calc-alkaline rocks, however with a higher content in incompatible elements (U, Th, and K) and a weaker depletion in Nb and Ta in trace-elements patterns (Fig.9b). Decreasing of MgO and CaO with increasing silica as well as depletion in Sr and Eu suggest a fractionation dominated by plagioclase. These geochemical features, together with the chemical mineral composition, could suggest any genetic link between calc-alkaline volcanics, diorite, granodiorite and monzogranite but Nd and Sr isotopic data reveal the presence of a continental crustal component in the monzogranite (Fig.12). However one can follow to use "calc-alkaline suite" to depict these rocks suggesting that they were generated from a similar source composition characterized by LREE, LILE and incompatible elements enrichment probably related with both differentiation and increase of continental crust component in the most felsic terms.

Table 1: Sm-Nd and Rb-Sr isotopic data for granitoids from the Northern Vosges after Altherr et al. (2000) recalculated at 330 Ma. New isotopic data (in bold) are included.

Sample		Rb (ppm)	Sr (ppm)	$^{87}Rb/^{86}Sr$	$^{87}Sr/^{86}Sr$	2σ(m)	$(^{87}Sr/^{86}Sr)_{330}$	Sm (ppm)	Nd (ppm)	$^{147}Sm/^{144}Nd$	$^{143}Nd/^{144}Nd$	2σ(m)	ε^{330}_{Nd}	T^{Nd}_{DM} (Ga)
Devonian volcanism														
	VON1	**27.9**	**480.1**	**0.1681**	**0.70445**	**0.000006**	**0.70366**	**4.83**	**22.9**	**0.1275**	**0.512746**	**0.000005**	**5.0**	**0.72**
	VON11	**14.0**	**58.6**	**0.6910**	**0.70899**	**0.000007**	**0.70574**	**5.23**	**20.9**	**0.1513**	**0.512681**	**0.000006**	**2.7**	**1.14**
"Calc-alkaline suite"														
Diorite	N-4			0.57	0.70742		0.70474	6.28	27.3	0.1390	0.512422		-1.8	1.48
	N-79			0.70	0.70880		0.70552	5.66	25.6	0.1334	0.512353		-2.9	1.51
	M-52			0.47	0.70833		0.70612	6.04	28.7	0.1272	0.512394		-1.9	1.33
Granodiorite	HS-25			0.69	0.70855		0.70531	4.69	26.3	0.1078	0.512431		-0.3	1.03
	HN-86			0.47	0.70755		0.70534	4.39	27.4	0.0969	0.512444		0.4	0.92
	CFS-114			1.15	0.71069		0.70529	4.95	25.7	0.1165	0.512439		-0.5	1.11
Older granite	CFN-90			3.55	0.72203		0.70535	7.17	40.6	0.1068	0.512311		-2.6	1.20
	W-38			2.31	0.71694		0.70609	8.52	53.2	0.0968	0.512324		-2.0	1.08
	F-59			2.36	0.71689		0.70580	6.91	35.4	0.1179	0.512343		-2.5	1.28
Younger granite														
	A-1			1.84	0.71422		0.70558	5.38	31.2	0.1042	0.512265		-3.4	1.23
	N-96			1.15	0.70997		0.70457	9.20	68.4	0.0813	0.512257		-2.6	1.03
	S-76			0.98	0.71059		0.70598	10.60	71.0	0.0902	0.512310		-2.0	1.04

Younger Granites, emplaced at about 310 Ma, are characterized by a high content of Mg, Cr, and Ni, strong REE fractionation with Eu anomaly roughly constant and high LILE content (Fig.10). Moreover, the total REE decreases according to the increase of silica content whereas the chemical composition of minerals remains rather constant (Fig.4). All these geochemical features are typical of Mg-K magmatism (Rossi & Cocherie, 1991; Holub, 1997; Tabaud et al., submitted).

The latest magmatic event, composed of S-type granite and Permian volcanic rocks, is characterized by a strong fractionation of REE together with a deep Eu anomaly and high content of incompatible elements, significant of partial melting of crustal components (Fig.11).

All these observations show that the Northern Vosges Mts are characterized by successive magmatic pulses spaced out of about 10 Ma which display a transition from tholeiitic to calc-alkaline to high-K calc-alkaline to Mg-K and to S-type magmas. Clearly, such a global magmatic trend which encompasses the result of successive magmatic pulses generated from different sources in different geodynamic environments cannot be seen as a simple differentiation process.

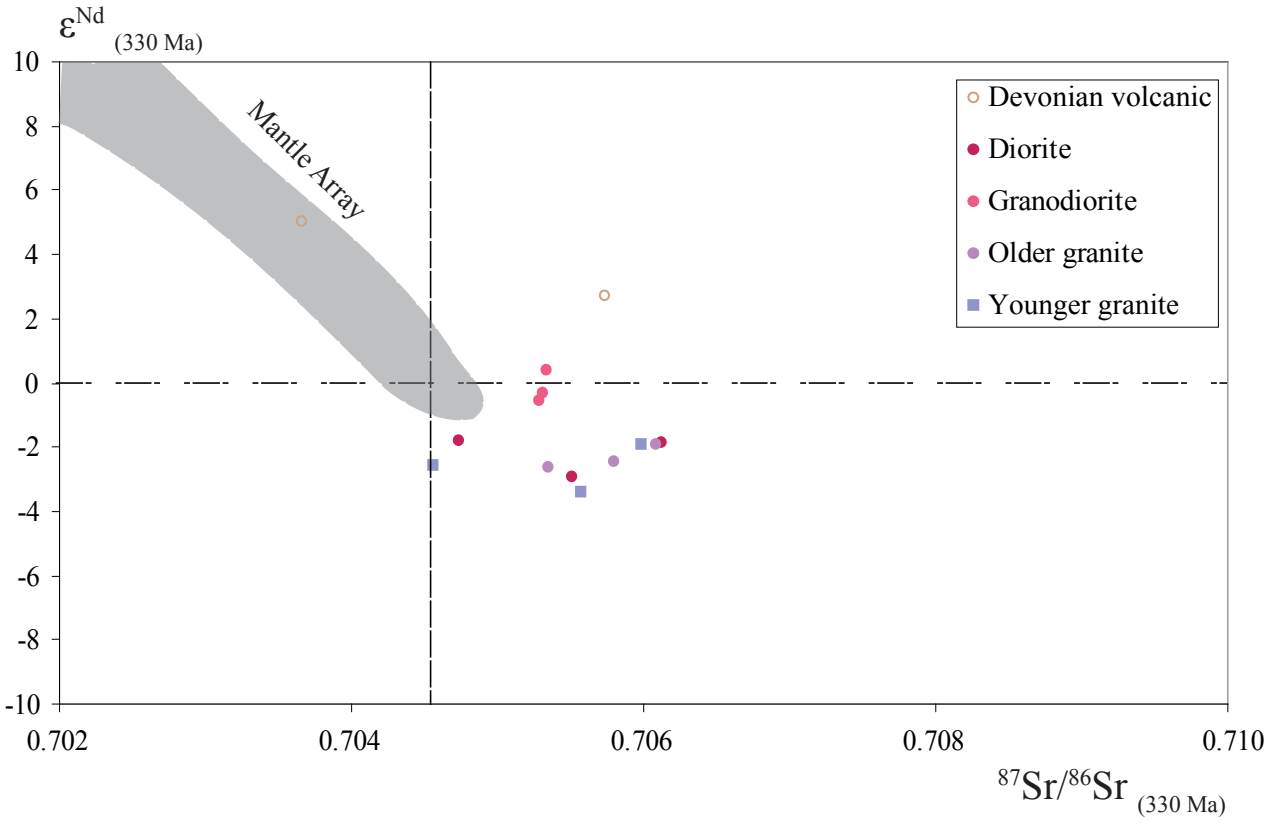

Figure 12: $(^{87}Sr/^{86}Sr)_{330}$ vs. ε^{Nd}_{330} plot for granitoids of Northern Vosges Mts (Altherr et al., 2000 and this study).

8.2. Genesis and tectonic implications of Northern Vosges magmatic events

8.2.1 Devonian volcanism

Continental tholeiite could have been generated either during the early evolution of a new ocean or during continental extension in a back-arc setting or even in post-tectonic extensional basins (Duncan, 1987; Lightfoot et al., 1993; Peate & Hawkesworth, 1996).

Multi-element patterns (Fig.7b) which show strong depletion in Nb, Ta and Ti and enrichment in LILE suggest that these rocks could have been generated from an enriched lithospheric mantle source contaminated by fluids expelled from a subduction zone. In the same way, the isotopic compositions of these volcanic rocks that display following isotopic value: $+3 < \varepsilon_{Nd} < +5$ and $0.704 < (^{87}Sr/^{86}Sr) < 0.706$ point to a minor contribution of depleted mantle source (Fig.12). The enrichment of the mantle source could have been caused by the Early Devonian subduction of the Rhenohercynian oceanic crust from the North (Franke, 2000; Edel & Schulmann, 2009; Leveridge & Shail, 2011).

Occurrence of arc-related magmatic rocks further to the north (Altenberg & Besch, 1993; Dombrowski et al., 1995; Edel & Schulmann, 2009) suggests that these continental tholeiites could have occurred in a back-arc setting (Fig.13a).

The lack of either voluminous continental flood basalts, high-Mg basalt flows or depleted N-MORB rocks suggests that no mantle plume was necessary to initialize the rifting and that this rifting did not lead to development of oceanic crust. Extension in the Saxothuringian crust could have been related to the roll-back of the Rhenohercynian oceanic slab further to the north (Fig.13a) accompanied by a possible upwelling of asthenospheric mantle. The temporal shift from tholeiitic to calc-alkaline magmatism (Devonian to Visean) in the same place might have occurred owing to change in angle of dip of the oceanic slab, which could have been related to onset of continental collision with arrival of Rhenohercynian continental crust in the subduction zone (Fig.13b).

Figure 13: Sketch of the geotectonic scenario for the development of magmatic intrusions and extrusions during late stages of the Variscan Orogeny. Rhenohercynian and Saxothuringian crust after Oncken et al., 2000; Leveridge & Shail, 2011; Edel & Schulmann, 2009. See text for discussion. Next double pages.

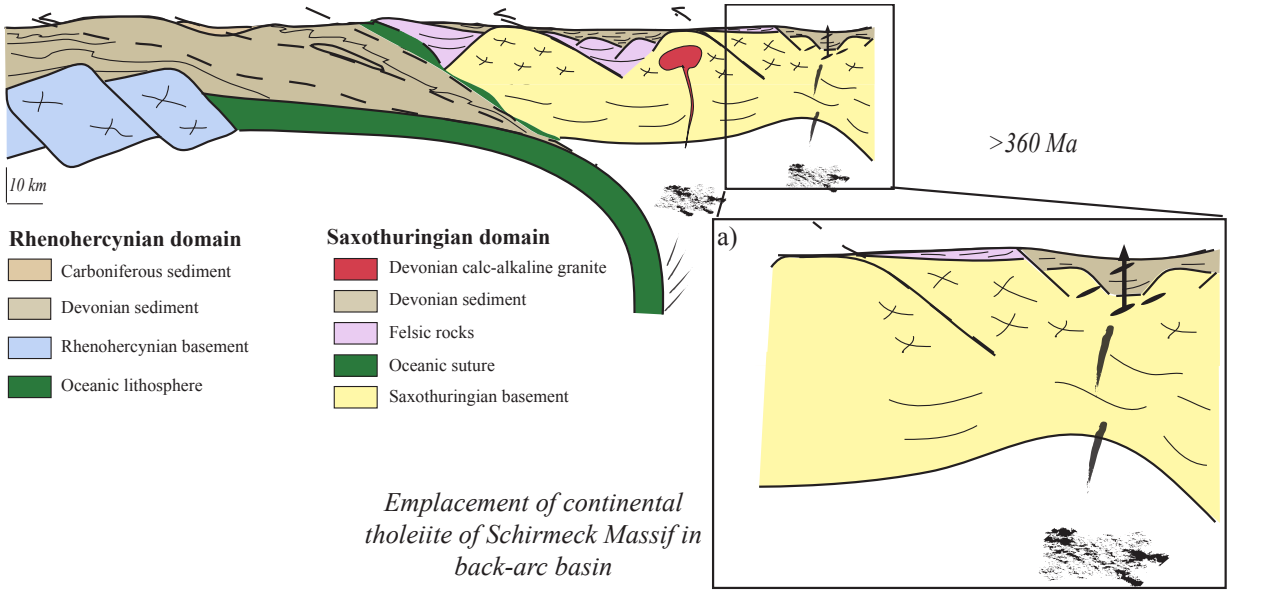

Emplacement of continental tholeiite of Schirmeck Massif in back-arc basin

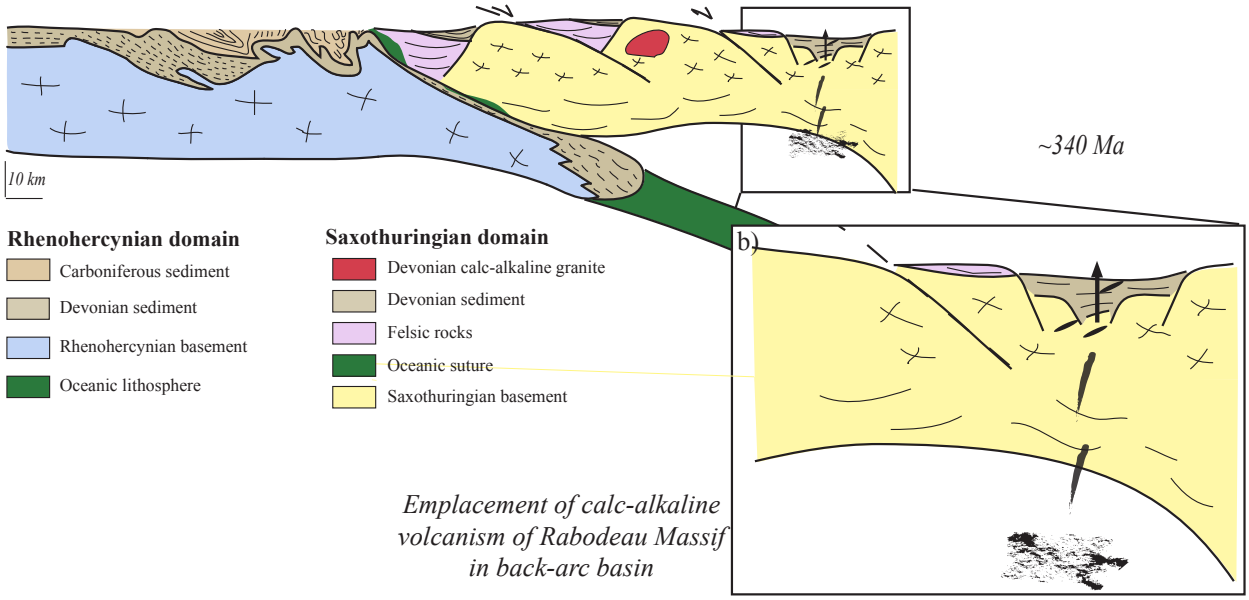

Emplacement of calc-alkaline volcanism of Rabodeau Massif in back-arc basin

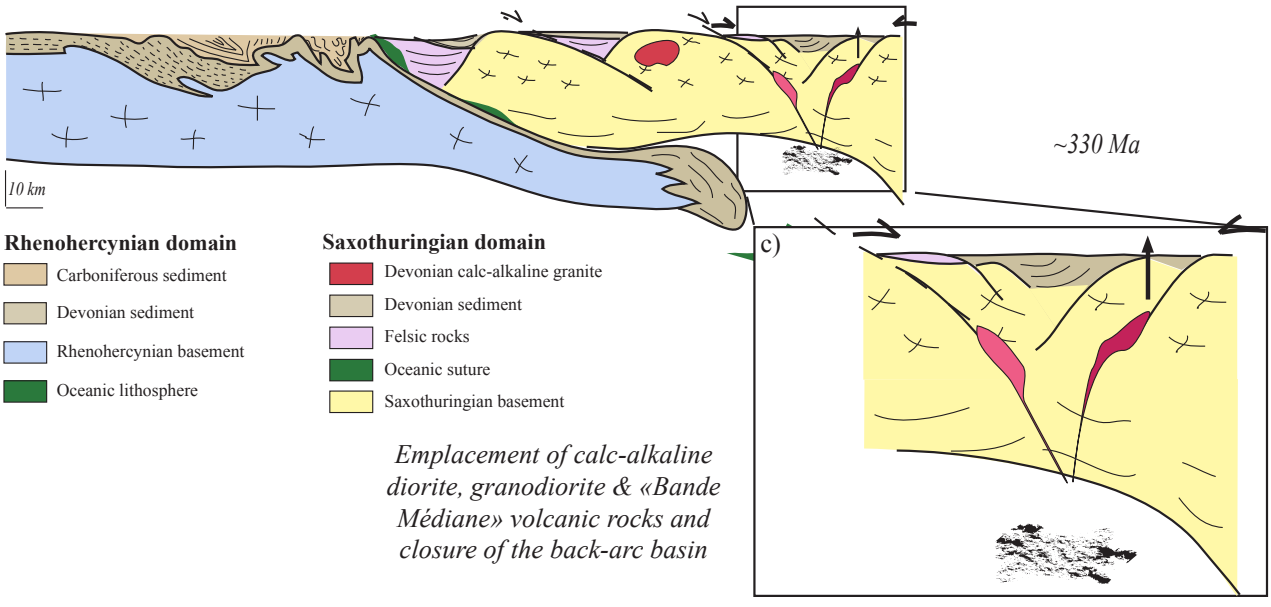

Emplacement of calc-alkaline diorite, granodiorite & «Bande Médiane» volcanic rocks and closure of the back-arc basin

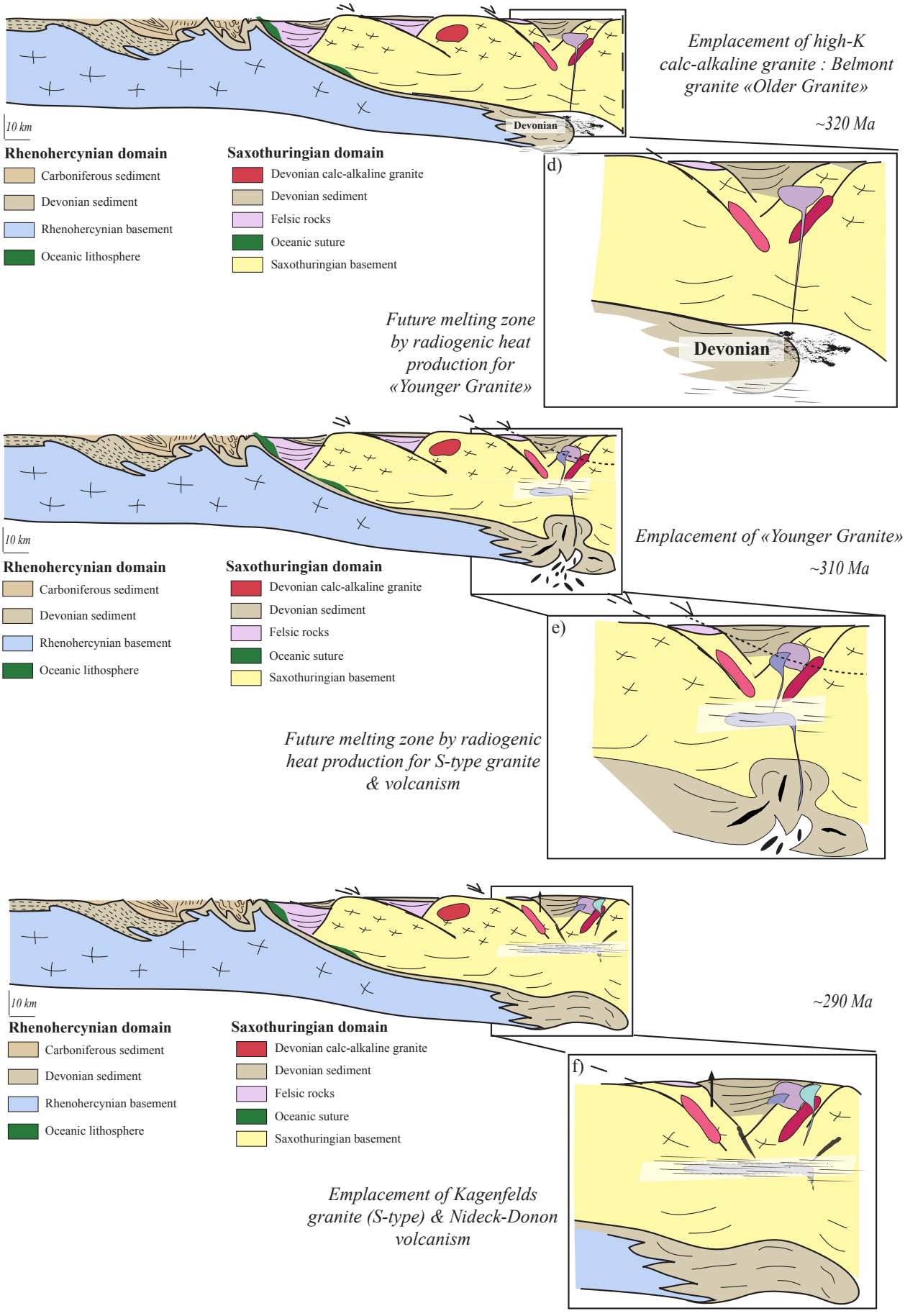
10 km
Rhenohercynian domain
Carboniferous sediment
Devonian sediment
Rhenohercynian basement
Oceanic lithosphere
Saxothuringian domain
Devonian calc-alkaline granite
Devonian sediment
Felsic rocks
Oceanic suture
Saxothuringian basement
Devonian
Emplacement of high-K calc-alkaline granite : Belmont granite «Older Granite»
~320 Ma
d)
Future melting zone by radiogenic heat production for «Younger Granite»
Devonian
10 km
Rhenohercynian domain
Carboniferous sediment
Devonian sediment
Rhenohercynian basement
Oceanic lithosphere
Saxothuringian domain
Devonian calc-alkaline granite
Devonian sediment
Felsic rocks
Oceanic suture
Saxothuringian basement
Emplacement of «Younger Granite»
~310 Ma
e)
Future melting zone by radiogenic heat production for S-type granite & volcanism
10 km
Rhenohercynian domain
Carboniferous sediment
Devonian sediment
Rhenohercynian basement
Oceanic lithosphere
Saxothuringian domain
Devonian calc-alkaline granite
Devonian sediment
Felsic rocks
Oceanic suture
Saxothuringian basement
~290 Ma
f)
Emplacement of Kagenfelds granite (S-type) & Nideck-Donon volcanism

8.2.2 Calc-Alkaline suite

In a previous work, chemical and isotopic constrains led Altherr et al. (2000) to propose that dioritic and granodioritic magmas, emplaced at 10 km depth, could have been derived from an enriched lithospheric mantle contamined by a metaigneous crust. The monzogranite of the northern "*Champ du Feu massif*" part, emplaced at 3 km depth, shows geochemical characteristics that are both consistent either i) with magma generation in a volcanic-arc setting above a subduction slab or ii) by dehydration melting of metagreywackes. Geochemical characteristics of volcanic of "*Bande Médiane*", diorite and granodiorite may point to an origin in a continental-arc environment, as suggested by its calc-alkaline nature (Fig.8a), pronounced Nb, Ta, Ti throughs and enrichment in LILE on primitive-mantle normalized multi-elementary diagrams (Fig.9b). Moreover, initial ε_{Nd} values from +0.4 to -3.0 and initial ($^{87}Sr/^{86}Sr$) ratios between 0.7047 and 0.7061 (Fig.12) of the southern "*Champ du Feu massif*" suite (Altherr et al., 2000) are in the range of subduction-related magmatic rocks (Hildreth & Moorbath, 1988) and point to partial melting of an enriched mantle which was metasomatized by fluids (Hawkesworth et al., 1993; Rottura et al., 1998; Cameron et al., 2003). Intrusion of this calc-alkaline suite could be directly related to an active subduction or alternatively post-dated an ancient subduction-related mantle enrichment processes. Indeed, the production of calc-alkaline magmas may post-date the cessation of subduction by as much as 30-50 My (Bonin, 1990). However, Schmidberger & Hegner (1999) proposed that the closure of Rhenohercynian basin was not complete at the end of Lower Carboniferous because the culmination of HP-LT metamorphism in the Northern Phyllite zone and southern Rhenohercynian is only slightly older than 325 Ma (Fig.13c). This hypothesis is in agreement with other recent studies (Edel & Schulmann, 2009; Leveridge & Shail, 2011).

Notwithstanding U-Pb zircon age at 319 Ma (this study) reveals that monzogranite of the northern "*Champ du Feu massif*" part is significantly younger than both dioritic and granodioritic intrusions, they all present similar geochemical calc-alkaline characteristics with however an increasing continental crustal influence (enrichment in incompatible elements such as Th, U, Zr, K and LILE; Fig.9b). As isotopic composition of the monzogranite remains in the range of calc-alkaline suite (Fig.12), it will be considered that sources of similar composition were involved in the generation of the magmas of the "calc-alkaline suite".

Sr and Nd isotopic compositions of the calc-alkaline suite and monzogranite also argue for crustal component in sources of magmas. Inherited zircon population is in agreement with this consideration. Analyzed zircons of calc-alkaline suite reveal Pb component of Neoproterozoic to Lower Carboniferous ages (600-350 Ma; Edel et al., submitted). The age of this population is similar to ages of weakly-metamorphosed sediments of *Steige and Villé* unit (Doubinger, 1963; Doubinger & von Eller, 1963a, 1963b; Ross, 1964; Reitz & Wickert, 1989). Analyzed zircons of monzogranite

reveal Middle Devonian to Lower Carboniferous ages which are similar to ages of sediments of *Bruche* unit (Firtion, 1945, 1957; Figge, 1968; Juteau, 1971; Blanalt & Lillié, 1973; Braun et al., 1992; Aghai Soltani et al, 1996) and Rhenohercynian upper-crust (Oncken et al., 2000).

In a geotectonic view, the shift from calc-alkaline to high-K calc-alkaline magmatism could have been caused by arrival of subducted Rhenohercynian continental crust underplating Saxothuringian crust (Oncken et al., 2000) with slab-break off of the Rhenohercynian oceanic crust which brought about upwelling of asthenospheric mantle (Fig.13c & 13d). Heat contribution from asthenospheric mantle could have caused the remelting of the enriched lithospheric mantle and during ascent in a shallower crustal level; magmas are contaminated by crustal component producing monzogranite of the northern "*Champ du Feu massif*" part (Fig.13d). Intrusion of the calc-alkaline magmas could be synchronous with closure of the back-arc basin due to their emplacement in fine elongated bodies oriented NE-SW (Fig.13c).

8.2.3 Younger Granites

Altherr et al. (2000) proposed that Younger Granites could originated by dehydration of metasedimentary sources at greater depths than monzogranite of northern "*Champ du Feu massif*" part.

As we demonstrated above, Younger Granites belongs to Mg-K magmatism. Their particular geochemical trend and isotopic composition (Fig.10 & 12) resemble the SVMg-K association of the southern Vosges Mts. As proposed in a previous paper (Tabaud et al., submitted), this Mg-K magmatism would result from partial melting of both metasomatized lithospheric mantle and Early Paleozoic mafic rocks of the Saxothuringian crust underplated at Moho depth under the Moldanubian continental crust. The melting was mainly due to radiogenic heat production of Saxothuringian lower crust. In the same way, we proposed a same geodynamic scenario to generate Younger Granites of the northern Vosges Mts where Rhenohercynian Devonian continental crust was underplated under Saxothuringian crust (Fig.13e). Fields relationship (intrusion into monzogranite) and rounded shapes of Younger Granites indicate that back-arc basin was totally closed at 310 Ma (Fig.13e).

8.2.4 S-type granite and Permian rhyolite

Peraluminous S-type granite and Permian rhyolite show geochemical features consistent with only a crustal component involved in magmas sources (Fig.11). In the Southern Vosges Mts, the results of numerical modelling (Tabaud et al., submitted) has shown that intrusion of Mg-K magmas at 20 km deep could have caused, after about 10 Ma partial melting of surrounding country rocks thanks to radiogenic heat production. The same scenario could also be applied to the northern Vosges Mts where the intrusion of Younger Granites could have involved partial melting of the Upper Carboniferous Saxothuringian crust (cf. presence of inherited zircon of this age in Kagenfels granite) by radiogenic heat production (Fig.13f). This melting underwent in an extensional environment (orogenic collapse) and was probably accompanied by an upwelling of lithospheric mantle due to the simultaneous onset of magmatism at about 300 Ma over a large area within Northern Europe (Wilson et al., 2004).

9. Conclusion

The northern Vosges Mts expose occurrences of magmatic rocks emplaced from Devonian to Permian within a small area (250 km²) and displaying a large variety of petrological and geochemical characteristics. The range of composition of the Northern Vosges magmatism changes respectively from mafic to acidic rocks, and from tholeiitic, calc-alkaline, high-K, Mg-K and S-type compositions according to the time.

The succession of changing of the Variscan geotectonic environment through time can explain the nature and variation of composition of the different magmatic pulses of the Northern Vosges Mts. The main process that controlled changes in the composition of the magmatic pulses is the progress of the subducted Rhenohercynian oceanic and continental crust under the Saxothuringian continental crust.

Collaborators: Alain Cocherie, Catherine Guerrot, Philippe Elsass, Philippe Rossi & Hubert Whitechurch.

REREFENCES CITED

Aghai Soltani, L., Bender, P., Braun, A. & Schmidt-Effing, R. (1996). Oberdevonische Radiolarien aus Kieselgesteinen des Breuschtales (Vallé de la Bruche, Nord-Vogesen, Frankreich). *Jahresbericht und Mitteilungen des oberrheinischen geologischen Vereins*, **78**, 183-208.

Altenberger, U. & Besch, T. (1993). The Böllstein Odenwald evidence for pre- to early variscan plate convergence in the central European Variscides. *Geologische Rundschau,* **82**, 475-488.

Altherr, R., Holl, A., Hegner, E., Langer, C. & Kreuzer, H. (2000). High-potassium, calc-alkaline I-type plutonism in the European Variscides: northern Vosges (France) and northern Schwarzwald (Germany). *Lithos*, **50**, 51-73.

Blanalt, J. G. & Lillié, F. (1973). Données nouvelles sur la stratigraphie des terrains sédimentaires dévono-dinantiens de la vallée de la Bruche (Vosges septentrionales). *Sciences Géologiques*, **26**, 69-74.

Benecke, W. & Bücking, H. (1898): Calceola sandalina im oberen Breuschtal. *Mitteilungen der Geologischen Landesanstalt von Elsass-Lothringen*, **4**, 105 - 111.

Bonin, B. (1990). From orogenic to anorogenic settings: evolution of granitoid suites after a major orogenesis. *Geological Journal, W.S. Pitcher Special Issue*, **25**, 261-270.

Boutin, R., Montigny, R. & Thuizat, R. (1995). Chronologie K-Ar et 39Ar/40Ar du métamorphisme et du magmatisme des Vosges. Comparaison avec les massifs varisques avoisinants. *Géologie de la France*, **1**, 3–25.

Boynton, W. V. (1984). Cosmochemistry of the rare earth elements meteoritic studies. In: Henderson, P. (ed.) *Rare Earth Elements Geochemistry*. *Amsterdam: Elsevier*, 63–114.

Braun, A., Maass, R. & Schmidt-Effing, R. (1992). Oberdevonische Radiolarien aus dem Breuschtal (Nord-Vogesen, Elsaß) und ihr regionaler und stratigraphischer Zusammenhang. *Neues Jahrbuch für Geologie und Paläontologie. Abhandlungen*, **185**, 161-178.

Cameron, B. I., Walker, J. A., Carr, M. J., Patino, L. C., Matias, O. & Feigenson, M. D. (2003). Flux versus decompression melting at stratovolcanos in southeastern Guatemala. *Journal of Volcanology and Geothermal Research,* **119**, 21–50.

Carasco B. (1897) - Les grabens stéphano-permiens de l'Est de la France. Evolution tec-tono-sédimentaire, développement des faciès lacustres carbonatés et sapropéli-ques. Ph.D. thesis, Strasbourg, 161 p.

Carlson, R. W. (1984). Isotopic constraint on Columbia River flood basalt genesis and the nature of the subcontinental mantle. *Geochimica et Cosmochimica Acta*, **48**, 2357-2372

Cocherie A., Robert M. (2008). Laser ablation coupled with ICP-MS applied to U-Pb zircon geochronology: A review of recent advances. *Gondwana Research*, doi:10.1016/j.gr.2008.01.003.

Cocherie A., Legendre O. (2007). Potential minerals for determining U-Th-Pb chemical age using electron microprobe. *Lithos*, **93,** 288-309.

Cocherie A., Albarède F. (2001). An improved U-Th-Pb age calculation for electron microprobe dating of monazite. *Geochimica et Cosmochiica. Acta*, **65**, 4509-4522.

de Béthune, P., Lapania, E., Rousseau-Turay, M. & von Eller, J. P. (1968). Les diorites du Neuntelstein et du Neugrunrain près du Hohwald Vosges, et leurs enclaves. *Bulletin du Service de la Carte Géologique d'Alsace-Lorraine*, **21**, 23-24.

Debon F. & Le Fort, P. (1983). A chemical–mineralogical classification of common plutonic rocks and associations. *Transactions of the Royal Society of Edinburgh, Earth Sciences,* **73**, 135–149.

de la Roche, H. & von Eller, J. P. (1969). Caractères et tendances géochimiques des bandes granodioritiques et granitiques formant le massif du Champ-du-Feu Vosges cristallines du Nord. *Bulletin du Service de la Carte Géologique d'Alsace-Lorraine*, **22**, 199-223.

Deschamps, M. (1995). Le magmatisme du Champ du Feu (Vosges septentrionales) : Caractérisation et signification géodynamique. *Bulletin des Académie et Société Lorraines des Sciences*, **34**, 131-149.

Didier, J. (1991). The various types of enclaves in the Hercynian granitoids of the Massif Central, France. In: Didier, J., Barbarin, B. (eds.). *Enclaves and Granite Petrology. Developments in Petrology, Elsevier, Amsterdam*, **13***,* 47–62.

Dombrowski , A., Henjes-Kunst, F., Höhndorf, A., Kröner, A., Okrusch, M. & Richter, P. (1995). Orthogneisses in the Spessart Crystalline Complex, north-west Bavarian: Silurian granitoid magmatism at an active continental margin. *Geologische Rundschau*, **64**, 399-411.

Doubinger, J. (1963). Chitinozoiares ordoviciens et siluriens des schistes de Steige dans les Vosges. *Bulletin du Service de la Carte Géologique d'Alsace-Lorraine*, **16**, 125-136.

Doubinger, J. & von Eller, J.-P. (1963a). Présence de Spongiaires dans les schistes précambriens métamorphiques des Vosges. *Bulletin du Service de la Carte Géologique d'Alsace-Lorraine*, **16**, 111-123.

Doubinger, J. & von Eller, J.-P. (1963b). Découverte de Chitinozoaires d'âge silurien dans les schistes de Steige (vallée de l'Andlau, Vosges). *Comptes Rendus de l'Academie des Sciences*, **256**, 469-471.

Duncan, A. R. (1987). The Karoo igneous province - a problem area for inferring tectonic setting from basalt geochemistry. *Journal of Volcanology and Geochemical Research,* **32**, 13-34.

Edel, J. B., Schulmann, K., Skrzypek, E. & Cocherie, A. (*submitted*). Coupling between oblique subduction zone dynamics and transtensional emplacement of magmatic arc exemplified by AMS and paleomagnetic study (N Vosges, E France).

Edel, J.-B. & Schulman, K. (2009). Geophysical constraints and model of the ''Saxothuringian and Rhenohercynian subductions–magmatic arc system'' in NE France and SW Germany. *Bulletin de la Société Géologique de France,* **180,** 545–558

Edel, J. B., Montigny, R., Royer, J. Y., Thuizat, R. & Troland, F. (1986). Paleomagnetic investigations and K–Ar dating on the Variscan plutonic massif of the Champ du Feu and its volcanic-sedimentary environment, northern Vosges, France. *Tectonophysics,* **122**, 165–185.

Faul, H. & Jäger, E. (1963). Age of some granitic rocks in the Vosges, the Schwarzwald and the Massif Central. *Journal of Geophysical Research*, **68**, 3293–3300.

Figge, K. (1968). Ober-Devon im Breuschtal der Vogesen. *Neues Jahrbuch für Geologie und Paläontologie. Monatshefte*, **4**, 195-199.

Finger, F., Roberts, M. P., Haunschmid, B., Schermaier, A. & Steyrer, H. P. (1997). Variscan granitoids of central Europe: their typology, potential sources and tectonothermal relations. *Mineralogy and Petrology*, **61**, 67-96.

Firtion, F. (1957). Les éléments paléontologiques dévoniens du Val de Bruche. *Annales Universitatis Saraviensis, Scientia*, **5-6**, 97-184.

Firtion, F. (1945). Apports à la connaissance paléontologique du Dévono-Dinantien de la région de Schirmeck. *Comptes rendus sommaires de la Société Géologique de France*, **4**, 39-41.

Fluck, P., Edel, J. B., Gagny, C., Montigny, R., Piqué, A., Schneider, J. L. & Whitechurch, H. (1989). Carte synthétique et géotraverse N-S de la chaine varisque des Vosges (France). Synthèse des travaux effectués depuis deux décennies. *Comptes-rendus Academie des Sciences, Série II,* **309**, 907-912.

Fluck, P. (1980). Métamorphisme et magmatisme dans les Vosges moyennes d'Alsace. Contribution à l'histoire de la chaine Varisque. *Mémoires des Sciences Géologiques*, **62**, 248 p.

Franke, W. (2000). The mid-European segment of the Variscides: Tectonostratigraphic units, terrane boundaries and plate tectonic evolution, In: Franke W., Haak V., Oncken O., Tanner D. (eds). *Orogenic processes; quantification and modelling in the Variscan Belt. Geological Society Special Publications*, **179**, 35-56.

Geldron, A. (1986). Genèse et contexte magmatique des stockworks à molybdenite de la chaîne hercynienne française : étude comparative des gisements à Mo-W de Breitenbach (Bas-Rhin) à Mo-Cu de Beauvain (Orne) et à Mo-W-Sn-Ag-Sb-Bi de la Rousselière (Loire-Atlantique). Ph D. thesis, Université of Orléans, 450 p.

Hahn-Weinheimer, P., Propach, G. & Raschka, H. (1971). Zur Genese des Kagenfels Granits Nordvogesen. *Bulletin du Service de la Carte Géologique d'Alsace-Lorraine*, **24**, 5-56.

Hawkesworth, C. J., Gallagher, K., Herot, J. M. & McDermott, F. (1993). Mantle and slab contributions in arc magmas. *Annual Review of Earth and Planetary Sciences,* **21**, 175–2004.

Hess, J. C., Lippolt, H. J. & Kober, B. (1995). The age of the Kagenfels granite (northern Vosges) and its bearing on the intrusion schem of late Variscan granitoids. *Geologische Rundschau*, **84**, 568-577.

Hess, J.C. & Lippolt, H. J. (1986). Kinetics of Ar isotopes during neutron-irradiation. ^{39}Ar loss from minerals as a source of error in ^{40}Ar/^{39}Ar dating. *Chemical Geolology*, **59**, 223-236.

Hildreth, W. & Moorbath, S. (1988). Crustal contributions to arc magmatism in the Andes of Central Chile. *Contributions to Mineralogy and Petrology*, **98**, 455-489.

Holm, P. E. (1985). The geochemical fingerprints of different tecton-magmatic environments using hygromagmatophile element abundances of tholeiitic basaltic and basaltic andesites. *Chemical Geology*, **51**, 303-323.

Holub, F. V. (1997). Ultrapotassic plutonic rocks of the durbachite series in the Bohemian Massif: petrology, geochemistry and petrogenetic interpretation. *Sborník geologických ved, Lozisková geologie–mineralogie,* **31**, 5–26.

Holub, F. V., Klecka, M. & Matejka, D. (1995). Igneous activity (Moldanubian Zone). In: Dallmeyer, R. D., Franke, W. & Weber, K. (eds). *Pre-permian Geology of Eastern and Central Europe. Springer-Verlag, Berlin*, 444-452.

Ikenne, M., Rasamimanana, G., Baroz, F. & Bébien, J. (1991). Magmatismes tholéiitiques et calco-alcalins dévono-dinantien dans le massif du Rabodeau (Vosges septentrionales). *Géologie de la France*, **1**, 3-16.

Ikenne, M. (1986). Le volcanisme dévono-dinantien du massif du Rabodeau, un témoin de l'évolution orogénique des Vosges du Nord dans l'Europe moyenne varisque. Ph.D. thesis, Nancy.

Janoušek, V., Farrow, C. M. & Erban, V. (2003). GCDkit: new PC software for interpretation of whole-rock geochemical data from igneous rocks. *Geochimica et Cosmochimica Acta,* **A67**, 186.

Juteau, T. (1971). Nouvelles données cartographiques, pétrographiques et chimiques sur le massif dévono-dinantien du Rabodeau (Vosges septentrionales). Pétrogénèse d'une série spilite-kératophyre « hercynotype » complexe. *Sciences de la Terre*, **16**, 45-106.

Kossmat, F. (1927). Gliederung der varistischen Gebirgsbaues. *Abhandlungen des Sächsischen geologischen Landesamts,* **1**, 1-39.

Laubacher, G. & von Eller, J. P. (1966). Contribution à l'étude géologique des dépôts permiens du bassin de Villé. *Bulletin du Service de la Carte Géologique d'Alsace-Lorraine,* **19**, 163-186.

Leake, B.E., Woolley, A.R., Arps, C.E.S., Birch, W.D., Gilbert, M.C., Grice, J.D., Hawthorne, F.C., Kato, A., Kisch, H.J., Krivovichev, V.G., Linthout, K., Laird, J., Mandarino, J.A., Maresch, W.V., Nickel, E.H., Rock, N.M.S., Schumacher, J.C., Smith, D.C., Stephenson, N.C.N., Ungaretti, L., Whittaker, E.J.W., and Youzhi, G. (1997) Nomenclature of amphiboles: Report of the Subcommittee on Amphiboles of the International Mineralogical Association, Commission on New Minerals and Mineral Names. *American Mineralogist*, **82**, 1019–1037.

Leterrier, J. (1978). Aspects chimiques des interactions entre les magmas basiques et leur encaissant pélitique dans le plutonisme. *Bulletin de la Société Géologique de France,* **20,** 21–28.

Leveridge, B. E. & Shail, R. K. (2011). The Gramscatho Basin, south Cornwall, UK: Devonian active margin successions. *Proceedings of the Geologists' Association*, **122**, 568-615.

Lightfoot, P. C., Hawkesworth, C. J., Hergt, J., Naldrett, A. J., Gorbachev, N. S., Fedorenko, V. A. & Doherty, W. (1993). Remobilisation of the continental lithosphere by a mantle plume: major-, trace- and Sr-, Nd-, and Pb-isotope evidence from picritic and tholeiitic lavas of the Noril'sk district, Siberian Trap, Russia. *Contributions to Mineralogy and Petrology*, **114**, 171–188.

Ludwig K.R. (2003). ISOPLOT/EX, version 3. A geochronological toolkit for Microsoft Excel. *Berkeley Geochronology Center*, *Special Publication*, **4**, 70 p.

Oncken, O., Sobolev, S. V., Stiller, M., Asch, G., Haberland, C., Mechie, J., Yuan, X., Lüchen, E., Giese, P., Wigger, P., Lueth, S., Scheuber, E., Götze, H. J., Brasse, H., Buske, S., Yoon, M. K., Shapiro, S., Rietbrock, A., Chong, G., Wilke, H. G., Gonzales, G., Bravo, P., Vieytes, H., Martinez, E., Rössling, R. & Ricaldi, E. (2003). Seismic imaging of a convergent continental margin and plateau in the central Andes (Andean Continental Research Project 1996 (ANCORP'96)). *Journal of Geophysical Research*, **108**, 2328.

Oncken, O., Plesch, A., Weber, J., Ricken, W. & Scharder, S. (2000). Passive margin detachment during arc-continental collision (Central European Variscides). In: Franke W., Haak V., Oncken O., Tanner D. (eds). *Orogenic processes; quantification and modelling in the Variscan Belt. Geological Society Special Publication*, **179**, 199-216.

Owens, T. J. & Zandt, G. (1997). Implications of crustal property variations for models of Tibetan Plateau evolution. *Nature*, **387**, 37–43.

Peacock, M. A. (1931). Classification of igneous rock series. *Journal of Geology,* **39**, 54–67.

Peate, D. W. & Hawkesworth, C. J. (1996). Lithosphere to asthenosphere transition in low-Ti flood basalts from southern Paraná, Brazil. *Chemical Geology,* **127**, 1–24.

Pupin, J. P. (1980). Zircon and granite petrology. *Contributions to Mineralogy and Petrology,* **73**, 721-725.

Reitz, E. & Wickert, F. (1989). Late Cambrian to early Ordovician acritarchs from the Villé unit, northern Vosges Mountains (France). *Neues Jahrbuch für Geologie und Paläontologie. Monatshefte*, **6**, 375-384.

Rizki, A. & Baroz, F. (1988). Le volcanisme tholéïtique du massif de Schirmeck (Vosges septentrionales, France), témoin d'une zone de convergence de plaques au Paléozoïque supérieur. *Comptes Rendus de l'Academie des Sciences*, **307**, 511-516.

Robert, J. L. (1976). Titanium solubility in synthetic phlogopite solid solutions. *Chemical Geology,* **17**, 213-227

Ross, P. H. (1964). Fossilfunde in den Steiger und Weiler Schiefern (Vogesen). *Nachrichten der Akademie der Wissenschaften zu Göttingen, Mathematisch-Physikalische Klasse*, **3**, 37-43.

Rossi, P. & Cocherie, A. (1991). Genesis of a Variscan batholith: field, petrological and mineralogical evidence from the Corsica–Sardinia batholith. *Tectonophysics*, **195**, 319–346.

Rottura, A., Bargassi, G. M., Caggianelli, A., Delmoro, A., Visonà, D. & Tranne, C. A. (1998). Origin and significance of the Permian high-K calc-alkaline magmatism in the central-eastern Southern Alps, Italy. *Lithos*, **45**, 329-348.

Sabatier, H. (1991). Vaugnerites: special lamprophyre-derived mafic enclaves in some Hercynian granites from Western and Central Europe. In: Didier, J., Barbarin, B. (eds.). *Enclaves and Granite Petrology. Developments in Petrology*, *Elsevier, Amsterdam*, **13**, 47–62.

Sawyer, E. W. (1994). Melt segregation in the continental crust. *Geology*, **22**, 1019–1022.

Schaltegger, U. (1997). Magma pulses in the Central Variscan Belt: episodic melt generation and emplacement during lithospheric thinning. *Terra Nova*, **9**, 242-245.

Schmidberger, S. S. & Hegner, E. (1999). Geochemistry and isotope systematics of calc-alkaline volcanic rocks from the Saar-Nahe basin (SW Germany)-implications for Late-Variscan orogenic development. *Contributions To Mineralogy and Petrology,* **135**, 373-385.

Schmidt, M. W. (1992). Amphibole composition in tonalite as a function of pressure: an experimental calibration of the Al-in-hornblende barometer. *Contributions To Mineralogy and Petrology,* **110**, 304-310.

Sun, S. S. & McDonough, W. F. (1989). Chemical and isotopic systematics of oceanic basalts: implications for mantle composition and processes. In: Saunders, A. D. & Norry, M. (eds) *Magmatism in the Ocean Basins. Geological Society, London, Special Publications,* **42**, 313–345.

Tabaud, A. S., Rossi, P., Whitechurch, H., Skrzypek, E., Schulmann, K., Guerrot, C. & Paquette, J. L. (*submitted*). Chronology, petrogenesis and heat sources for successive Carboniferous magmatic events in the Variscan Vosges Mts (NE France).

Tera, F. & Wasserburg, G. (1972). U-Th-Pb systematics in three Apollo 14 basalts and the problem of initial Pb in lunar rocks. *Earth and Planetary Science Letters,* **14**, 281-304.

Thompson, R. N., Morrison, M. A., Hendry, G. L. & Parry, S. J. (1984). An assessment of the relative roles of crust and mantle in magma genesis an elemental approach. *Philosophical Transactions of the Royal Society,* **310**, 549-590.

Tobschall, H. J. (1974). Geochemische Untersuchungen zum stofflichen Bestand und Sedimentationsmilieu paläozoischer mariner Tone: Die Gehalte der Hauptelemente und der Spurenelemente Ni, Cu, Zn, Rb, Sr, Y, Zr, Nb und Ba in den Steiger Schiefern (Vogesen). Habilitationsschrift, Mainz, 142 p.

von Eller, J.P., Hameurt, J., Ruhland, M. (1971a). Evolutions métamorphiques et ignées dans les Vosges. *Comptes rendus de la Société Géologique de France*, 296–306.

von Eller, J.P., Lapania, E., Laduron, D., Béthune de, P. (1971b). Caractères polymétamorphiques des cornéennes de la région de Barr Andlau Vosges. *Bulletin du Service de la Carte Géologique d'Alsace-Lorraine,* **24**, 127–148.

von Eller, J. P., Blanalt, J. G., Hameurt, J. Hollinger, J. & Hoepffner, C. (1970). Carte géologique du socle vosgien, partie septentrionale. *Bulletin du Service de la Carte Géologique d'Alsace-Lorraine*, **23**, 5-28.

von Eller, J.P. (1969). Granitisation, dioritisation et métamorphisme dans les Vosges cristallines du Nord: V. Le massif d'Etival. *Bulletin du Service de la Carte Géologique d'Alsace-Lorraine,* **22**, 185–198.

von Eller, J.P. (1968). Granitisation, dioritisation et métamorphisme dans les Vosges cristallines du Nord: IV. La zone comprise entre Saales et Denipaire. *Bulletin du Service de la Carte Géologique d'Alsace-Lorraine,* **21**, 3–22.

von Eller, J. P. (1965). Granitisation, dioritisation et métamorphisme dans les Vosges cristallines du Nord. II.-La région comprise entre la faille vosgienne à l'Est de Grendelbruch et la vallée de la Bruche à la hauteur de Fouday-Rothau. *Bulletin du Service de la Carte Géologique d'Alsace-Lorraine*, **18**, 117-144.

von Eller, J.-P. (1964). Dioritisation, granitisation et métamorphisme dans les Vosges cristallines du Nord. I Région comprise entre la plaine d'Alsace, d'Andlau à Saint-Nabor et le Champ du Feu. *Bulletin du Service de la Carte Géologique d'Alsace-Lorraine*, **17**, 171-210.

Wickert, F. & Eisbacher, H. (1988). Two-sided Variscan thrust tectonics in the Vosges Mountains, north-eastern France. *Geodinamica Acta*, **2**, 101–120.

Wilson, M., Neumann, E. R., Davies, G. R., Timmerman, M. J., Heeremans, M. & Larsen, B. T. (2004). Permo-Carboniferous magmatism and rifting in Europe: introduction. In: Wilson, M., Neumann, E. R., Davies, G. R., Timmerman, M. J., Heeremans, M. & Larsen, B. T. (eds) *Permo-Carboniferous Magmatism and Rifting in Europe. Geological Society, London, Special Publications*, **223**, 1-10.

Chapitre 6 : Synthèse & Conclusion

A l'issue de présentation des différents évènements magmatiques affectant les deux domaines, Saxothuringien et Moldanubien, qui composent le Massif des Vosges, nous pouvons proposer un modèle d'évolution et de développement de la croûte continentale des Vosges en prenant en compte toutes les données acquises (pétrologie, géochimie, géochronologie et structurale) sur l'intégralité de ce massif.

1. Au Dévonien supérieur (Famennien : 375- 360 Ma)

C'est le début de la collision continentale entre les domaines Rhénohercynien et Saxothuringien (Fig1a). Cette collision permet la mise en place des ophiolites du Lizard et la nappe de Giessen (Leveridge & Shail, 2011; Franke, 2000).

- Dans les Vosges septentrionales, le retrait de la subduction rhénohercynienne a permis la mise en place d'un bassin d'arrière-arc où se mettent en place les tholéiites continentales du massif de Schirmeck en même temps que le dépôt des sédiments dévonien de la Bruche. Les données géochimiques (majeurs et traces) montrent que ces roches sont enrichies en éléments lithophiles et les analyses isotopiques ($+ 3 < \varepsilon_{Nd} < + 5$) suggèrent une faible contribution d'un manteau appauvri. Nous en avons déduit que ce bassin ne se créé pas par une remontée du manteau asthénosphérique mais plutôt au droit de la zone de subduction rhénohercynienne située plus au nord (Chapitre 5).

- Dans les Vosges moyennes et méridionales, le bassin d'arrière arc créé au droit de la subduction vers le nord de la Paléothéthys au sud et qui a fourni les blocs ophiolitiques observés dans la ligne des Klippes, se ferme. Nous avons vu que ces blocs ophiolitiques présentent des lithologies différentes, essentiellement des gabbros et des lherzolites. Les nouvelles datations (Sm-Nd roche totale et minéraux) donne un âge de 372 ± 18 Ma pour les gabbros. Les analyses géochimiques (majeurs et traces) ainsi que isotopiques ($\varepsilon_{Nd} = + 11.3$) montrent que ces gabbros se sont mis en place dans un bassin d'arrière-arc mature. Ce bassin se forme, sans doute, loin de la fosse de subduction située au Sud des Vosges moldanubiennes (Chapitre 2). La croûte saxothuringienne comprenant les protolites Protérozoique et Cambro-Ordovicien du magmatisme Mg-K est sous plaquée à la profondeur du Moho sous la croûte moldanubienne (Chapitre 3).

2. Au Carbonifère (Viséen : 340 Ma)

La croûte continentale rhénohercynienne rentre dans la zone de subduction située au Nord des Vosges et entraine une diminution d'angle de son pendage (Fig1b).

- Dans les Vosges septentrionales, le changement de pendage de la lithosphère océanique de l'océan rhéno-hercynien permet la mise en place du volcanisme calco-alcalin du massif de Rabodeau et vers 334 Ma (Viséen supérieur), la mise en place du volcanisme calco-alcalin de la bande médiane du Champ du Feu (ignimbrite de Saint-Nabor) dans le bassin d'arrière-arc précédemment ouvert. Ces phases volcaniques présentent des caractéristiques géochimiques (enrichissement en éléments lithophiles, anomalies en Ta, Nd et Ti) et isotopiques ($-3 < \varepsilon_{Nd} < +0.4$; $0.7047 < {}^{87}Sr/{}^{86}Sr < 0.7061$) qui les classent dans les roches magmatiques issus de la fusion partielle d'un manteau enrichi et métasomatisé par des fluides expulsés d'une zone de subduction (Chapitre5).

- Dans les Vosges moyennes et méridionales, les magmas Mg-K : CVMg-K (anciennement durbachite, granite des Crêtes, granite de Metzeral et granite de Goldbach) et SVMg-K (anciennement granite des Ballons, granite de Corravillers, complexe volcanique de Crémillot et rhyolite du Molkenrain) que nous avons datés entre 345-335 Ma (Viséen) sont issus de la fusion partielle par apport de chaleur par désintégration radiogénique d'un mélange de magmas entre le manteau lithosphérique enrichi et d'un protolithe Protérozoïque (anomalie en Sr ; $\varepsilon_{Nd} \sim -7$; $0.710 < {}^{87}Sr/{}^{86}Sr < 0.714$; zircon hérités) pour CVMg-K et d'un protolithe Cambro-Ordovicien (anomalie en P ; $-5 < \varepsilon_{Nd} < +1.4$; $0.705 < {}^{87}Sr/{}^{86}Sr < 0.708$; zircon hérités) pour SVMg-K. Nous avons aussi démontré que ce magmatisme est homogène d'un point de vue pétrographique (chimie homogène de la biotite), géochimique, isotopique et géochronologique dans toute la partie interne de la chaine varisque. L'association CVMg-K se retrouve dans le massif de la Forêt Noire (Durbach) et dans le massif de Bohème (Čertovo Břemeno) et l'association SVMg-K se retrouve aussi dans le massif de la Forêt Noire (Rand granite) ainsi que dans les massifs cristallins externes des Alpes et dans le bloc Corso-Sarde (Chapitre 3). Ces magmas sont accompagnés des granulites et gneiss variés du type Sainte-Marie-aux-Mines (Skrzypek, 2011) et remonte à différents niveaux de la croûte continentale moldanubienne. Cette remontée est verticale et est suivie par un aplatissement vertical comme l'atteste les données ASM (Chapitre 4) et les structures métamorphiques (Skrzypek, 2011).

Figure 1 : Schematic cross-section illustrating the development of magmatic intrusions and extrusions of the Northern, Central and Southern Vosges Mts between 360 and 340 Ma. Rhenohercynian domain after Levridge & Shail, 2011 at ~360 Ma and after Oncken et al., 2000 at ~340 Ma. Saxothuringian domain after Edel & Schulmann, 2009. *Figure ci-contre.*

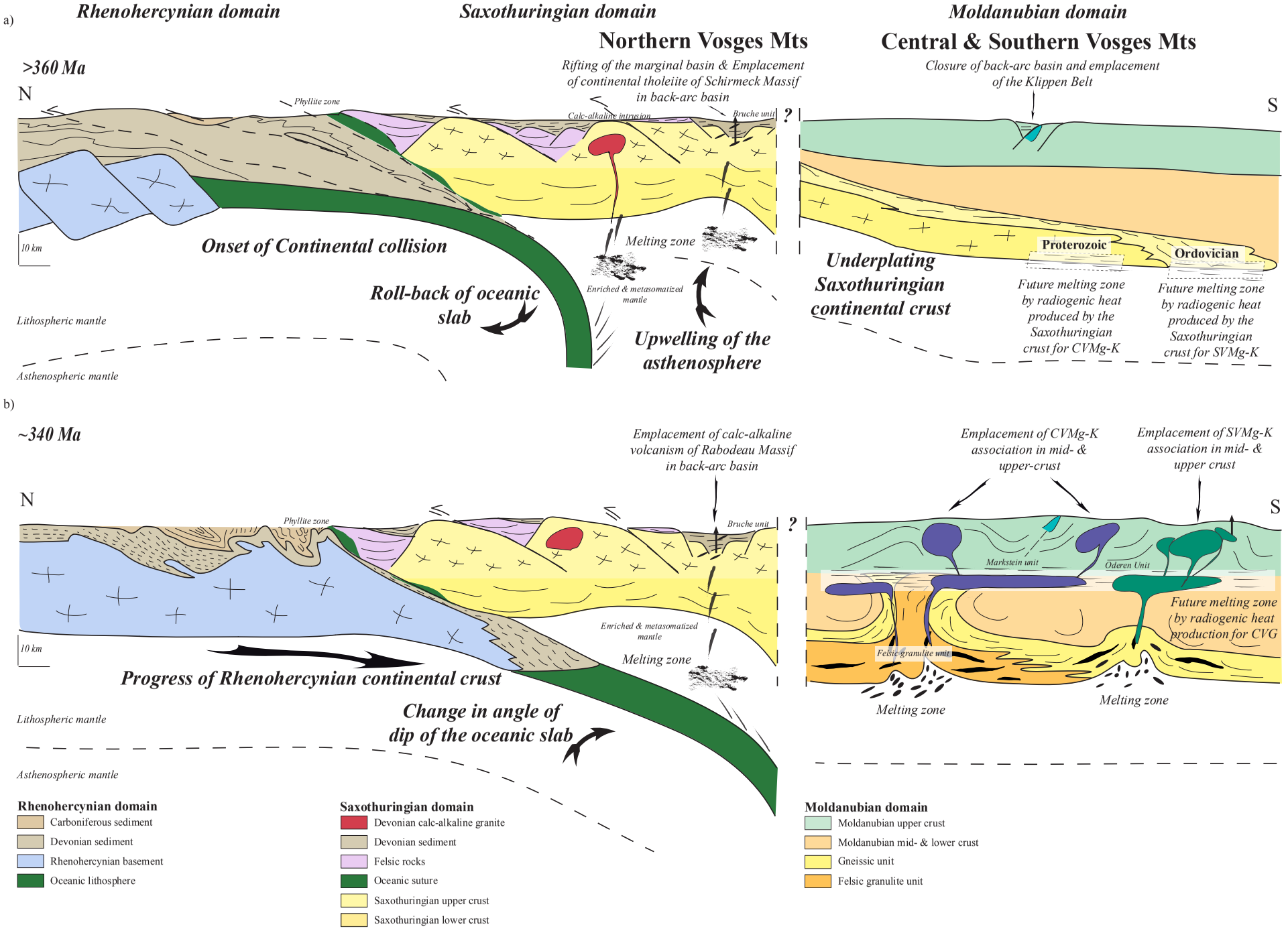
a)
Rhenohercynian domain
Saxothuringian domain
Moldanubian domain
Northern Vosges Mts
Central & Southern Vosges Mts
>360 Ma
N
S
Phyllite zone
Calc-alkaline intrusion
Bruche unit
?
Rifting of the marginal basin & Emplacement of continental tholeiite of Schirmeck Massif in back-arc basin
Closure of back-arc basin and emplacement of the Klippen Belt
10 km
Onset of Continental collision
Melting zone
Enriched & metasomatized mantle
Roll-back of oceanic slab
Upwelling of the asthenosphere
Lithospheric mantle
Asthenospheric mantle
Underplating Saxothuringian continental crust
Proterozoic
Ordovician
Future melting zone by radiogenic heat produced by the Saxothuringian crust for CVMg-K
Future melting zone by radiogenic heat produced by the Saxothuringian crust for SVMg-K
b)
~340 Ma
Emplacement of calc-alkaline volcanism of Rabodeau Massif in back-arc basin
Emplacement of CVMg-K association in mid- & upper-crust
Emplacement of SVMg-K association in mid- & upper crust
Markstein unit
Oderen Unit
Future melting zone by radiogenic heat production for CVG
Felsic granulite unit
Melting zone
Progress of Rhenohercynian continental crust
Change in angle of dip of the oceanic slab
Rhenohercynian domain
Carboniferous sediment
Devonian sediment
Rhenohercynian basement
Oceanic lithosphere
Saxothuringian domain
Devonian calc-alkaline granite
Devonian sediment
Felsic rocks
Oceanic suture
Saxothuringian upper crust
Saxothuringian lower crust
Moldanubian domain
Moldanubian upper crust
Moldanubian mid- & lower crust
Gneissic unit
Felsic granulite unit

3. Au Carbonifère (Viséen supérieur : 330 Ma)

La croûte continentale rhénohercynienne avance dans la zone de subduction (Fig2a). La rupture de la lithosphère océanique rhénohercynienne (slab-break-off) peut être déjà amorcée.

- Dans les Vosges septentrionales, cette avancée de la croûte continentale rhénohercynienne entraine la fermeture du bassin d'arrière-arc lors de la mise en place des diorites (Neuntelstein et Muckenbach), granodiorites (Hohwald) calco-alcaline (Chapitre 5) formant la partie sud du Champ du Feu ainsi que du granite calco-alcalin de Soultz-sous-Forêt plus au nord (expression plutonique du volcanisme de la Bande Médiane du Champ du Feu). Les données ASM (Edel et al, submitted) montrent que cet ensemble se met en place dans un contexte de compression régionale.

- Dans les Vosges moyennes et méridionales, par modélisation thermique, nous avons montré que la mise en place du magmatisme Mg-K dans la croûte continentale moldanubienne entraine la fusion partielle de la croûte moyenne gneissique et de sa couverture sédimentaire de type grauwacke (faciès Culm) d'âge Dévonien supérieur à Carbonifère inférieur (Chapitre 3).

4. Au Carbonifère (Namurien : 320 Ma)

La croûte continentale rhénohercynienne arrive dans la zone de fusion. La rupture de la lithosphère océanique rhénoherynienne (slab break-off) permet la remontée de manteau asthénosphérique chaud (Fig2b).

- Dans les Vosges septentrionales, l'arrivée de la croûte rhénohercynienne est montrée par la mise en place du granite de la partie nord du Champ du Feu (granite de Belmont, Fouday Waldersbach ; Chapitre 5) que nous avons daté à 319 Ma. Les données géochimiques montrent que ce granite fait partie des séries dites « calco-alcaline riche en potassium » par son enrichissement en éléments incompatibles (U, Th et K) qui montre une contribution crustale d'âge dévonien (zircons hérités) plus importante dans sa source que celle des séries calco-alcaline (diorite, granodiorite). Les données ASM (Edel et al., submitted) montrent que la mise en place de ce granite se fait lorsque le bassin d'arrière-arc est complètement fermé.

- Dans les Vosges moyennes et méridionales, le Granite Central Vosgien (anciennement granite fondamental, granites Brézouard-Bilstein-Thannenkirch, leucogranite de Dambach et du Valtin, granite du Bramont-Lac Vert…) que nous avons daté entre 330 Ma et 320 Ma, est formé. Les analyses géochimiques et isotopiques nous ont révélé que ce granite peut être divisé en deux groupes séparés par le système de la faille de Sainte-Marie-aux-Mines et la dislocation de Bilstein (Chapitre 3). Le groupe (W-CVG) situé à l'Ouest et au Nord de ce système provient de la fusion partielle d'un mélange de magma Mg-K et de roche gneissique (anomalie en Sr ; $-6.8 < \varepsilon_{Nd} < -6.1$; $0.715 < {}^{87}Sr/{}^{86}Sr < 0.720$; zircon hérités) alors que le groupe situé à l'Est et au Sud du système provient de la fusion partielle d'un mélange de magma Mg-K et de la couverture sédimentaire de la croûte moldanubienne (anomalie en P ; $-5.4 < \varepsilon_{Nd} < -4.1$; $0.709 < {}^{87}Sr/{}^{86}Sr < 0.712$; zircon hérités). La mise en place de ces granites au niveau actuel se fait par l'intermédiaire d'une faille de décrochement orientée E-W qui pente vers le S (Chapitre 4).

Figure 2 : Schematic cross-section illustrating the development of magmatic intrusions and extrusions of the Northern, Central and Southern Vosges Mts between 330 and 320 Ma. Rhenohercynian domain after Oncken et al., 2000. Saxothuringian domain after Edel & Schulmann, 2009. *Figure ci-contre.*

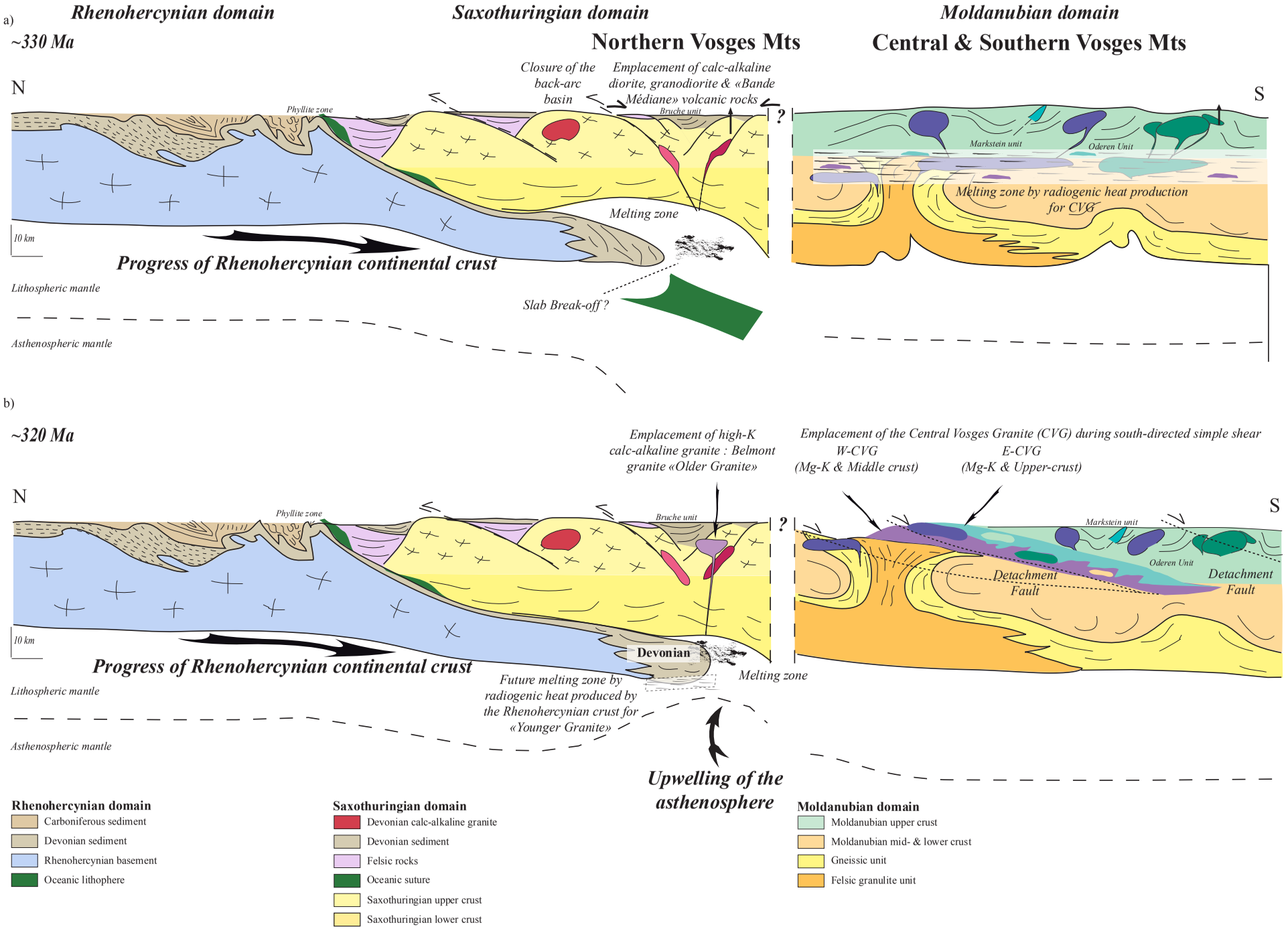
a)
Rhenohercynian domain
Saxothuringian domain
Moldanubian domain
~330 Ma
Northern Vosges Mts
Central & Southern Vosges Mts
N
S
Closure of the back-arc basin
Emplacement of calc-alkaline diorite, granodiorite & «Bande Médiane» volcanic rocks
Phyllite zone
Bruche unit
?
Markstein unit
Oderen Unit
Melting zone by radiogenic heat production for CVG
Melting zone
10 km
Progress of Rhenohercynian continental crust
Lithospheric mantle
Slab Break-off ?
Asthenospheric mantle
b)
~320 Ma
Emplacement of high-K calc-alkaline granite : Belmont granite «Older Granite»
Emplacement of the Central Vosges Granite (CVG) during south-directed simple shear
W-CVG
(Mg-K & Middle crust)
E-CVG
(Mg-K & Upper-crust)
N
S
Phyllite zone
Bruche unit
?
Markstein unit
Oderen Unit
Detachment Fault
Detachment Fault
10 km
Devonian
Progress of Rhenohercynian continental crust
Melting zone
Lithospheric mantle
Future melting zone by radiogenic heat produced by the Rhenohercynian crust for «Younger Granite»
Asthenospheric mantle
Upwelling of the asthenosphere
Rhenohercynian domain
Carboniferous sediment
Devonian sediment
Rhenohercynian basement
Oceanic lithophere
Saxothuringian domain
Devonian calc-alkaline granite
Devonian sediment
Felsic rocks
Oceanic suture
Saxothuringian upper crust
Saxothuringian lower crust
Moldanubian domain
Moldanubian upper crust
Moldanubian mid- & lower crust
Gneissic unit
Felsic granulite unit

5. Au Carbonifère (Westphalien : 310 Ma)

La croûte rhénohercynienne est sous-plaquée au niveau du Moho sous la plaque saxothuringienne (Fig3a).

- Dans les Vosges septentrionales, le sous-plaquage de roches dévoniennes de la croûte rhénohercynienne a permis la fusion partielle, une des sources du magmatisme Mg-K (granite de Senones, granite de Natzwiller et granite d'Andlau) qui s'intruse dans les formations précédentes (Chapitre 5). Les caractéristiques géochimiques de ce magmatisme Mg-K (anomalie en P ; $-5.4 < \varepsilon_{Nd} < -4.1$; $0.709 < {}^{87}Sr/{}^{86}Sr < 0.712$; zircon hérités) sont proches de celle de l'association SVMg-K Les données ASM (Edel et al., submitted) montre que ces granites se mettent en place dans un niveau supérieur de la croûte continentale par une faille de décrochement de direction ENE-WSW qui pente vers le SSE. Cette direction est celle déjà observée pour la mise en place plus au sud des migmatites (Schulmann et al., 2009) et est proche de la direction de celle permettant la mise en place du Granite Central Vosgien et du magmatisme Mg-K au niveau actuel (Chapitre 4).

Nous n'avons actuellement pas de données nous permettant de dire si ces décrochements se font par l'intermédiaire d'un système de failles qui progressent du Sud vers le Nord de 320 Ma à 310 Ma ou par l'intermédiaire d'une seule faille de décrochement. Cette direction de décrochement est reconnue dans d'autres massifs de la chaine varisque (Verner et al., 2006 ; Žák et al., 2011).

6. Au Permien (290 Ma)

C'est le stade final de l'orogène varisque (Fig3b) avec une relaxation des forces de volume, dans toute la chaine (collapse orogénique). Ceci entraine la formation de zones d'extension qui sont suivies par une remontée de chaleur asthénosphérique. Cette remontée de chaleur est mise en évidence par la perpétuité du volcanisme durant le Permien dans toute l'Europe (Wilson et al., 2004).

- Dans les Vosges septentrionales, la mise en place du magmatisme Mg-K entraine la fusion partielle de la croûte continentale saxothuringienne et permet dans un contexte d'extension la mise en place du leucogranite de Kagenfels et du volcanisme du Nideck-Donon (rhyolites et tufs) présentant des caractéristiques géochimique de source purement crustale (fort enrichissement en éléments lithophiles et en éléments incompatibles) (Chapitre 5).

- Dans les Vosges moyennes et méridionales, ce volcanisme se met en place dans le bassin de Villé au sud de la faille de Lalaye-Lubine.

Figure 3 : Schematic cross-section illustrating the development of magmatic intrusions and extrusions of the Northern, Central and Southern Vosges Mts between 310 and 290 Ma. Rhenohercynian domain after Oncken et al., 2000. Saxothuringian domain after Edel & Schulmann, 2009. *Figure ci-contre*.

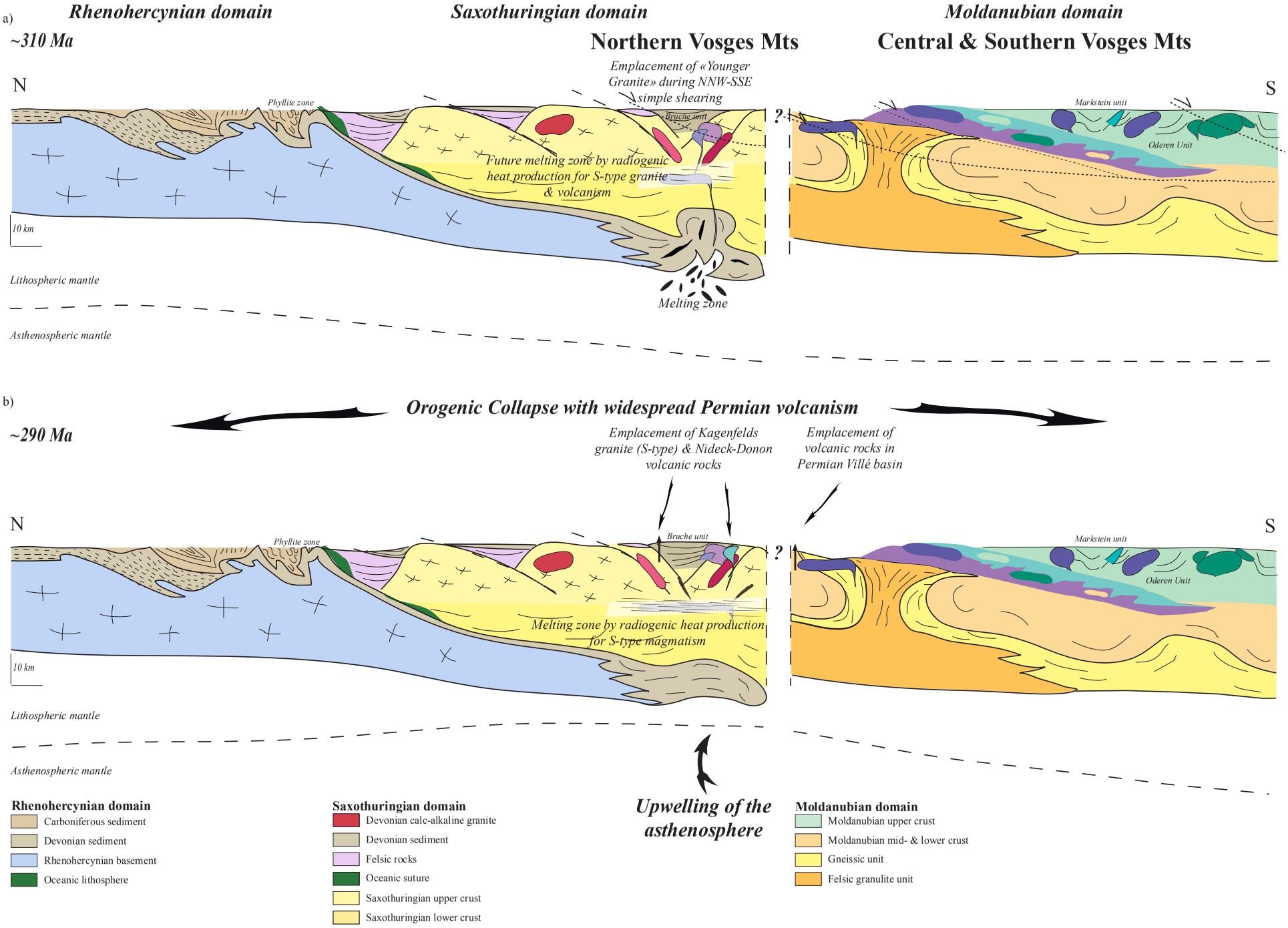
a)
Rhenohercynian domain
Saxothuringian domain
Moldanubian domain
~310 Ma
Northern Vosges Mts
Central & Southern Vosges Mts
N
S
Emplacement of «Younger Granite» during NNW-SSE simple shearing
Phyllite zone
Bruche unit
Future melting zone by radiogenic heat production for S-type granite & volcanism
Markstein unit
Oderen Unit
?
10 km
Lithospheric mantle
Melting zone
Asthenospheric mantle
b)
Orogenic Collapse with widespread Permian volcanism
~290 Ma
Emplacement of Kagenfelds granite (S-type) & Nideck-Donon volcanic rocks
Emplacement of volcanic rocks in Permian Villé basin
N
S
Phyllite zone
Bruche unit
Markstein unit
Oderen Unit
?
Melting zone by radiogenic heat production for S-type magmatism
10 km
Lithospheric mantle
Asthenospheric mantle
Upwelling of the asthenosphere
Rhenohercynian domain
Carboniferous sediment
Devonian sediment
Rhenohercynian basement
Oceanic lithosphere
Saxothuringian domain
Devonian calc-alkaline granite
Devonian sediment
Felsic rocks
Oceanic suture
Saxothuringian upper crust
Saxothuringian lower crust
Moldanubian domain
Moldanubian upper crust
Moldanubian mid- & lower crust
Gneissic unit
Felsic granulite unit

Néanmoins, quelques questions restent encore à élucider pour améliorer ce modèle de mise en place du Massif des Vosges :

- Quel est l'âge précis (U-Pb sur zircons) du volcanisme du Massif de Schirmeck-Rabodeau (zircons arrachés lors du polissage) ?

- ***La faille de Lalaye-Lubine*** :

Est-ce une zone de suture entre le domaine Saxothuringien et le domaine Moldanubien ?

Est-ce une zone de suture entre le domaine Teplà-Barradienne et le domaine Moldanubien ?

Est-ce un détachement lors de l'orogène varisque ?

- ***Les Vosges septentrionales*** :

A quel domaine (Moldanubien, Saxothuringien ou Teplà-Barrandien) appartiennent-elles ?

Si elles appartiennent au domaine Moldanubien, est-ce que le bassin d'arrière-arc dévonien où se mettent en place les tholéiites continentales et celui qui a fournis les blocs ophiolitiques de la ligne des Klippes ne formeraient qu'un seul et même bassin ?

En conclusion, deux successions d'évènements magmatiques identiques, mais décalées dans le temps, caractérisent les domaines Moldanubien (de 360 à 320 Ma) et Saxothuringien (de 335 à 295 Ma) de la partie Est de l'orogène varisque (Vosges, Forêt Noire, Massif de Bohème, Alpes et Corse-Sardaigne). Ces successions d'évènements magmatiques commencent par un magmatisme calco-alcalin suivi par un magmatisme dit « calco-alcalin riche en potassium » puis un magmatisme Magnésio-Potassique et enfin un magmatisme d'origine crustale.

Ces deux successions ne sont pas toujours complètes tout le long des deux domaines. La succession dans le domaine Moldanubien est complète dans le Massif de Bohème (Sázava, Blatná, Čertovo Břemeno et South Bohemian Batholith) et vers l'Ouest cette succession n'est composée que du magmatisme Mg-K et du magmatisme d'origine crustale. Alors que pour le domaine Saxothuringien, la succession est complète dans le Massif des Vosges et est incomplète en allant vers l'Est.

Les processus principaux liés à ces successions d'évènements magmatiques qui se sont mis en place dans un espace restreint, sont :

- d'une part, la progression des croûtes continentales Saxothuringienne et Rhenohercynienne subduites au niveau du Moho sous les croûtes continentales Moldanubienne et Saxothuringienne respectivement, qui permet la transition entre le magmatisme calco-alcalin et le magmatisme calco-alcalin riche en potassium

- et d'autre part, l'apport de chaleur par désintégration des éléments radiogéniques (U, Th, K) présents dans les croûtes continentales subduites et sous-plaquées au niveau du Moho (formation du magmatisme Magnésio-potassique) et dans le magmatisme Magnésio-potassique (formation du magmatisme d'origine crustale).

Bibliographie: Introduction & Synthèse

Altherr, R., Holl, A., Hegner, E., Langer, C. & Kreuzer, H., (2000). High-potassium, calc-alkaline I-type plutonism in the European Variscides: northern Vosges (France) and northern Schwarzwald (Germany). *Lithos*, **50**, 51-73.

Barbarin, B. (1990). Granitoids: main petrogenetic classifications in relation to origin and tectonic setting. *Geological Journal*, **25**, 227–238.

Condie, K. C. (1998). Episodic continental growth and supercontinents: a mantle avalanche connection. *Earth and Planetary Science Letters*, **163**, 97–108.

Downes, H., Shaw, A., Williamson, B. J. & Thirlwall, M. F. (1997). Sr, Nd and Pb isotopic evidence for the lower crustal origin of Hercynian granodiorites and monzogranites, Massif Central, France. *Chemical Geology*, **136**, 99-122.

Downes, H. & Duthott, J. L. (1988). Isotopic and trace element arguments for the lower crustal origin of Hercynian granitoids and pre-Hercynian orthogneisses, Massif Central (France). *Chemical Geology*, **68**, 291-308.

Edel, J. B., Schulmann, K., Skrzypek, E. & Cocherie, A. (submitted). Coupling between oblique subduction zone dynamics and transtensional emplacement of magmatic arc exemplified by AMS and paleomagnetic study (N Vosges, E France).

Edel, J. B. & Schulman, K. (2009). Geophysical constraints and model of the ‘‘Saxothuringian and Rhenohercynian subductions–magmatic arc system’’ in NE France and SW Germany. Bulletin de la Société Géologique de France, 180, 545–558.

Floyd, P. A. & Winchester, J. A. (1975). Magma type and tectonic setting discrimination using immobile elements. *Earth and Planetary Science Letters*, **27**, 211–218.

Foerster, H. J., Tischendorf, G. & Trumbull, R. B. (1997). An evaluation of the Rb vs. (Y+Nb) discrimination diagram to infer tectonic setting of silicic igneous rocks. *Lithos*, **40**, 261–293.

Franke, W. (2000). The mid-European segment of the Variscides: Tectonostratigraphic units, terrane boundaries and plate tectonic evolution, In: Franke W., Haak V., Oncken O., Tanner D. (eds). *Orogenic processes; quantification and modelling in the Variscan Belt*. *Geological Society Special Publications*, **179**, 35-56.

Kossmat, F. (1927). Gliederung der varistischen Gebirgsbaues. *Abhandlungen des Sächsischen geologischen Landesamts,* **1**, 1-39.

Kratinová, Z., Schulmann, K., Edel, J. B., Ježek, J. & Schaltegger, U. (2007). Model of successive granite sheet emplacement in transtensional setting: Integrated microstructural and anisotropy of magnetic susceptibility study. *Tectonics,* **26**, TC6003.

Kuno, H. (1968). Differentiation of basalt magmas. In, Hess, H. H., and Poldervaart, A. (Eds.) *Basalts (Vol. 2): New York (Wiley)*, pp. 623-688.

Leveridge, B. E. & Shail, R. K. (2011). The Gramscatho Basin, south Cornwall, UK: Devonian active margin successions. *Proceedings of the Geologists' Association*, **122**, 568-615.

Maniar, P. D. & Piccoli, P. M. (1989). Tectonic discrimination of granitoids. *Geological Society of America Bulletin*, **101**, 635–643.

Oncken, O., Plesch, A., Weber, J., Ricken, W. & Scharder, S. (2000). Passive margin detachment during arc-continental collision (Central European Variscides). In: Franke W., Haak V., Oncken O., Tanner D. (eds). *Orogenic processes; quantification and modelling in the Variscan Belt. Geological Society Special Publication*, **179**, 199-216.

Pearce, J. A., Harris, N. B. W. & Tindle, A. G. (1984). Trace element discrimination diagrams for the tectonic interpretation of granitic rocks. *Journal of Petrology*, **25**, 956–983.

Petro, W.L., Vogel, T.A. & Wilband, J.T. (1979). Major-element chemistry of plutonic rock suites from compressional and extensional plate boundaries. *Chemical Geology*, **26**, 217–235.

Pin, C. & Duthou, J. L. (1990). Sources of Hercynian granitoids from the French Massif Central: Inferences from Nd isotopes and consequences for crustal evolution. *Chemical Geology*, **83**, 281-296.

Pitcher, W. S. (1983). Granite Type and Tectonic Environment. In: Hsu, K. (ed.) *Mountain Building Processes, Academic Press, London*, pp. 19–40.

Schaltegger, U., Fanning, C. M., Günther, D., Maurin, J. C., Schulmann, K. & Gebauer, D. (1999). Growth, annealing and recrystallization of zircon and preservation of monazite in high-grade metamorphism: conventional and in situ U–Pb isotope cathodoluminescence and microchemical evidence. *Contributions to Mineralogy and Petrology*, **134**, 186–201

Schaltegger, U., Schneider, J. L., Maurin, J. C. & Corfu, F. (1996). Precise U–Pb chronometry of 345–340 Ma old magmatism related to syn-convergence extension in the Southern Vosges (Central Variscan Belt). *Earth and Planetary Science Letters*, **144**, 403–419.

Schneider J. L. (1990). Enregistrement de la dynamique varisque dans les bassins volcano-sédimentaires dévono-dinantiens: exemple des Vosges du Sud (zone moldanubienne). Ph.D. thesis, University of Strasbourg, 222 p.

Schulmann, K., Edel, J. B., Hasalová, P., Cosgrove, J. Ježek, J. & Lexa, O. (2009). Influence of melt-induced mechanical anisotropy on the magnetic fabrics and rheology of deforming migmatites, Central Vosges, France. *Journal of Structural Geology,* **31**, 1223-1237.

Schulmann, K., Schaltegger, U. Ježek, J., Thompson, A. L. & Edel, J. B. (2002). Rapid burial and exhumation during orogeny: thickening and synconvergent exhumation of thermally weakened and thinned crust (Varican orogen in Western Europe). *American Journal of Science*, **302**, 856-879.

Skrzypek, E. (2011). Contribution structurale, pétrologique et géochronologique à la tectonique intracontinentale de la chaîne hercynienne d'Europe (Sudètes, Vosges). Ph.D. thesis, University of Strasbourg, 381 p.

Shaw, A., Downes H. & Thirlwall, M. F. (1993). The quartz-diorites of Limousin: Elemental and isotopic evidence for Devono-Carboniferous subduction in the Hercynian belt of the French Massif Central. *Chemical Geology*, **107**, 1-18.

Verner, K., Žák, J., Hrouda, F. & Holub, F. V. (2006). Magma emplacement during exhumation of the lower- to mid-crustal orogenic root: The Jihlava syenitoid pluton, Moldanubian Unit, Bohemian Massif. *Journal of Structural Geology*, **28**, 1553-1567.

Williamson, B. J., Shaw, A., Downes, H. & Thirlwall, M. F. (1996). Geochemical constraints on the genesis of Hercynian two-mica leucogranites from the French Massif Central. *Chemical Geology*, **127**, 25-42.

Wilson, M., Neumann, E. R., Davies, G. R., Timmerman, M. J., Heeremans, M. & Larsen, B. T. (2004). Permo-Carboniferous magmatism and rifting in Europe: introduction. In: Wilson, M., Neumann, E. R., Davies, G. R., Timmerman, M. J., Heeremans, M. & Larsen, B. T. (eds) *Permo-Carboniferous Magmatism and Rifting in Europe. Geological Society, London, Special Publications*, **223**, 1-10.

Žák, J., Verner, K., Finger, F., Faryad, S. W., Chlupáčová, M. & Veselovský, F. (2011). The generation of voluminous S-type granites in the Moldanubian unit, Bohemian Massif, by rapid isothermal exhumation of the metapelitic middle crust. *Lithos*, **121**, 25-40.

Annexes

Int J Earth Sci (Geol Rundsch) (2012) 101:803–817
DOI 10.1007/s00531-011-0711-x

ORIGINAL PAPER

AMS record of brittle dilation, viscous-stretching and gravity-driven magma ascent in area of magma-rich crustal extension (Vosges Mts., NE France)

Zuzana Kratinová · Karel Schulmann · Jean-Bernard Edel · Anne-Sophie Tabaud

Received: 12 September 2010 / Accepted: 28 August 2011 / Published online: 17 September 2011

Abstract Orogenic compression-related fabrics (~340–335 Ma) were reworked during regional extensional deformation (~328–325 Ma) in a large anatectic crustal domain of the Central Vosges (NE France). The extension was first accommodated by brittle dilation affecting vertically anisotropic high-grade rocks associated with emplacement of subvertical granitic sheets. The AMS fabric of granitoids is consistent with highly partitioned transtensional deformation marked by alternations of flat and steep foliations and development of orthogonal lineations. This deformation passes to top-to-the-southwest ductile shearing expressed in southerly migmatitic middle crust. The AMS fabric revealed moderately west-dipping foliations bearing subhorizontal NNW–SSE-trending lineations and predominantly plane strain to prolate shapes. This fabric pattern is interpreted as a viscous response of stretched partially molten crust during continuous ductile extension. Vertical ascent of voluminous granites and stoping of the upper crust occurs further south. This gravity ascent triggered by extension leads to development of south-dipping AMS foliations, south-plunging lineations and oblate fabrics in various crustal granites. Vertical shortening related to ascent of these (~325 Ma) granitoids and persistent N–S stretching is responsible for reworking and remelting of originally vertical compression-related fabric in roof supracrustal granites (~340 Ma) and development of highly prolate fabrics in these rocks. This work shows that the finite shape of AMS fabric ellipsoid is highly sensitive to both strain regime and superpositions of orthogonal deformation events.

Keywords Anisotropy of magnetic susceptibility · Crustal extension · Magmatic fabrics · Carboniferous

Z. Kratinová (✉)
Geophysical Institute, Czech Academy of Sciences, Boční II/1401, Praha 4 14131, Czech Republic
e-mail: kratinova@ig.cas.cz

K. Schulmann · J.-B. Edel
Institut Physique du Globe, EOST, UMR 7517 Université Louis Pasteur, Strasbourg cedex, France

A.-S. Tabaud
Centre de Géochimie de la Surface, EOST, UMR 7516 Université Louis Pasteur, Strasbourg cedex, France

Introduction

Crustal extension is an integral part of orogenic evolution representing the final event in tectono-thermal histories of the Variscan belt of the Western Europe (Burg et al. 1994). Generally, the late orogenic post-thickening extension is characterized by thermal re-equilibration (England and Thompson 1986), providing conditions suitable for high-temperature low-pressure metamorphism associated with crustal magmatism. Modern research in domain of extensional tectonics has brought new insights into extensional structural features (Rey et al. 2001), but understanding of structural and mechanical relationship with the magma emplacement dynamics is still required.

The Carboniferous extensional tectonics linked with the emplacement of voluminous bodies of crustal magmas has been recognized in the Variscan belt of the Western Europe for two decades (e.g. Faure 1995; Ledru et al. 2001). The present paper discusses structural data from the Central Vosges Mountains (NE France), where the extensional deformation has been already described and well characterized (Rey et al. 1992). This study is intended to investigate relations between tectonic switches characterized by

alternations of compressional and extensional deformation and associated dynamics of magmatism at crustal scale, recorded in the final fabric pattern of granitoids.

Internal fabric pattern of magmatic rocks represents critical memory about emplacement and ascent processes, regional deformation and its successions in time. Although their interpretation may be still controversial (Paterson et al. 1998), the systematic mapping of magmatic fabric patterns in larger scale is required in order to understand the flow and type of deformation related to orogenic processes, such as exhumation of lower crustal material and its subsequent deformation history. The common problem in magmatic structural geology is the lack of strain markers, and therefore, the application of anisotropy of magnetic susceptibility (AMS) has recently become very useful and extensively used in magmatic regions (e.g. Bouchez et al. 1990).

Anisotropy of magnetic susceptibility (AMS; Tarling and Hrouda 1993) has become a powerful tool in structural analysis providing information about igneous fabrics and is nowadays broadly accepted method, which is systematically used for structural mapping of granites (Bouchez 1997). This method provides integral information of fabric pattern, which can be potentially correlated with finite strain (Hrouda 1993). Recent numerical models (Benn 1994; Schulmann et al. 2009; Kratinová et al. 2010) show that the AMS is very sensitive to small strain increments, which is reflected in the final shape and intensity of AMS fabrics.

The aim of this study is to document a relationship between magmatic fabrics related to regional extensional deformation superposed on magmatic fabrics produced during previous compressional event. The present-day erosion level exposes the juxtaposed lower crustal and supracrustal rocks, which show different structural record related to compressional and extensional cycles. Finally, the study discusses the fabric record within the large anatectic domain in the Central Vosges in terms of combined extensional tectonics and gravity-driven ascent of partially molten crust.

Geological setting

Regional geological framework

The studied area is located in the central zone of the Vosges massif (Fig. 1a), which consists of central high-grade domain bordered to the south and north by the Paleozoic volcano-sedimentary sequences (Fluck 1980; Fluck et al. 1987) (Fig. 1b). The volcano-sedimentary basins were formed at 345–340 Ma in the south (Schaltegger et al. 1996) and before 331 Ma in the north (Hess et al. 1995). The central domain is composed of high-grade

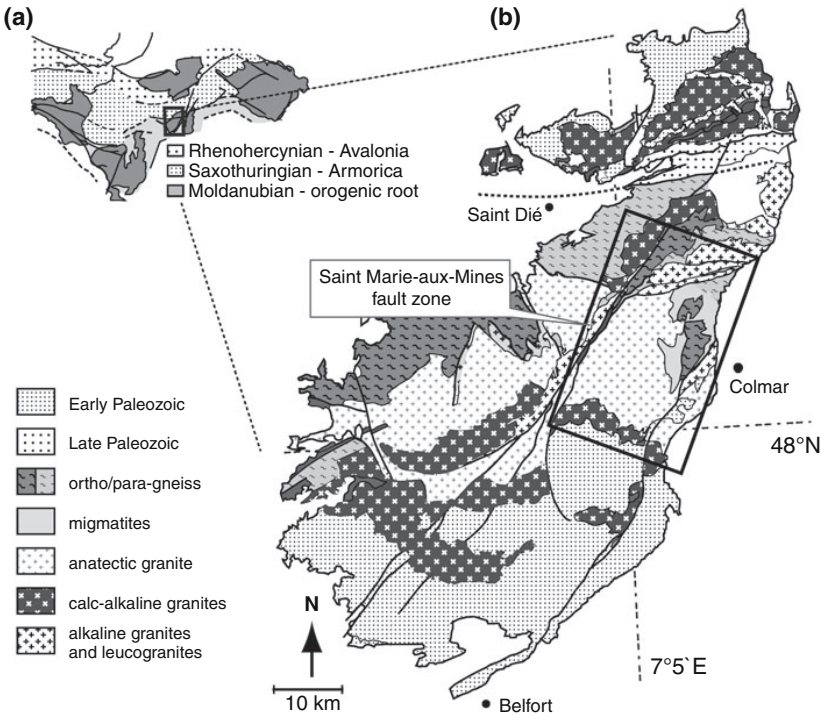

Fig. 1 Geological map and the position of the Vosges Mountains (NE France) within the European Variscides. **a** Location of the study area in the framework of the European Variscides (*black square marks* the Vosges Mountains), modified after Edel and Weber (1995). **b** Simplified geological map of the Vosges Mountains. The region of interest is demarcated by the *black rectangle* and details are shown in Fig. 2

gneisses, granulite rocks, voluminous granites and migmatites corresponding to the narrow (~ 50 km wide) root zone of the Variscan orogen (Schulmann et al. 2002).

The high-grade gneiss unit in the east of the Saint Marie-aux-Mines fault zone (Figs. 1b and 2) is made up of a granulite facies unit including lenses of peridotites, felsic granulites and amphibolites (Fluck 1980). The underlying mid-crustal rocks are composed of monotonous paragneisses (Rey et al. 1989), which were intruded by ENE–WSW-trending crustal granite intrusions—the BBTC complex (the Brézouard, Bilstein and Thannenkirch granites; Fig. 1b) (Fluck 1980; Kratinová et al. 2007). South of the BBTC intrusive complex, the adjacent monotonous paragneiss shows high degree of partial melting; this area is built of the migmatite complex and several bodies of felsic orthogneiss (Fluck 1980; Schulmann et al. 2009). The degree of partial melting increases to the south and west with migmatites being progressively evolved into heterogeneous granites (so called anatectic granite, Fig. 1b). This granitic domain is limited to the south by the low-grade to non-metamorphosed upper Devonian to Visean volcano-sedimentary sequences—the Markstein unit, which is intruded by the calc-alkaline the Crêtes granites.

Within the migmatitic unit (Fig. 2), two major lithologies have been distinguished. The orthogneiss bodies represented by highly annealed, recrystallized solid-state rock related to high-grade granulitic or orthogneiss protolith subjected to a partial melting (Fluck 1980; Schulmann et al. 2009). The surrounding rocks are represented by large domain composed of meta- and diatexites associated with

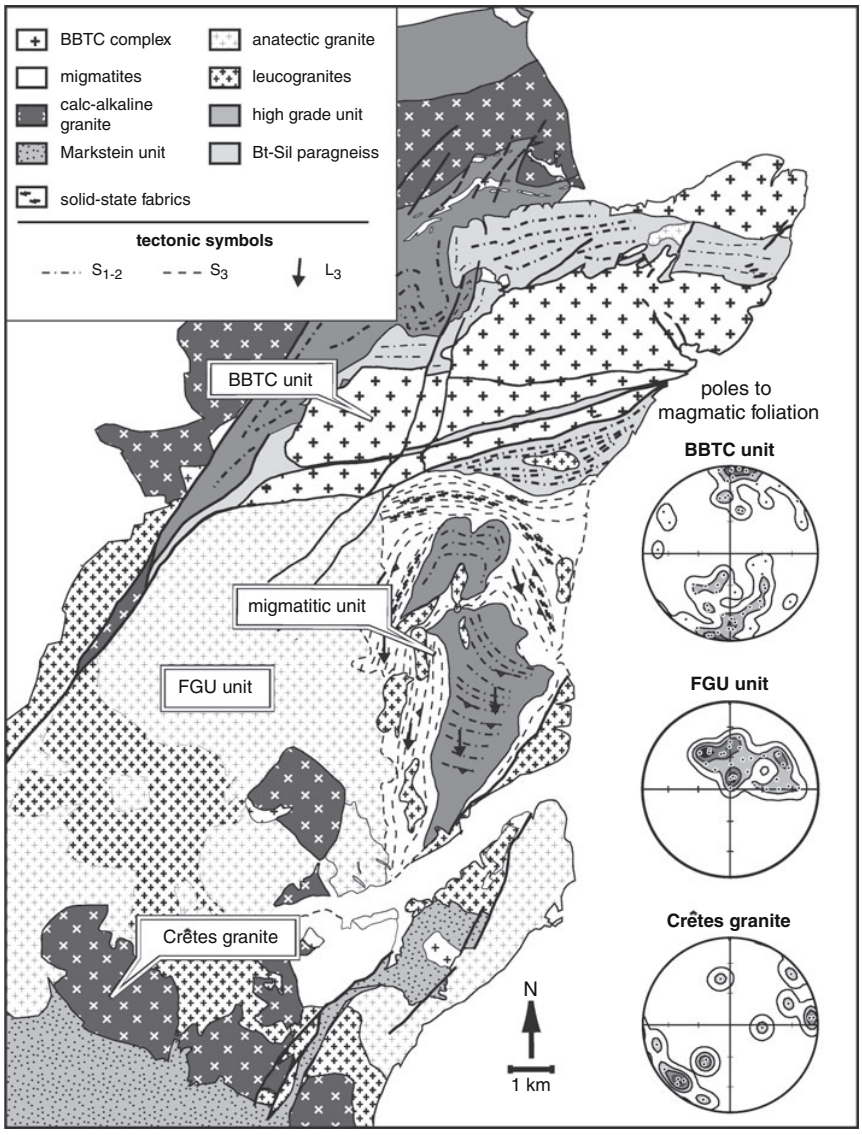

Fig. 2 Detailed map of the studied area, close-up of the Fig. 1. The map shows the southern anatectic unit, which is limited in the north by the BBTC complex and to the south by the sedimentary basin (the Markstein unit). Contoured stereonets (equal-area lower hemisphere projection) of poles to S_2 foliation planes

local intrusions of porphyritic to medium-grained granite veins. These migmatites and granitoids have been related to partial melting of a fertile metasedimentary protolith (Schaltegger et al. 1999; Schulmann et al. 2009). The major part of the studied area is formed by the anatectic granites (so called granite fundamentale), which are represented by the heterogeneous crustal granites and leucogranites (Hameurt 1967; Eller et al. 1970). In order to distinguish the migmatitic unit from the large unit of heterogeneous granite, we introduce the term fundamental granite unit (FGU) for the latter unit.

Geochronologic and pressure–temperature constrains

The granulites of the gneiss unit reveal an early high-grade stage (temperature = 750°C, pressure = 9–11 kbar) (Rey et al. 1989), followed by re-equilibration in amphibolite facies conditions (temperature = 650°C, pressure = 4–6 kbar) (Rey et al. 1989, 1992). South of the BBTC, the adjacent Crd-Bt-Sil migmatized paragneiss is characterized by pressure and temperature conditions of 640 ± 80°C and ~6–4 kbar (Latouche et al. 1992). The petrological data suggest 'clockwise' retrograde pressure–temperature path, including high-temperature decompression documented by the growth of late poikilitic cordierite (Rey et al. 1992). The published U–Pb geochronological data compiled in Table 1 compare the ages determined by the U–Pb geochronology on zircon and monazite with the K–Ar and ^{39}Ar–^{40}Ar analyses. The age of early metamorphism was determined in various granulites using U–Pb zircon method at around 335 Ma (Schaltegger et al. 1999). Re-equilibration of the high-grade orthogneiss occurred at 327.9 ± 4.4 Ma (Schaltegger et al. 1999).

Two types of granitoids are distinguished within the Central Vosges. First group of granites intruded shallow crustal units and produced a contact metamorphism in the sediments of the southern sedimentary basin (the Markstein unit). This group comprises the Crêtes granite, which occupies the south region of the studied area (Fig. 2) and which was constrained by the U–Pb at 340 ± 1 Ma (Schaltegger et al. 1999). The second group of granites crystallized between 330 and 325 Ma. This group comprises the granites of the migmatitic unit, dated at 325.8 ± 4.8 Ma (Schaltegger et al. 1999), which is synchronous with the crystallization ages of surrounding crustal granites of the FGU. This age is also contemporaneous with the intrusion of the leucogranites of the BBTC unit (Kratinová et al. 2007; Schulmann et al. 2002). K–Ar cooling ages from the migmatitic unit and from the BBTC yield consistent ages of ~323 Ma for muscovite and slightly older ^{39}Ar–^{40}Ar muscovite cooling ages similar to those in the granulite gneiss unit ranging between 327 and 332 Ma (Boutin et al. 1995). The 340-Ma-old Crêtes

Table 1 Summary table of published geochronological data. The Ar^{40}–Ar^{39} data are from Boutin et al. (1995), the U–Pb zircon and monazite data from Schaltegger et al. (1996, 1999), Schulmann et al. (2002) and Kratinová et al. (2007)

Southern domain					BBTC unit			North gneiss unit		Method
Crets granite	Leucogranites	FGU granite	Kaysersberg granite	Trois-Epis orthogeness	Bilstein	Brézouard	Thannenkirch	Bt-Sil metapelites	Granulite geneiss	
			326 ± 5 Ma	328 ± 4 Ma		329 ± 2 Ma	326 ± 1 Ma		335 ± 4 Ma	U–Pb
340 ± 10 Ma	334 ± 11 Ma	336 ± 10 Ma	333 ± 10 Ma	328 ± 10 Ma	323 ± 10 Ma	323 ± 10 Ma	314 ± 9 Ma			K–Ar
Biotite	Biotite	Biotite	Biotite	Biotite	Muscovite	Muscovite	Chlorite			
323 ± 10 Ma	328 ± 10 Ma	322 ± 10 Ma								
Biotite and amphibole	Biotite	Biotite								
	331 ± 5 Ma				327 ± 2 Ma	332 ± 2 Ma		330 ± 7 Ma	332 ± 4 Ma	$^{39}_{Ar}$–$^{40}_{Ar}$
	Biotite				Muscovite	Muscovite		Biotite	Phlogopite	
									337 ± 4 Ma	
									Amphibole	

granite show ^{39}Ar–^{40}Ar cooling ages in the range 335–330 Ma similarly to those of the northern part of high-grade Central Vosges.

Lithology, petrography and microstructures of principal granitoids

The studied complex consists basically of migmatite and granite units (Fig. 2), which occupy 50% of the surface of the Central Vosges. The migmatitic unit was recently studied in detail by Kratinová et al. (2007) and Schulmann et al. (2009), and therefore, we only refer to most important results of these studies, complemented with fabric data of the westerly and southerly anatectic granites and of the older Crêtes granite.

Anatectic granites and leucogranites form essential intrusive rocks of the migmatitic unit (Fig. 2). These granites are located in the NE of the studied area and are formed by crustal granite to granodiorite bodies which host abundant metasedimentary enclaves intruded by dykes of leucogranites. The typical anatectic granite is medium-grained biotite-rich, locally porphyritic granite associated with the abundant migmatites, which exhibit various degree of melting from meta- to diatexites (Schulmann et al. 2009). The microstructure of this rock is magmatic which progressively evolve into solid-state deformation characterized by strong recrystallization of quartz and micas, and by the fracturing of feldspars (Kratinová et al. 2007).

The fundamental granite unit (FGU) covers the major part of the region (Fig. 2). It consists essentially of medium- to coarse-grained granite formed by idiomorphic plagioclase and K-feldspar, quartz, biotite, minor muscovite and accessory zircon, apatite and magnetite. Plagioclase grains display inverse zoning with albite cores (An0) and distinct oligoclase rims (An14-20). Biotite (Ti = 0.21–0.26 p.f.u., XMg = 0.57–0.59) is arranged into aggregates or is elongated along plagioclase and K-feldspar grain boundaries (Fig. 3a). This granite is developed in various facies, which preserves sings of crustal anatexis and hybridization. The microstructures of quartz grains characterized by the formation of subgrains and fine recrystallization into K-feldspar suggest low-temperature deformation (Hirth and Tullis 1992; Stipp et al. 2002). The low-temperature overprint is localized in anastomosing zones, which heterogeneously affect the magmatic microstructure. Locally, the deformation is accompanied by the weak dynamic recrystallization of K-feldspar grains, suggesting that the plastic deformation started at higher temperatures. These granites are intruded by the medium-grained leucogranites characterized by magmatic fabric without any significant solid-state overprints.

The Crêtes granite intrusion (Fig. 2) is emplaced along the southern limit with the Markstein unit. These intrusions represent special sub-alkali granites, which are close to syenites, rich in Rb, Cs, U, Th, Ba, K and Mg. The original mantle source of these magmas was enriched in K and depleted in Ca and presumably mixed with more silicate magma (Gagny 1968). The Crêtes granite represents coarse-grained granite characterized by idiomorphic K-feldspar, and plagioclase (An0), quartz, biotite and muscovite, zircon, apatite, magnetite are present as accessory phases. Absence of zoning of plagioclase grains suggests a slow crystallization. Quartz occurs in large grains with lobate boundaries and is divided into subgrains. Biotite (Ti = 0.21–0.26 p.f.u., XMg = 0.64–0.68) and muscovite are arranged into large grain aggregates or are elongated along grains boundaries and show strongly corroded shapes (Fig. 3b). The common porphyritic texture is defined by the K-feldspar phenocrysts and characteristic overgrowth of K-feldspars and plagioclase as well as corroded feldspar boundaries, indicating that this granite microstructure was not in equilibrium with late melt.

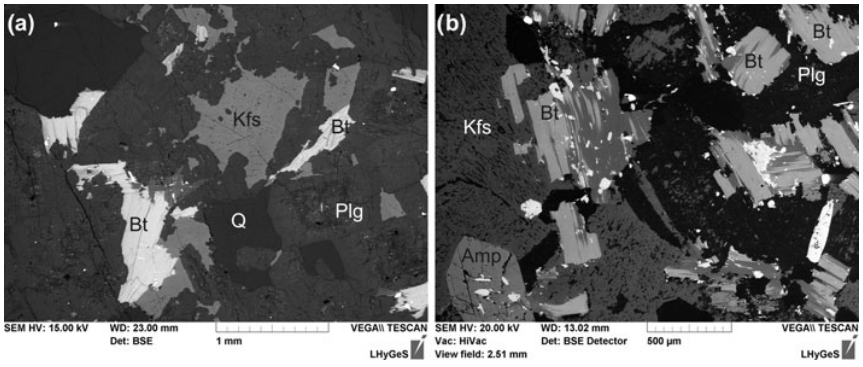

Fig. 3 Principal microtextures of the rock types. **a** The fundamental granite showing the idiomorphic shapes of K-feldspars and plagioclase and zoning of plagioclase. **b** The Crêtes granite composed of idiomorphic K-feldspars and plagioclase and quartz and biotite arranged into aggregates. Remelting of the Crêtes granite composed of irregular corroded K-feldspars and plagioclase (Mineral abbreviations after Kretz 1983)

Macroscopic structural pattern

The gneiss unit north of the BBTC complex reveals presence of steep E–W-trending granulitic fabric S_1 reworked by amphibolite facies foliation S_2 moderately dipping to the north. This deformation is associated with thrusting of granulites over mid-crustal Bt-Sill paragneisses that show similar polyphase structural pattern (Kratinová et al. 2007). The BBTC magmatic suite further south represents a sequence of magmatic pulses successively emplaced in a transtensional regime. Kratinová et al. (2007) proposed a model of sequential granite sheet emplacement parallel to $S_{1–2}$ composite vertical anisotropy during NW–SE extension. The BBTC granitoid fabrics recorded both pure extensional component in the northern part of intrusions and wrench component in the south.

The migmatitic unit south of the BBTC complex is characterized by the pervasive overprint by the D_3 Carboniferous extensional deformation and widespread melting (Blumenfeld and Bouchez 1988; Schulmann et al. 2009), which has been previously described to the west of the Saint Marie-aux-Mines fault zone by Rey et al. (1992). This unit is characterized by superposition and often complete reworking of early compressional and steep $S_{1–2}$ fabric by later extensional deformation S_3. Here, the early deformation $D_{1–2}$ is represented by solid-state fabrics variably preserved in two large strongly recrystallized felsic orthogneiss bodies (Fig. 2) and locally also in metasedimentary migmatites (Schulmann et al. 2009). The S or SSW steeply dipping S_{1-2} fabric is defined by the polycrystalline aggregates of K-feldspar, plagioclase and biotite. The D_{1-2} fabric in the host meta- and diatexites is pervasively reworked by the flat migmatitic layering S_3 and intrusion of S-type granites. The S_3 lit-par-lit banding is defined by mafic schlieren, layers of metagraywackes and enclaves in diatexites. In anatectic granites, the planar fabric is marked by the alignment of biotite and feldspar phenocrysts. The gently dipping magmatic foliation S_3 dips uniformly to SW and bears mineral lineation plunging to S or SSE. The transition from magmatic to sub-magmatic and solid-state deformation leads to the development of strongly non-coaxial deformation manifested by C–S fabrics (Berthé et al. 1979; Blumenfeld and Bouchez 1988), indicating top-to-the-SSE movement. The localized greenschist facies normal shear zones are developed parallel to the principal S_3 fabric, represented by the retrograde lineations defined by muscovite and chlorite flakes. The similar structural pattern of large-scale normal shear deformation was described by Rey et al. (1992), where the mylonitic zone separates the hanging wall granulites and footwall schists.

The large FGU domain is characterized by the presence of various types of granites, which show only exceptionally planar and linear structures. In general, the fabric of most of granites is rather isotropic so that the structural data cannot be obtained using classical field structural methods. Locally, south-dipping shear bands occur indicating normal post-solidus shearing affecting already solidified granite. However, the hypothesis of continuity or fabric discontinuity between the easterly migmatites and the FGU cannot be solved.

In contrast to anatectic granites of the FGU, the Crêtes granite reveals strong alignment of feldspar phenocrysts. This mineral fabric is clearly of magmatic origin as confirmed by the absence of plastic deformation of matrix minerals (Paterson et al. 1989) and defines steep NW–SE-trending foliation. The fabric intensity is highly variable in the field so that in many places the alignment of feldspar could not be determined. The foliation of the Crêtes granite is parallel to the cleavage and folded bedding of Carboniferous sediments of the Markstein Unit (Petrini and Burg 1998; Krecher et al. 2007). Here, the bedding is folded by open-to-close steep folds, with axial planes striking NW–SE parallel to trend of fold hinges. The disjunctive cleavage is replaced by metamorphic schistosity in the direct vicinity of the Crêtes granite (Petrini and Burg 1998), which is also parallel to its internal magmatic fabric.

In summary, the structural analysis revealed that the southern region is represented by the large migmatite-magmatic unit that shows a superposition of the extensional syn-anatectic D_3 deformation superimposed on earlier solid-state $S_{1–2}$ fabric. In contrast, the gneiss unit to the north reveals total absence of D_3 deformation, and it is marked only by existence of compressional fabrics S_1 and S_2, related both to exhumation of granulitic lower crustal rocks (Fig. 4). Kratinová et al. (2007) pointed out to a mechanical role of the BBTC complex which separated the northern compression-dominated tectonic domain from the southern extensional migmatitic domain during major transtensional event at 328–326 Ma (Fig. 4). The structural analysis presented in this work shows absence of magmatic to mylonitic fabric D_3 in the FGU in contrast to adjacent migmatites (Fig. 2). The structural relationships between the early Carboniferous (340 Ma) Crêtes granites and late Carboniferous (327–325 Ma) anatectic granites are difficult to assess using macroscopic structural analysis and therefore the AMS method is used in order to evaluate the fabric pattern of these geochronologically distinct intrusions.

Magnetic fabric pattern in the granite unit

We have employed the technique of anisotropy of magnetic susceptibility (AMS; Tarling and Hrouda 1993) in the whole southern part of the Central Vosges in order to complement the structural data acquired in the field and AMS data published elsewhere (Kratinová et al. 2007;

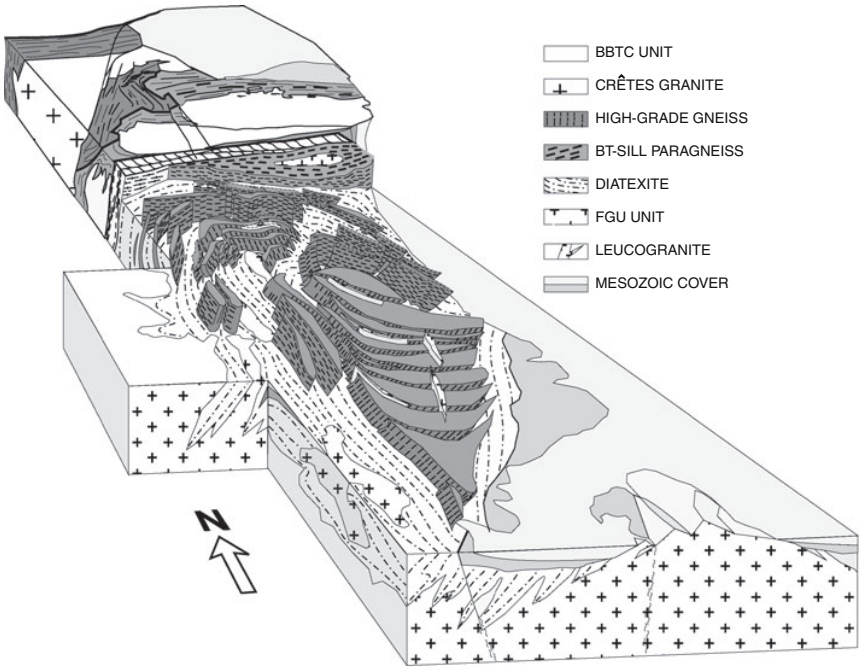

Fig. 4 Schematic 3D block diagram showing the main structural features in the southern anatectic domain. The earlier fabric is reworked by the subhorizontal extension-related S_3 fabrics, where the earlier structures are dismembered and merged within the partially anatectic crust. The whole migmatite unit is supported by the voluminous anatectic granites

Schulmann et al. 2009). Samples were drilled with a portable drilling machine, and locally, some large oriented hand specimens were collected, plastered and cored in the laboratory. The low-field AMS was measured with KLY-3S Kappabridge (Jelínek and Pokorný 1997) and also in part, with DIGICO instruments in Ecole et Observatoire des Sciences de la Terre, Strasbourg. The data were statistically evaluated using the ANISOFT package of programs (Jelínek 1978; Hrouda et al. 1990) and MOYASM1 (Westphal unpublished). In order to characterize the intensity and shape of the magnetic fabric ellipsoid, two parameters were calculated (Jelínek 1978): the degree of anisotropy $P = k1/k3$, and the shape factor $T = 2\ln(k2/k3)/\ln(k1/k3)-1$, where $0 < T < 1$ indicates oblate and $-1 < T < 0$ prolate shapes of magnetic susceptibility ellipsoids. The $k1 \geq k2 \geq k3$ are the principal susceptibility axes. Orientation of AMS is characterized by the planar structures (magnetic foliations, defined as planes perpendicular to $k3$) and linear structures (magnetic lineations, defined as directions parallel to $k1$).

Magnetic mineralogy

The magnetic mineralogy was investigated to characterize magnetic carriers and better interpret the bulk magnetic data. The contribution of particular minerals to the bulk rock susceptibility was established by analysis of the bulk susceptibility variations with temperature. The powder specimens were measured with a temperature interval of −195 to 700°C, using the CS-3 Apparatus and KLY-3S Kappabridge (Parma and Zapletal 1991; Hrouda 1994).

The bulk susceptibility (Km) of analyzed rocks was relatively low, ranging from 20×10^{-6} to 320×10^{-6} (SI) (Fig. 5a). The Km data show lower values for the anatectic granites (average Km = 147×10^{-6}, standard deviation = 60×10^{-6}) then for the calk-alkaline granites (average Km = 197×10^{-6}, standard deviation = 41×10^{-6}). Within the anatectic granites, the lowest values of Km show the leucogranites (Km = 112×10^{-6}) with respect to similar values of biotite-rich FGU granite (Km = 151×10^{-6}) and Kaysersberg granite (Km = 134×10^{-6}).

The thermomagnetic curves document predominantly hyperbolic courses, indicating the importance of a paramagnetic phase in all granitoids (Fig. 5b). According to petrographic analysis, the paramagnetic phase is mainly represented by abundant biotite. Rarely, some samples of the Crêtes granite have pronounced peaks followed by acute decrease in the proximity of 560–570°C (Curie temperature of magnetite). These samples show Km values around 320×10^{-6} (SI), suggesting minor contribution of ferromagnetic minerals (Rochette 1987) which is mainly represented by magnetite inclusions in biotite or chlorite (Fig. 3a).

Magnetic fabric

The distribution of AMS foliations and lineations is presented in the Fig. 6, which shows more complex pattern in case of magnetic foliations (Fig. 6a) with respect to

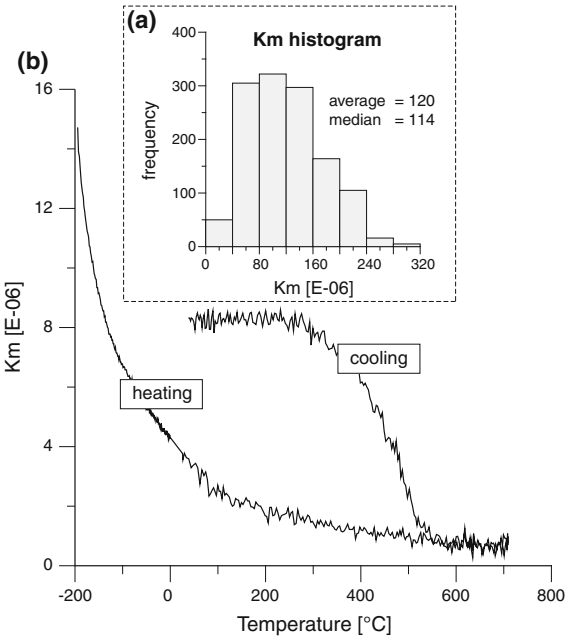

Fig. 5 Magnetic mineralogy diagrams. **a** Histogram of mean susceptibility (Km) for all AMS data shows very low values of Km clustered around average Km = 120. **b** Representative diagram of granite total susceptibility versus temperature from a sample from Crêtes granite shows hyperbolic heating curve documenting dominant presence of paramagnetic phase

relatively consistent lineation trends (Fig. 6b). In the northern region close to the BBTC unit, magnetic foliations (pole to *k*1–*k*2 plane) trend predominantly E–W and dip at moderate angles to the south. The AMS fabric pattern in the adjacent BBTC unit has been previously described by Kratinová et al. (2007). These authors showed that the central and northern parts of intrusions are characterized by subhorizontal NW–SE-trending fabric pattern, while the southern margins of intrusions are marked by steep ENE–WSW-striking foliations and strong AMS lineations. South of the BBTC, the foliation trends in the migmatitic unit gradually change into the N–S orientation, and the AMS foliation here dips predominantly to the W at moderate to steep angles. The AMS data from the northern part of the FGU show clear continuation of foliation trends from the migmatitic unit. However, the southernmost part of the anatectic granites is characterized by foliations dipping at moderate to shallow angles to the S. In the Crêtes granite, the foliation trend is distributed consistently with the NW–SE elongation of the intrusion and shows variable dips from steep NW and SE toward the subhorizontal foliations. Magnetic lineations generally exhibit subhorizontal plunges in all studied units. The northern region close to the BBTC unit exhibits NW–SE-trending orientation of magnetic lineation. This trend changes into the pervasive N–S orientation and represents the dominant fabric in the main region of the anatectic granite and migmatites. In the Crêtes granite, the magnetic lineations are trending NW–SE parallel with the intrusion shape.

The degree of magnetic anisotropy expressed by *P* parameter is generally relatively low (Fig. 7). In anatectic granites and migmatites, the *P* parameter is higher (*P* values ranging from 1.066 to 1.186) in comparison with the Crêtes granite (*P* values ranging from 1.015 to 1.074). In the migmatitic region, the most intensive fabrics are associated with the subhorizontal foliations dipping to S, which often shows features of subsolidus deformation. These zones are located partly in the southern region of the FGU and mainly in the northern migmatite unit (Schulmann et al. 2009). The weakest AMS fabrics in the anatectic granite are associated with foliations steeply dipping to the W.

In the migmatitic unit and the northern part of the FGU, the shapes of AMS ellipsoids expressed by parameter *T* are mostly of plane strain shapes to oblate in metatexites and metagraywackes (Fig. 7). The prolate fabrics are associated with the W-dipping foliations in the partially molten orthogneiss and diatexites. The southern regions reveal homogeneously developed oblate ellipsoids, which are associated with the subhorizontal-to-moderate S-dipping foliations. In contrast to the predominantly oblate to plane strain character of the AMS ellipsoids in the anatectic granites and migmatites, the AMS in the Crêtes granite is significantly more prolate (Fig. 7).

Discussion

We discuss the fabric pattern as well as the whole geometry of AMS fabric of anatectic granites in terms of deformation behavior of brittle highly partitioned transtension in the north, evolving to ductile homogeneous extension in the central migmatites, and finally gravity-extension-driven ascent of granites in the south.

Crustal extension and diapiric granite ascent in the Central Vosges

The late Carboniferous extension in the Vosges and the Black Forest (Germany) was first reported by Eisbacher et al. (1989). In the southern Black Forest, roughly N–S stretching associated with crustal extension produced the west-dipping ductile shear zone within the high-grade metamorphic HT-LP gneisses (Echtler and Chauvet 1991). These authors relate the extension to rapid uplift, exhumation and thinning due to a gravitational collapse of a previously thickened crust. In the Vosges, the extensional deformation has been studied in detail by Rey et al. (1992)

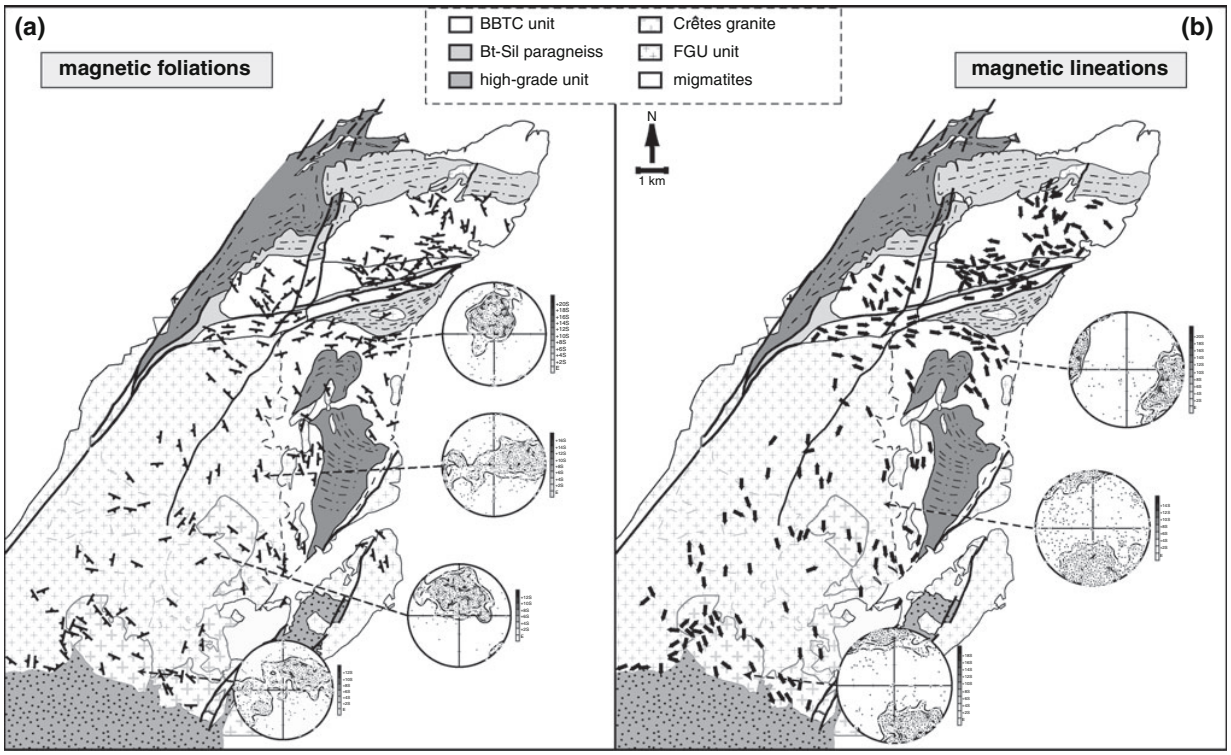

Fig. 6 Map of AMS fabric data of the southern domain and also of the BBTC intrusions. **a** Magnetic foliations. Contoured stereonets of poles to magnetic foliation (k3 direction) show the distribution of k3 for northern, central and southern parts and the Crêtes granite; see discussion in the text (equal area, lower hemisphere projection, contoured at multiples of uniform distribution). **b** Magnetic lineations (*k*1 direction). Contoured stereonets of magnetic lineations are shown for the northern, central and southern parts of the anatectic domain and for the Crêtes intrusion, for the detailed discussion see the text (equal area, lower hemisphere projection, contoured at multiples of uniform distribution)

in the western region of the Central Vosges that is separated by the NE–SW-trending Saint Marie-aux-Mines fault zone from the studied area located in the eastern high-grade part of the Vosges Mountains (Fig. 1). These authors documented the SW–NE extension accommodated by the southwestward detachment shear zone accompanied by nearly isothermal decompression (suggesting nearly 15 km thinning) and granite intrusion.

The fabric pattern summarized in Fig. 8 shows the AMS trajectories in the whole anatectic region and also in the BBTC unit. The data reveal the importance of S- and SW-dipping subhorizontal foliations bearing N–S-plunging horizontal lineations in the whole FGU and easterly migmatites. These orientations are consistent with the central and northern parts of granites of the BBTC unit, which alternate with NE–SW-oriented steep foliations associated with the NE–SW-trending horizontal lineations. The subhorizontal S-dipping fabrics in the BBTC are characterized by the plane strain to weakly prolate ellipsoid shapes, and the E–W vertical fabrics are marked by the highly oblate fabrics and high degree of AMS anisotropy (Kratinová et al. 2007). This pattern has been interpreted to result from highly partitioned transtensional deformation with NNW–SSE-oriented stretching axis. In addition, Schulmann et al. (2009) showed that this extensional deformation produced moderately to gently west-dipping migmatitic foliation and SSW–NNE-stretching direction in migmatitic domain. Kratinová et al. (2007) suggest that the intrusions of the BBTC granite sheets are entirely controlled by extensional stress obliquely oriented with respect to rheologically strong and vertical S_{1-2} anisotropy of northern gneiss and micaschist units. All that indicates that the crust in the northern part of high-grade Vosges core was relatively strong so that it reacted first by brittle failure during sequential emplacement of the BBTC sheets followed by viscous stretching of partially molten migmatitic unit.

In this work, we show that the AMS fabric pattern developed in the northern part of the FGU is broadly similar to fabrics reported from central migmatitic unit. Here, the magnetic foliation and lineation show geometrical and kinematical continuity with the S_3 migmatitic fabric of easterly meta- and diatexites. This similarity in magnetic foliation and lineation trends between migmatites and granites can be interpreted as a result of continuous

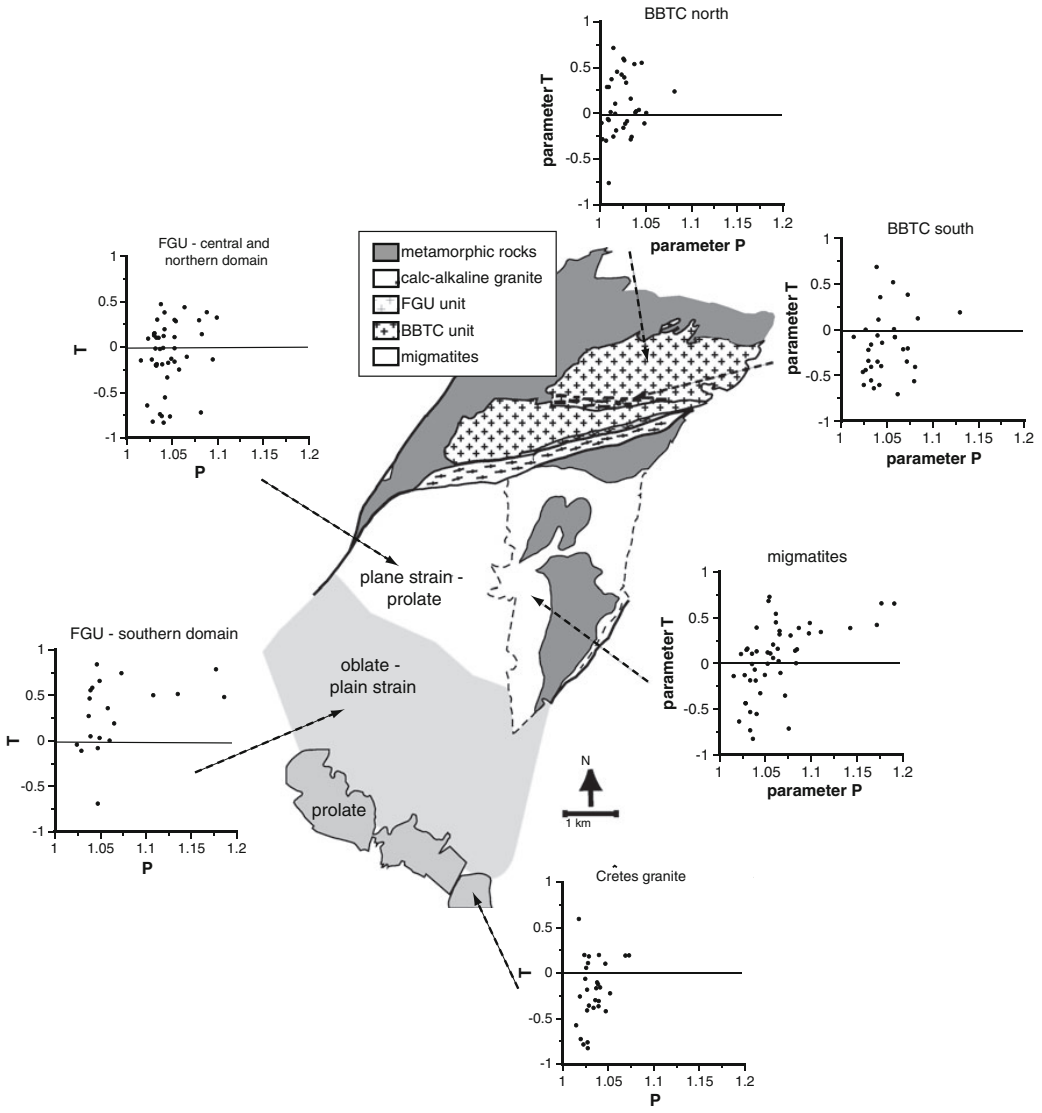

Fig. 7 Map showing the Jelínek plots (*P* vs. *T*) for selected areas: northern, central and southern domains and for the calk-alkaline granites. The differences between the anatectic and calk-alkaline granites are presented in two uppermost Jelínek plots (*P*—degree of AMS, *T*—shape of AMS ellipsoid, see text for parameter definition)

subhorizontal flow associated with increased melting of the progressively extended crust. Schulmann et al. (2009) discussed variations in shape of AMS ellipsoid in the migmatitic unit as a result of two factors: (1) the oblate fabric of relict metagraywackes and metatexites was explained as a typical fabric of pre-anatectic biotite-rich layering of schists, (2) the plane strain to weakly constrictional strains of highly molten diatexites were interpreted as a result of slightly constrictional flow associated with the extensional deformation superimposed on previous steep fabrics. This study also shows that the deformation of anatectic granites is characterized by the plane strain in the north and oblate fabrics in the south-dipping AMS foliations in the south of the FGU (Fig. 7). These differences of fabric symmetry, intensity and orientation within one predominantly magmatic unit cannot be explained by lithological differences.

We suggest that the regional variations in fabric shapes are related to complex history of crustal extension in time and space. We propose a model of tectono-magmatic evolution in which the early stages of extension are preserved in rather weakly molten rocks of migmatitic unit, which reflects the strain associated with extensional deformation, i.e. intense extensional stretching leading to

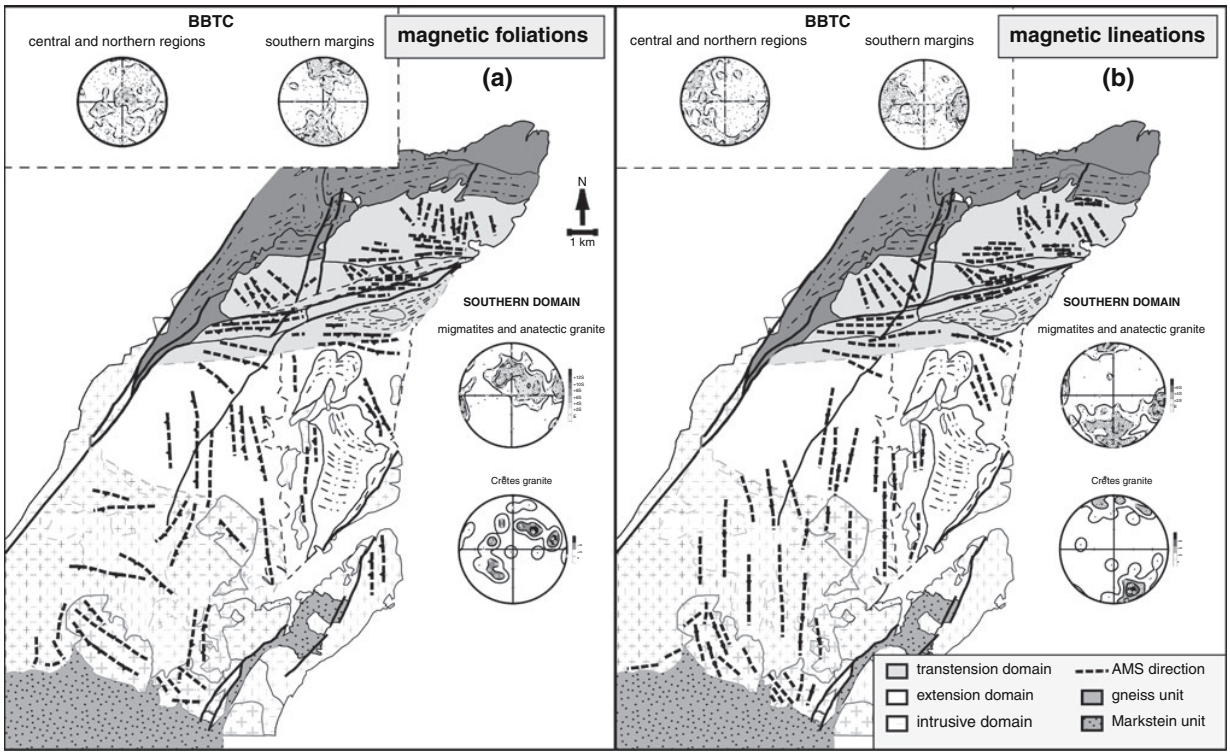

Fig. 8 Interpretative map of AMS fabric distribution in the southern anatectic domain and BBTC intrusions. **a** Distribution of AMS foliation. **b** Distribution of AMS lineation. The AMS measurements are grouped into trends showing the homogeneous fabric in the southern anatectic domain, parallel to the central-northern parts of the BBTC granites, which contrasts with the southernmost margins of the BBTC marked by steep foliations and margin-parallel horizontal lineations

the development of weakly prolate strains. Here, the deformation of relatively viscous material is purely controlled by kinematics of crustal extension and horizontal stress. The northern part of the FGU followed this simple pattern so that the magnetic fabrics of granites are similar to fabrics of migmatites.

However, this model cannot explain the development of south-dipping AMS fabric associated with oblate strains in southern part of the FGU. This regional modification of fabric is related to late stages of extensional deformation, progressive melting and intrusions of anatectic granites in the south. Such a massive crustal anatexis may produce a regional scale gravity-driven ascent of partially molten crystal mush that can generate flat fabrics and oblate strains in the roof parts of granite–migmatite body (e.g. Jackson and Talbot 1989; Paterson et al. 1998). The development of oblate fabrics at the top of gravity-driven intrusions is proposed by a number of numerical models (e.g. Cruden 1990) and recent analogue AMS plaster diapiric models of Kratinová et al. (2006). Therefore, we interpret the fabric pattern of southern part of the FGU as a result of pure shear deformation of granite roof associated with diapiric ascent of large portion of crustal melts. Our model is compatible with the presence of roof pendants preserved in SE part of the FGU in form of large stoped blocks of the Carboniferous sediments (Fluck 1980) in the FGU granite. The diapiric ascent is not the unique mechanism responsible for fabric acquisition in granitoids as shown by AMS lineation which continuously trend N–S from northern migmatites to southern granites. The persistence of AMS lineation trends can be explained by combination of gravity-driven granite ascent and continuous extensional deformation. However, the role of extensional tectonics was already limited as shown by absence of sheeted intrusions and rather irregular pattern of elliptical granites favoring gravitational ascent-emplacement processes.

The transition from tectonically driven crustal extension to gravity-driven ascent of crustal melts is a process proposed for hot orogenic domains by number of authors in last two decades (Talbot 1979; Vanderhaeghe 1999, 2001; Rey et al. 2001). In analogy to these models, we suggest that the emplacement of FGU granitoids was driven at first stage by horizontal extension when the crust was strong and reacted by brittle failure to tensile stress (BBTC intrusions), followed by viscous stretching in weakly molten rocks (northern migmatite unit) and terminated by dominantly gravity-driven ascent of FGU granitoids (southern granites).

Interactions between orogenic suprastructure and infrastructure

Previous structural studies revealed existence of earlier subvertical E–W-trending solid-state foliation, which has been documented in the granulitic gneiss unit and monotonous paragneiss north of the BBTC, as well as in paragneiss south of the BBTC (Kratinová et al. 2007). In addition, the folded remnants of earlier solid-state, vertical and NW–SE-trending fabrics were also described in the disintegrated orthogneiss bodies in the central part of the migmatitic unit (Fig. 3; Schulmann et al. 2009). Schulmann et al. (2002) proposed that this early structural pattern developed via viscous extrusion of high-grade rocks in front of indenting rigid basement promontory located further to the north (Fig. 9a). In this model, the orogenic lower crust flows along a steep channel in mid-crustal levels resulting in the development of steep metamorphic fabric as proposed by Štípská et al. (2004) in similar setting of the Variscan belt. According to this model, the vertical S_1 fabric in higher-grade units of the crustal domain reflects the geometry imposed by the horizontal SW–NE-oriented shortening at about 340–330 Ma (Fig. 9a; Schulmann et al. 2002). This fabric was further locally superimposed by the subsequent moderately dipping compressional fabrics affecting early steep fabrics during extrusion of partially molten lower crust over orogenic middle crust at depth levels of about 3–4 kbar, and the whole region was further affected by the regional extension deformation D_3 (Fig. 9b).

There are a number of studies showing that the Carboniferous sediments of the Markstein Unit were affected by important Carboniferous folding and development of steep NW–SE-striking cleavage (e.g. Krecher et al. 2007). Petrini and Burg (1998) show that the disjunctive cleavage characteristic for supracrustal folding passes to metamorphic schistosity in the vicinity of the Crêtes granite. The existence of structural and contact metamorphic aureole of the Crêtes granite led Schulmann et al. (2002) to propose that the emplacement of 340 My old Crêtes granite is coeval with the compressive deformation of the Carboniferous sediments. This means that the deformation affecting the upper crust occurred ~15 millions years before the onset of the extensional deformation dated by U–Pb zircon age of porphyritic granite intruding the S_2 flat migmatite fabric (Schaltegger et al. 1999).

This study shows that the AMS fabric, i.e., foliation trends and lineation strike of the Crêtes granite, is subparallel to the cleavage trend and fold hinges affecting southerly Carboniferous sediments of the Markstein Unit

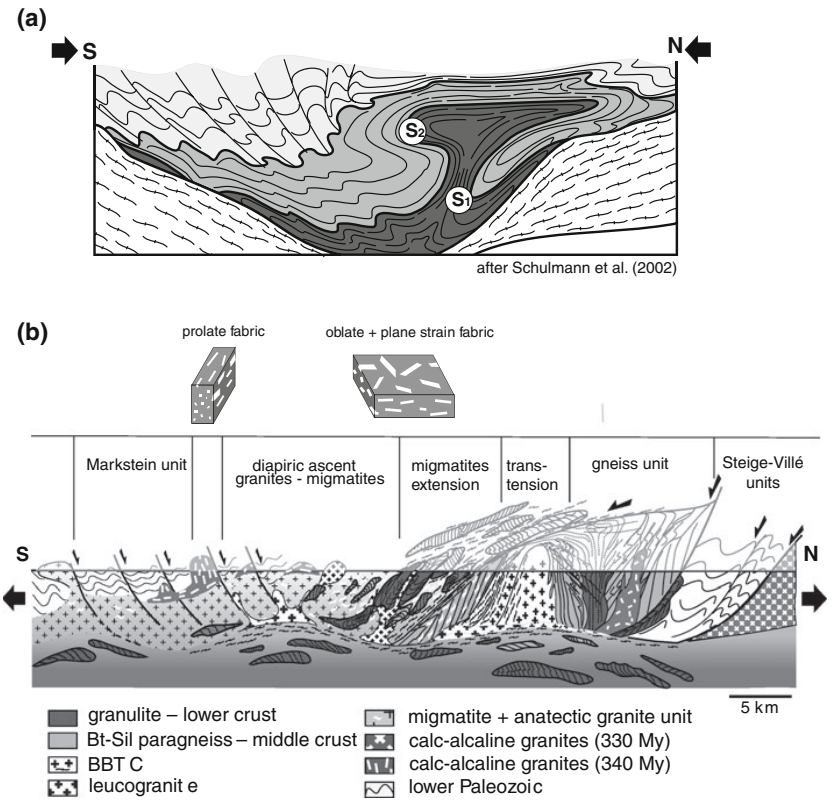

Fig. 9 Schematic orogenic scale cross-sections showing the interpretative tectonic evolution of the studied area. **a** Late convergent deformation of the crustal section is associated with the development of the steep foliation S_1 due to the vertical extrusion of the lower crustal rocks which is locally overprinted by subhorizontal foliations S_2 associated with the subsequent lateral spreading of partially molten rocks over the middle crustal unit (modified after Schulmann et al. 2002, 2005). **b** The region is overprinted by the subsequent extensional deformation D_3 structures. The BBTC unit intruded the inherited vertical anisotropy developed during the compressive stage, the high-grade unit towards the south is subjected to large-scale boudinage and the background anatectic crust shows the pervasive ductile flow and diapiric intrusions

(Fig. 8). This geometrical conformity is just another argument for coeval horizontal NE–SW compression and emplacement of the Crêtes granite in the supracrustal levels. The structural observations from the upper and lower orogenic crust show that both deeply seated high-grade rocks (orthogneiss in migmatitic domain) and the unmetamorphosed sediments were affected by the same compressional event at early Carboniferous. This deformation produced steep fabric in both crustal levels. However, the actual fabric pattern of granitoids and migmatites shows that the vertical fabrics of the upper crust units are separated from deeper steep fabrics of orogenic lower crust by a zone of flat foliations that developed in relatively shallow crustal levels.

It is therefore evident that the zone of migmatites and anatectic granites played a major role for decoupling between supracrustal units and orogenic lower crust during late stages of orogenesis. The AMS fabric contrast between supracrustal 340 Ma Crêtes granite and infrastructural FGU unit is therefore of vital importance for understanding the mechanical role of this weak layer. Our AMS study shows that the foliations in the Crêtes granite are not exclusively steep, but their poles form a NE–SW-trending girdle, with a maximum indicating presence of flat fabrics similar to those of the adjacent FGU granites (Fig. 6a). In addition, the AMS ellipsoids reveal predominance of strongly prolate fabrics which contrast with oblate fabrics in the nearby FGU granites (Fig. 7). In analogy to model of Kratinová et al. (2007) and Schulmann et al. (2009), the fabric pattern of the Crêtes granites (steep to flat foliation, horizontal NW–SE-trending lineation and prolate shape of AMS ellipsoid) may be interpreted as a result of superposition of vertical shortening on early vertical intrusive emplacement fabric of the Crêtes granite. Based on structural observations discussed above, fabric data from both the Crêtes and subjacent FGU granites and numerical modeling of Schulmann et al. (2009) and Schulmann and Ježek (2011), it is proposed that the fabric of the Crêtes granite results from important vertical shortening superimposed on originally vertical magmatic fabric. These conclusions corroborate microstructural observations in Fig. 3b, showing re-equilibration of early magmatic textures in the Crêtes granites. Overgrowths and resorption microstructures observed here suggest a second stage of melting which is not preserved in the FGU granitoids.

In conclusion, it is well known that the crustal extension settings are associated with the vertical maximum principal compressive stress (Dewey 1988; Cosgrove 1997). It follows that during extensional deformation, the occurrence of a substantial component of coaxial strain implies subvertical shortening, which induces the dominant subhorizontal planar and/or linear anisotropy within rocks. In the region of migmatitic unit, the extension is principally accommodated by horizontal flow that is amplified by vertical ascent of the FGU granites. Some fabric variations like prolate fabrics in orthogneiss migmatites and the Crêtes granite can be explained as modification of early solid state microstructure of steeply oriented fabric during horizontal shortening and complete or partial reset of original AMS record. Recent studies and numerical modeling of Schulmann and Ježek (2011) confirm that prolate AMS fabrics of low degree of anisotropy may result from such deformation overprints.

Conclusions

This structural and AMS analysis of a large anatectic crustal domain in the Central Vosges provides further evidence for the late Carboniferous extensional tectonics, synchronous with the partial melting. The inherited compressional fabrics preserved in the orogenic lower and middle crust were overprinted by the late Carboniferous regional extension, which accounts for the low-pressure–high-temperature metamorphism associated with the emplacement of numerous crustal granites.

The regional AMS fabric pattern reflects (1) transtensional emplacement of granite sheets in brittle vertical anisotropy of high-grade gneiss in the north followed by (2) homogeneous viscous flow related to the regional extensional deformation in migmatitic rocks in the central part of high-grade Vosges and (3) diapiric ascent of crustal granites associated with the vertical shortening of partially molten roof and stoping of brittle parts of the upper crust in the south. This study predominantly based on the AMS documents the importance of superposed deformation overprints for the bulk AMS pattern in the granites and contributes to understanding of anatomy of magma-rich crustal extensional zones.

Acknowledgments This research is a contribution of UMR 7516 Institut de Physique du Globe of CNRS and University of Strasbourg and was supported financially by the Grant Agency of the Academy of Sciences of the Czech Republic (GAAV) (grant no. KJB300120702 to Z. Kratinová) and Fundacao para a Ciencia e a Tecnologia (FCT) project (AMS progress, n. PTDC/CTE-GIX/098696/2008).

References

Benn K (1994) Overprinting of magnetic fabrics in granites by small strains: numerical modelling. Tectonophysics 184:153–162

Berthé D, Choukroune P, Jegouzo P (1979) Orthogneiss, mylonite and non coaxial deformation of granites; the example of South Armorican shear zone. J Struct Geol 1:31–42

Blumenfeld P, Bouchez JL (1988) Shear criteria in granite and migmatite deformed in the magmatic and solid states. J Struct Geol 10:361–372

Bouchez JL (1997) Granite is never isotropic: an introduction to AMS studies of granitic rocks. In: Bouchez JL, Hutton DHW, Stephens

WE (eds) Granite: from segregation of melt to emplacement fabrics. Kluwer academic Publishers, Dordrecht, pp 95–112
Bouchez JL, Gleizes G, Djouadi T, Rochette P (1990) Microstructure and magnetic susceptibility applied to emplacement kinematics of granites: the example of the Foix pluton (French Pyrenees). Tectonophysics 184:157–171
Boutin R, Montigny R, Thuizat R (1995) Chronologie K-Ar et 39Ar-40Ar du métamorphisme et du magmatisme des Vosges. Comparaison avec les massifs varisques avoisinants. Géologie de la France 1:3–25
Burg JP, Van Den Driessche J, Brun JP (1994) Syn- to post-thickening extension in the Variscan Belt of Western Europe: Modes and structural consequences. Géologie de la France 3:33–51
Cosgrove JW (1997) The influence of mechanical anisotropy on the behaviour of the lower crust. Tectonophysics 280:1–14
Cruden AR (1990) Flow and fabric development during the diapiric rise of magma. J Geol 98:681–698
Dewey JF (1988) Extensional collapse of orogens. Tectonics 7:1123–1139
Echtler P, Chauvet A (1991) Carboniferous convergence and subsequent crustal extension in the southern Schwarzwald (SW Germany). Geodin Acta 5:37–49
Edel JB, Weber K (1995) Cadomian terranes, wrench faulting and thrusting in the central Europe Variscides: geophysical and geological evidence. Geol Rundsch 84:412–432
Eisbacher GH, Luschen E, Wickert F (1989) Crustal-scale thrusting and extension in the hercynian Schwarzwald and Vosges, central Europe. Tectonics 8:1–21
Eller JPV, Fluck P, Hameurt J (1970) Carte géologique des Vosges moyennes, partie centrale et partie orientale. Bull Serv Carte géol Als Lorr 23:29–50
England PC, Thompson AB (1986) Some thermal and tectonic models for crustal melting in continental collision zones. In: Coward MP, Ries AC (eds) Collision tectonics. Geol Soc Spec Publ 19: 83–94
Faure M (1995) Late orogenic carboniferous extensions in the Variscan French Massif Central. Tectonics 14:132–153
Fluck P (1980) Métamorphisme et magmatisme dans les Vosges Moyennes d'Alsace. Contribution a l'histoire de la chaine Varisque. Memoire de these, Strasboug, p 245
Fluck P, Edel JB, Gagny C, Montigny R, Piqué A, Schneider JL, Whitechurch H (1987) Le socle Vosgien, segment de la chaine Varisque d'Europe. Géologie profonde de la France. Project Vosges, Strasbourg, Nancy, p. 84
Gagny C (1968) Pétrogenese du granite des Crêtes. Vosges méridionales, Fac Sci Nantes, p 546
Hameurt J (1967) Les terrains cristallins et cristallophylliens du versant occidental des Vosges moyennes. Mém Serv Carte géol Als Lorr 26:402
Hess JC, Lippolt HJ, Kober B (1995) The age of the Kagenfels granite (Northern Vosges) and its bearing on the intrusion scheme of late Variscan granitoides. Geol Rundsch 84:568–577
Hirth G, Tullis J (1992) Dislocation creep regimes in quartz aggregates. J Struct Geol 14:145–159
Hrouda F (1993) Theoretical-models of magnetic-anisotropy to strain relationship revisited. Phys Earth Planet In 77:237–249
Hrouda F (1994) A technique for the measurement of thermal-changes of magnetic-susceptibility of weakly magnetic rocks by the Cs-2 apparatus and Kly-2 Kappabridge. Geophys J Int 118:604–612
Hrouda F, Jelínek V, Hrušková L (1990) A package of programs for statistical evaluation of magnetic data using IBM-PC computers. EOS Trans, AGU, San Francisco, p 1289
Jackson MPA, Talbot CJ (1989) Anatomy of mushroom-shaped diapirs. J Struct Geol 11:21l–230
Jelínek V (1978) Statistical processing of anisotropy of magnetic susceptibility measured on groups of specimens. Stud Geophys Geod 22:50–62
Jelínek V, Pokorný J (1997) Some new concepts in technology of transformer bridges for measuring susceptibility anisotropy of rocks. Phys Earth Planet In 22:179–181
Kratinová Z, Závada P, Hrouda F, Schulmann K (2006) Non-scaled analogue modelling of AMS development during viscous flow: A simulation on diapir-like structures. Tectonophysics 418:51–61
Kratinová Z, Schulmann K, Edel JB, Ježek J, Schaltegger U (2007) Model of successive granite sheet emplacement in transtensional setting: integrated microstructural and AMS study. Tectonics 26. doi:10.1029/2006TC002035
Kratinová Z, Ježek J, Schulmann K, Hrouda F, Shail RK, Lexa (2010) Non-coaxial K-feldspar and AMS sub-fabrics in the Land's End Granite, Cornwall: evidence of magmatic fabric decoupling during late deformation and matrix crystallization. J Geophys Res 115:B09104. doi:10.1029/2009JB006714
Krecher M, Behrmann JH, Muller-Sigmund H (2007) Sedimentology and tectonic setting of Devonian-Carboniferous turbidites and debris flow deposits in the Variscan Vosges Mountains (Markstein Group, NE-France). Z dt Ges Geowiss 158(4):1063–1087
Kretz R (1983) Symbols for rock-forming minerals. Am Mineral 68:277–279
Latouche L, Fabries J, Guiraud M (1992) Retrograde evolution in the Central Vosges Mountains (northeastern France): implications for the metamorphic history of high-grade rocks during the Variscan orogeny. Tectonophysics 205:387–407
Ledru P, Courrioux G, Dallain C, Lardeaux JM, Montel JM, Vanderhaeghe O, Vitel G (2001) The Velay dome (French Massif Central): melt generation and granite emplacement during orogenic evolution. Tectonophysics 342:207–237
Parma J, Zapletal K (1991) CS-1 apparatus for measuring the temperature dependence of low-field susceptibility of minerals and rocks (in cooperation with KLT-2 Kappabridge). Geofyzika Brno, Unpublished Report
Paterson SR, Vernon RH, Tobisch OT (1989) A review of criteria for identification of magmatic and tectonic foliations in granitoids. J Struct Geol 11:349–363
Paterson SR, Fowler TK, Schmidt KL, Yoshinobu AS, Yuan ES, Miller RB (1998) Interpreting magmatic fabric patterns in plutons. Lithos 44:53–82
Petrini K, Burg JP (1998) Relationship between deformation, plutonism and regional metamorphism in the Markstein area (southern Vosges). Géologie de la France 2:13–26
Rey P, Burg JP, Lardeaux JM, Fluck P (1989) Evolution métamorphiques contrastée dans les Vosges orientales: témoins d'un charriage dans la chaine varisque. C R Acad Sci Paris 309:815–821
Rey P, Burg JP, Caron JM (1992) Middle and Late Carboniferous extension in the Variscan Belt: structural and petrological evidences from the Vosges massif (Eastern France). Geodin Acta 5:17–36
Rey P, Vanderhaeghe O, Teyssier C (2001) Gravitational collapse of the continental crust: definition, regimes and modes. Tectonophysics 342:435–449
Rochette P (1987) Magnetic susceptibility of the rock matrix related to magnetic fabric studies. J Struct Geol 9:1015–1020
Schaltegger U, Schneider JL, Maurin JC, Corfu F (1996) Precise U–Pb chronometry of 345–340 Ma old magmatism related to syn-convergence extension in the Southern Vosges (Central Variscan Belt). Earth Planet Sci Lett 144:403–419
Schaltegger U, Fanning CM, Gunther D, Maurin JC, Schulmann K, Gebauer D (1999) Growth, annealing and recrystallization of zircon and preservation of monazite in high-grade metamorphism:

conventional and in situ U–Pb isotope, cathodoluminiscence and microchemical evidence. Contrib Mineral Petr 134:186–201

Schulmann K, Ježek J (2011) Some remarks on fabric overprints and constrictional AMS fabrics in igneous rocks. Int J Earth Sci. doi: 10.1007/s00531-011-0681-z

Schulmann K, Schaltegger U, Ježek J, Thompson AB, Edel JB (2002) Rapid burial and exhumation during orogeny: thickening and synconvergent exhumation of thermally weakened and thinned crust (Variscan orogen in Western Europe). Am J Sci 302:856–879

Schulmann K, Kröner A, Hegner E, Wendt I, Konopásek J, Lexa O, Štípská P (2005) Geodynamics of eastern margin of the Variscan thickened orogenic root, model based on structural, petrological and new geochronological data. Am J Sci 305:407–448

Schulmann K, Edel JB, Hasalová P, Cosgrove JW, Ježek J, Lexa O (2009) Influence of melt induced mechanical anisotropy on the magnetic fabrics and rheology of deforming migmatites, Central Vosges, France. J Struct Geol 31(10):1223–1237. doi:10.1016/j.jsg.2009.07.004

Stipp M, Stunitz H, Heilbronner R, Schmid SM (2002) The eastern Tonale fault zone: a 'natural laboratory' for the crystal plastic deformation of quartz over a temperature range from 250 to 700°C. J Struct Geol 24:1861–1884

Štípská P, Schulmann K, Kroner A (2004) Vertical extrusion and middle crustal spreading of omphacite granulite: a model of syn-convergent exhumation (Bohemian Massif, Czech Republic). J Metamorph Geol 22:179–198

Talbot CJ (1979) Infrastructural migmatitic upwelling in East Greenland interpreted as thermal convective structures. Precambrian Res 8:77–93

Tarling DH, Hrouda F (1993) The magnetic anisotropy of rocks. Chapman and Hall, London

Vanderhaeghe O (1999) Pervasive melt migration from migmatites to leucogranite in the Shuswap metamorphic core complex, Canada: control of regional deformation. Tectonophysics 312:35–55

Vanderhaeghe O, Teyssier C (2001) Partial melting and flow of orogeny. Tectonophysics 342:451–472

Anne-Sophie TABAUD

Le magmatisme des Vosges

Résumé

Les Vosges sont caractérisées par la présence de nombreuses intrusions et extrusions magmatiques d'affinités variées. Elles constituent donc un excellent site d'étude pour contraindre, par la datation et la géochimie, l'évolution des évènements de ce segment de l'orogène Varisque. Ce travail révèle ainsi deux successions d'évènements magmatiques identiques, décalées dans le temps, caractérisant les domaines Moldanubien (360 à 320 Ma) et Saxothuringien (335 à 295 Ma). Ces successions d'évènements magmatiques résultent de deux processus majeurs. L'avancée des croûtes continentales subduites et sous-plaquées au niveau du Moho sous les blocs continentaux permet le passage du magmatisme calco-alcalin au magmatisme calco-alcalin riche en potassium. L'apport de chaleur par désintégration des éléments radiogéniques (K, U et Th) présents dans ces croûtes continentales subduites permet, dans un premier temps, la formation du magmatisme magnésio-potassique en profondeur. Dans un second temps, elle permet la formation du magmatisme d'origine crustale par l'intrusion du magmatisme magnésio-potassique, riche en K, U et Th, à la limite croûte moyenne - croûte supérieure. Ces successions d'évènements magmatiques et particulièrement, la présence des granites magnésio-potassiques, relient clairement les Vosges à la partie Est de l'orogène Varisque (Forêt Noire, Massif de Bohème, Alpes et Corse-Sardaigne).

Mots clés : Magmatisme, Orogène varisque, Vosges, Géochimie, Pétrologie magmatique, Géochronologie, ASM.

Abstract

The Vosges Mountains are characterized by the presence of numerous magmatic intrusions and extrusions of varied affinities. Accordingly, they constitute the best site to investigate, by dating and geochemistry, the evolution of the events affecting this segment of the Variscan orogeny. Two successions of identical magmatic events, shifted in the time, are identified, characterizing both Moldanubian (360 to 320 Ma) and the Saxothuringian (335 to 295 Ma) domains. These successions of magmatic events result of two major process. The progress of subducted and underplated continental crusts at Moho depth under continental blocks permits to shift from calc-alkaline to high potassic calc-alkaline magmatism. The radiogenic heat production from latter underplated continental crusts, in a first time, permits to generate magnesio-potassic magmas at depth. Then, this radiogenic heat permits to generate crustal magmas by intrusion of magnesio-potassic magmas rich in K, U and Th at mid-upper crust boundarie. These successions of magmatic events and particularly, the presence of the magnesio-potassic granites, imply a strong link between the Vosges Mts. and the eastern part of the Variscan orogeny (Black Forest, Bohemian Massif, the Alps and Corsica Batholith).

Keywords: Magmatism, Varican Orogeny, Vosges Mts, Geochemistry, Magmatic petrology, Geochronology, AMS.